

University of Southampton Research Repository
ePrints Soton

Copyright © and Moral Rights for this thesis are retained by the author and/or other copyright owners. A copy can be downloaded for personal non-commercial research or study, without prior permission or charge. This thesis cannot be reproduced or quoted extensively from without first obtaining permission in writing from the copyright holder/s. The content must not be changed in any way or sold commercially in any format or medium without the formal permission of the copyright holders.

When referring to this work, full bibliographic details including the author, title, awarding institution and date of the thesis must be given e.g.

AUTHOR (year of submission) "Full thesis title", University of Southampton, name of the University School or Department, PhD Thesis, pagination

**AN INVESTIGATION INTO THE IMPACT OF SEQUENTIAL FILLING ON
PROPERTIES OF EMPLACED REFUSE LIFTS AND MOISTURE STORED IN A
MUNICIPAL SOLID WASTE LANDFILL**

by

Olayiwola Ademola Oni

A thesis submitted for the degree of

Doctor of Philosophy

IN THE FACULTY OF ENGINEERING AND APPLIED SCIENCE
DEPARTMENT OF CIVIL AND ENVIRONMENTAL ENGINEERING
UNIVERSITY OF SOUTHAMPTON
SOUTHAMPTON
DECEMBER 2000

This thesis is dedicated to my beautiful wife, Olayinka, and lovely daughter, Oludemilade for their patience and sacrifice. The thesis is the fruit of their support and encouragement.

ABSTRACT

FACULTY OF ENGINEERING AND APPLIED SCIENCE CIVIL AND ENVIRONMENTAL ENGINEERING

Doctor of Philosophy

AN INVESTIGATION INTO THE IMPACT OF SEQUENTIAL FILLING ON PROPERTIES OF EMPLACED REFUSE LIFTS AND MOISTURE STORED IN A MUNICIPAL SOLID WASTE LANDFILL

by Olayiwola Ademola Oni

The majority of investigations on municipal solid waste (MSW) landfills have been undertaken during the post-closure period, and therefore, the changes that occur in the properties of refuse layers placed during the period of infilling are often ignored. The impact of further tipping of refuse loads on the moisture content, hydraulic and geotechnical properties of emplaced refuse lifts, and the daily cover was examined in this study by undertaking field and laboratory tests on the refuse fill at White's Pit landfill, Poole, Dorset.

The field tests involved mainly pit tests and cone penetration tests. The porosity and field capacity of the refuse excavated from the pits were determined in 210 litre drums. In addition, factors that influence leachate production, which include the moisture stored in the topsoil and the runoff from the landfill were measured. The laboratory tests involved the determination of compression, porosity, and hydraulic conductivity of pulverised refuse samples with and without a cover soil, under increasing vertical loading. The data obtained from the tests were used in the simulation of moisture in refuse lifts at the site, using the Hydrologic Evaluation of Landfill Performance (HELP) model. The data were also used to formulate characteristic equations used for determining temporal changes in the physical properties of emplaced refuse lifts.

The results of the investigation show a reduction in porosity and hydraulic conductivity, and increase in the density of an emplaced refuse layer according to the quantity of further filling of refuse loads. The density of an emplaced refuse is further increased by the ravelling of the daily cover materials, but its permeability decrease as a result. Under an applied vertical load of 6 kPa, the hydraulic conductivity and density of refuse-only samples were 1.4×10^{-3} m/s and 291 kg/m³, while that for refuse with 7.5 % cover soil were 9.4×10^{-4} m/s and 353 kg/m³ respectively. The hydraulic conductivity of a refuse lift with a slightly clay/silt sand cover, however, appeared greater than its calculated value (10^{-5} m/s) at low effective stresses.

The similarity between the results of refuse tested in experimental cells in present study and Beaven and Powrie's (1995) large-scale compression cell suggests that empirical models can be derived from the data obtained from cell tests to predict the behaviour of refuse with different densities. Furthermore, relatively small cells can be used in preliminary study of the behaviour of refuse if the particle sizes are reduced in proportion to the size of the test cell.

Apart from direct infiltration of water during waste placement, the volumetric moisture content and degree of saturation of a refuse lift increase during the fill period due to compression from overlying lifts. The saturation of the refuse fill is further enhanced by channelled water through the macropores in the cover soil system. The simulation technique used in this study may be used in evaluating alternative designs and plans of a MSW landfill. Large-scale testing of refuse with an intermediate cover soil is recommended.

Table of Contents

Abstract.....	ii
Table of Contents.....	iii
List of Figures.....	viii
List of Plates.....	x
List of Table.....	xi
Acknowledgements.....	xii
Chapter 1: Introduction.....	1
1.1 The Problem.....	1
1.2 Objectives.....	3
1.3 Outline and Scope.....	4
Chapter 2: Review of Landfill Practice.....	6
2.1 Summary.....	6
2.2 Landfill.....	6
2.2.1 Types of Refuse Landfill Sites.....	7
2.2.2 The Landfill Process.....	8
2.2.3 Post-Closure.....	13
2.3 Impact of Overburden on Refuse fills.....	14
2.3.1 Introduction.....	14
2.3.2 Mechanisms of Compression in Refuse Fills.....	15
2.4 Determination of Settlement in Refuse Fills.....	17
2.4.1 Introduction.....	17
2.4.2 Conventional Methods.....	17
2.5 Effective Stress.....	21
2.6 Research Considerations.....	23
2.6.1 Aims and Approach	23

Chapter 3: Review of Leachate Production in Landfills.....	25
3.1 Summary.....	25
3.2 Introduction.....	25
3.3 Formation of Leachate.....	26
3.4 Determination of the Quantity of Leachate Generated in Landfills	27
3.4.1 The Water Balance Method.....	28
3.5 Factors Influencing the Quantity of Leachate Generated in Landfills.....	29
3.5.1 Precipitation.....	30
3.5.2 Evapotranspiration.....	30
3.5.3 Moisture Storage.....	33
3.5.4 Surface Runoff.....	37
3.5.5 Microbial Degradation.....	38
3.6 Simulation of Leachate Quantity in Landfills.....	42
3.7 Research Needs.....	44
Chapter 4: The Site.....	45
4.1 Summary.....	45
4.2 Location and Topography.....	45
4.3 Geology.....	47
4.3.1 Regional.....	47
4.3.2 Local.....	50
4.4 Refuse Disposal in Dorset.....	53
4.4.1 Refuse Tipping at White's Pit Landfill.....	54
4.5 Conclusion.....	55
Chapter 5: Field Investigations into the Changes in the Properties of an Emplaced Refuse Fill.....	58
5.1 Summary.....	58
5.2 Introduction.....	58
5.3 Test Pits.....	59
5.3.1 Density of the Emplaced Refuse Fill.....	60
5.3.2 Physical Composition of the Emplaced Refuse	65

5.3.3	Macroporosity, Absorption Capacity and Field Capacity of the Emplaced Refuse Fill	67
5.3.4	Results.....	69
5.3.5	Discussion.....	77
5.4	Determination of the Secondary Compression Index of the Refuse fill.....	80
5.5	Static Cone Penetration Tests.....	85
5.5.1	Introduction.....	85
5.5.2	Testing Technique.....	86
5.5.3	Results.....	87
5.5.4	Discussion.....	87
Chapter 6: Field Measurements of Factors Influencing Leachate Production		92
6.1	Summary.....	92
6.2	Introduction.....	92
6.3	Determination of the Moisture Content in the Cover Soil System.	93
6.3.1	The Neutron Probe.....	93
6.3.2	Method of Measurement.....	93
6.3.3	Results and Discussion.....	97
6.4	Surface Runoff Measurements.....	102
6.4.1	Introduction.....	102
6.4.2	Field Measurement.....	103
6.4.3	Results and Discussion.....	106
Chapter 7: A Laboratory Investigation into Changes in the Properties of Refuse Llifts under Loading.....		110
7.1	Summary.....	110
7.2	Introduction.....	110
7.3	Experimental Set-up.....	112
7.4	Materials and Methodology.....	116
7.4.1	Refuse Material.....	116
7.4.2	Determination of Compression, Porosity, and Hydraulic Conductivity of Refuse (With Cover Soil) under Loading	118
7.5	Results.....	120

7.6	Discussion.....	128
7.6.1	Compression and Density of the refuse fill.....	129
7.6.2	Porosity and Hydraulic Conductivity.....	130
7.6.3	Comparison of Experimental Results with Data Obtained from Large-scale Cells.....	131
7.6.4	The Impact of Cover Soil on the Properties of Refuse Layer and Implications for Landfilling.....	135
Chapter 8: The Help Model - An Overview.....		136
8.1	Summary.....	136
8.2	The HELP Model.....	136
8.2.1	Modelling Procedure.....	137
8.2.2	Limitations in the Application.....	141
Chapter 9: Simulation of Moisture Stored in Refuse Lifts in a Municipal Landfill.....		144
9.1	Summary.....	144
9.2	Introduction.....	144
9.3	The Empirical Models for Refuse Properties.....	145
9.4	Moisture Simulation at White's Pit Landfill.....	147
9.4.1	Introduction.....	147
9.4.2	HELP Input.....	148
9.4.3	Solution Method.....	151
9.5	Actual Leachate Level in the Landfill.....	153
9.6	Results.....	154
9.7	Discussion.....	164
9.7.1	Modelling Results.....	164
9.7.2	Validity of the Simulation Technique.....	167
Chapter 10: General Discussion and Recommendations.....		169
10.1	Summary.....	169
10.2	General Discussion.....	169
10.3	Recommendations for Future Investigations.....	174

Chapter 11: Conclusions

11.1 Conclusions.....	177
References.....	179
Bibliography.....	192

Appendices

Appendix A: Errors in Measurement and Some Useful Geotechnical Terms

Appendix B: Tables and Curves

List of Figures

Figure 2.1: Development and completion of a solid waste landfill.....	10
Figure 3.1: Water movement at a landfill.....	26
Figure 3.2: Water Holding Characteristic of Soils.....	37
Figure 3.3: Major degradative steps during the anaerobic decomposition phase..	41
Figure 3.4: Schematic of landfill stabilisation, organic, components.....	42
Figure 4.1: Topographical Map of White's Pit Landfill.....	46
Figure 4.2: Sketch map of the geology of the Bournemouth-Poole-Wimborne area	49
Figure 4.3: The Schematic of the Poole Formation at White's pit.....	51
Figure 4.4: Map of the top and thickness of Broadstone clay at White's pit, Poole, Dorset.....	52
Figure 4.5: Controlled waste to landfill in Dorset 1993/94 - 1,144994 tonnes ...	54
Figure 4.6: The tipping faces and waste thickness at the site.....	57
Figure 5.1: Locations for test pits and cone penetration tests.....	60
Figure 5.2: Schematic of the test pit.....	65
Figure 5.3: Particle size distribution curves of fines (<10mm) in refuse and the cover soil at the site.....	75
Figure 5.4: Densification of the emplaced refuse.....	80
Figure 5.5: Vertical strain versus logarithm of the refuse fill.....	83
Figure 5.6: Pore pressure and soil behaviour type vs depth for CPT 14.....	88
Figure 5.7: Cone resistance and friction ratio vs depth for CPT 14.....	89
Figure 5.8: Soil behaviour type index vs depth for CPT 14.....	90
Figure 6.1: The neutron probe access tubes.....	94
Figure 6.2: Location of neutron probe access tubes and V-notches at the site...	96
Figure 6.3: Calibration curve for the topsoil at the site.....	98
Figure 6.4a: Topsoil moisture profile for point NP 4 at the site on 09/07/1997..	99
Figure 6.4b: Topsoil moisture profile for point NP 4 at the site on 22/12/1997..	99
Figure 6.5a: Topsoil moisture profile for point NP 5 at the site on 11/9/1997...	100
Figure 6.5b: Topsoil moisture profile for point NP 5 at the site on 22/12/1997..	100
Figure 6.6: The V-notch used at the site.....	104
Figure 6.7: Runoff versus $H^{2.5}$	104

Figure 6.8: The precipitation and runoff at the site.....	107
Figure 7.1: The permeameter used for measuring the hydraulic conductivity of waste.....	113
Figure 7.2: Compression of refuse at different applied vertical stress.....	122
Figure 7.3: The dry density of refuse at different applied vertical stresses.....	123
Figure 7.4: The porosity of refuse at different dry densities.....	124
Figure 7.5a: Hydraulic conductivity of refuse vs. applied vertical stress.....	125
Figure 7.5b: Expanded hydraulic conductivity vs. applied vertical stress.....	125
Figure 7.6: Hydraulic conductivity vs. dry density.....	127
Figure 7.7: Hydraulic conductivity vs. porosity.....	128
Figure 7.8: Porosity versus dry density of refuse tested in small cells and large-cell	133
Figure 7.9: Hydraulic conductivity versus dry density of refuse tested in small cells and large cell.....	133
Figure 7.10: Hydraulic conductivity versus porosity of refuse tested in small cells and large-scale cell.....	133
Figure 7.11: Fied capacity versus dry densisty (Beaven, 2000).....	134
Figure 8.1: Schematic profile view of a typical hazardous waste landfill.....	138
Figure 9.1: Flow chart for the simulation of moisture routing in refuse layers at White's pit.....	149
Figure 9.2: Standing leachate levels at White's pit in December 1998.....	153
Figure 9.3: Simulated height of waste lifts above basal clay liner.....	159
Figure 9.4: Simulated dry density of waste lifts.....	159
Figure 9.5: Simulated field capacity of the waste lifts.....	160
Figure 9.6: Simulated porosity of the waste lifts.....	160
Figure 9.7: Simulated hydraulic conductivity of waste layers.....	161
Figure 9.8: Simulated moisture content of waste lifts.....	161
Figure 9.9: Comparison of simulated and measured moisture content.....	162
Figure 9.10: Simulated moisture content of waste lifts with and without compression.....	163

List of Plates

Plate 5.1 a: Excavation of a uniform void.....	62
Plate 5.1 b: Loading of spoil into the skip.....	62
Plate 5.2 a: Loading of spoil into the drums.....	63
Plate 5.2 b: Drums including the measuring stick.....	63
Plate 5.3 a: Compaction of small refuse loads with a steel plate rammer.....	68
Plate 5.3 b: Draining water from the compacted refuse in the drum.....	68
Plate 6.1: The use of the Neutron probe.....	94
Plate 6.2: Surface runoff measurement at the site.....	105
Plate 7.1: Cell and other components.....	114
Plate 7.2: Assembled cell in operation.....	114

List of Tables

Table 2.1: Performance characteristic of landfill equipment.....	12
Table 2.2: Suitability of general soil types as cover material.....	12
Table 3.1: Consumptive Use of Water.....	31
Table 3.2: Evapotranspiration equations.....	34
Table 3.3: Typical Composition of Urban Collection and Civic Amenity Wastes as Delivered to Landfill.....	35
Table 3.4: Moisture content and water retention of domestic refuse, vol/vol.....	36
Table 3.5: Typical values of coefficient of runoff.....	39
Table 4.1: Geological Succession in Bournemouth – Poole – Wimborne area..	48
Table 4.2: Phases of Filling at the Dilute Disperse site of White's landfill.....	56
Table 5.1: The length of Pit A at regular depth intervals.....	70
Table 5.2: The length of Pit B at regular depth intervals.....	70
Table 5.3: Unit weights and overburden of refuse and composite cover soil at pits A and C.....	71
Table 5.4: Physical composition and moisture content of fresh and aged refuse obtained from the site.....	73
Table 5.5: Absorption, macroporosity and field capacity of fresh and aged refuse	76
Table 5.6: Typical unit weights of emplaced refuse fills.....	78
Table 5.7: The temporal spot heights at the site.....	82
Table 5.8: Compression index of waste.....	85
Table 6.1: Calibration of Neutron Probe – Soil moisture and count rate data.....	96
Table 6.2: 5-day precipitation and temperature before moisture measurement...	102
Table: 6.3: The precipitation and temperature during the continuous period of surface runoff measurement.....	108
Table 7.1: Composition of waste materials used in the permeability test.....	117
Table 7.2: Porosity, dry density, and hydraulic conductivity of refuse at different applied stresses.....	121
Table 9.1: Simulated temporal moisture content and properties of refuse lift 1...	155
Table 9.2: Simulated temporal moisture content and properties of refuse lift 2...	156
Table 9.3: Simulated temporal moisture content and properties of refuse lift 3...	157

ACKNOWLEDGEMENTS

Praise, Glory and Honour be unto our Lord and Saviour, JESUS CHRIST whose grace is more than sufficient in adversity. His love, compassion and magnanimity are untold and forevermore. “ Jesu o se pupo o.”

I am very grateful indeed to my supervisor, Dr David Richards for his invaluable advice. His commitment to the completion of the research is highly commendable and appreciated.

I am indebted to my sponsors, Commonwealth Scholarship Commission, London for giving me the opportunity to carry out the research. The effort of the Awards Administrator, Ms Anna Gane to the success of the research is appreciated. I am very much obliged to W H White plc for supporting the field tests. The previous financial assistance from EEC, Lagos is also acknowledged.

I wish to express my heartfelt gratitude to Ken Yeates, Derek Taylor, John Adams, Trevor Croumbs, Jonathan Fryett and Ewan Huc for their assistance during the laboratory and field tests. I thank Drs. Mike Cooper, Paul Tossell, Tony Lock, Habib Mahama; Profs. Trevor Tanton, William Powrie; Barbara Hudson and members of the Civil Engineering Department that contributed to the completion of the research. I am extremely grateful to friends at Portswood Church, Southampton, notably, Abi, Ade, Badmus, John Symons, Mike and Pearl Matthews.

I thank my entire family and friends including my parents, Mr & Mrs David Oladimeji Oni; Mrs Grace Akinwamide, Chief & Mrs Adewale Oni, Bros. Dayo, Akanni and Sesi, Niyi and Bola. Their prayers were vital to the success of this study. Words alone cannot express my gratitude to Mr & Mrs Akin Alagbe and Mama, who nurtured Demi during the period of the research.

May God bless you all (Amen).

CHAPTER

1

Introduction

1.1 The Problem

Approximately 70% of the waste (excluding agriculture, mining and quarrying wastes) produced in the UK is disposed to landfill sites, which are acknowledged to remain the ultimate disposal destinations for waste and residues in the foreseeable future (DoE, 1995B). The composition of waste landfilled in the UK has changed over the years (Hutchinson, 1995). As a result of 1956 Clean Air Act, the proportion of the more stable ash content has reduced while the volume of paper, rag, and plastic has increased considerably (Watts and Charles, 1999). It now takes decades rather than years for the refuse constituents in landfills to stabilise, thereby increasing aftercare costs and limiting afteruse. In addition, the location and operation of landfill sites is becoming increasingly difficult due to public awareness of the environmental impact of refuse landfill and the shortage of suitable locations that can be developed.

Consequently, landfill tax was introduced in October 1996 (Biffaward, 2000) to encourage waste reduction by increasing the cost of waste disposal. Twenty percent of the tax collected may be designated for environmental projects under the Landfill Tax Credit Scheme (Waste Management, 1998). Among the environmental projects being funded by the scheme is the research into properties of emplaced waste, landfill gas, and leachate produced in refuse landfills. It is believed that a better understanding of physical and biochemical processes in refuse landfills will enhance the objectives of environmental protection and early stabilisation for sustainable development.

The hydraulic and geotechnical properties of refuse are needed for the design of an efficient leachate control system, and also a leachate recirculation system, which is used to accelerate the stabilisation process in landfills (Leckie and Pacey, 1979; Pohland, 1980; Barlaz et al, 1989; Knox, 1998). Unfortunately, the majority of field investigations have been undertaken on properties of refuse fills during post-closure (Holmes 1984; Edil et al, 1990; Bengtsson et al, 1994; Ling et al, 1998). This may be due to the difficulty in obtaining reliable data from waste lifts during the active (filling) period of a landfill. Notwithstanding this, field tests may be undertaken on closed landfills to infer the impacts of the active period (overburden) on the properties of emplaced lifts.

Investigations into the properties of refuse during the active fill period have been carried out by modelling the essential behaviour of the emplaced refuse. Bleiker et al (1995) used a rheological model to simulate compression in refuse lifts during both the active and post closure periods of a landfill. They used data presented by Rao et al (1977) to calibrate their model and were able to simulate the observed settlement trend in waste lifts in municipal solid waste (MSW) landfills. Beaven and Powrie (1995) used a large-scale compression cell to simulate changes in the hydraulic and geotechnical properties of a waste lift placed at the base of a 60-metre landfill. They reported increased compression and variations in the density, stiffness, absorptive capacity, effective porosity and hydraulic conductivity of the waste lifts. These simulations, however, did not consider the influence of the daily cover on the waste properties.

The influence of the daily cover materials on the geotechnical and hydraulic properties of waste lifts in a landfill may have received less attention due in part to the volume of cover materials being relatively small compared to the waste volume involved. Moreover, fines are also inherent in the waste placed in landfills. However, daily cover materials are interbedded between waste lifts and they also vary in quantities and types from site to site.

Daniel (1993) reported that an impermeable cover material might cause hydraulic isolation of waste cells, thus encouraging differential settlement in landfills. Morris and Woods (1990) also suggested that the thickness of daily cover material might

reduce from 20% to 5% of the overall thickness of waste lift after the assimilation of the cover material into adjacent waste lift. Bleiker et al (1995), however, assumed the thickness of the daily cover soil to be unchanged in a study of landfill settlement and the impact on site capacity and refuse hydraulic conductivity. These assumptions are no longer adequate as the impact of daily cover material on the properties of waste lifts emplaced in landfills needs to be more fully understood and quantified. The effect of sequential filling on refuse properties and the possible interactions between waste and cover materials can more readily be determined through appropriate field and laboratory investigations.

The prediction of the volume of leachate generated in a landfill is paramount to the effective design, planning and management of a MSW landfill. The water balance method (WBM) is generally used to estimate the volume of water present in a refuse fill (Holmes, 1984; Blight et al, 1989; Bengtsson, 1994). This estimate provides an indication of leachate volumes in the landfill. Currently, computer models based on WBM are used routinely for moisture routing in MSW landfill. Of these, the Hydrologic Evaluation of Landfill Performance (HELP) model is commonly used (Farquhar, 1989, Blight et al., 1992).

As in field studies on MSW landfills, the majority of investigations on leachate generation (Dass et al., 1977; Gee, 1981; Blakey, 1982; Blight et al., 1992) have been carried out on completed landfills. However, refuse infilling is not instantaneous, but takes place over a significant period of time. The continuous sequential placement of waste loads results in a temporal changing structure of the emplaced waste fill. Any attempt to include the impact of waste filling in the modelling of moisture stored in waste lifts placed at MSW landfill sites will obviously enhance leachate predictions.

1.2 Objectives

A series of field and laboratory tests has been undertaken in the present study to quantify the effects of continuous placing of waste on the physical properties of emplaced refuse lifts in a MSW landfill. The refuse properties determined are those commonly used in the design of leachate control and recirculation systems. They include compressibility, dry density, porosity, and hydraulic conductivity. In

particular, the effect of daily cover material on these properties is studied.

To achieving this objective, field tests were carried out at White's pit landfill, Magna Road, Poole, Dorset. The tests include a pit test and static-electric cone penetration tests. Classification and geotechnical tests were conducted on the samples obtained from the pit tests. Laboratory tests were also undertaken on waste samples (including cover soil) obtained from the active filling face of the landfill to determine the impact of overburden on the geotechnical and hydraulic properties of waste lifts with and without daily cover material used at White's Pit.

The impact of refuse filling on the volume of moisture stored in emplaced waste lifts in the landfill was also determined. This process required a technique for simulating moisture in refuse lifts during the active period of landfill to be developed.

The HELP model was used to simulate the moisture stored in the restored landfill at White's pit from inception in 1985, through the active filling period that ended in 1991, to 1998, when field tests were undertaken at the site. The modelling was conducted sequentially to reflect the pattern of refuse filling in the landfill. Waste characteristic models were used in conjunction with the HELP model to determine the changing properties of waste lifts during the active fill period of the landfill. These empirical models, which are for estimating porosity, field capacity, and hydraulic conductivity of refuse lifts, were obtained by fitting characteristic curves to the experimental data. Conventional settlement models, whose parameters were determined from White's pit landfill, were used to estimate the compression of the waste lifts. Field measurements of runoff and the moisture stored in topsoil of the landfill were also considered in an effort to improve the accuracy of the moisture simulation through improved input data.

1.3 Outline and Scope

The structure of this thesis is as follows: -

- Chapter 2 reviews landfill practice in the UK. It describes the landfill process and various types of landfill sites. The impact of imposed loads on emplaced waste lifts, compression mechanisms, and the methods commonly used to estimate

settlement in landfills are reviewed.

- Chapter 3 reviews leachate generation in landfills. It includes the principles of and factors affecting leachate generation in landfills. Important geotechnical issues relevant to the research are reported.
- The study site is described in Chapter 4, including the geology and waste disposal at the site.
- Chapter 5 discusses the field tests carried out in the study area. It includes classification and geotechnical tests of the spoil from the pit test. The implications of overburden on waste properties are discussed.
- The field measurement of factors influencing leachate production is reported in Chapter 6. The tests include the runoff and moisture stored in the topsoil of the landfill.
- The laboratory tests conducted on refuse and cover material collected from the site are reported in Chapter 7. The tests include porosity, compression, and field capacity. Three different methods of waste placement are considered in the tests. The effect of a daily cover soil on the hydraulic and geotechnical properties of refuse lifts is discussed.
- The overview of the HELP model is in Chapter 8. The simulation of moisture stored in refuse lifts in the landfill using the HELP model in conjunction with waste characteristic models is described in Chapter 9. The validity and implications of the simulation is also discussed.
- The general discussion of the research and recommendations are given in Chapter 10 while Chapter 11 contains the conclusion of the research.

CHAPTER

2

Review of Landfill Practice

2.1 Summary

This chapter reviews the landfill process and the potential impact that current placement and operational practices may have on the physical properties of refuse lifts. The mechanisms of refuse compression and the empirical models commonly used to simulate settlement of refuse fills are discussed.

2.2 Landfill

Landfill is generally acknowledged to be the most economic method of solid waste disposal (ASCE, 1959; Rovers and Farquhar, 1973; Thompson and Zandi, 1975; Tchobanoglou et al, 1993 Ling et al., 1998). Formal sanitary landfill practice started in the USA and England in 1930 and 1916 respectively; informal practice probably goes back to man's beginning (Yen and Scalon, 1975). Over the years, strategies have been developed to minimise the volume of refuse disposed to landfills. They include, in order of priority (Qasim and Chiang, 1994; NRA, 1995):

- waste minimisation (reducing waste production)
- recycling (reuse of various waste streams, composting)
- waste conversion to energy and waste pre-treatment (incineration)

However, the residue from these waste reduction strategies will ultimately need to be landfilled.

In the following sections, refuse landfilling and its impact on the physical properties of emplaced refuse lifts is reviewed.

2.2.1 Types of Refuse Landfill Sites

Landfill sites are the physical facilities used for the disposal of residual solid wastes in the surface of the earth. They are commonly classified according to the kinds of waste accepted for disposal. Recent planning conditions and restrictions with increasing understanding of the processes that occur within the waste mass have also affected the classification of landfill sites. The typical sites in the UK are described as follows (DoE, 1992; Hutchinson, 1995):

- **Inert sites**

Inert sites are licensed to receive wastes that will present no potential harm to the environment, as they will not degrade under normal environmental conditions. They accept uncontaminated wastes like rubble and soil. It is unlikely that significant quantities of leachate or gas will be produced, and as such, limited engineered barriers are required for their safe containment.

- **Organic (biodegradable) sites**

Organic refuse sites are licensed to receive household, commercial and biodegradable industrial wastes. They are the most common types of landfill sites in the UK because of the range of refuse materials they receive. They contain predominantly biodegradable wastes, which will readily degrade under the action of bacteria normally present in the landfill environment. Organic landfill may be operated as a dry vault, to prevent moisture from entering it, or as a bioreactor in which organic-rich leachate and significant amount of gas may be produced under certain conditions that may develop in the site. Some organic landfill sites are used for co-disposal of biodegradable waste and controlled quantities of special or difficult wastes. In this case, they make use of the physical and biochemical changes occurring in biodegradable wastes to detoxify components of the difficult waste. Organic landfills are required to be operated under strict safety standards and contained in well-

engineered cells, fitted with a leachate control regime and a gas collection systems to prevent pollution of the environment. Most research has been undertaken on organic landfills because they receive most of the waste produced in the community, and more importantly, due to the non-stability of its emplaced waste. Much of this research has sought to enhance the stability of waste, provide optimal economic gains from gas production, and to increase landfill capacity through waste volume reduction.

- **Hazardous refuse sites**

Hazardous waste sites are licensed to receive refuse designated as difficult and special industrial wastes. Special wastes are controlled wastes, which contain or are contaminated with, materials dangerous to human health. They include poisons, corrosives and flammable materials as well as prescription-only medicines. Difficult wastes include those wastes not defined as special but harmful either in the short or long term to humans as a result of their chemical and toxicological properties. Hazardous refuse sites are required to be well engineered and to act as vaults for emplaced waste. The containment systems are engineered with the objective of providing long term integrity. There are usually no provisions for gas emission because the wastes are not degradable, and if there is any gas produced, it will be toxic and thus harmful to human health and the environment. There are relatively few Hazardous waste sites and are mostly operated by highly specialised organisations to avoid any environmental pollution, which is likely to be extremely damaging if allowed to occur.

2.2.2 The Landfill Process

The landfill process has changed over the years due to an increased understanding of the behaviour of emplaced waste and strict regulations, which now control the disposal of waste onto land. The process has transformed from uncontrolled backfilling of mineral excavations or raising the level of natural depressions in landscape and low adjoining river estuaries to controlled filling of refuse in highly engineered facilities. Some of the methods of refuse landfill include: (a) excavated cell/trench, (b) area, and (3) canyon. The process of landfill for all the methods of landfill is similar. The excavated/trench method is discussed in details below.

The processes involved in the excavated/trench method of landfill are well described by Tchobanoglou et al (1993). The first step involves the preparation of the site for landfill construction. The existing site drainage is modified to route any runoff away from the intended area of landfill construction. Side drainage is provided along the perimeter of the intended landfill to intercept run-off from adjacent areas. Access roads are then constructed together with the weighing facilities while the fences are installed.

The next development is the excavation and preparation of the landfill bottom and surface areas. Modern landfills are now constructed in sections to limit the portion of the waste surface that is exposed to precipitation at any time. Excavation can be carried out gradually and sequentially rather than preparing the entire landfill base at once. By doing this, the problem of water accumulating in excavations is reduced considerably. The spoil is stockpiled on adjacent unexcavated soil. In many cases, the excavated soil, if suitable, is used as cover material during waste placement to reduce operating costs.

The initial working area of the landfill is excavated to its design depth and the base of the landfill is profiled to provide effective drainage of leachate produced in the waste mass. The groundwater level monitoring equipment is installed, prior to lining of the landfill. A low permeability material is used to line the base and the walls of the excavation to prevent any escape of leachate from the landfill. The basal lining is not required if the native soil is a low-permeability material. Leachate collection and extraction facilities are placed within or on top of the liner to control leachate levels and more importantly, to enhance the drainage of the leachate produced within the waste mass to a collection system. The excavation of the landfill and installation of landfill liner are shown in Figure 2.1. Horizontal gas recovery trenches are installed if emissions from the newly placed refuse are expected to be a problem or energy recovery is likely to be practised. A soil berm is sometimes constructed at the downwind side of the planned fill area to serve as windbreak and to act as a face against which the refuse can be compacted above grade. The walls of the excavation serve as the compaction face for the filling below the ground level.

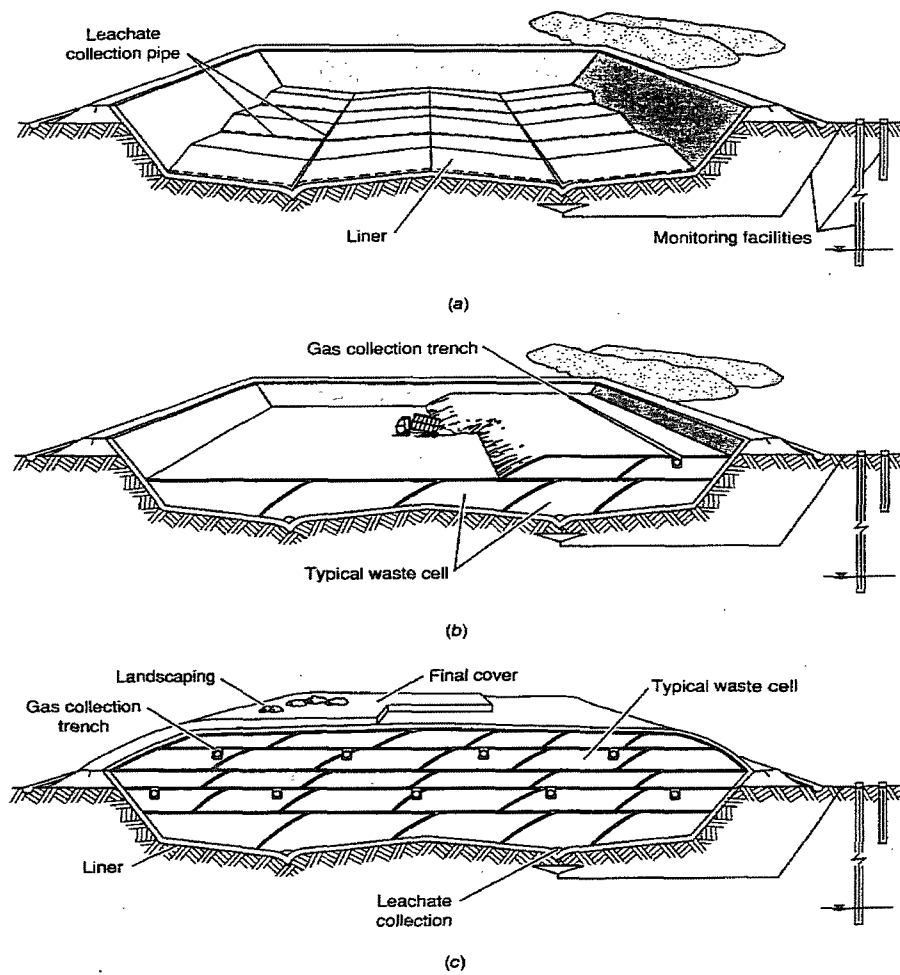


Figure 2.1: Development and completion of a solid waste landfill: (a) excavation and installation of the landfill liner, (b) placement of solid waste (c) cutaway through completed landfill. (Tchobanoglous, 1993)

The next step in the landfill process is the placement of the refuse (Figure 2.1b). The refuse deposited by the collection and transfer vehicles is spread out in layers of approximately 0.45 m to 0.6 m and then compacted uniformly by roller plant to achieve uniform volume reduction and stability of the waste fill. The performance characteristic of equipment used for landfill operations is presented in Table 2.1. The type, size, and amount of equipment required will depend on the size of the landfill and the method of operation. The refuse is placed in cells starting from the compaction face, continuing outward from the face (Figure 2.1b). A cell is described as the volume of material placed in a landfill during one operating period.

The length of the working face of the landfill varies with site conditions and the size of operation. The working face is the area where refuse is being placed and compacted during a given operating period. The width of a cell varies from approximately 3 m to 9 m, depending on design capacity. The typical height of completed cells varies from 2 m to 4 m. The exposed faces of each cell are covered with a thin cover material at the end of each operating period to minimise odour emissions and prevent infestation by flies and rodents. This material, which is known as daily cover is also used to limit surface infiltration, prevent rodent and fly infestation, and to enhance the aesthetic appearance of the landfill. The suitability of the general soil type used as cover material is presented in Table 2.2. The compost obtained from shredded refuse is often used as a daily cover material. The use of compost as a daily cover is expected to increase, as the optimal utilisation of the landfill capacity becomes a front issue.

Landfills are made up of lifts. A refuse lift is a complete layer of cells over the active area of the landfill. Once one or more lifts have been placed, horizontal gas recovery trenches are excavated in the complete surface (Figure 2.1c). These are typically filled with gravel, and perforated pipes are installed in the trenches to manage and control gas that is produced within the waste mass. Successive refuse lifts are placed upon

Table 2.1: Performance characteristic of landfill equipment (Tchobanoglou et al., 1993).

Equipment	Solid waste		Cover material			
	Spreading	Compacting	Excavating	Spreading	Compacting	Hauling
Crawler tractor	E	G	E	E	G	NA
Wheeled compactor	E	E	P	F-G	E	NA
Scraper	NA	NA	G	E	NA	E

E = excellent; G = good; F = fair; P = poor; NA = not applicable

Table 2.2: Suitability of general soil types as cover material (Qasim, 1994)

Function	Clean Gravel	Clayey Silty Gravel	Clean Sand	Clayey Silty Sand	Silt	Clay
Prevents rodents from borrowing and tunnelling	G	F-G	G	P	P	P
Keep flies from emerging	P	F	P	G	G	E
Minimise moisture entering fill	P	F-G	P	G-E	G-E	E
Minimise landfill gas venting through cover	P	E	P	E	G-E	E
Provide pleasing appearance and control blowing paper	E	G	E	E	E	E
Grow vegetation	P	P	P-F	E	G-E	F-G
Be permeable for venting decomposition gas	E	P	G	P	P	P

E = excellent; G = good; F = fair; P = poor; NA = not applicable

each other until the final design grade is reached. Additional leachate collection facilities may be placed within successive lifts, depending on the depth of landfill. Finally, a cover material is applied to the completed area of the landfill to minimise infiltration of precipitation and to route drainage away from the active portion of the landfill. The cover is also landscaped to control erosion. The final cover is likely to be a composite material consisting of vegetation top layer and a low permeability mineral layer sometimes in contact with dense membrane layer. Vertical gas extraction wells are installed through the completed landfill surface. The gas extraction system is connected together and the extracted gas may be flared or routed to an energy recovery facility as appropriate. Gas collection systems may be either passive or active. A passive system utilises the principle of natural pressures and conventional mechanisms to move the landfill gas away from the site. Active systems extract the landfill gas under an induced negative pressure or vacuum.

The exploitation of the gases produced in landfills for energy is increasing due to the economic benefits that may be derived from energy utilisation and also the reduction in environmental damage caused by flaring of gas. Once a section in the landfill is completed, the next section will be constructed outward, repeating the construction process outlined above. Wind blown paper, plastics, and other debris can be a problem at some landfills. This is solved by installing screens near the face of operating face of the landfill. The material accumulated on the screens are removed daily to avoid problems with flies. Water is regularly sprayed on the roads within the site to control dust and thereby minimise any nuisance to local residents.

2.2.3 Post Closure

During the post-closure period, considerable effort is expended in maintaining the integrity and effectiveness of the final cover system. The landfill construction activities during the post-closure period include refilling and repairing landfill areas of settlement to maintain the desired final grade and drainage. The gas and leachate collection systems are maintained, and extended if necessary. The most frequent activity undertaken during post-closure period is the monitoring of groundwater to detect possible pollution caused by leachate produced within the refuse fill. This is accomplished by analysing samples obtained from monitoring wells located adjacent

to the landfill. At least one observation from the monitoring wells is usually done per week in most landfills. The post-closure care usually allows for the planned uses of the site following a stabilisation period.

The monitoring and maintenance of landfills may continue for 30 to 50 years after closure (Tchobanoglous et al., 1993; Qasim, 1994; DoE, 1995B). However, recent developments such as operating and controlling the landfill as a bio-reactor have been postulated and being undertaken to minimise the active waste period following closure (Pohland, 1980; Barlaz et al, 1989; Richards et al., 1997; Knox, 1998).

2.3 The Impact of Overburden on Refuse Fills

2.3.1 Introduction

The process of landfilling involves continuous placement of new refuse lifts over and above previously emplaced lifts during the active period. This involves the application of vertical loads on emplaced refuse lifts during the fill period of the landfill. The application of these loads is not instantaneous and depends on the fill rate of refuse in a landfill. In landfill simulations, imposed loads on refuse fills are usually applied sequentially to enhance the accuracy of simulation results (Bleiker et al., 1995). The imposition of refuse loads is the main physical activity on emplaced lifts and is likely to be the principal cause of physical changes in properties of underlying refuse lifts during the active period of a landfill.

Beaven and Powrie (1995) simulated the effect of further waste placement on the properties of an underlying refuse layer in a landfill. They used a purpose-built large-scale compression cell to simulate sequential loads applied to a basal refuse-lift in a 60-metre depth landfill. The compression cell consists of a steel cylinder, 2 metre diameter and 3 metre high. The upper platen in the cell compresses the waste, and is connected to and moved by two 200 mm diameter hydraulic pistons. While vertical loads were being applied to the domestic refuse (crude and pulverised), some hydrogeological parameters were determined. The geotechnical properties of the refuse were also determined by determining key parameters and applying conventional soil mechanics relationships. They observed changes in density,

porosity, stiffness, and hydraulic conductivity of the refuse layer with an increase in vertical stress. As expected, there was a general increase in the density of the refuse layer with an increase in applied stress. The effective porosity of the domestic refuse decreased from an initial value of 30% to less than 2 % at an applied stress of 600 kPa. The stiffness of the crude refuse tested increased from 250 kPa to 1985 kPa at an applied stress of 600 kPa. The hydraulic conductivity fell from 10^{-4} m/s at placement to 10^{-7} m/s at a burial depth of 60 m. The results were valid for non-degraded unsaturated refuse.

Bleiker et al. (1995) developed a settlement model to predict the settlement of a refuse layer in response to the applied load of overlying refuse in deep landfills. They applied the rheological model to determine the compression of refuse lifts in landfills using the parameters determined from Rao et al. (1977) data for the model. It was reported the density and compression of refuse layers increased as the vertical applied stresses increased. Based on previously established relationships (Parker et al., 1987) between strain and hydraulic conductivity, it was concluded that refuse hydraulic conductivity of refuse decreases significantly with the compression.

2.3.2 Mechanisms of Compression of Refuse Fills

Without any doubt, the compression of emplaced refuse lifts is caused mainly by an increase in overburden during the active period of a landfill. The change in hydraulic and geotechnical properties of refuse lifts due to overburden is influenced greatly by the degree of compression of the particulate waste. The mechanisms of settlement in a refuse fill are complex due to the variable nature of refuse constituents the degree of saturation in landfills. Unlike soil, the particles of refuse may be compressible, and its rate of degradation depends on a number of factors including temperature and moisture content (Farquhar, 1989; Ling et al. 1998).

Sowers (1973) originally described the mechanisms of settlement of refuse as:

- Mechanical compression: Distortion, bending, crushing and reorientation of the materials similar to the consolidation of organic soils

- Ravelling: The erosion and or sifting of fine materials into voids between larger particles.
- Physico-chemical change: Corrosion, oxidation and combustion
- Bio-chemical decay: Fermentation and decay, both aerobic and anaerobic
- Interaction: Organic acid from decaying organic matter may cause corrosion and volume changes from consolidation may trigger ravelling.

Mechanical compression is caused by vertical stresses due to the applied vertical load (overburden) as well as self-weight of the waste. It comprises initial and primary compression. The initial compression is caused by immediate distortion of refuse particles and void space upon applied vertical loading. This is analogous to the elastic compression in partially saturated fine-grained soils and coarse graded soils. Sowers (1973) stated that mechanical settlements in refuse occur rapidly with little or no pore pressure build-up, and it is usually completed within one month of the applied surcharge. Such settlements account for most of the settlement during the active period of the landfills. Edil et al. (1990) stated that typical primary settlement values range from 5-30%.

Physico-chemical mechanisms are caused by in-situ conditions such as the available moisture content, dissolved oxygen, and waste composition. They affect refuse settlement through the weakening and collapse of the waste skeleton. Bio-chemical decay or biodegradation of refuse is caused by aerobic, anaerobic and facultative microorganisms in the waste. The rate of biodegradation depends on a number of ambient conditions in waste, such as the dissolved oxygen (for aerobic); moisture conditions, temperature, and pH (for anaerobic). Rovers and Farquhar (1989), El-Fadel et al. (1997), and Knox (1998) have reported conditions for optimal anaerobic digestion of waste. Secondary settlement in waste fills is caused by a combination of creep and biodegradation of waste particles (Sowers, 1973).

Richards et al. (1997) stated that an additional mechanism of refuse settlement (that might be classified as either primary or secondary) is the settlement that occurs on wetting of the waste, leading to the loss of strength or structure of certain components

on contact with moisture. This type of settlement though possibly minor, should not be ignored.

2.4 Determination of Settlement in Refuse fills

2.4.1 Introduction

The mechanisms involved in refuse settlement are interdependent and thus extremely difficult for any model to accommodate. Some of the factors influencing the magnitude of settlement include: (1) initial refuse density or void ratio; (2) the amount of degradable materials in the refuse; (3) fill height; (4) stress history; (5) leachate level; and (6) environmental factors (such as moisture content, temperature and gases present or generated within the landfill).

Many authors (Wall and Zeiss, 1995; Bleiker et al, 1995; Charles and Burland, 1982; Yen and Scalon, 1975; Sowers, 1973) have adapted soil settlement models to refuse landfills. The validations of the models have been undertaken with pilot cells and landfills, and real landfills. In fact, Sowers (1973) and Charles and Burland (1982) reported small-scale laboratory tests were of limited use when studying the settlement of MSW landfills because of the diverse particle sizes found in refuse. Edil et al. (1990) stated that settlement-time curves of refuse are similar to those of organic soils and peats. However, recent developments in this area question the validity of fitting settlement data to such creep models as there is lack of consideration of degradation occurring within the waste. Biodegradation of refuse is very difficult to model, therefore various stages of secondary settlement are now being modelled separately with appropriate models to enhance simulation results (Watts and Charles, 1999).

2.4.2 Conventional methods

The initial settlement can be modelled with reasonable success using the following equation (Wall and Zeiss, 1995).

$$S_i = \frac{\Delta q H_0}{E_s} \quad [2.1]$$

where:

S_I = initial settlement of the refuse fill

Δq = change in applied stress

E_s = modulus of elasticity of the refuse fill

H_o = initial thickness of refuse fill

This equation is for immediate settlement, which is instantaneous in a loose fill.

Charles and Burland (1982) reported that the initial compression in refuse is due to self-weight effects and will occur during load application in poorly compacted fills.

ASCE (1959) reported that the initial settlement due to compaction by landfill plants (equipment) and self-weight of lift can be up to 24% while a further 25% settlement can occur after 5 years of refuse emplacement due to combined effects of creep and biodegradation. Immediate settlement of refuse will vary within a site as it depends on the applied stress and modulus of elasticity of the refuse fill.

The primary compression or settlement may be modelled using the common compression equation for partially saturated soils. Primary settlement have been modelled with reasonable success using the following equation (Sower, 1973; Morris and Wood, 1990; Wall and Zeiss, 1995):

$$S_p = H_i C_{ce} \log \left(\frac{P_0 + \Delta P}{P_0} \right) \quad [2.2]$$

where:

$$C_{ce} = \frac{C_c}{1 + e_0}$$

S_p = primary settlement occurring in the refuse fill being considered

H_i = initial thickness of the refuse fill being considered

C_{ce} = primary compression ratio

C_c = primary compression index of refuse fill.

e_0 = initial void ratio of the refuse fill

P_0 = existing overburden pressure acting at the mid-level of the refuse fill

ΔP = increment in overburden pressure on the refuse fill

Creep compression shows a linear relationship when plotted against the logarithm of time (Charles and Burland, 1982). Some researchers (Sowers, 1973; Buisman, 1973; Chen and Scalon, 1982; Wall and Zeiss, 1995) reported that the secondary settlement in refuse landfills can be reasonably modelled using the following equation:

$$S_s = H_i C_{se} \log\left(\frac{t}{t_p}\right) \quad [2.3]$$

where:

$$C_{se} = \frac{C_s}{1 + e_0}$$

S_s = secondary settlement from time period t_p to t .

H_i = initial thickness of refuse fill

C_{se} = secondary compression ratio, which is the slope of strain versus log-time curve of the refuse fill.

C_s = secondary compression index usually determined in oedometer tests

e_0 = initial void ratio of the refuse fill

The traditional models (equations 2.1 – 2.3) are based on empirical data. Any use of these equations will require the determination of the compression index from the field data of the landfill.

Watts and Charles (1999) reported that compression could be modelled according to the moisture condition of the refuse fill as follows:

1. Immediate compression of partially saturated fill.

There is immediate compression in a partially saturated refuse fill upon load application. The amount of immediate compression is expressed in equation 2.1.

2. Creep compression of partially saturated fill.

Creep compression occurs in partially saturated refuse fill under constant applied load and constant moisture content. The compression is caused by physical creep processes in the particulate refuse. The linear relationship between creep compression and the logarithm of time since fill placement can be expressed by the parameter α_c

$$\alpha_c = 2.303t \frac{\partial \varepsilon_v}{\partial t} \quad [2.4]$$

where

$(\delta \varepsilon_v / \delta t)$ = the rate of vertical compression due to physical processes at time t after fill placement.

α_c = secondary compression index, which is similar to C_s (equation 2.3).

3. Primary consolidation of saturated fill

When load is applied to saturated fill, there is a generation of positive pore water pressures, which dissipates resulting in settlement of the fill. The compression is related to the increase in effective stress $\delta \sigma'_v$ by a constrained modulus D' given as:

$$D' = \frac{\partial \sigma'_v}{\partial \varepsilon'_v} \quad [2.5]$$

where:

$\delta \varepsilon_v$ = The increase in vertical strain

4. Secondary consolidation of saturated fill

Secondary consolidation takes place once the pore pressure has dissipated in a saturated fill. The long-term movement of refuse particles, which will continue due to physical creep effects, can be modelled as α_c .

5. Bioconsolidation

Biodegradation is likely to be the major cause of long-term settlement in refuse fills with high organic and moisture contents. As mentioned earlier, no settlement model

has been developed that incorporates the rate of degradation of refuse particles. However, the settlement due to bioconsolidation is described by a parameter α_b similar to α_c but is somewhat larger since it is likely to be affected not only by effective stress but the biochemical environment within the refuse fill. The parameter α_b is determined similar to α_c from a compression-log time graph, but at a much later period in the life of a landfill when biodegradation is assumed to be the main cause of settlement.

Ironically, the settlement processes described by Watts and Charles (1999) are based on traditional models (equations 2.1-2.3), which do not consider the moisture content of the refuse fill. Furthermore, accurate partition of the different creep stages in the compression-log time graphs will be very difficult to achieve. Consequently, these methods may not be accurate in determining the compression of a refuse fill.

Other models proposed for estimation of landfill settlement include the power creep model, and the rheological model (Edil et al., 1990). These models are based primarily on the post-closure settlement of the refuse fill, and therefore are not discussed in this study.

Generally, the compression models do not consider recycling of leachate, which is often used to accelerate degradation of refuse and enhance gas production. The models are based on uniformity in settlement of the particulate refuse in landfills. However, differential settlement often occurs in landfills because of the variation in the composition, moisture conditions, properties, and rate of degradation of refuse within the refuse fill. This often leads to undesirable effects such as channelling of moisture in the refuse fill, and tilting and distortion of structures erected on the landfill. The modelling of differential settlement caused in this manner is complex and outside the scope of this study.

2.5 Effective Stress

The effective stress exerted on the fabrics of the refuse is very important in analysing the behaviour of refuse due to changes in loading and subsurface water pressure.

Terzaghi (1936) first discovered the principle of effective stress and expressed effective stress as follows:

$$\sigma' = \sigma - u \quad [2.6]$$

where:

σ' = the effective stress

σ = total or bulk stress

u = pore pressure

However, Skempton (1960) in his work on effective stress in soils, concrete and rocks proposed a more comprehensive expression for effective stress in fully saturated materials as follows:

(a) for shear strength

$$\sigma' = \sigma - \left(1 - \frac{a \cdot \tan \psi}{\tan \phi'} \right) u_w \quad [2.7]$$

(b) for volume change

$$\sigma' = \sigma - \left(1 - \frac{C_s}{C} \right) u_w \quad [2.8]$$

where

σ' = effective stress

σ = total or bulk stress

a = specific area of contact between particles

ψ = angle of intrinsic friction

ϕ' = angle of shearing resistance of porous material

u_w = water pressure

C_s = compressibility of the solid substance comprising the particles (fabrics)

C = compressibility of the porous material

Skempton (1960) reported that for soils, $\tan\psi / \tan\phi'$ is usually between 0.15 to 0.3 but a is very small at pressures normally encountered in engineering and geological problems. In addition, C_s/C is extremely small under low pressures, therefore equations 2.7 and 2.8 reduces to Terzaghi's standard equation. However, Beaven (2000) reported that the specific area for refuse at high refuse densities is not small because many of the macro voids in the refuse would have collapsed due to the relatively high compressibility of some components of refuse e.g. paper and plastic. In the absence of further work on effective stress on refuse, he proposed the continued use of the Terzaghi theory, which has been extended from soils to refuse.

2.6 Research Considerations

The practice of landfill involves additional placement of refuse lifts upon emplaced refuse fills during the active life of the landfill. Since a refuse lift is made up of a refuse layer together with a daily cover material, the increase in vertical stress on emplaced refuse fill will not only affect the refuse layer but also the daily cover material of each refuse lift. The composition or nature of the daily cover may affect the properties of the underlying refuse layer under vertical loading through assimilation of the cover material within the waste. The impact of daily cover on the properties of the refuse layer subjected to a sequence of vertical loading (filling) has not been adequately investigated. Also, sufficient field tests to corroborate either the laboratory or mathematical simulation of the effect of increased vertical loading on refuse lifts are still lacking. A good understanding of these aspects of landfill is likely to enhance optimal landfill processes and maintenance to achieve the objective of environmental protection and beneficial afteruse, currently the goal for sustainable development.

2.6.1 Aims and Approach

The aim of this study is to investigate the consequence of sequential filling on emplaced refuse fill by carrying out field and laboratory tests. In order to obtain

sufficient information from emplaced refuse lifts at a landfill site, the following approach was used:

- Excavation of trial pits at locations that have different thickness top cover soil system in order to determine the variation in density of waste layers subjected to different overburden.
- Classification of the refuse excavated from the different experimental pits to determine the difference in refuse constituents, most importantly, the fines content.
- Determining the particle size distribution of fines content in the excavated refuse and daily cover material from sieve analysis. Any interaction between the daily cover and the underlying refuse layer is likely to be observed by comparing their particle size distribution curves.
- Undertaking cone penetration tests (CPT) at different locations in the landfill since the test pits are restricted to the upper zone of the landfill.
- Investigating the impact of overburden stress on the hydraulic and geotechnical properties of a waste layer with, and without a cover soil in the laboratory.

CHAPTER

3

Review of Leachate Production in Landfills

3.1 Summary

The physical processes involved in the formation of leachate are described in this chapter. The application of the water balance method of estimating leachate volumes in MSW landfill is reviewed. The various reported moisture simulations of refuse fills are also considered.

3.2 Introduction

Public concern for the environment is now considerably greater than it was in the mid-1980s (The Engineering Council, 1994). Among the main concerns for the location of landfills are the emission of leachate and gas to the environment (Farquhar, 1973; Thompson and Zandi, 1976). Prior to 1965, most people were unaware that water having passed through a waste deposit may be highly contaminated. This was due to few cases of pollution caused by leachate from landfills (Qasim and Chiang, 1994). However, cases of groundwater pollution near landfills have shown that the drainage water from waste fills become contaminated. (Kelly, 1976; Johnson et al., 1981; Lyngkilde and Christensen, 1992; Kjedsen, 1993) and may present considerable risk to the environment.

Precipitation, evapotranspiration, surface runoff, moisture storage and microbial degradation influence the leachate generated in a refuse fill. These factors are interdependent and may vary from site to site. The moisture storage of refuse

significantly influences the gas production in a landfill. Problems associated with uneven water storage between cells which may cause both clogging and differential settlement in landfills are particular problems requiring attention at a number of closed landfill sites (Charles and Burland, 1982).

The mechanisms of leachate production and the estimation of water storage in landfills are reviewed in the following sections.

3.3 Formation of Leachate

In simple terms, leachate is generated in landfills when water percolates through a partially saturated refuse and extracts contaminant into the liquid phase through physical, chemical and microbial processes. The volume of leachate produced is directly related to the input of water to the landfill. The water movement in a landfill is depicted in Figure 3.1.

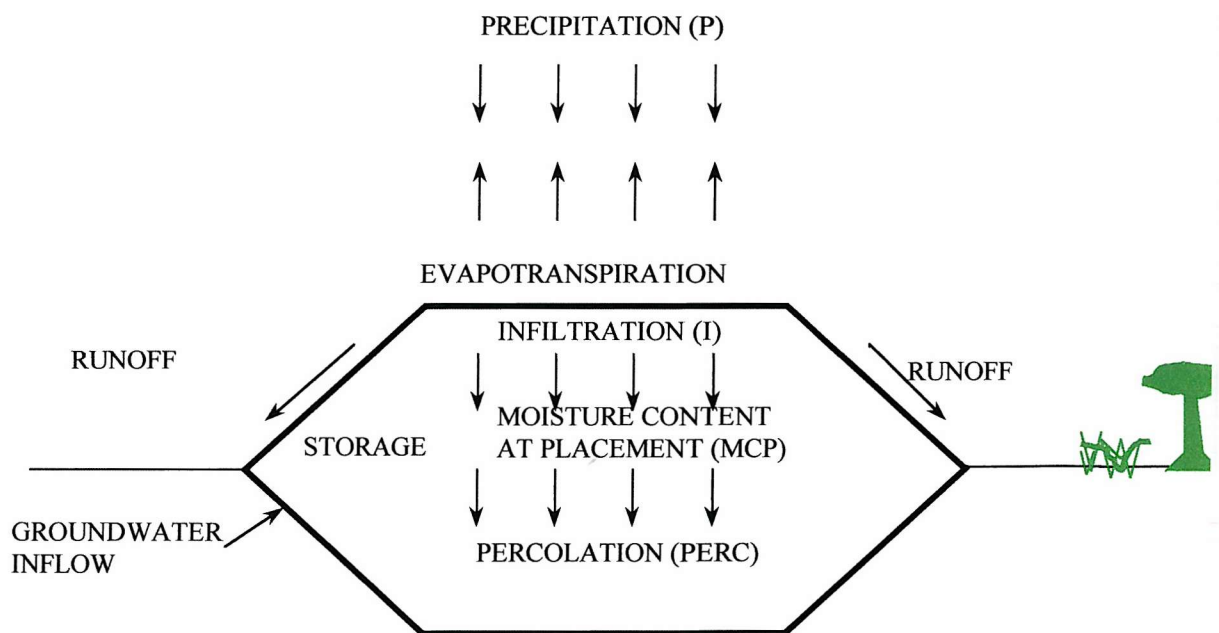


Figure 3.1: Water movement at a landfill. (Farquhar, 1989)

Farquhar (1989) described the major processes involved in the formation of leachate as follows:

- a) Precipitation falls on to the landfill and some of it is lost as runoff
- b) Precipitation infiltrates the surface (uncovered refuse, daily cover, or final cover).
- c) Some of the infiltration evaporates from the surface and (or) transpires through the vegetative cover (if it exists).
- d) Some of the infiltration may make up a deficiency in soil moisture storage (the difference between field capacity and the existing moisture content).
- e) The remaining infiltration, after evaporation, transpiration, and soil moisture storage have been satisfied, percolates downward, eventually forming leachate as it reaches the base of the landfill.
- f) The percolate may be augmented by infiltration of groundwater.

The quantity and the rate of leachate formation depend on a number of factors. Some of the factors include temperature, relative humidity, wind speed, initial moisture content of the refuse, and hydraulic and geotechnical properties of the emplaced refuse. The amount of leachate produced through the above mentioned leachate-forming processes is typically obtained from a water balance analysis of the landfill.

3.4 Determination of the Quantity of Leachate Generated in Landfills

The volume of leachate generated during the life of a landfill is an essential parameter in the design, operation, and post-closure maintenance of a landfill. Basically, the water routing through a landfill consists of moisture moving through the cover and waste layers. The quantitative estimation of leachate produced in the landfills is based on the principle of the water balance method (Dass et al., 1977; Holmes, 1980; Campbell, 1983; Blight et al., 1989; Bengtsson et al., 1994).

3.4.1 The Water Balance Method

The water balance method has various forms and is widely used in soil science and surface hydrology. It is based on the principle of mass conservation and continuity of fluid flow. Thus:

$$\text{Water Input} = \text{Water Output} + \text{Water retained} \quad [3.1]$$

The generalised water balance of a landfill can be represented as follows (Lu et al., 1985):

$$W_P + W_{SR} + W_{IR} = I + R \quad [3.2]$$

where:

W_P = input water from precipitation

W_{SR} = input water from surrounding surface runoff

W_{IR} = input water from irrigation

I = infiltration

R = surface runoff

$$PER_S = I - E - \Delta S_S \quad [3.3]$$

$$PER_R = I - E - \Delta S_S + W_D - \Delta S_R \quad [3.4]$$

$$= PER_S + W_D - \Delta S_R \quad [3.5]$$

where:

PER_S and PER_R = percolation in soil and refuse respectively

W_D = water contributed by soil waste decomposition

ΔS_S = change in moisture storage in soil

ΔS_R = change in moisture storage in refuse

E = evapotranspiration

Finally,

$$L = PER_R + W_{GW} \quad [3.6]$$

where:

L = quantity of leachate generated

W_{GW} = input water from underflow

The water balance of the landfill surface is represented by equation [3.2]. The water contributed by precipitation, surface runoff from the surrounding area or irrigation will either become surface runoff or infiltrate into the cover soil of the landfill. A portion of the infiltrated water leaves by evapotranspiration and the rest recharges the cover soil. Once the water in storage exceeds the amount of water that can be held under gravity (field capacity) in the cover soil, vertical percolation (PER_S) of the water will occur. The percolate from the soil will be absorbed in the underlying refuse until field capacity is reached. Then, the percolate in the refuse (PER_R) eventually becomes the refuse leachate and may be recharged with groundwater, if it exists at the landfill site.

There are different conditions in various landfills, so, some of the terms represented above in equations 3.2 - 3.6 may not be applicable in some situations. In cases where the landfill site is not susceptible to groundwater intrusion and the inflow of water from adjacent areas is insignificant, W_{GW} and W_{SR} may be neglected. Input from irrigation (W_{IR}) will be significant where leachate recirculation is practised. If the water balance method is applied to a refuse fill without any cover material, the initial moisture content of incoming waste load should be considered as a water input, although it makes a once-off contribution to the water balance process.

3.5 Factors Influencing the Quantity of Leachate Generated in Landfills

As can be seen in equations 3.1 – 3.6, the parameters that influence the quantity of leachate produced in a landfill are precipitation, evapotranspiration, runoff, moisture storage, and microbial degradation. The contribution due to microbial degradation was often ignored by most authors (Dass et al., 1977; Gee 1981; Blight et al., 1989). Currently, optimal gas utilisation and accelerated stabilisation are often the objectives

in refuse landfilling (Knox, 1998), and as such, biodegradation is accelerated through techniques that include leachate recirculation. This activity also enhances the settlement of the cover system leading to increased infiltration. In view of this, the contribution of biodegradation to the leachate volume in refuse fills should not be ignored in present landfill practice.

3.5.1 Precipitation

Precipitation is the main water input in the determination of leachate volumes in landfills, and therefore the primary source of moisture in leachate production. The amount of precipitation is expressed as the quantity of water (in millimetres) that will accumulate on a sealed surface and comprises all the water that falls from the atmosphere to the landfill area. Precipitation occurs in the form of rainfall, snow, hail, or sleet. Upon striking the ground, it will either accumulate in low-lying areas, runoff the landfill, evaporate or infiltrate the capping layer and then percolates through the refuse layer.

Campbell (1983) stated that rainfall is likely to vary between 500-1200 mm per annum in the landfill locations in the UK. Blight (1992) reported that the 30-year average precipitation for Johannesburg and Cape Town landfill areas, which are in the semi-arid regions of South Africa were 745 mm/yr and 550 mm/yr respectively. There are also a number of interpretations to the precipitation that falls initially as snow. Rovers and Farquhar (1973) used a conversion factor of 0.1 for all snowfalls that fell on test cells used to study the infiltration and landfill behaviour in Canada. In contrast, Dass et al. (1977) assumed that all precipitation during freezing period results in runoff during the warmer periods of the year, following a study of leachate production at Sanitary landfills at Blue Valley, Wisconsin. In the UK, all precipitation data are obtained from the Meteorological Office at Bracknell.

3.5.2 Evapotranspiration

Linsley et al. (1982) defined evapotranspiration (or total evaporation) as the evaporation from all water, soil, snow, ice, and other surfaces plus transpiration (plant water consumption). He defined potential evapotranspiration as the amount of water

that would evaporate when there is no deficiency of water in the soil for the use of vegetation and actual evapotranspiration as the loss of water, which is controlled by the amount of water actually available for plant use. He further stated that the rate of evaporation depends on the vapour pressure of the body of water and that of air for a free-water surface. The major factors affecting vapour pressures include temperature (both water and air), wind, humidity, atmospheric pressure, quality of the water, and the nature and shape of the surface. Apart from the last two, these factors will vary seasonally and geographically.

The factors influencing transpiration are due to both physiological and environmental factors. Physiological factors include the type and density of vegetation, leaf structure, plant condition, and age. Environmental factors include the season, temperature, solar radiation, relative humidity, wind speed, and soil moisture when the permanent wilting point is reached. The seasonal variation in sunlight conditions affects temperature of the leaf and thus, transpiration. Solar radiation is particularly important because it stimulates the opening of leaf pores. Approximately 95% of daily transpiration occurs between sunrise and sunset (Lu et al., 1985). The consumptive use of water shown in Table 3.1 indicates that a substantial amount of water can be lost by transpiration from the soil.

Table 3.1: Consumptive Use of Water (Qasim and Chiang, 1994).

Crop	Consumptive Use (m/year)
Alfalfa	3.5
Pasture	3.5
Wild Hay	2.6
Grass/Weeds	1.8
Small Grain	1.6
Oats	1.2
Wheat	1.3

Dass et al. (1977) reported that one of the objectives in the design of sanitary landfills is to increase the evapotranspiration in an effort to reduce leachate production. Holmes (1984) also reported that, encouraging vegetation to grow on a completed or

partially completed landfill such as Pitsea landfill, UK would increase moisture loss through transpiration by 11%. However, Campbell (1983) reported that evapotranspiration is unlikely to be a major source of water loss except on completed parts of the landfill where natural vegetation has become established. He reported that evaporation could be responsible for up to 70% and 40% of water lost annually in vegetated landfills and active landfills respectively. The moisture in the evaporative zone of uncovered landfill is too low to maintain potential evaporation. Bengtsson et al. (1994) reported that the water loss due to evaporation in a landfill with a thick soil cover corresponds to the regional evaporation.

The evapotranspiration at a site can be measured or estimated. Some of the methods applicable to landfills are described below (Lu et al., 1985):

a) The soil-moisture sampling method:

In this method, soil samples are taken at different time intervals from different depths in the landfill cover to determine the moisture content profile. The rate of change of water loss due to evapotranspiration is calculated after determining the moisture content. Modern equipment (i.e. neutron probe) allows immediate results without the need for sampling.

b) The lysimeter method:

Evapotranspiration is determined by growing the vegetation in lysimeters and measuring the losses of water necessary to maintain satisfactory growth. The lysimeter may not truly simulate the field conditions due to small-scale effects and thus needs to be treated with caution.

c) The pan evaporation adjusted method:

The rate of evaporation from a free water surface is the potential evapotranspiration from a vegetated soil surface. The annual distribution of potential evapotranspiration is obtained by multiplying the monthly pan evaporation by the pan coefficient (the ratio of annual free water evaporation to annual pan evaporation). Linsley et al. (1982) reported that pan coefficient ranges between 0.67 to 0.81.

d) Evapotranspiration equations:

Evapotranspiration equations are commonly used to obtain the evapotranspiration rates from landfill sites. Many of these equations are empirical and they depend on climatic factors such as temperature, humidity, and solar radiation. Some evapotranspiration equations are presented in Table 3.2. Of these, the Penman and Thornwaite equations are most commonly used for estimating evapotranspiration in landfills because of their accuracy (Lu et al., 1985).

3.5.3 Moisture Storage

In most landfills the moisture retained within the refuse represents the largest volume of moisture within the system. Moreover, a certain amount of moisture is needed for microbial degradation of the refuse especially if optimal gas production and accelerated waste stabilisation are practised as part of the landfill management. The moisture storage of the soil and waste materials changes according to infiltration and evapotranspiration of water in the landfill. There is a variation in moisture storage within the landfills due principally to the heterogeneity of the emplaced refuse materials.

The amount of moisture that can be stored in a waste layer depends on the initial moisture content and the absorptive capacity of the waste material. The overall moisture content of a waste fill is the sum of individual moisture contents of the constituents. The large variation in the sizes of refuse particles makes it imperative for large samples of refuse to be tested for moisture content. Landva and Clark (1990) stated that large samples of waste could be dried in a pottery type kiln furnace for accurate determination of moisture content and organic content of refuse provided provision is made for proper ventilation. The moisture content of refuse is normally determined by drying a sample at a temperature of $105^{\circ}\text{C} - 110^{\circ}\text{C}$ for 16 hours – 24 hours (BS 1377). Engineers usually use and report gravimetric moisture content but some hydrological models (e.g. HELP) require moisture content to be represented as volumetric data (as in agronomy and soil physics). Bengtsson et al. (1994) stated that most reported initial volumetric moisture content in municipal solid waste landfills vary between 0.15 – 0.2. Typical composition and average moisture content of refuse in the UK is shown in Table 3.3.

Table 3.2: Evapotranspiration equations (Lu et al., 1985)

Name of equation	Date	Period for E	Unit for E	Equation
Hedke	1930	Annual	Feet	$E = KH$ [3.7]
Lowry-Johnson	1942	Annual	Feet	$E = 0.000156H + 0.8$ [3.8]
Blaney-Morin	1942	m months	Inches	$E = k \sum_1^m pt(114 - h)$ [3.8]
Thornwaite	1944	Monthly	Centimetres	$E = 1.6 \left(\frac{10t}{TE} \right)^a$ [3.9] where $a = 0.000000675(TE)^3 - 0.0000771(TE)^2 + 0.0179TE + 0.49239$ [3.10]
Penman	1948	Daily	Millimetres	$E = \frac{AH - 0.27e}{A - 0.27}$ where $e = 0.35(e_a - e_d)(1 + 0.0098w_2)$ and $H = R(1 - r)(0.18 + 0.55S) - B(0.56 - 0.092e_d^{0.5})(0.10 + 0.905)$ [3.11]
Blaney-Criddle	1950	m months	Inches	$E = k \sum_1^m pt = kF$ where $F = \sum_1^m pt$ [3.12]

E = evapotranspiration or consumptive use for given period

A = slope of saturated-vapour curve of air at absolute temperature in $^{\circ}\text{F}$, or de_a/dt in mm

$\text{Hg}/^{\circ}\text{F}$

B = a coefficient depending on temperature

e_a = saturation vapour pressure at mean air temperature in mm Hg

e_d = saturation vapour pressure at dew point (i.e., actual vapour pressure in the air) in mm Hg,
being equal to e_a multiplied by relative humidity in percent.

e = daily evaporation in mm

h = annual mean relative humidity in per cent, in Eq.(7)

H = accumulated degree-days above minimum growing temperature for growing season, in
Eq. (5); or accumulated degree-days of maximum daily temperature above 32°F for
growing

season, in Eq. (8) or daily heat budget at surface in mm of water, in Eq. (9)

k = annual seasonal or monthly consumptive-use coefficient.

p = percent of daytime hours of the year, occurring during the period, divided by 100.

r = estimated percentage of reflecting surface.

R = mean monthly extraterrestrial radiation in mm of water evaporated per day.

TE = Thornwaite temperature-efficiency index, being equal to the sum of 12 monthly values
of

heat index $i = (t/5)^{1.514}$ where t is mean monthly temperature in $^{\circ}\text{C}$.

t = mean monthly temperature in $^{\circ}\text{F}$ in Eqs. (7), (10) or in Eq. (8).

w_2 = mean wind velocity at 2m above the ground in miles/days, or equal to
 $w_1(\log 6.6 / \log h)$

where w_1 is measured wind velocity in miles/day at a height h in ft

S = estimated ratio of actual duration of sunshine to maximum possible duration of sunshine

Table 3.3: Typical Composition of Urban Collection and Civic Amenity Wastes as Delivered to Landfill (DoE, 1995).

Constituents	Weight, % (as received)
Paper	29.2
Putrescible	19.0
Unsorted fines	8.6
Glass	8.4
Ferrous metal	8.0
Misc. Combustible	5.8
Plastic-film	4.2
Misc. Non-combustible	4.0
Garden waste	3.8
Textile	3.0
Dense plastic	2.8
Wood	2.2
Non-ferrous metal	1.0

Moisture content = 33% (by wet weight)

Bulk density, uncompressed = 170 kg/m³

Porous materials have the ability to absorb and hold water due to capillary forces or suctions (negative pore pressure) within the material. The maximum moisture a porous material can hold against the force of gravity is known as its field capacity. Blight (1989) referred to it as the material moisture storage capacity. The “field capacity” terminology was initially used for soil but has since been extended to waste by many investigators. Rovers and Farquhar (1973) in an investigation into infiltration and landfill behaviour in Canada, observed leachate flow in a cylindrical test cell filled with refuse at a moisture content which was then compared to the field capacity in soils, since no piezometric head was observed.

In general terms, absorptive capacity of a waste fill denotes the amount of liquid uptake before the field capacity of the refuse is reached. However, leachate has been observed shortly after refuse placement in many landfills (Blight et.al, 1989; 1992; Blakey, 1982; Bengtsson et al.1994). This was found to be as a result of channelling of water in macropores initiated by differential settlement of the refuse fill. In order to account for this phenomenon, Campbell (1983) defined absorptive capacity of refuse as the volume of water added to domestic refuse before leachate is generated. Blakey (1982) also defined actual field capacity as the moisture content when 90% of infiltration appears as leachate. Holmes (1980) reported the water retention of domestic refuse emplaced at a landfill in Southeast England (Table 3.4). Voids of approximately 6.25 m³ of refuse of different ages were excavated. The samples were then compacted to a predetermined in situ density, saturated, and drained in 45 gallon containers to determine certain geotechnical properties.

Table 3.4: Moisture content and water retention of domestic refuse, volume/volume (Holmes, 1980)

Age (years)	Density (T/m ³)	Initial moisture content (v/v)	Moisture retained (v/v)	Field capacity (v/v)	Void ratio (v/v)	No of samples		
4	0.638	19.14	19.47	38.60	26.44	3	4	2
10	0.814	24.83	15.35	40.19	25.51	6	4	3
17	0.96	31.68	10.97	42.65	24.65	4	4	4

v/v – volume per volume

The water storage of the cover topsoil is always changing due to evapotranspiration processes. The moisture holding capacity of soil available to plants is defined as the difference between the field capacity and the moisture content at wilting point; this being the minimum moisture available to vegetation to prevent wilting. The water holding characteristics of soils is shown in Figure 3.2. Cohesive soils have a higher field capacity and available water for evapotranspiration than the coarser soils.

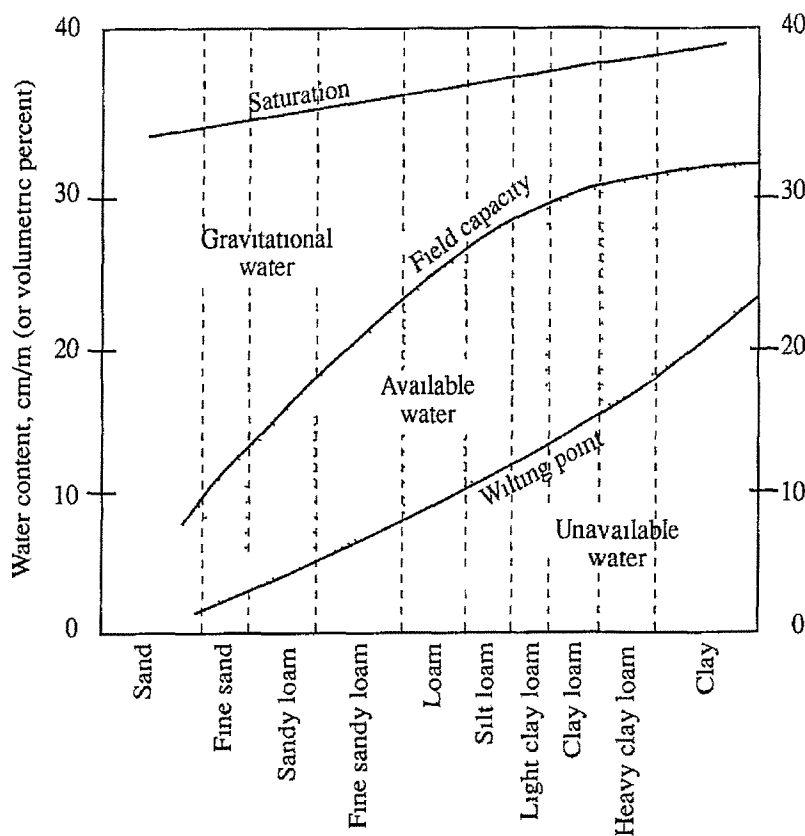


Figure 3.2: Water Holding Characteristics of Soils (Qasim and Chiang, 1994)

3.5.4 Surface Runoff

During periods of runoff, part of the incident precipitation runs off the landfill site and is lost to the overland flow before it can infiltrate. The term surface runoff is often called overland flow in surface hydrology (Price, 1985; Linsley et al., 1982) and is defined as water which travels over the ground surface to a channel. The surface runoff depends on many factors such as the surface slopes, the intensity and duration of storm, the antecedent soil moisture condition, the permeability of the cover soil and the amount and type of vegetation.

Several methods may be used to estimate the runoff from a landfill. These methods include surface measurements, empirical relationships and graphical methods. Surface runoff can be measured directly in the field or laboratory. The drainage from a fenced plot, which is representative of the landfill is sometimes used in the field. The drainage area to a side drain may also be estimated from the topographical map of the

landfill. Kjeldsen (1993) used a weir installed on the perimeter drainage ditch to obtain the surface runoff from Vejen Landfill, Denmark.

The most commonly used method of estimating runoff is the rational method. The runoff coefficient used in the rational equation depends upon surface characteristics, type and extent of vegetation, and the surface slope. The runoff coefficients used in this method are provided in Table 3.5. In most cases it is expected that the runoff for sanitary landfill conditions will lie within the range 0.07 to 0.2 (Qasim and Chiang, 1994).

The use of empirical runoff coefficients for designing surface water drainage systems is a convenient method but requires some caution. Dass et al. (1977) reported that the runoff coefficients customarily used in the design of 5 year to 10 year frequency storms gives high values of runoff from landfills. Landfill sites will typically have potholes and depressions due to differential settlement that may interrupt the surface runoff processes. The use of runoff coefficients may yield unrealistically high values and greatly underestimate infiltration. Ettala (1987) supported this opinion when he reported an infiltration in excess of 60mmh^{-1} through the clay cover of Lahti and Hollola landfills in southern Finland. In addition, Berger et al. (1996) stated that cohesive soils (e.g. clay used for capping) may develop desiccation cracks as a result of water uptake by plant roots. Precipitation channels through these leading to a reduction in the surface runoff.

The graphical method used in estimating runoff is called the curve number method, proposed by the U.S. Soil Conservation Service (SCS) to predict surface runoff from agricultural lands. The method incorporates rainfall, soil type, land cover, land use, and antecedent moisture condition. The curve number method is used to calculate runoff in the HELP model.

3.5.5 Microbial Degradation

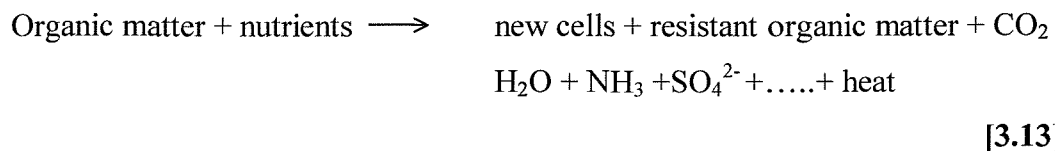
The decomposition of biodegradable organic matter present in refuse usually results in water, which will contribute to the moisture in refuse for leachate production. The extent and rate of microbial degradation and consequent water generation depend

Table 3.5: Typical values of coefficient of runoff (Qasim and Chiang, 1994)

Surface Type	Coefficient of Runoff
Bituminous Streets	0.7-0.95
Concrete Streets	0.8-0.95
Driveways, Walks	0.75-0.85
Roofs	0.75-0.95
Lawns; Sandy Soil	
Flat 2%	0.05-0.1
Average, 2-7%	0.1-0.15
Steep, 7%	0.15-0.2
Lawns, Heavy Soil	
Flat, 2%	0.13-0.17
Average, 2-7%	0.18-0.22
Steep, 7%	0.25-0.35

upon the amount and pH of interstitial water, presence of oxygen, the composition and particle size of the refuse, the type of organic matter present, and the degree of the refuse mixing (Lu te al., 1985). The two types of refuse decomposition by organisms present in the refuse fill are aerobic digestion and anaerobic digestion.

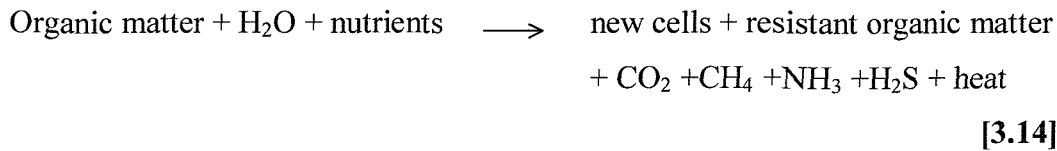
During the placement of waste, oxygen present in the void space give rise to aerobic decomposition. The general aerobic transformation of solid waste can be described by means of the following equation (Tchobanoglous et al., 1993):



This phase is generally very short because of the limited amount of oxygen in landfills and the high biochemical oxygen demand (BOD) of the solid waste. Leachate

produced during this phase is expected to dissolve highly soluble salts, such as NaCl and others (Qasim and Chiang, 1994).

As oxygen is used up, the decomposition by facultative anaerobic organism predominates. The general anaerobic transformation of solid waste can be described with the following equation:



As can be seen in equation (3.14), water is consumed during the anaerobic digestion of organic constituents in MSW. An estimate of the amount of water consumed per cubic metre of gas produced in a typical landfill is 0.19 kg while the amount lost as vapour is 0.035 kg of water /m³ landfill gas (Tchobanoglous et al, 1993). These values may be taken as the optimal quantity since gas production depends on ambient conditions and will vary considerably within landfills. However, they are small if compared to other terms in the water balance equation.

Several authors have reported the major phases involved in the anaerobic decomposition in which organic materials are converted to methane and carbon dioxide (Barlaz et al., 1989; Qasim and Chiang, 1994, WS Atkins environment, 1994; El- Fadel et al., 1995; Knox, 1998). The steps are highly inter-dependent and include hydrolysis, acidogenesis, acetogenesis, and methanogenesis (Figure 3.3).

The attainment of the stages above depends on a suitable and favourable environment, which depends on temperature, pH, moisture content, nutrients, composition, particle size, and microbes. Farquhar (1989) stated that vigorous methanogenesis does not always occur in the landfills because the environment is much less than optimal for the methanogenic bacteria.

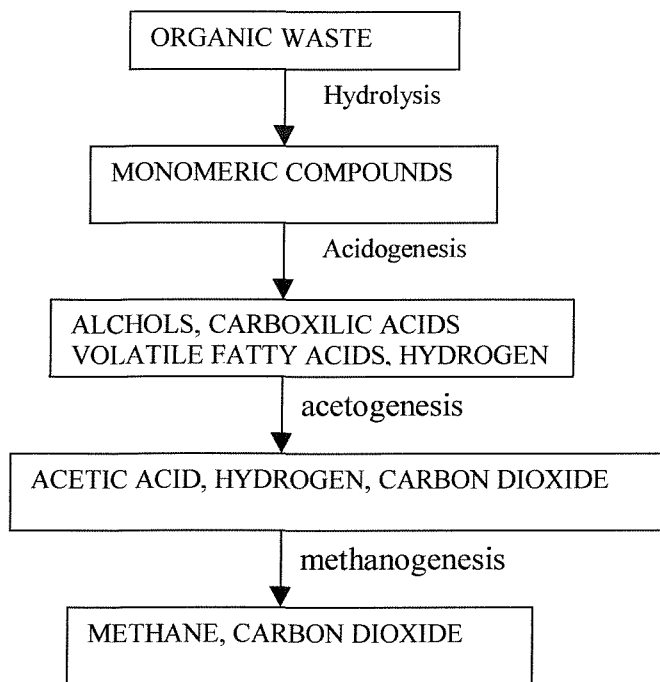


Figure 3.3: Major degradative steps during the anaerobic decomposition phase (El-Fadel et al. 1997)

The phases of landfill gas production are shown in Fig 3.4. The five phases are:

- I. Aerobic
- II. Anaerobic
- III. Anaerobic methanogenic unsteady
- IV. Methanogenic steady state
- V. Transition from anaerobic back to aerobic

Farquhar and Rovers (1973) stated that results from test cells showed that phases I and II may be completed between 11 days and 40 days, and phase III between 180 days and 500 days after waste placement. However, these values may be atypical of actual landfill conditions. Phase III is unsteady, as the concentration of CH_4 is increasing. The composition of the gases produced and rate of production remain steady at their peak for the prevailing conditions in phase IV.

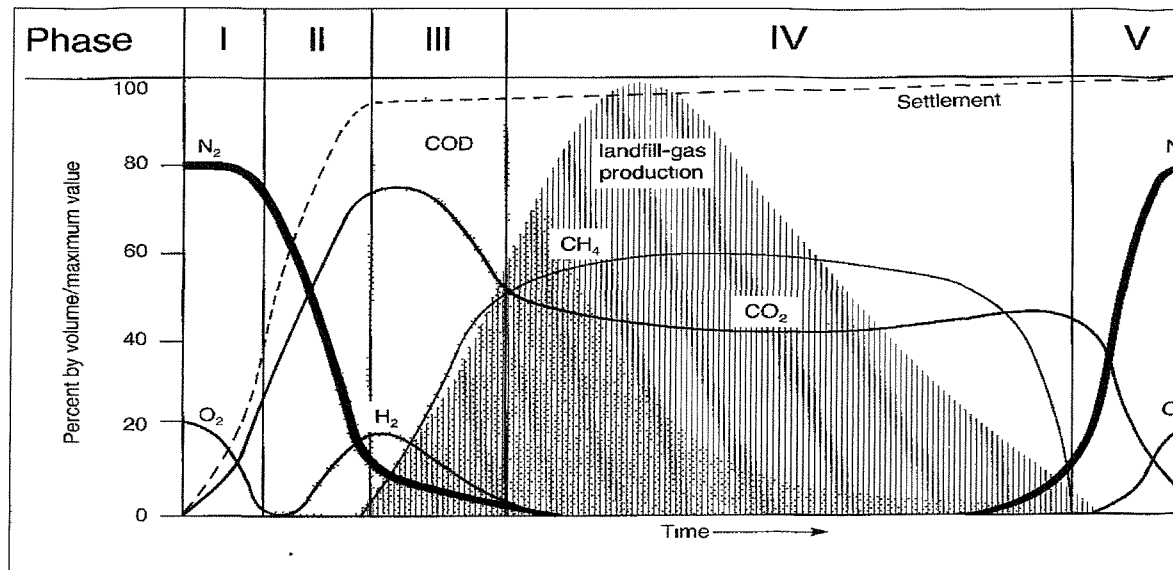


Figure 3.4: Schematic of landfill stabilisation, organic, components (DoE, 1995)

3.6 Simulation of Leachate Quantity in Landfills

Ability to simulate the quantity of leachate produced in a landfill is vital for good planning and management of a landfill. As mentioned earlier, the water balance method is used to estimate leachate volume in landfills. Farquhar (1989) reported that accurate prediction of leachate is difficult because of the uncertainties involved in determining some of the terms in the water balance equation. He stated that some of the data of the water balance are stochastic in nature (temperature, heat index, precipitation, wind, vegetation growth); other data are poorly defined (runoff coefficients, refuse and cover density, moisture storage capacities). Parsons (1995) stated that the inability to accurately measure the parameters in water balance method is its major limitation. Zeiss (1997) stated that matching the predicted and measured quantities of leachate in a landfill depends on the parameters of the water balance model.

Reliable results have been obtained from the application of water balance method to moisture routing in landfills. Blight et al. (1989) used a water balance method to predict the time taken for two sanitary landfills in a water deficient area of South Africa to produce leachate. The calculated values were compared with direct sampling

results and it was concluded that the water balance method was accurate and provided realistic values if the input data is measured accurately. Holmes (1984) used the water balance method to estimate the effective rainfall at Pitsea co-disposal landfill, UK.

The input and output values were found to balance within 10% of each other.

Farquhar (1989) reported that Kmet (1982) used the water balance method to simulate leachate production in eight field lysimeters. In this case, leachate flows from the field lysimeters ranged from 16.6% to 22.1% of the annual precipitation. The water balance method predicted an average of 22% of annual precipitation, providing good agreement. However, Gee (1981) found a 94% error in the predicted volume of leachate determined from the water balance method as compared with measured values at GROWS landfill, Bucks County, Pennsylvania. The runoff and infiltration of the landfill were obtained by measuring the runoff from a rainfall simulator in the laboratory. The discrepancy in the leachate volumes is therefore likely to arise from the use of these simulated values of runoff and infiltration used in the water balance method.

Advancements in computing have created a shift from the manual procedures of utilising the water balance method at landfill sites to computer based water balance models. The ability to analyse rapidly and to incorporate many sub-models in the simulation has made computer models more robust and accurate. Farquhar (1989) reported that the computer models widely used for estimating leachate volumes in landfill sites are the hydrologic simulation of solid waste disposal site (HSSWDS) model developed by Perrier and Gibson (1981), and the hydrologic evaluation of landfill performance (HELP) model developed by Schroeder et.al. (1994). Both were developed by researchers at U.S Army Engineer Waterways Experiment Station (WES), Vicksburg, for the U.S. Environmental Protection Agency (EPA), Risk Reduction Engineering Laboratory Cincinnati, OH, in response to needs in the Resource Conservation and Recovery Act (RCRA) and the Comprehensive Environmental Response, Compensation and Liability Act (CERCLA, better known as Superfund) as identified by the EPA Office of Solid Waste, Washington, DC (Schroeder et.al.,1994).

The HSSWD model simulates only the cover system and does not model lateral flow through drainage layers and handles vertical percolation only in a rudimentary

manner. In contrast, the HELP model simulates the entire refuse fill process including the drainage and liner systems (Schroeder et. 1994). The HELP model is widely regarded as the best available and the most commonly used computer model for the estimation of leachate in landfills (Blight et al., 1992; Nixon et al., 1997). The HELP model is described in Chapter 8.

3.7 Research Needs

As stated earlier, the quantity of leachate produced in a refuse fill is often determined from the water balance method of the landfill. However, the water balance equation (including HELP) does not account for the changing physical characteristics of a refuse fill (Farquhar, 1989; Schroeder et. 1994). Surprisingly, little work has been reported on the simulation of leachate volumes with consideration to the changing environment of a landfill. This was investigated in this research by undertaking the following approach:

- Simulating moisture stored in refuse lifts in a landfill in sequence to reflect the pattern of refuse tipping in a landfill site.
- Using the HELP model in conjunction with characteristic models that determine temporal changes in properties of an emplaced refuse fill, to simulate the moisture storage in a landfill.
- Utilising the data from the field and laboratory tests (e.g. moisture changes in the topsoil of the landfill) in the simulation to improve results.

For workability and simplification of the simulation, biodegradation was not considered in the characteristic models. This is reasonable since the study is mainly concerned about the fill period of the landfill, when biodegradation is small.

CHAPTER

4

The Site

4.1 Summary

The site used for undertaking field tests on municipal refuse is described in this chapter. In particular, the topography, geology and refuse disposal practices at the site are outlined. The suitability of the site for landfilling is also reported.

4.2 Location and Topography

The site used in the present study is the White's Pit landfill, located towards the north end of Canford Heath, Poole, Dorset (British National Grid SZ030971). It lies approximately 6km north of Poole and about 8km northwest of Bournemouth. The site is bounded by a wooded area with sparse residential structures in the north, and by 800 acres of the Canford Heath Site of Special Scientific Interest, one of the largest surviving fragments of lowland heath in the south. The site and the heath are owned by WH White Plc., Wimborne, Dorset.

The topographical map of the site is shown in Figure 4.1. The site consists of two major areas of refuse landfill: a “dilute and disperse” landfill area, and a containment landfill area. The dilute and disperse area occupies the northern part of the site and it comprises two areas of refuse in-fill, namely the biodegradable area, and the inert area. The biodegradable area is well vegetated with grass while the inert area is poorly

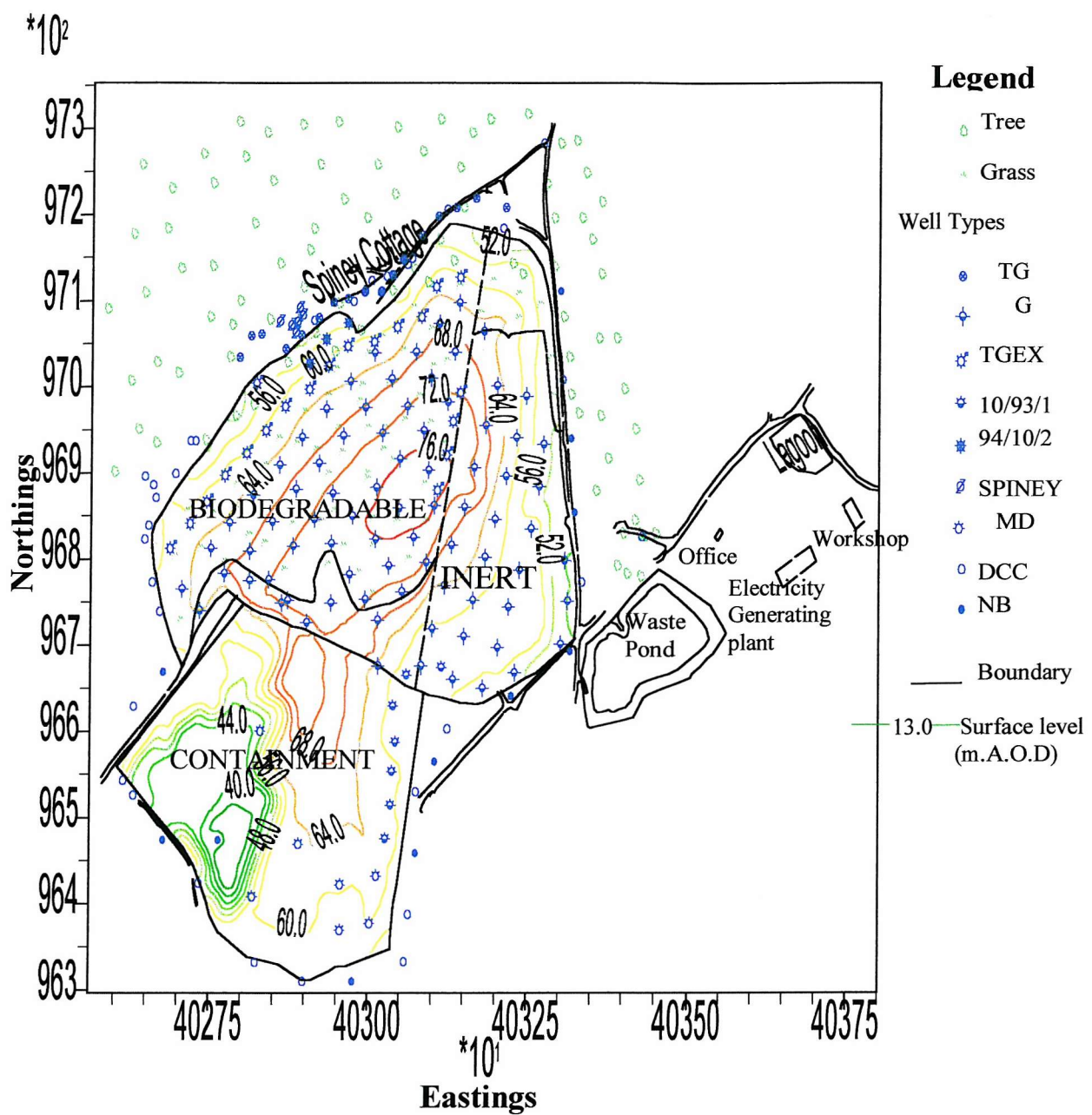


Figure 4.1: Topographical Map of White's Pit Landfill

vegetated because of the placement of inert soil, which is still taking place on the southern part of the area. The containment landfill area is located at the southern part of the site. Refuse is currently being disposed to cells in the containment area of the site.

Gas production wells and leachate-monitoring wells are located within and outside the landfill. The gas produced at the landfill is used to generate electricity. The power station is located on site and comprises seven spark ignition engines generating 7000 kilowatts of electricity into the National Grid (W H White Plc., 1995). The power station is one of the largest gas power installations in a single landfill site in Europe (W H White Plc., 1995). Other on-site infrastructure includes two office buildings and a workshop. There is a recycling facility situated at the southern boundary of the containment site that produces metals for re-use, soil and hardcore for landscaping and construction, and paper and wood for composting.

A perimeter ditch collects the surface runoff from the landfill. The water that drains into an excavated cell in the containment area is also pumped to the ditch. Water from the ditch drains to a wastewater pond located at the eastern part of the site. A lagoon, currently under construction, is located in the top corner of access roads at the eastern part of the site. On completion, the lagoon will be used to treat wastewater collected from the landfill.

4.3 Geology

4.3.1 Regional

The regional geology of the Bournemouth-Poole-Wimborne district has been described by Freshney et al. (1985). They reported that the geological succession present in the district consists of drift deposits of the Quaternary age overlying rocks of the Palaeocene and Cretaceous periods (Table 4.1). The highest beds of the cretaceous upper chalk have been proved only in boreholes. The chalk is smooth, white and massively bedded, with flints occurring throughout. The rocks of the Palaeocene system crop out at the surface in many areas of the district (Figure 4.2),

Table 4.1: Geological Succession in the Bournemouth - Poole - Wimborne Area (Freshney et al., 1985).

DRIFT DEPOSITS				
Quaternary	Drift deposits			
	Brown Sand			
	Alluvium			
	River Terrace Deposits			
	Marine Beach Deposits			
	Estuarine Alluvium			
	Storm Gravel Beach			
	Deposits			
	Head			
SOLID FORMATION				
System	Group	Formation	Member	Thickness(m)
	Barton	Boscombe		18
	Group	Sand		
		Branksome		
		Sand		c70
	Bournemouth		Parkstone Clay	0-22
	Group		Broadstone Clay	0-19
Palaeocene		Poole Formation	Haymoor Bottom Clay	0-3
			Creekmoor Clay	0-54
			Oakdale Clay	0-27
			Unnamed Clay	0-45
		London Clay		12-35
		Reading Formation		12-21
Cretaceous		Upper Chalk		30 proved

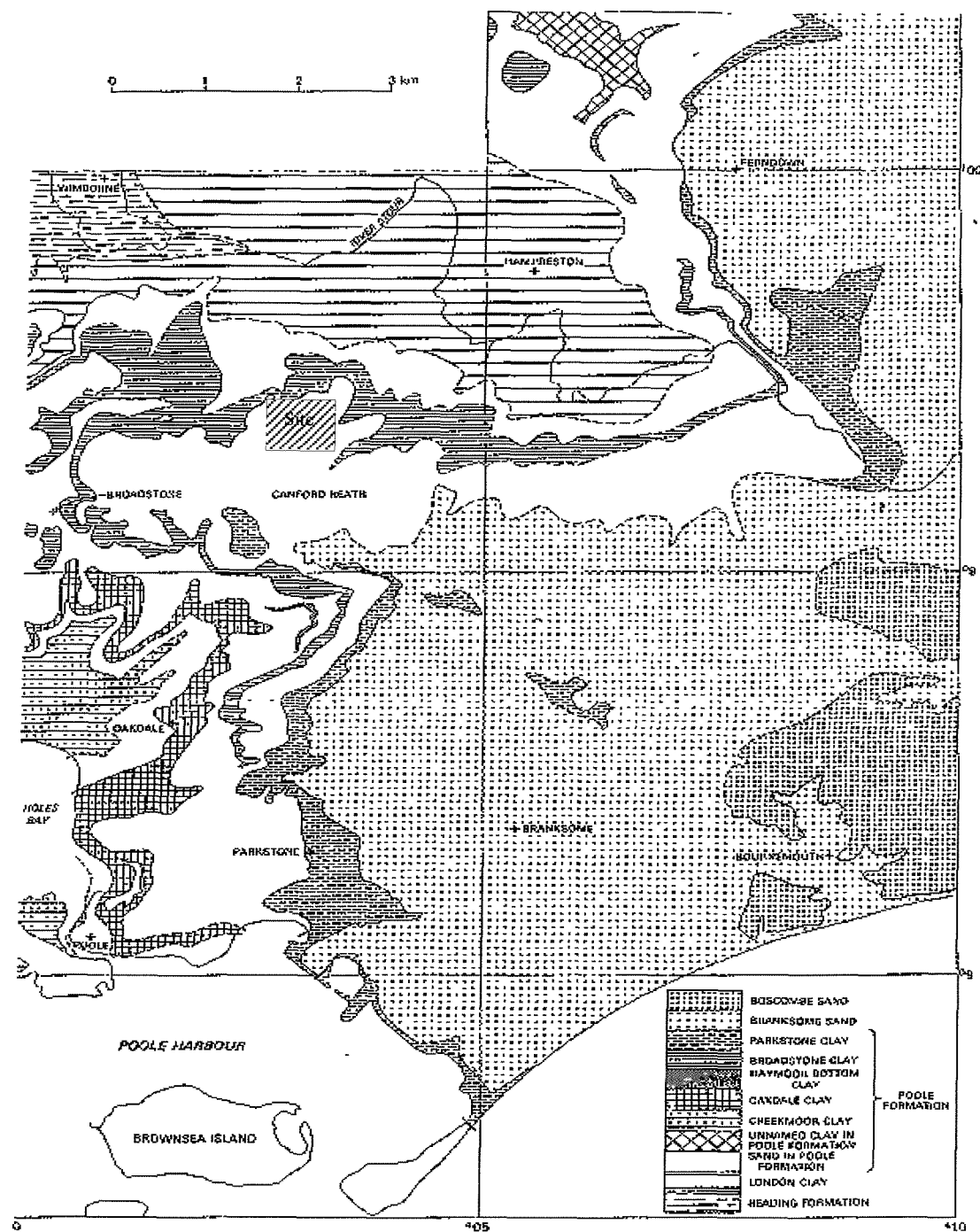


Figure 4.2: Sketch map of the geology of the Bournemouth-Poole-Wimborne area (Freshney et al., 1985)

but the basal beds of the Reading Formation were proved only in boreholes. The River Terrace deposits are the most prominent of the drift deposits in the district. They are found on the flanks of Stour Valley and the area south of the Stour, around Merley and Canford Heath. They consist of flint gravels, commonly very sandy and locally very clayey. The pebbles have a maximum size of approximately 5cm and are usually subangular to subrounded but well-rounded flints from the Tertiary deposits are usually present. The thickness of the River Terrace Deposit in the district is generally between 4m and 6m.

4.3.2 Local

According to Figure 4.2, the site is situated in the Poole Formation of the Palaeocene system. The Poole Formation consists of an alternating sequence of fine to very coarse-grained, locally pebbly, cross-bedded sands, and pale grey to dark brown, carbonaceous, commonly laminated, locally red-stained, clays and silty clays. The sands generally are thicker than the clays and occupy approximately two-thirds of the area where the formation outcrops (Freshney et al., 1985).

In accordance with the previous geologic mapping by Freshney et al., (1985), the borehole logs from the ground investigation carried out at Whites pit landfill by Mott MacDonald (1990 a & b) show that the site is underlain by River Terrace deposits of the Quaternary period over deposits of Poole formation of the Palaeocene system. The clays of the Poole Formation present in the pit are Parkstone clay and Broadstone clay. The schematic sequence of the Poole Formation at the site is as below (Mott MacDonald, 1990a)

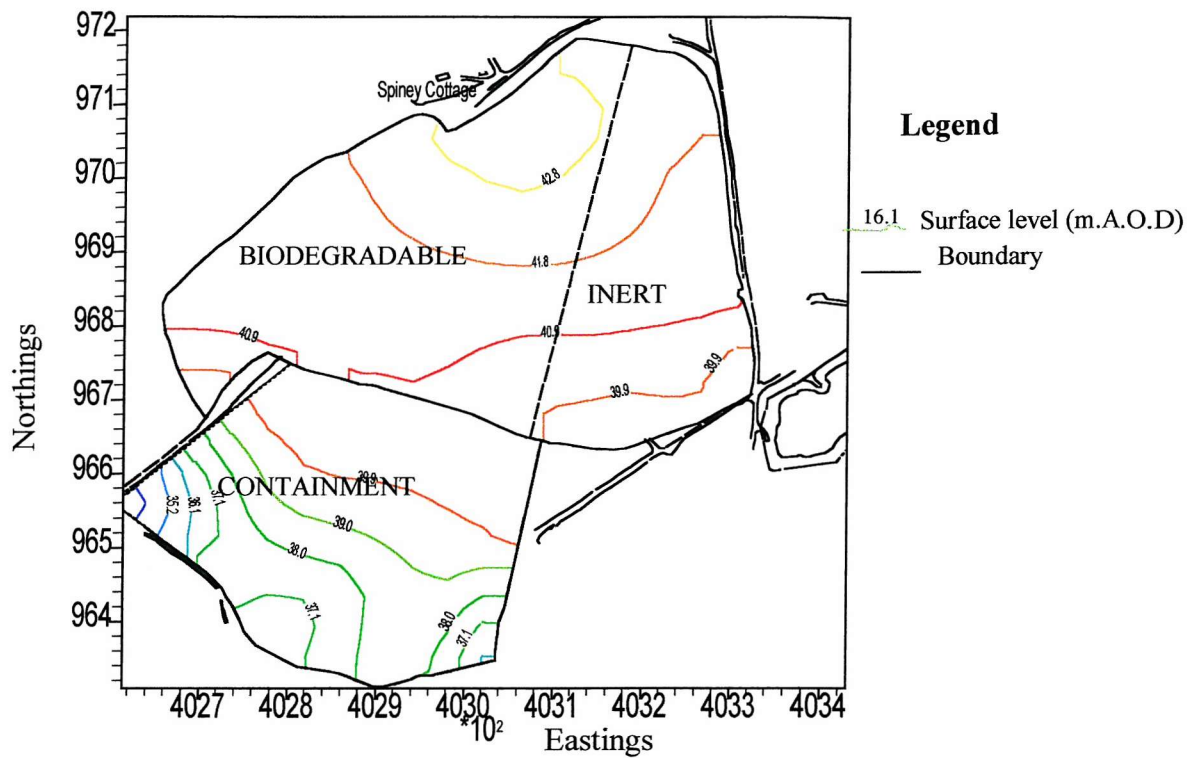
Parkstone clay comprises a bluish grey, commonly laminated, clay. The underlying lower sand varies from silty and fine grained to very coarse-grained and pebbly, with medium to coarse the commonest grain size. Only a patch of the Parkstone clay is present in the landfill. It also outcrops in the southern part of the landfill where the River Terrace deposit has been eroded (C L Associates, 1991; Dorset Drilling Services, 1994 & 1996; Environment Agency, 1996).

Broadstone Clay takes its name from the nearby town of Broadstone where the clay was used for brickmaking. It is the most laterally consistent of the clays in the Poole formation and underlies the entire site. It varies from a pale grey silty clay, through to a medium grey silty clay, to laminated, silty and fine-grained sandy clay. Results of the ground investigation undertaken by Mott MacDonald (1990b) shows that the sand in the Poole formation at the site (Figure 4.3) varies from a silty, very fine to very coarse-grained sand with medium-grained sand being common. The laboratory examination of undisturbed samples from the ground investigation shows that the Broadstone clay at the site has an average gravimetric moisture content of 20 %, mean bulk density of 2000kg/m^3 , and mean hydraulic conductivity of the order of 10^{-10} m/s .

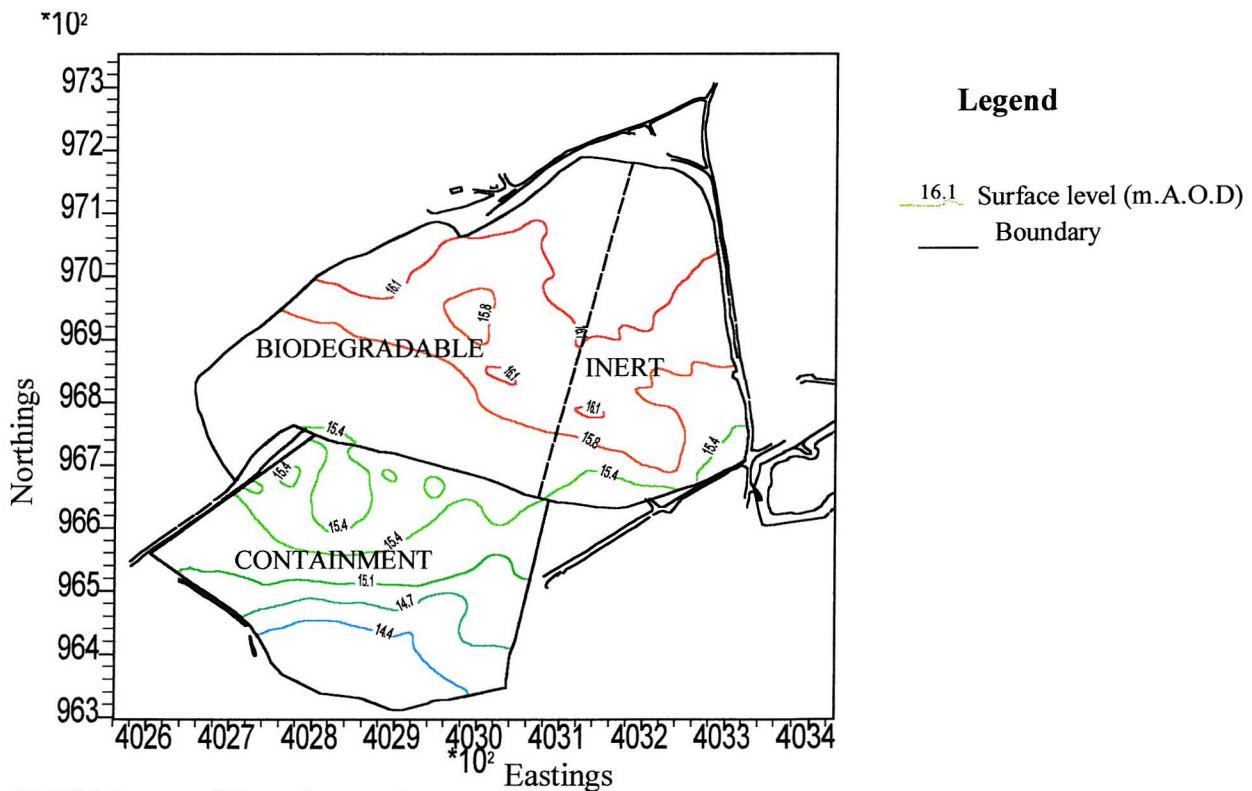
River Terrace Deposit
Parkstone Clay
Sand
Broadstone Clay

Figure 4.3: The schematic of the Poole Formation present at White's pit.

The data obtained from borehole logs of the site (M J Carter, 1989; Mott MacDonald 1990b; C.H Steavenson, 1992; Dorset Drilling Services, 1993 & 1994) have been used to depict the top, and thickness of the basal Broadstone clay in White's pit, using UNIMAP 2000, an advanced visualisation software (UNIRAS, 1989). The top of the Broadstone clay is shown in Figure 4.4a. The average surface level of Broadstone clay in the dilute and disperse part of the site is approximately 41 m above ordnance datum (A.O.D) while the average surface elevation of the containment area is approximately 38 m A.O.D. By considering the vertical elevation of the Broadstone clay in relation to horizontal distance in Figure 4.4a, the top of the Broadstone clay slopes down to the southwest of the site at approximately 0.7%. The thickness of Broadstone clay is shown in Figure 4.4b. The average thickness of the Broadstone clay in the “dilute and disperse” and containment areas are approximately 16 m and 15 m respectively.



(a) Top of Broadstone clay



(b) Thickness of Broadstone clay

Figure 4.4: Map of the top and thickness of Broadstone clay at White's pit, Poole, Dorset.

4.4 Refuse Disposal in Dorset

The waste produced in Dorset has changed significantly in composition in recent years. The waste disposal practice in Dorset was reported by Hutchinson (1995). He reported a sharp increase in the disposal of paper and plastics, which were unknown in 1935, but constitutes a significant quantity of household waste in 1993/99. Over one million tonnes of waste was disposed to landfills in Dorset in 1993/94. The average Dorset household produces approximately one tonne of domestic waste annually (WH White plc, 1996). The waste includes household waste, commercial and industrial waste, and hazardous waste.

The controlled waste going to landfills in Dorset is indicated in Figure 4.5. Out of 292,116 tonnes of household waste produced in Dorset in 1993/94, approximately 29796 tonnes was recycled while the remaining 262,116 was landfilled. Commercial waste is collected from the premises used for trade and business while industrial waste includes factory waste, construction and demolition waste, waste oil and scrap metal. The quantity of commercial and industrial waste landfilled in 1993/94 was 882.674 tonnes. Hazardous waste consists of toxic, flammable, corrosive or pharmaceutical materials, which are deemed harmful to human health and the environment. Of the residual 1753 tonnes produced in the county, 1663 tonnes was asbestos or asbestos contaminated material that was landfilled while the remaining 90 tonnes, consists of waste solvents were recovered at various solvent recovery plants (Hutchinson, 1995). The bulk of the clinical waste generated from hospitals in Dorset was incinerated at five existing hospital incinerators at Poole General, Royal Bournemouth, Christchurch, West Dorset and Bransford hospitals.

The non-controlled wastes comprise agricultural, mining and quarrying wastes disposal of which is not controlled by County Council. Most of the agricultural wastes are recycled or reused while almost all-mining and quarrying wastes are returned to the mineral voids.

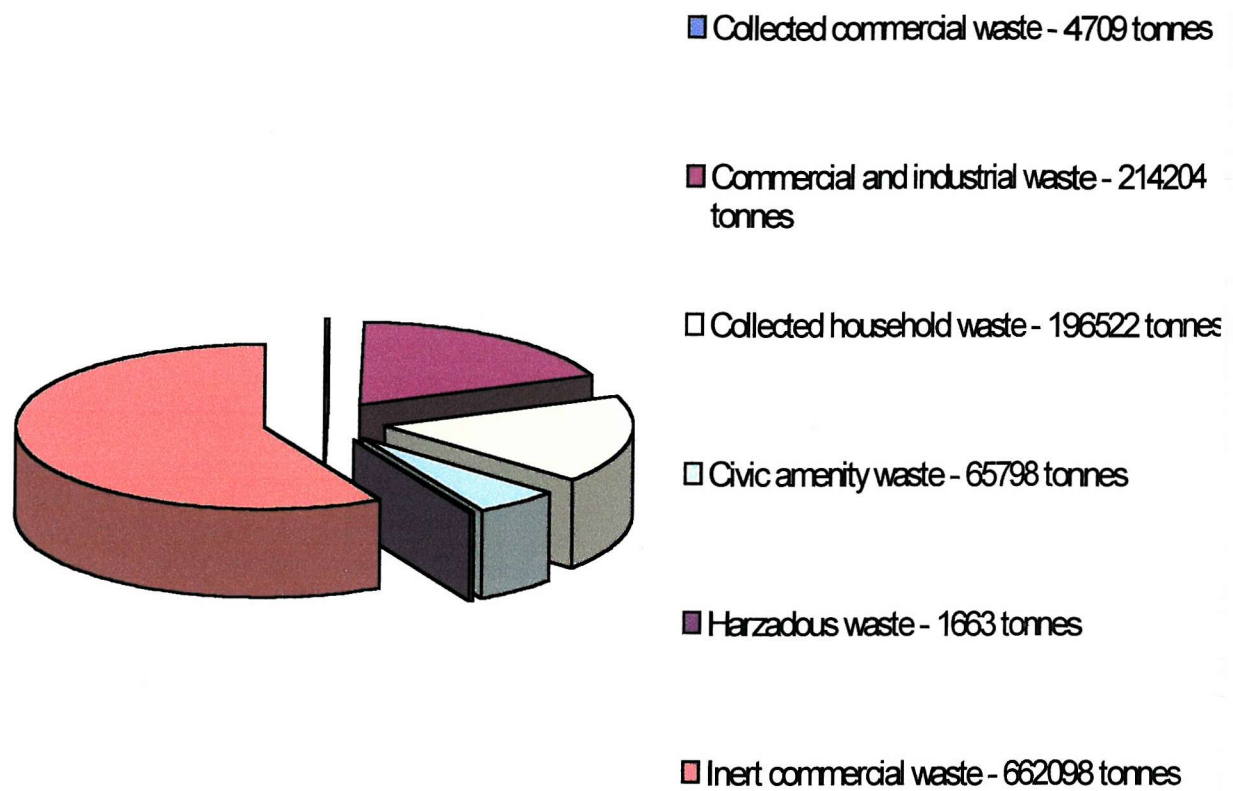


Figure 4.5: Controlled waste to landfill in Dorset 1993/94 - 1,144994 tonnes (Hutchinson, 1995)

4.4.1 Refuse Tipping at White's Pit Landfill

Approximately 330,000 tonnes of controlled waste, mainly from Poole, Bournemouth, and Christchurch are landfilled annually at the site (W H White Plc., 1995). The site is the largest landfill site in Dorset. Refuse was emplaced in the void originally created by sand quarrying in the dilute disperse area of the site. In the active containment area of the site, excavation proceeds into the Broadstone clay to obtain materials for capping and lining of the refuse cells. The excavated clay is stockpiled at the eastern part of the site prior to use. Approximately two thirds of the site's area has been landfilled with refuse.

Landfilling of refuse started at the site in 1977 by Phillips Ltd. (Leach, 1994). Infilling of inert waste and commercial waste started from the northern and eastern parts of the site. Shortly afterwards, the placement of inert materials at the site was undertaken by Drinkwater Sabey Ltd., which filled a 150 m wide strip of the quarrying void from the eastern boundary of the site to restoration level.

In 1982, Dorset County Council started filling the biodegradable area of the site with household and commercial waste. The phases of tipping of the biodegradable area of the site are shown in Table 4.2. Placement of the household and the commercial waste started at the western boundary of the site and continued through to the boundary of the inert waste area. On many occasions, different areas were filled simultaneously. Tipping of refuse stopped at the biodegradable area in 1989. However, inert materials are still being used to fill depressions caused by differential settlement of refuse in this area.

The tipping faces and thickness of waste at the biodegradable part of site are shown in Figure 4.6. The refuse fill in the “dilute and disperse” area rises steadily from the boundary to approximately 30m above the Broadstone clay, at the centre of the site. The final depth of the emplaced refuse in the containment area is likely to be more than 30m because of the extra space created by the excavation of the Broadstone clay for lining and capping purposes. Over three million tonnes of household and commercial waste have been disposed to the site (Leach, 1994).

4.5 Conclusion

The area geology is among the main factors influencing the location of a landfill site. Even though the site was formed from the void created by mineral excavation, the Broadstone clay, which underlies the entire site, provides the landfill with a natural liner. The hydraulic conductivity of 10^{-10} m/s (Mott MacDonald, 1990b) of the clay will reduce significantly the vertical leakage of leachate from the site. Vertical seepage will be further reduced due to the 16 m thickness of the clay formation. The

Table 4.2: Phases of Filling at the Dilute Disperse site of White's landfill (Hutchinson, 1990).

Date	Areas of Fill (See Figure 4.6)								
	A	B	C	D	E	F	G	H	I
1982 Summer	x								
Autumn	x								
1983 Winter	x								
Spring	x	x							
Summer	x	x							
Autumn	x	x		x					
1984 Winter	x	x	x	x					
Spring	x	x	x	x					
Summer	x	x	x	x		x			
Autumn	x			x		x			
1985 Winter				x		x			
Spring				x	x	x			
Summer				x	x				
Autumn				x					
1986 Winter				x					
Spring				x			x		
Summer							x	x	
Autumn							x	x	
1987 Winter							x	x	
Spring	x						x	x	
Summer	x						x		
Autumn	x					x	x		
1988 Winter	x				x				x
Spring					x				x
Summer					x		x	x	
Autumn	x					x	x		
1989 Winter	x								x
Spring	x					x	x	x	
Summer					x		x	x	
Autumn					x		x	x	

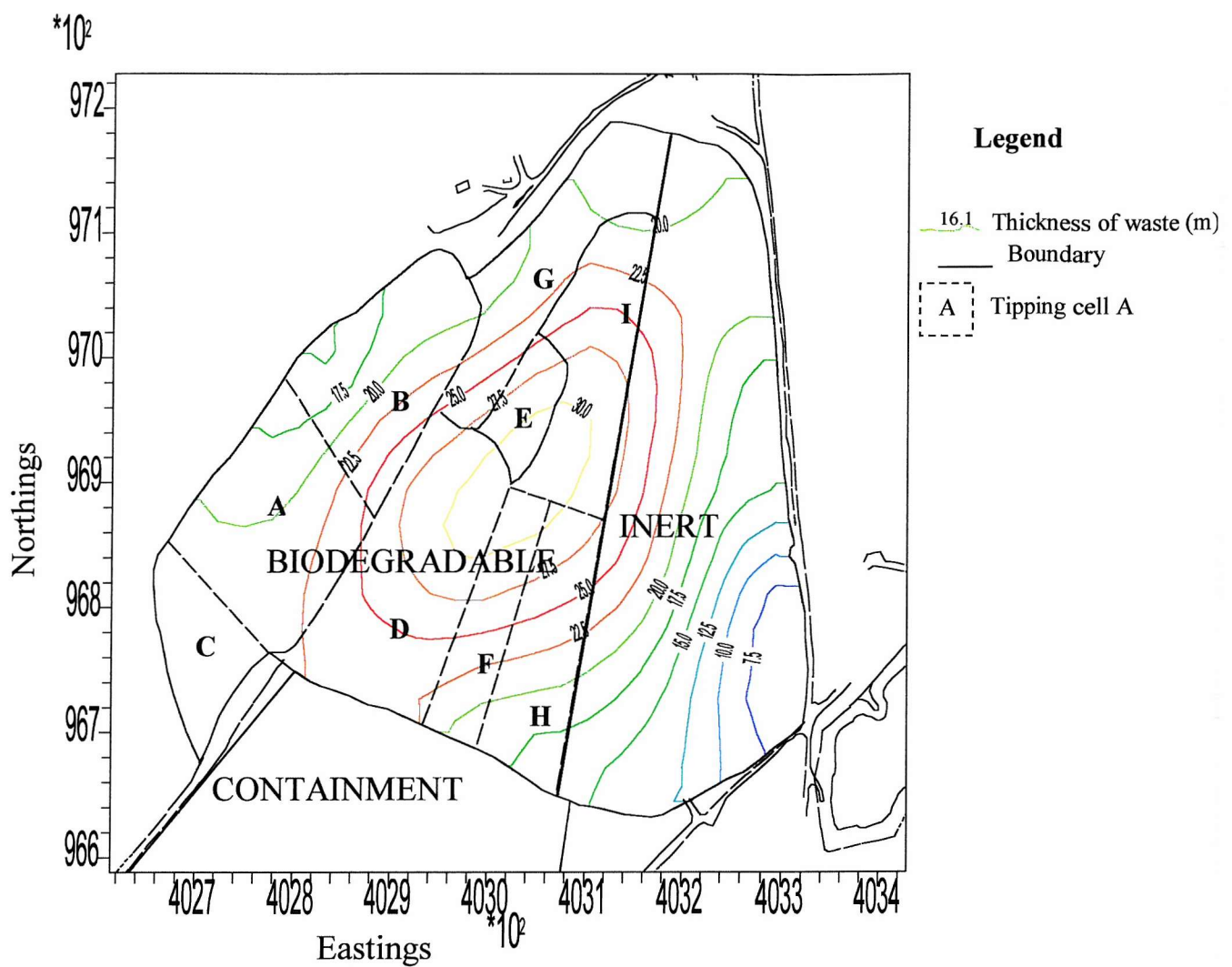


Figure 4.6: The tipping cells and waste thickness at the site

clay is stiff and therefore suitable as a platform for refuse infilling, and also for clay capping. The excavated sand that cannot be sold is used as a daily soil cover for the waste placed at the site. The site thus appears suitable for refuse landfilling.

CHAPTER

5

Field Investigations into Changes in the Properties of an Emplaced Refuse Fill

5.1 Summary

This chapter describes the determination of common physical properties such as density, porosity, absorption, and field capacity of emplaced refuse fills at the site. These were determined following excavation of emplaced refuse, followed by controlled tests on recompacted samples in 210-litre drums. The determination of the rate of post-closure compression, and the cone penetration tests undertaken to study in situ properties of the emplaced refuse at various depths are also presented.

The impact of overburden stress on the physical properties of emplaced refuse lifts during the fill period is discussed. The influence of other factors including daily cover and biodegradation on the properties of the particulate refuse is also considered.

5.2 Introduction

The landfill process has been reviewed in Chapter 2. Beaven and Powrie (1995), and Bleiker et al. (1995) simulated the impact of applied vertical stress on refuse layers and reported that the physical properties of refuse fills such as density, porosity, and field capacity change with increasing sequential loading. These changes were further investigated in field tests undertaken on the refuse fill at White's pit, Poole. The tests were necessary, as the temporal variation in properties of refuse were required for the

(modified) simulation technique to determine moisture stored in the landfill in Chapter 9.

5.3 Test Pits

Test pits have always been vital to the ground investigation of a landfill, even though they are usually limited to the unsaturated upper zone (< 4m) of the landfill.

Observations of the spoil from test pits usually reveal the nature, composition and the variability of the refuse fill. Gifford et al. (1990) stated that test pits could potentially yield more continuous visual information on emplaced refuse than conventional borings.

Some of the important physical properties of refuse fill that can be determined in situ from test pits include the unit weight and the hydraulic conductivity. However, the hydraulic conductivity measurement was not conducted in situ in this study, as the landfill operator did not approve it. Some refuse properties (field capacity, porosity, and absorption capacity) that are also difficult to determine in situ are usually obtained from tests on large representative samples of the refuse that are compacted to the in-situ density. Landva and Clark (1990) reported that results from such tests are comparable to the in-situ properties of refuse.

Currently, there is no universal classification system used to identify waste components but researchers usually group similar constituents of refuse together. Sowers (1973) classified waste into the following: Garbage; Paper and cloth; Lawn and garden refuse; Hollow metal; Massive metal; Rubber; Glass; Lumber from demolition; Rubble; and Ashes and chemical wastes. Considering the variability in the degradation rate of waste components, Landva and Clark (1990) however, proposed that waste can be classified into the following: Organic putrescible; Organic non-putrescible; Inorganic degradable; and Inorganic non-degradable.

The refuse properties determined from pit tests in this study include density, classification, moisture content, field capacity, absorption capacity, and porosity of the excavated refuse. The refuse density was determined in situ while other tests were carried out in the laboratory.

5.3.1. Density of Emplaced Refuse

Excavation of Pit

Prior to the commencement of works, the grid positions of the pits were measured with a Global Positioning System (GPS) in order to locate the pits correctly on the topographical map of the site (Figure 5.1). Preliminary survey indicated that an average of six readings was needed for accurate location with a GPS 45XL (Solomat, 1994).

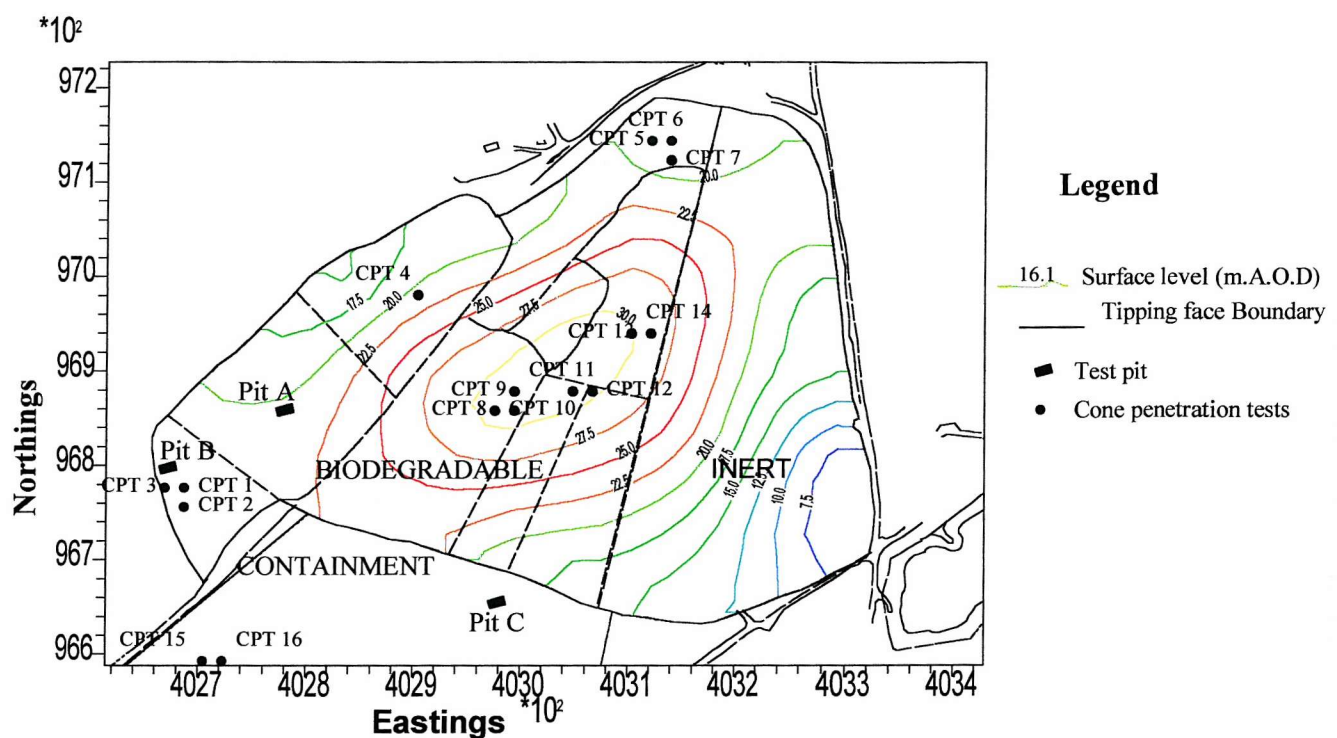


Figure 5.1: Locations for test pits and cone penetration tests.

Experimental pits were excavated at pit A and pit B in the dilute and disperse area, and pit C in the containment area of the site (Figure 5.1). However, the excavation at pit B, which was located at the edge of the landfill, was refilled because the excavated material consisted mainly of soil materials. The terrain of the site locations at pit A and pit C was flat, therefore enhancing access during excavation of the pits. The

topmost refuse lift at pit A was covered with approximately 1 m clay soil in 1984 while the topmost refuse lift at pit C was covered with about 0.5 m clay soil in 1993. These locations were chosen to compare changes in properties of the refuse lifts under different overburden.

A surface area of 5m x 1 m was marked at each test point with survey pegs, which were tied with a line. A hydraulic excavator was used to dig a pit along the perimeter of the tied lines. (Plate 5.1a). The cover soil materials (topsoil, clay, and daily cover) was stripped to just below the daily cover/waste interface to ensure complete removal of the cover materials. The cover materials were loaded into the tipper truck, which has been previously weighed at the weighbridge, with the bucket of the excavator. The weighbridge has an error of $\pm 10\text{kg}$, which translates to $<\pm 1\%$ (Appendix A) for weighing loads in excess of 20 Mg, which is the total mass of the tipper truck and the soil materials. The errors in all measurements in this study are discussed in appendix A.

Excavation of the refuse was done in small scraping movements to avoid compression of the refuse particles and to create a uniform trapezoidal void (Plate 5.1a). The refuse materials were carefully loaded into six pre-weighed steel drums and a tipper truck (Plates 5.1b & 5.2a). Each drum was sealed and all spills during loading with the excavator were carefully loaded back into the tipper truck with a shovel. The spoil in the tipper truck was then covered with a plastic sheet to prevent moisture loss through evaporation. Ten samples of the waste ($\sim 5\text{ kg}$) were taken periodically to determine the moisture content of the refuse fill. The tipper truck including the excavated waste material, filled steel drums, moisture content samples, and the plastic covering sheets were reweighed at the weighbridge to determine the mass of the excavated refuse from the test pit.

Pit Measurements

Determination of the volume the test pit is always the most difficult task in determining the density of refuse fills from test pit excavations. Landva and Clark (1990) reported that the jagged nature of the walls of test pits and the often very considerable variations in pit dimensions tend to make pit measurements imprecise.



Plate 5.1a: Excavation of a uniform void.



Plate 5.1b: Loading of the spoil into the tipper truck



Plate 5.2a: Loading of spoil into the drums



Plate 5.2b: Drums including the measuring stick

These sources of error were taken into consideration by limiting the width of the pit to the width of the excavator's bucket (~ 1 m) and also taking many measurements.

Unlike previous studies where a sliding stick was used to measure pit dimensions without entering the test pit (Holmes, 1980; Landva and Clark; 1990), an improvised measuring stick (Plate 5.2b) was used in this study. It consists of a portable-measuring instrument called Distomat, which is attached to a wooden rod that was graduated in centimetres. A Distomat is a measuring device commonly used by Surveyors and Builders to quickly measure the internal dimensions of enclosures such as rooms in buildings. The Distomat measures distances by sending an infra red beam to the surface or wall whose distance is to be measured. Through appropriate calibration, the distance measured is immediately displayed on the Distomat screen. The error in measuring with a Distomat is in Appendix A.

The instant measuring mechanism of the distomat enabled readings to be taken faster than the conventional sliding stick, therefore enabling many pit measurements to be taken to improve the volume calculation of the refuse void. The excavator could effectively dig a void of approximately 10 m^3 in pit A due to the length of its arm. The small thickness of the topmost refuse lift at pit B limited the void excavated to approximately 8 m^3 .

In measuring the dimensions of the void, the surface measurements of the width and length of the test pit were measured with a steel tape. Due to the constant width of the void, the measuring instrument was used to measure only the length of the void at constant depths from the ground level to the base of the pit. Eight measurements were taken at evenly spaced distances across the pit at each depth. Measurements were taken by pressing the measuring stick firmly against the wall of the pit and pulling the string, which switches on the distomat. A plumb line was attached to the measuring rod to ensure verticality during measurements. A wooden plank was placed across the pit and adjacent to the measuring stick. The plank served as a horizontal reference line for the measuring stick, thereby ensuring that readings were taken at constant depth across the pit. Preliminary measurements taken by the measuring instrument, close to the surface of the pit were checked against tape measurements, and the Distomat had to be slightly tilted on the wooden stick to enable its line of sight parallel to the

ground surface. The dimensions of the base of the pit were measured with a steel tape because accurate measurements could not be obtained with the Distomat due to obstructions caused by jagged refuse at the bottom of pit.

The volume of the pit includes in situ volumes of the excavated topsoil, clay, daily cover, and refuse. A schematic of the test pit is shown in Figure 5.2. Ten measurements each of the thickness and the bottom length of the composite cover soil (topsoil, clay, and daily cover) was undertaken to enable the volume calculations of the cover soil system.

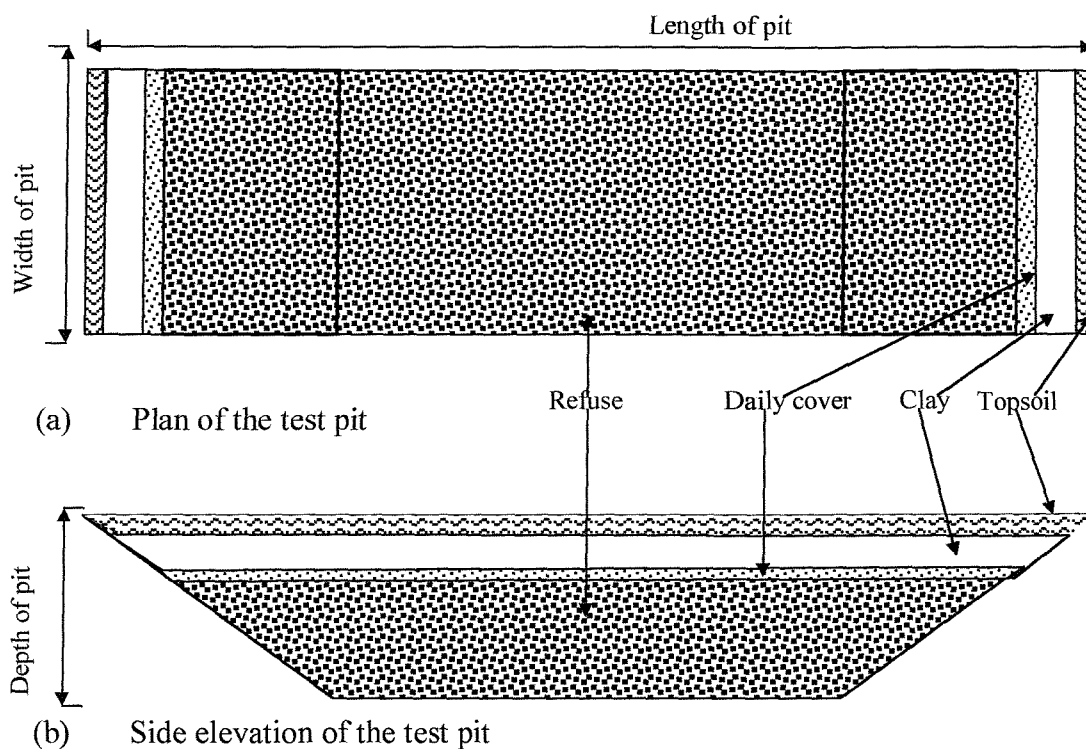


Figure 5.2: Schematic of the test pit

5.3.2 Physical Composition of the Emplaced Refuse

The physical composition of refuse disposed to landfills is usually of considerable interest. Qdais et al. (1997) and Musa and Ho (1981) reported that the quantities and composition of refuse is an essential preliminary step in effective management of

municipal refuse. The physical composition of refuse disposed to landfills varies within and in landfills (Tchobanoglous, 1993).

Fresh refuse, in addition to aged refuse was excavated from the working face of the containment area of the site for testing in the laboratory. The refuse samples for classification tests were stored and transported in plastic bags from the site to the laboratory to prevent loss of moisture through evaporation. The refuse was sorted into the following categories (Beaven and Powrie, 1995; Weymouth and Sherborne Recycling. 1997): Paper and cardboard; Thick plastic; Thin plastic; Textiles; Glass; Food waste; Ferrous metals; Non-ferrous metals; Combustible; Garden, Wood, Rubble; and Fines < 10 mm.

40 kg refuse samples from the landfill were sorted by hand in 5 kg sub-samples into the constituents listed above. Sorting small quantities of the refuse reduced evaporation of moisture that would have occurred from the surface of the bulk sample. The particles sorted were put in plastic bags which had been previously weighed to further minimise moisture lost through evaporation. The process involved immediate sorting of the putrescible food and then, particles that were distinct and easy to handle (fraction size > 10 mm). Some of the small waste particles of paper and cardboard were partially decomposed and therefore required extreme care to separate the compost from the non-degraded matter. The smaller particles were gently sieved through a 10mm sieve, of the type normally used in particle size distribution tests. The particles retained on the sieve were sorted into the various refuse components. The particles less than 10 mm constituted the fines and were put into plastic bags. Soil particles that adhered to the waste components were carefully removed with a small medium hard brush and added to the fines. Finally, the plastic bags including the waste components were reweighed to determine the proportion of each refuse component in the emplaced fill.

The in situ (non-evaporated) masses of the sorted refuse components were determined from their dry masses and in situ moisture contents*. The samples of the sorted refuse

* $M_{wet} = M_{dry} (m_{dry} + 1)$. M_{wet} and M_{dry} are wet and dry masses of each refuse component respectively. m_{dry} is the gravimetric dry moisture content of each refuse component.

components (excluding the non-absorbent components; glass and metals) were dried in an oven at 105°C for 24 hours (BS 1377 Part 2) to obtain their dry masses. The in situ moisture contents (by dry mass) of the components were determined by drying the refuse components, which have not been previously exposed or handled in the oven at 105°C for 24 hours. Samples up to 10kg of the waste were dried in a number of pans, this being the capacity of the available drying pan and oven.

A sieve analysis (BS 1377: Part 2) was undertaken on the dry samples of fines less than 10 mm in the refuse samples to determine the particle size distribution of their particles. A sample of the daily cover material used at the site was also dried and sieved to determine any similarity or interaction between the fines in the emplaced refuse and its overlying cover material.

5.3.3 Porosity, Absorption Capacity and Field Capacity of the Emplaced Refuse

Landva and Clark (1990) reported that visual examination alone is not adequate for geotechnical classification of emplaced refuse. Some of the most important physical properties of refuse often required for design and operation of a waste disposal facility include porosity, absorption capacity, and field capacity. These properties are very difficult to determine in situ and are often obtained from controlled tests in large cells (Beaven and Powrie, 1995).

The porosity, absorption capacity, and field capacity of emplaced fresh refuse and emplaced refuse in pit A and pit B were determined in the laboratory. The tests for each refuse type were carried out in three 210-litre steel drums, which have been previously weighed. The refuse was loaded into each of the drums to the in situ density of the emplaced refuse fills. The field density of the emplaced refuse in pit A and pit B (Table 5. 3) were determined on site while an in situ unit weight of 5.88 kN/m³ (Huc, 1997), was used for the fresh refuse fill. Measured quantities of loose refuse were loaded into the drum in small volumes and compacted in 15 cm layers to the in situ density (15 cm-depths were marked on the drum). The compaction was undertaken uniformly in the drum with a 10 kg steel plated rammer (Plate 5.3a).

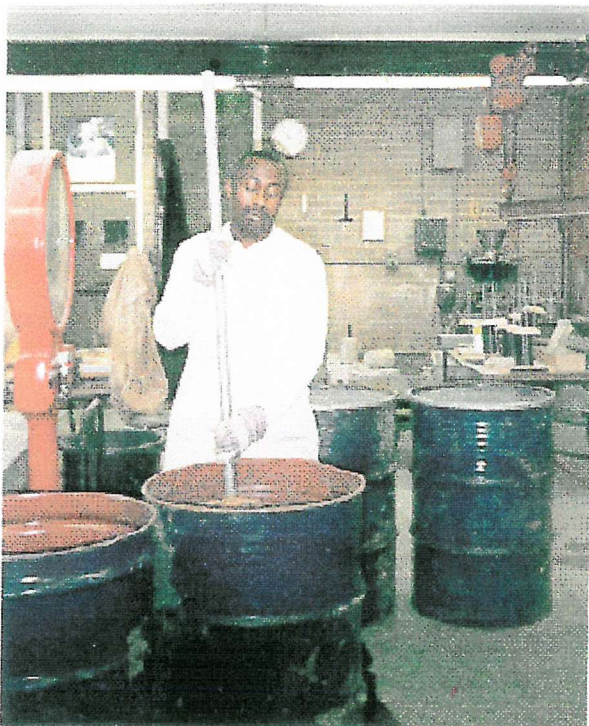


Plate 5.3a: Compaction of small refuse loads with a steel plated rammer



Plate 5.3b: Draining water from the compacted refuse in the drum

In cases where adequate compaction was difficult to achieve (as in fresh waste), a measured quantity of water was applied to enhance workability.

After compaction, the drum was sealed to minimise moisture loss through evaporation. The sealed drum was tilted to approximately 60°C to the horizontal by an overhead hydraulic lift and small measured quantities of water were applied carefully through one of the two openings at the top of the drum. The drum was vibrated at regular intervals to remove any trapped air through the openings in the steel drum lid. As the wetting of the refuse with water progressed, the steel drum was gradually tilted back to the vertical position, allowing the waste to be thoroughly saturated with water. The process took between 48 hours and 60 hours for complete saturation of the refuse in each of the nine steel drums used for the experiment.

When the saturation process was completed, the steel drum was weighed and then overturned so that water could drain away under gravity (Plate 5.3b). During the initial drainage stage, the outflow was rapid and the drained water was collected and weighed immediately. In the later stages, the outflow was very slow and the drainage was collected with a container having a small surface area to minimise evaporation. The experiment was stopped when there was no drainage from the drum over a period of 6 hours. The steel drum was then reweighed to determine the volume of water drained from the saturated refuse under gravity and the volume of water absorbed by the refuse fill.

5.3.4 Results

The lengths of the pits recorded at various depths from ground level to the base are shown in Tables 5.1 and 5.2. Measurements of lengths were taken at 0.3 m-depth intervals in pit A and mainly at 0.2 m-depth intervals in pit C. The longitudinal cross sectional areas of the pits were obtained from a summation of the area enclosed by adjacent lengths measured at regular depth intervals (footnote page 71). With average top and base lengths of 4.84 m and 2.06 m, and an average cover soil thickness of 1.59 m, the longitudinal cross sectional area of the refuse and composite soil cover in pit A were 6.54 m² and 3.86 m² respectively (Table 5.3). Similarly, the longitudinal

Table 5.1: The length of Pit A at regular depth intervals

Depth to the base of pit (m)	Length of the pit (m)								Average length (m)	
	Points of measurement along the width of pit									
	1	2	3	4	5	6	7	8		
3.0	4.89	4.91	4.80	4.78	4.79	4.83	4.86	4.84	4.84	
2.70	4.60	4.64	4.67	4.63	4.59	4.61	4.59	4.61	4.62	
2.40	4.32	4.29	4.34	4.36	4.33	4.34	4.34	4.30	4.33	
2.10	3.93	3.96	4.03	4.05	4.04	3.98	3.95	3.89	3.98	
1.80	3.76	3.69	3.61	3.75	3.87	3.80	3.78	3.80	3.76	
1.50	3.48	3.49	3.53	3.46	3.51	3.54	3.53	3.53	3.51	
1.20	3.11	3.12	3.14	3.17	3.15	3.13	3.14	3.13	3.14	
0.90	2.91	2.89	2.94	3.01	2.87	2.97	2.89	2.88	2.92	
0.60	2.59	2.60	2.58	2.62	2.60	2.54	2.57	2.61	2.59	
0.30	2.35	2.43	2.29	2.35	2.37	2.28	2.33	2.36	2.35	
0.00	2.07	2.06	2.04	2.07	2.05	2.05	2.06	2.08	2.06	

Table 5.2: The length of Pit B at regular depth intervals

Depth to the base of pit (m)	Length of the pit (m)								Average length (m)	
	Points of measurement along the width of pit									
	1	2	3	4	5	6	7	8		
1.87	4.91	4.93	4.99	4.98	4.96	5.01	5.02	4.99	4.97	
1.67	4.79	4.81	4.77	4.80	4.83	4.79	4.81	4.77	4.80	
1.47	4.55	4.59	4.57	4.52	4.55	4.57	4.52	4.51	4.55	
1.27	4.45	4.47	4.51	4.55	4.49	4.43	4.44	4.43	4.47	
1.07	4.30	4.34	4.31	4.29	4.36	4.28	4.32	4.30	4.31	
0.87	4.01	3.97	3.99	4.02	3.96	4.04	3.94	3.92	3.98	
0.67	3.79	3.82	3.84	3.78	3.87	3.94	3.93	3.90	3.86	
0.47	3.63	3.69	3.73	3.67	3.62	3.58	3.60	3.57	3.64	
0.27	3.48	3.52	3.49	3.51	3.53	3.49	3.51	3.47	3.50	
0	3.19	3.23	3.24	3.22	3.21	3.24	3.25	3.23	3.23	

Table 5.3: Unit weights and overburden of refuse and composite cover soil at pits**A and C**

Material		Age (Approximate) (yrs)	Thickness of emplaced material in pit (m)	Cross sectional area of pit ¹ (m ²)	Volume of Refuse (m ³)	Mass of refuse (kg)	Unit weight (kN/m ³)	Total overburden vertical stress ² (kPa)
Pit A	Cover Soil	14	1.59	6.54	6.28	11780	18.40	14.63
	Refuse	14	1.41	3.86	3.70	4430	11.75	37.54
Pit C	Cover Soil	5	0.91	4.07	3.91	7250	18.19	8.28
	Refuse	5	0.96	3.61	3.47	2640	7.46	20.13

¹ Pit A:

Cross sectional area of pit A

$$=0.3*0.5*(4.84+2.06+2(4.62+4.33+3.98+3.76+3.51+3.14+2.92+2.59+2.35))$$

$$=10.40 \text{ m}^2: \text{Average thickness of cover soil} = 1.59 \text{ m} : \text{Length of base of cover soil} = 3.39 \text{ m}$$
Cross sectional area of emplaced cover soil in pit A = $0.5*1.59*(4.84+3.39) = 6.54 \text{ m}^2$ Cross sectional area of emplaced refuse in pit A = $10.40 - 6.54 = 3.86 \text{ m}^2$

Pit B:

$$\text{Cross sectional area of pit B} = 0.2*0.5*(4.97+3.50+2(4.80+4.55+4.47+4.31+3.98+3.86+3.64)) + 0.27*0.5*(3.23+3.50) = 7.68 \text{ m}^2$$

Average thickness of cover soil = 0.91 m : Average length of the base of cover soil = 3.98 m

Cross sectional area of emplaced cover soil in pit B = $0.5*0.91*(4.97+3.98) = 4.07 \text{ m}^2$ Cross sectional area of emplaced refuse in pit B = $7.68-4.07 = 3.61 \text{ m}^2$ ² Pit A:

$$\text{Average overburden stress on refuse layer (excluding self weight of refuse layer)} = 18.40*1.59 = 29.26 \text{ kPa}$$

$$\text{Total overburden stress on refuse layer} = 0.5*11.75*1.41 + 29.26 = 37.54 \text{ kPa}$$

$$\text{Average self weight of composite soil cover} = 0.5*29.26 = 14.63 \text{ kPa}$$

Pit B:

$$\text{Average overburden stress on refuse layer (excluding self weight of refuse layer)} = 18.19*0.91 = 16.55 \text{ kPa}$$

$$\text{Total overburden stress on refuse layer} = 0.5*7.46*0.96 + 16.55 = 20.13 \text{ kPa}$$

$$\text{Average self weight of composite soil cover} = 0.5*16.55 = 8.28 \text{ kPa}$$

cross sectional area of the refuse and composite soil cover in pit C were 4.07 m^2 and 3.61 m^2 respectively.

A unit weight or specific weight is the weight of material per unit volume and is often used in waste technology to express the density of refuse (Tchobanoglous (1993)). The unit weights of the emplaced refuse and the overlying composite cover soil at pit A were 11.75 kN/m^3 and 18.40 kN/m^3 respectively. Likewise, the unit weight of the refuse layer at pit C was 7.46 kN/m^3 ; the unit weight of its overlying cover soil system was 18.19 kN/m^3 .

The refuse layer and composite soil cover in each pit were unsaturated, therefore, the total overburden stress on the refuse layers was taken as the effective vertical stress. The effective vertical stress on the refuse layer at pit A was 37 kPa while that of Pit C was 20.13 kPa. The vertical stress on the composite soil cover layer at pit A and pit C, which are also their self weights were 14. 63 kPa and 8.28kPa respectively.

The physical composition of fresh and aged refuse obtained from site is shown in Table 5.4. Paper and cardboard components have the highest percentage in the fresh and 5-year old refuse. The percentage of paper and cardboard was however, less than the fines in the 14-year old refuse. The percentages of paper and cardboard in fresh refuse, 5-year old refuse, and 14-year old refuse were 34.91%, 47.87%, and 16.16% respectively.

The proportion of fines in the refuse appeared to increase with the age of refuse. The percentages of fines were 6.89 %, 11.87 %, and 49.78 % in fresh refuse, 5-year old refuse, and 14-year old refuse respectively. In contrast, the percentage of green/garden waste and food in the refuse decreased with age of emplacement. The proportion of green/garden waste were 16.32%, 6.59%, and 0.89% while the proportion of food waste were 12.48%, 2.56%, and 0.37% for fresh refuse, 5-year old refuse, and 14-year old refuse respectively.

Table 5.4: Physical composition and moisture content of fresh and aged refuse obtained from the site

Component	Percentage by wet mass (%)			Moisture content (% by wet mass)		
	Fresh refuse	5-year old refuse	14-year old refuse	Fresh refuse	5-year old refuse	14-year old refuse
Paper and cardboard	34.91	47.87	16.16	9.84	61.70	63.44
Thick plastic	3.70	3.40	1.09	1.50	1.50	1.50
Thin plastic	5.73	8.45	6.63	2.50	1.50	1.50
Textiles	1.82	2.15	0.34	7.50	36.60	36.00
Glass	4.29	3.44	2.91	nd	nd	nd
Food waste	12.48	2.56	0.37	78.00	59.00	48.15
Ferrous metals	4.55	4.29	2.27	nd	nd	nd
Non-ferrous metals	1.49	0.88	0.65	nd	nd	nd
Combustible	6.43	4.01	5.33	6.50	6.50	23.00
Green/ garden waste	16.32	6.59	0.89	65.00	65.00	58.42
Wood	0.61	0.86	0.24	20.63	36.63	35.59
Rubble	0.78	3.64	13.34	5.94	5.94	4.99
Fines<10mm	6.89	11.87	49.78	17.36	17.36	28.57
Total	100.00	100.00	100.00	na	na	na
Average ³	na	na	na	25.90	39.15	27.38
Measured	na	na	na	28.09	36.27	33.58

nd – not determined.

na – not applicable

³ Average moisture content = $\sum (m_a * P_a)$: where m is the gravimetric moisture content of waste component, and P is the percentage of wet mass of waste component a in the wet bulk mass of the waste.

The in situ gravimetric moisture contents of the fresh and aged emplaced refuse are shown in Table 5.4. As expected, the refuse components with significant moisture contents were the materials with relatively absorbent characteristics. i.e. paper and cardboard, textiles, food waste, garden waste, and wood.

Food waste had high moisture content in both the fresh and aged refuse, and its moisture content seems to decrease with increasing age. In contrast, the moisture content of paper and cardboard seems to increase with increasing age, although it remains constant once field capacity is reached. The increase in moisture content of some materials such as wood and rubble, which have been exposed to precipitation before disposal at the landfill was not as significant as highly absorptive cardboard and paper. The moisture content of the aged refuse particles is at field capacity (Beaven and Powrie, 1996).

The overall moisture content of the refuse was influenced by the percentage of absorbent materials present, particularly paper and cardboard. The calculated moisture contents of the fresh refuse, 5-year old refuse, and 14-year old refuse were 25.90%, 39.15%, and 27.38% respectively. These, however, vary slightly from the measured values, which were 28.09%, 36.27%, and 33.58% for fresh refuse, 5-year old refuse, and 14-year old refuse respectively. The variance was likely to be due to the exclusion of the moisture content of glass and metals from the calculations. Even though these materials have a negligible absorption capacity, the moisture that adhered to their surface cannot be neglected.

The particle size distribution curves of fines (< 10 mm) in the refuse and the daily cover soil used at the site are shown in Figure 5.3. The daily cover soil can be classified as slightly silty/clayey gravelly sand and the fines in the 5-year-old, and 14-year old refuse as very gravelly sand and slightly silty/clayey very gravelly sand respectively.

The results of the porosity, absorption, and field capacity of the fresh and aged refuse are shown in Table 5.5. The initial moisture content of the refuse was previously determined as described in Section 5.3.2. The drainage porosity is the porosity at field capacity, and is therefore the effective porosity relevant to water flow in refuse. The

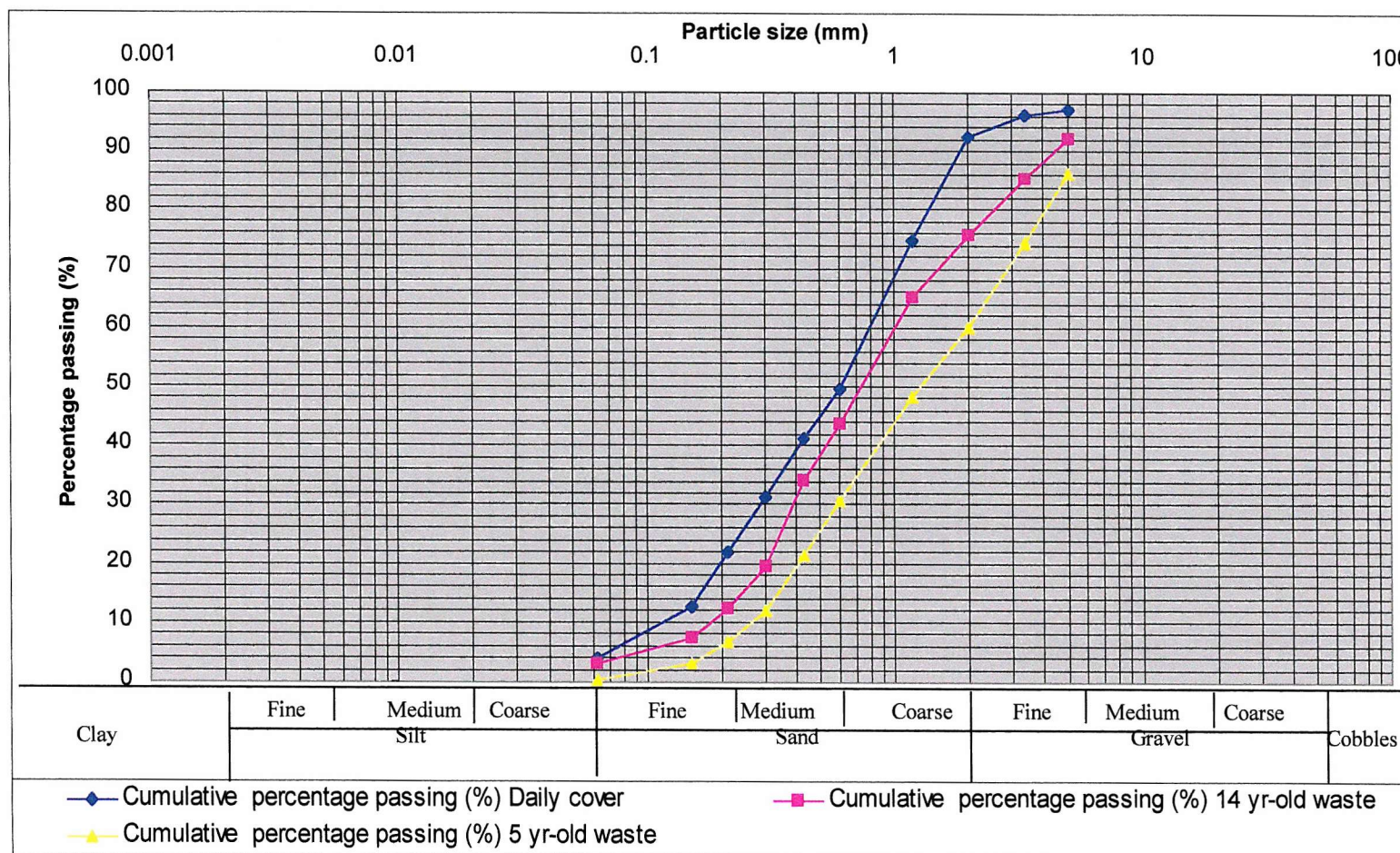


Figure 5.3: Particle size distribution curves of fines (<10mm) in refuse and the cover soil at the site

Table 5.5: Absorption, porosity and field capacity of fresh and aged refuse.

Age (years)	Bulk volume of waste (litres)	*Density kg/m ³ (wet)	Initial MC w/w (dry)	Initial MC ⁴ (v/v)	Volume added to saturate (litres)	Volume drained under gravity (litres)	Drainage ⁵ Porosity (v/v)	Absorption ⁶ (v/v)	Field ⁷ Capacity (v/v)	Porosity ⁸ @initial MC
Fresh	210	600	0.391	0.169	108.00	63.80	0.304	0.210	0.379	0.514
5	210	760	0.569	0.276	84.17	60.35	0.287	0.067	0.389	0.401
14	210	1198	0.506	0.402	48.00	38.28	0.182	0.046	0.449	0.229

MC – Moisture content; w/w – weight by weight (gravimetric ratio); v/v – volume by volume (volumetric ratio)

⁴ Volumetric moisture content (v/v) = (Initial) dry gravimetric moisture content x Bulk density of refuse / Density of water

⁵ Air porosity = (volume of water drained) / (Bulk volume of waste)

⁶ Absorption = (Volume of water added to saturation – Volume of water drained under gravity) / Bulk volume of waste

⁷ Field capacity = Initial moisture content + Absorption

⁸ Porosity at initial moisture content = Air porosity + absorption

drainage porosity of refuse decreased with increasing density and initial moisture content. The fresh refuse, which had initial moisture content of 0.169 and unit weight of 5.89 kPa had a drainage porosity of 0.304. Whereas the 5-year old and 14 year old refuse, which have much higher unit weights of 7.46 kPa and 11.75 kPa and initial moisture contents of 0.569 and 0.506 respectively have low drainage porosity values of 0.287 and 0.182 respectively.

As in the classification tests, the absorptive capacity of the refuse decreased with increasing initial volumetric moisture content. In contrast, the volumetric field capacity of the refuse increased with increasing initial volumetric moisture and density. The absorption capacities of the fresh, 5-year old refuse and 14 year-old refuse were 0.210, 0.067, and 0.046 respectively. Their field capacities were 0.379, 0.389 and 0.449 respectively.

5.3.5 Discussion

The density of emplaced refuse is a vital physical property used in the design and assessment of a waste disposal facility (Beaven and Powrie, 1999; Beaven, 2000). Typical uses of refuse density include estimating the effective stress in the waste mass, and the refuse volume that will be placed at a landfill site. The mean density of fresh emplaced refuse at the site is 5.89 kN/m³ (Huc, 1997). Typical densities of emplaced refuse in landfills are shown in Table 5.6.

Results from the pit tests show an increase in density of the emplaced refuse with overburden stress and age (Table 5.3). These support previous studies by Holmes (1980) which showed an increase in refuse density with age and Bleiker (1995), and Beaven (2000) that reported an increase in density with applied vertical stress. The activity responsible for temporal changes in refuse density is biodegradation, which reduces waste particles leading to refuse settlement. The extent and rate of biodegradation depend on many factors including the pH of interstitial water, presence of oxygen, the composition and particle size of the refuse, and the type of organic material present

Table 5.6: Typical unit weights of emplaced refuse fills

Type of refuse	Unit weight kN/m ³	Source
Normally compacted crude MSW	3.55 – 4.88	Tchobanoglous (1993)
Well compacted crude MSW	5.80 – 7.28	Tchobanoglous (1993)
Fresh crude domestic waste	5.23 – 5.80	Blakey (1982)
Pulverised domestic waste	7.85 – 9.81	
Crude domestic waste	6.12	Adapted from Holmes (1980)
4-year old crude domestic waste	6.26	Holmes (1980)
10-year old crude domestic waste	7.99	Holmes (1980)
17-year old crude domestic waste	9.42	Holmes (1980)

(Lu et al., 1985). Consequently, the extent of the impact of age on increased density of the emplaced refuse could not be determined from the pit (physical) tests alone. The densities of the emplaced refuse were higher than that of similar aged refuse tested by Holmes (1980). This may be attributed to variation in waste composition, initial compactive effort, overburden stress, moisture conditions, and errors in void volume measurements in the studies, among others. Landva and Clark (1990) reported the error in measuring refuse voids to be up to $\pm 15\%$, with the number of typical measuring points to be 50. The measured points in tests pits A and B were more; 88 and 80 respectively, and as such, the error in volume (and also density) calculations of the pits is expected to be lower than in previous studies.

As expected, the porosity of the refuse decreased with increasing density (Table 5.5). The classification tests and grading curves suggested that part of the daily soil cover migrated into the underlying emplaced refuse. The sifting of the daily soil cover was likely to be caused by differential settlement of the particulate waste. The ravelled soil would further reduce porosity and increase density of the emplaced refuse.

Results from the drum tests (Table 5.5) also showed similar changes in refuse behaviour with previous investigations (Blight et al., 1992; Beaven and Powrie, 1995). The field capacity increased with refuse density and age while the absorption capacity, as expected, decreased with increasing initial moisture content. An increase in field capacity with density indicates that the rate of decrease of the refuse pores is more than the reduction in water held under gravity as the waste compresses. As the applied load is increased, more water is squeezed out of the refuse particles and the increase in field capacity diminishes (Figures A2).

Based on the observations from the results of the tests, the impact of vertical stress on the particulate refuse at the site is depicted with a schematic of the emplaced refuse layer in Figure 5.4. In the initial condition, there were no external forces ($\sigma'_v = 0$), and the height of the refuse layer was the same as that immediately after placement (Figure 5.4a).

Upon the application of load (σ'_v), vertical stresses were distributed only onto the contact areas within the waste mass. The stresses exerted onto the initial refuse contact points were higher than the localised stress concentration caused by the application of the overburden. This resulted in the collapse of weaker components of the refuse and the sifting of the small particles into the interstices Figure 5.4b. The small particles included the refuse fragments and part of the overlying daily soil cover. The density of the refuse layer therefore increases due to a decrease in its overall volume (thickness). Some of the factors that might influence the magnitude of compression of the refuse mass included the applied vertical stress, the initial void ratio, and height of the refuse layer. The magnitude of immediate settlement of a refuse fill can be estimated from equation 2.1.

After the immediate compression, the refuse layer continued to settle mainly due to continued failure of the structures of individual refuse components. Settlement due to these effects is likely to be enhanced by infiltration of surface water leading to increased wetting of absorbent components such as cardboard, whose strength decreases rapidly with increased moisture content.

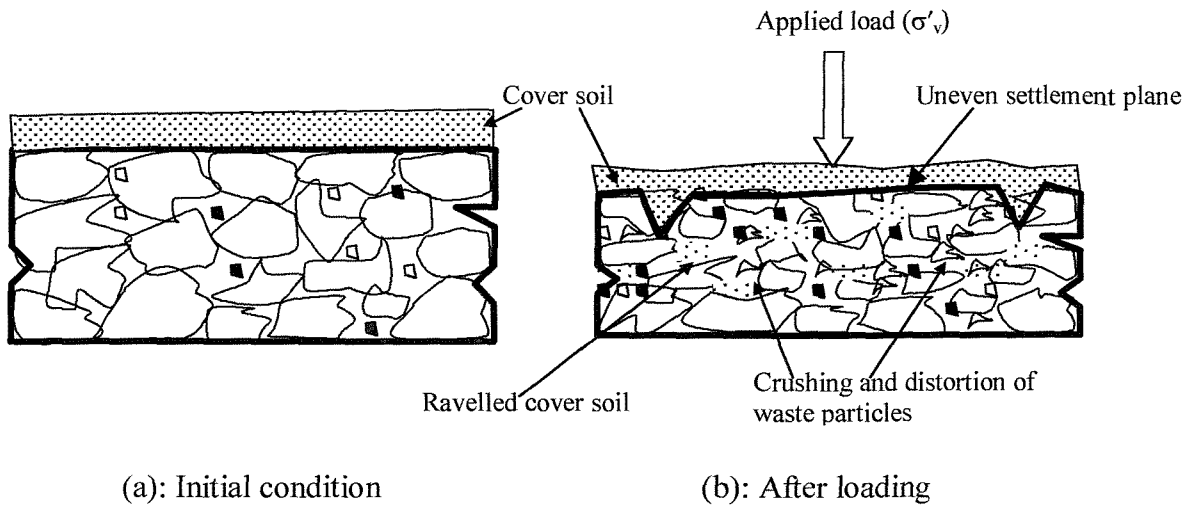


Figure 5.4: Differential settlement and ravelling of daily cover materials

In general, the changes in the properties of emplaced refuse in the test pits were similar to results from previous studies in test cells (Blight et al, 1992; Beaven, 2000), in experimental pits (Holmes, 1980) and simulations (Bleiker and Farquhar, 1995). The ravelling of the daily soil cover was expected to enhance (also modify) these changes, however, the classification and grading tests were not sufficient to determine their extent. Further tests on the ravelling of daily cover into the underlying refuse mass are needed.

The pit tests were undertaken in the unsaturated zone of the landfill, where the effective stress can be approximated to the overburden stress. In the saturated part of a landfill, the submerged unit weight is close to zero. The increase in total stress with depth is balanced by pore water pressures leading to a small change in effective stress in the refuse.

5.4 Determination of Compression Index of the Refuse Fill.

The state of the refuse i.e. density, porosity, and field capacity recovered from the pit tests was as a consequence of the compression experienced by the waste mass. A compression index parameter was required to apply simplified settlement models

(equations 2.2 and 2.3), which were useful in determining temporal changes in waste characteristics in the modified moisture simulation analysis in Chapter 9.

The rate of vertical compression of the refuse fill within the dilute and disperse area of the site (Figure 5.1) was determined from the level survey maps of Whites pit for 1985, 1986, 1987, and 1990 (Dorset county Council, 1997). Only the secondary compression of the fill was determined from the survey maps as they were compiled following closure.

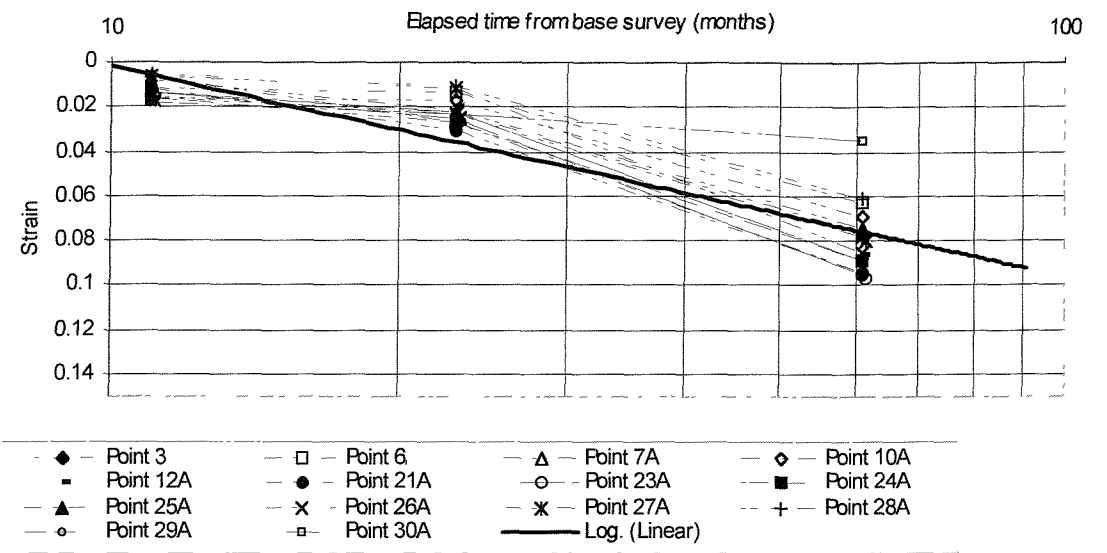
The landfill is underlain by stiff Broadstone clay, which is considered to have insignificant settlement potential due to the overlying refuse loading. Therefore, the total settlement observed from the maps was assumed to be solely due to the compression of the emplaced refuse.

The temporal elevations and the locations of key survey points are shown in Table 5.7. Each survey point represents a “fill column”, which is a unit column comprising of layers of waste and thin earth cover layers, on the basal Broadstone clay. A record of the phases of tipping at the site (Table 4.2) enabled the closure periods of the fill areas of the site to be determined. However, some parts of the completed landfill areas, which experienced significant differential settlements, were refilled with inert materials to re-profile the capping system. These areas were identified and their spot heights were not considered in the vertical compression analysis of the refuse fill.

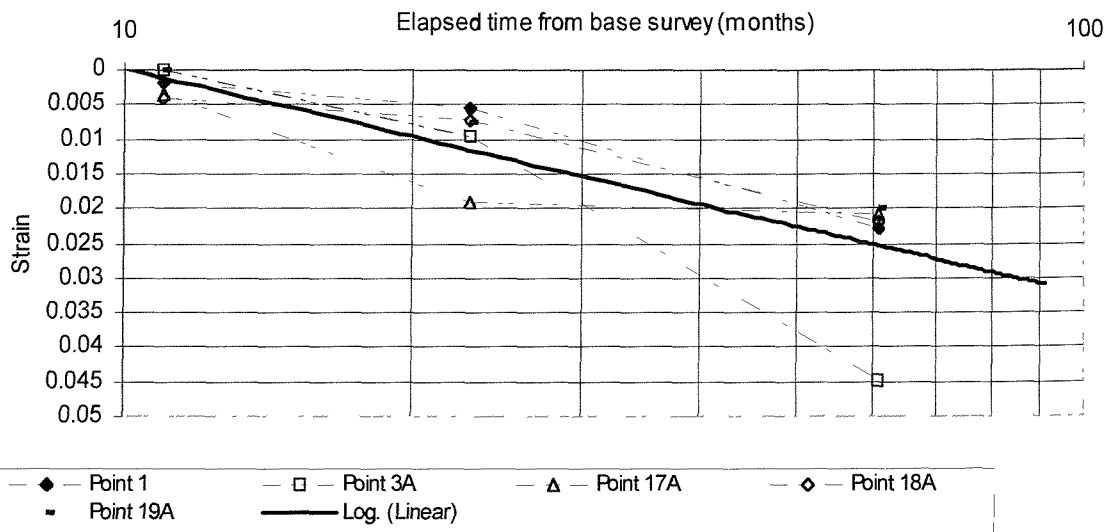
The initial thickness of the refuse fill was obtained by subtracting the spot height of the top of the basal Broadstone clay (Figure 4.4) from the spot heights of the refuse fill in 1985. The plot of vertical strain against logarithm of time for the restored part of the site is shown in Figure 5.5 (a & b). The survey data of 1985 were used as the baseline in calculating the vertical strain of the emplaced refuse. This period is close to the time of final placement of the cover soil system at the areas (Tipping areas A & C) of concern.

Table 5.7: The temporal spot heights at the site

Year	Spot height at non-boundary areas (m AOD)							
	Point 3 402700E 96850N	Point 6 402700E 96800N	Point 7A 402725E 96850N	Point 10A 402725E 96825N	Point 12A 402700E 96825N	Point 21A 402687.5E 96850N	Point 22A 402687.5E 96837.5N	Point 23A 96837.5N 402700E
1/7/85	61.73	63.15	62.20	62.92	62.56	62.01	61.93	62.25
5/6/86	61.60	62.88	62.02	62.54	62.27	61.75	61.70	61.95
6/87	61.13	62.84	61.72	62.54	62.12	61.35	61.57	61.69
1/8/90	59.67	61.70	60.55	61.33	60.61	59.93	59.89	60.13
Year	Spot height at non-boundary areas (m AOD)							
	Point 24A 402712.5E 96837.5N	Point 25A 402725E 96837.5N	Point 26A 402687.5E 96825N	Point 27A 402712.5E 96825N	Point 28A 402687.5E 96812.5N	Point 29A 402700E 96812.5N	Point 30A 402712.5E 96812.5N	
1/7/85	62.48	62.62	62.26	62.81	62.50	61.93		63.11
5/6/86	62.12	62.25	62.13	62.45	62.37	61.70		62.69
6/87	61.88	62.12	62.00	62.27	62.25	61.57		62.58
1/8/90	60.485	60.89	60.36	61.02	61.13	59.89		62.30
Year	Spot height at boundary areas (m AOD)							
	Point 1A 402712.5E 96837.5N	Point 3A 402725E 96837.5N	Point 17A 402687.5E 96825N	Point 18A 402712.5E 96825N	Point 19A 402687.5E 96812.5N			
1/7/85	58.74	59.83	51.54	56.90	52.10			
5/6/86	58.71	59.83	51.20	56.83	52.10			
6/87	58.64	59.64	51.32	56.78	52.01			
1/8/90	58.31	58.94	51.37	56.53	51.86			



(a) Main areas



(b) Boundary areas

Figure 5.5: Vertical strain versus logarithm of time of the refuse fill.

A linear fit to the plot in Figure 5.5 (a&b) gives the following relationship

$$\varepsilon_v = 0.09 \log t - 0.09 \quad - \text{Main areas} \quad [5.1]$$

$$\varepsilon = 0.03 \log t - 0.03 \quad - \text{Boundary areas} \quad [5.2]$$

where

ε_v = vertical compression of the refuse fill

t = elapsed time during post-closure period

The correlation coefficient for both linear fits is 0.8. From equations 5.1 and 5.2, the secondary compression rate for main landfill site and the boundary area are 0.09 and 0.03 respectively. Sower (1973) related the secondary index to the initial void ratio of the refuse as follows:

$$C_s = \left(\frac{e_0}{1 + e_0} \right) (0.03) : \text{ fills with low rate of biodegradation} \quad [5.3]$$

$$C_s = \left(\frac{e_0}{1 + e_0} \right) (0.09) : \text{ fills with high rate of biodegradation} \quad [5.4]$$

where:

C_s = secondary settlement index of waste layer

e_0 = initial void ratio

Sowers (1973) reported that initial void ratio of refuse fills commonly varies between 15 (uncompacted) to 2 (well compacted). If a void ratio of 2* is substituted in equations 5.3 and 5.4 as seen in Table 5.9, then the refuse fill at the site has a high rate of biodegradation. The compression rate is more than the pre-1980 data in Table 5.8 because of the increased quantity of biodegradable material emplaced in landfills over the years (Hutchinson, 1990; Watts and Charles, 1999). The low compression rate of the boundary areas was a result of the high soil content in the refuse at these areas (Section 5.3.1).

Table 5.8: Compression index of waste (Wall and Zeiss, 1995)

Reference	Primary (C_{ce})	Secondary (C_{se})
Rao et al (1977)	0.16 - 0.235	0.12 - 0.046
Converse (1975)	0.25 - 0.3	0.07
Zoino (1974)	0.15 - 0.33	0.013 - 0.03
Sowers (1973) ($e_0 = 2$)	0.1 - 0.4	0.02 - 0.06
Oweis and Khera (1986)	0.08 - 0.217	—
Landva et al. (1984)	0.2 - 0.5	0.0005 - 0.29
Wall and Zeiss (1995)	0.21-0.25	0.033-0.056

In general, the post-closure settlement of the site shows that the impact of bioconsolidation cannot be neglected. Even though the survey data are limited, the post-closure compression index of the refuse fill showed that the rate of biodegradation at the site is relatively high. Despite the inability to determine the primary (pre-closure) compression of the refuse fill from available survey data, the high post closure settlement justified the high density of the 14- year old refuse, which was determined from the pit tests (Table 5.3).

5.5 Static Cone Penetration Tests

5.5.1 Introduction

Cone penetration tests (CPT) were undertaken at the site to obtain information on waste properties beyond the depth of 3m, being that of the pit test. Landva (1990) stated that

* From Table 5.5, porosity of fresh refuse~0.5. \therefore void ratio = $1/(1-0.5) = 2$

CPT is possible in fine-grained fill but cannot be used in wastes such as domestic and industrial refuse. However, the difficulty in undertaking CPT at the site was seen as a challenge rather than a deterrent, and as such, a number of CPT were undertaken at the site to give allowance for drilling failures.

5.5.2 Testing Technique

The static cone penetration tests were carried out at sixteen locations at the site by GEOCONE, (Figure 5.1). The tests were undertaken using a 20-tonne capacity hydraulic penetrometer equipment mounted onto a lightweight crawler that is ballasted for stability during operation.

The tests were undertaken with both a 10cm^2 and 15 cm^2 two-channel electric friction cone capable of measuring cone resistance and local friction within the waste mass. The total applied load was governed by the reaction of the cone to penetration in the refuse together with the cone end resistance and local side friction sensors within their safe operating mode.

The operation of the CPT equipment has been reported by Georgiou (1998). The cone end resistance and local side friction were registered by load cells housed within the cone and transmitted by an umbilical cable through hollow push rods to a computerised data acquisition system. The rate of penetration was kept constant at 20mm per second except where penetration was in very dense or hard strata. The system provided instantaneous and continuous graphical records of cone end resistance and local side friction on a colour video monitor. The results were also recorded on a personal computer at 10mm depth intervals, thus allowing quick processing and plotting of the data.

The tests at each location were terminated when a combination of the following conditions occurred:

- High load (determined according to degree of rebound of test string)

- High load on the cone tip (generally 90% of rated capacity or suspected eccentric loading)
- Excessive inclination of the cone and test string (3 degrees or rapid inclination in any stroke)

Only three (CPT 7, CPT 11, CPT 14) of the sixteen tests exceeded depths more than 7m into the refuse fill.

5.5.3 Results

The results of CPT 14 are discussed in this chapter since the refuse fill at this location has been relatively undisturbed since completion in 1990. The data for CPT 7 and 11 are in appendix B.

The maximum cone penetration depth at CPT 14 was 7.65m. The pore pressure versus soil behaviour type at CPT 14 is shown in Figure 5.6. The maximum dynamic and static pore pressure within the refuse was 0.07 MPa but was approximately zero in most part of the length of cone penetration. The depth or extent of the standing water at a depth of 3m was not definite.

The cone resistance versus friction ratio for CPT 14 is shown in Figure 5.7 while the soil behaviour type index versus depth is shown in Figure 5.8. Generally, the cone penetration resistance and sleeve friction increase with the depth of cone penetration. However, there were sharp peak values at depths of 1m, 2.5 m, 3.8 m, 6.2 m, and 7.3 m that appeared not to follow any particular pattern in relation to depth. The friction ratio varied mostly between 0.5 % and 5%.

5.5.4 Discussion

The cone penetration tests provided some information about the characteristics of the emplaced refuse fill beyond the depth of the test pits. The near-zero static and dynamic

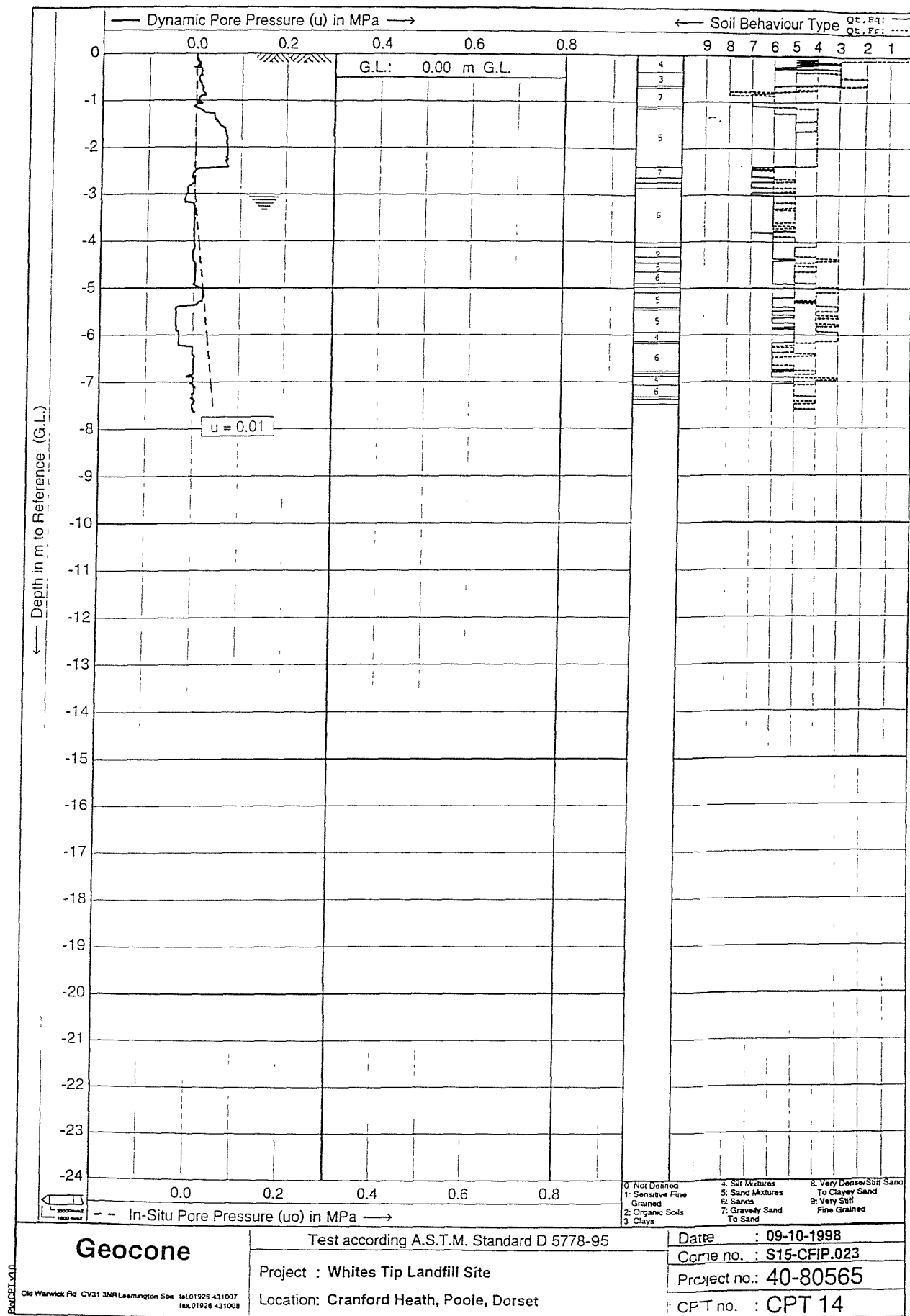


Figure 5.6: Pore pressure and the soil behaviour type vs depth for CPT 14

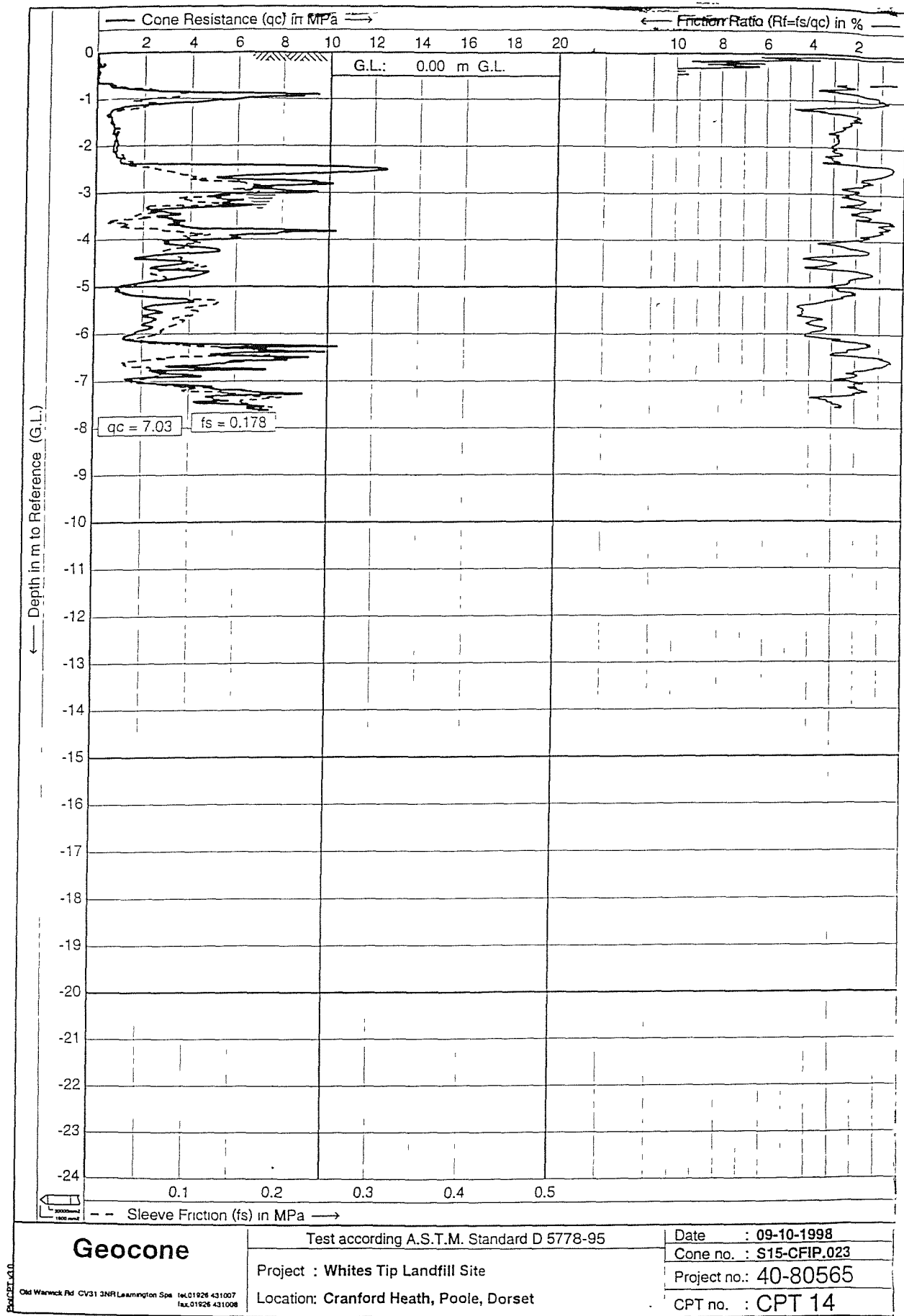


Figure 5.7: The pore pressure and the soil behaviour type vs depth for CPT 14

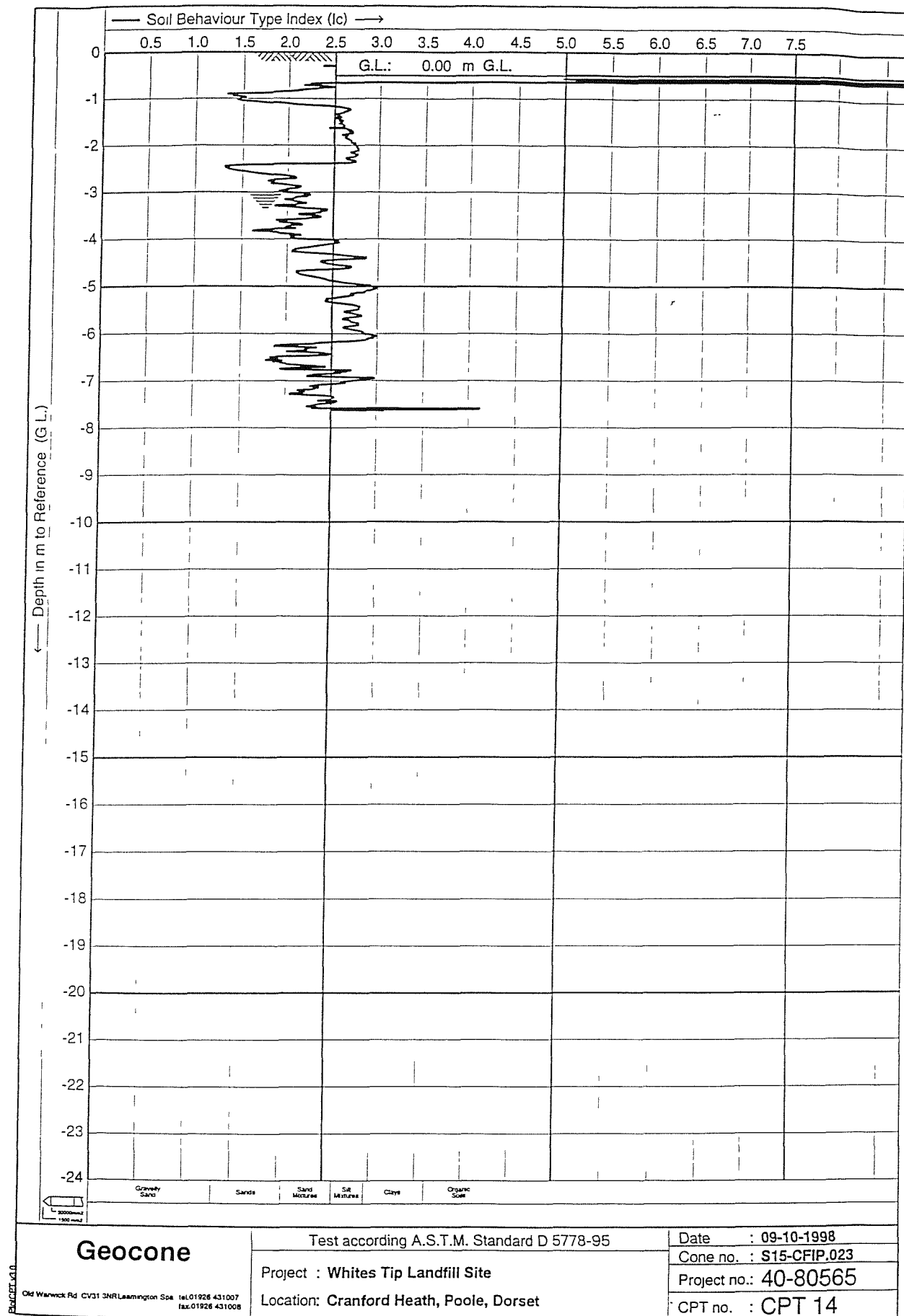


Figure 5.8: Soil behaviour type index vs depth for CPT 14

pore pressure in the refuse fill showed that the refuse was mainly unsaturated throughout the length of cone penetration.

Observations from the data interpretations of the cone penetrations showed the influence of overburden on waste properties (Figure 5.8). Neglecting the abrupt increases (i.e. the spikes) in cone resistance in the refuse fill, a general increasing trend in stiffness with depth was observed. It implies an increase in the density of the emplaced refuse with depth and overburden load together with associated changes in porosity and field capacity as encountered in the pit tests (Table 5.5).

The typical permeability of the soil behaviour type, which is sand/silt mixtures, is 10^{-5} m/s (McCarthy, 1982, Qasim and Chiang, 1994). Even though this value is similar to the hydraulic conductivity of a typical emplaced refuse (Landva and Clark, 1990), a decrease in hydraulic conductivity with overburden is not evident in the soil behaviour type profile.

In conclusion, the CPT indicated to some extent changes in properties of the emplaced refuse due to overburden. However, the quantity of data is extremely limited in determining the stiffness, pore pressure, and permeability profile in a landfill site. It is thus reasonable to say that the CPT is inappropriate for landfill studies.

CHAPTER

6

Field Measurement of Factors Likely to Influence Leachate Production

6.1 Summary

The field measurement and determination of some parameters required for water balance calculations typically used to predict leachate volumes in a municipal landfill site are presented in this chapter. The calibrations of the equipment used to undertake these tests within a period deemed suitable to obtain representative results are presented. The results of the tests are also discussed.

6.2 Introduction

The factors influencing the volume of leachate generated in a landfill site were described in Chapter 3. The importance of accurate measurement of the parameters of the water balance method in enhancing the prediction of leachate volumes was highlighted. Some of the parameters of the water balance that can be readily measured in a landfill site include the runoff, and the moisture storage in the topmost zone of the refuse fill. In this study, however, the field measurement of the temporal moisture storage in the cover soil system of the site was undertaken primarily to determine the depth of evaporative zone, which was consequently applied for simulation of moisture stored in the site in Chapter 7. The actual runoff from the site was measured and compared with typical runoff coefficients for similar natural soil surfaces.

6.3 Determination of the Moisture Content in the Cover Soil System

The volume of moisture stored in a refuse fill is greatly influenced by the infiltration of water and the evapotranspiration of moisture from the vegetated soil cover of the landfill. Campbell (1983) reported that evaporative loss is very low at operational areas of the landfill because the evaporative zone is mostly limited to the relatively small depth of daily cover. The evaporative zone of a vegetated surface, however, extends to the root depth, and as such, evaporation from the restored part of the landfill site usually accounts for a major loss of its incident rainfall.

The Neutron probe is a commonly used device for measuring the moisture content in the topsoil and that of the underlying unsaturated zone. The probe produces immediate reliable result without the requirement for soil sampling and is therefore acceptable for repeated measurements of soil water change over a long period of time.

6.3.1 The Neutron Probe

The neutron probe contains a sealed Americium-Beryllium radioactive source from which fast neutrons are emitted into the soil. Collisions with the nuclei of the soil atoms (mainly the hydrogen atoms of the soil water) cause the neutrons to scatter, to slow and to lose energy. When they have slowed to the so-called thermal energy, they are absorbed by other nuclear reactions. Hence, a cloud of slow neutrons (i.e. thermal) whose density is a function of the soil water content is generated within the soil and around the source. The density of the slow neutrons is sampled by a boron trifluoride slow neutron detector housed in the probe. The electrical pulses from the detector are amplified and shaped before passing to a ratescaler, where their mean count rate is displayed numerically as counts per second. The probe can be switched to a counting period of either 16 sec or 64 sec.

6.3.2 Method of Measurement

Prior to field measurements being undertaken, the neutron probe was calibrated by suspending the probe vertically in an access tube (Figure 6.1) in a 50 cm depth of water in a plastic drum (Plate 6.1a). The access tube was an aluminum alloy, 1m long,

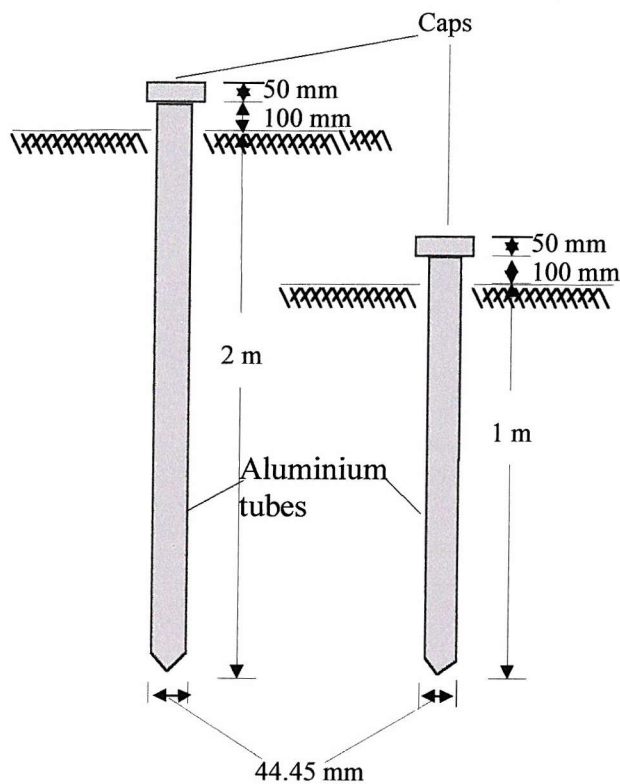
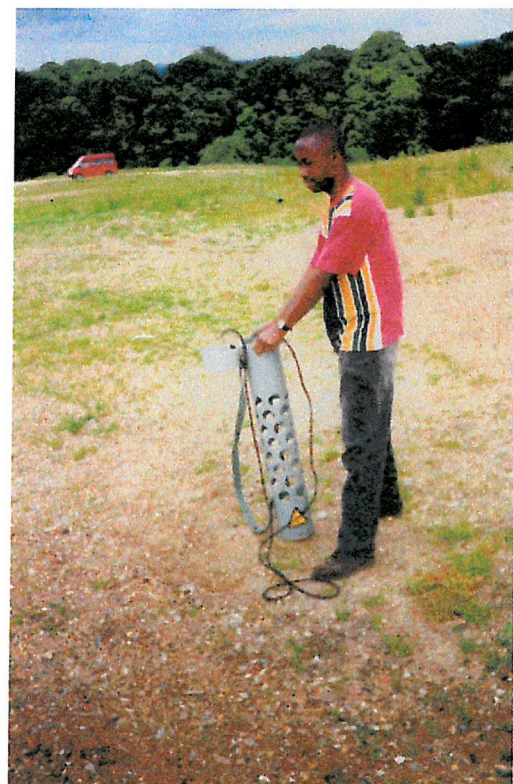


Figure 6.1: The neutron probe access tubes



(a) Calibration of the neutron probe



(b) Field measurement of moisture content at the site.

Plate 6.1: The use of the Neutron probe

44.45 mm diameter (O/D), with a wall thickness of 1.63 mm. Unlike plastic tubing, aluminum alloy has a relatively low absorption of slow and fast neutrons and is also mechanically strong and resistant to corrosion, making it appropriate as an access tube.

The standard count (full saturation count), R_w of the neutron probe was obtained from the mean of ten 64 -sec counts taken at the mid-point of water in the drum. The first two readings after switching on were discarded to reduce the error due to the startup period of the internal clock of the probe.

The field measurements of the soil water profile in the topsoil of the landfill were undertaken at four locations in the site (Figure 6.2). A hand auger was used to dig two 2 m depth holes at NP 3 and NP 4 and two 1 m depth holes at NP 1 and NP 2 into which the access tubes for the Neutron probe were installed. The tubes were placed such that approximately 10 cm of their lengths protruded above the ground surface to enable the probe carrier to be fitted in place without disturbing the surface soil and vegetation during measurements. Caps were provided for the tubes to prevent precipitation and particles from entering the hole between measurements.

The Institute of Hydrology (1979) recommended readings to be taken from 20 cm depth as neutrons are lost in any measurement above this depth. In one of the holes (NP 1), known-volume soil cores (samples) were taken 10 cm intervals from 20 cm depth to the bottom of the hole (Table 6.1). Thereafter, the neutron probe was used to take three 64-sec counts at each point where the samples were taken. The soil samples were later dried in an oven (BS 1377 Part 2) to obtain their moisture content.

The neutron probe was used to take soil water measurements at 100 mm depth intervals in the cover soil system of the site during the period June 1997 to May 1998. The use of the neutron probe for moisture content determination of the topsoil at the site is shown in Plate 6.1b.

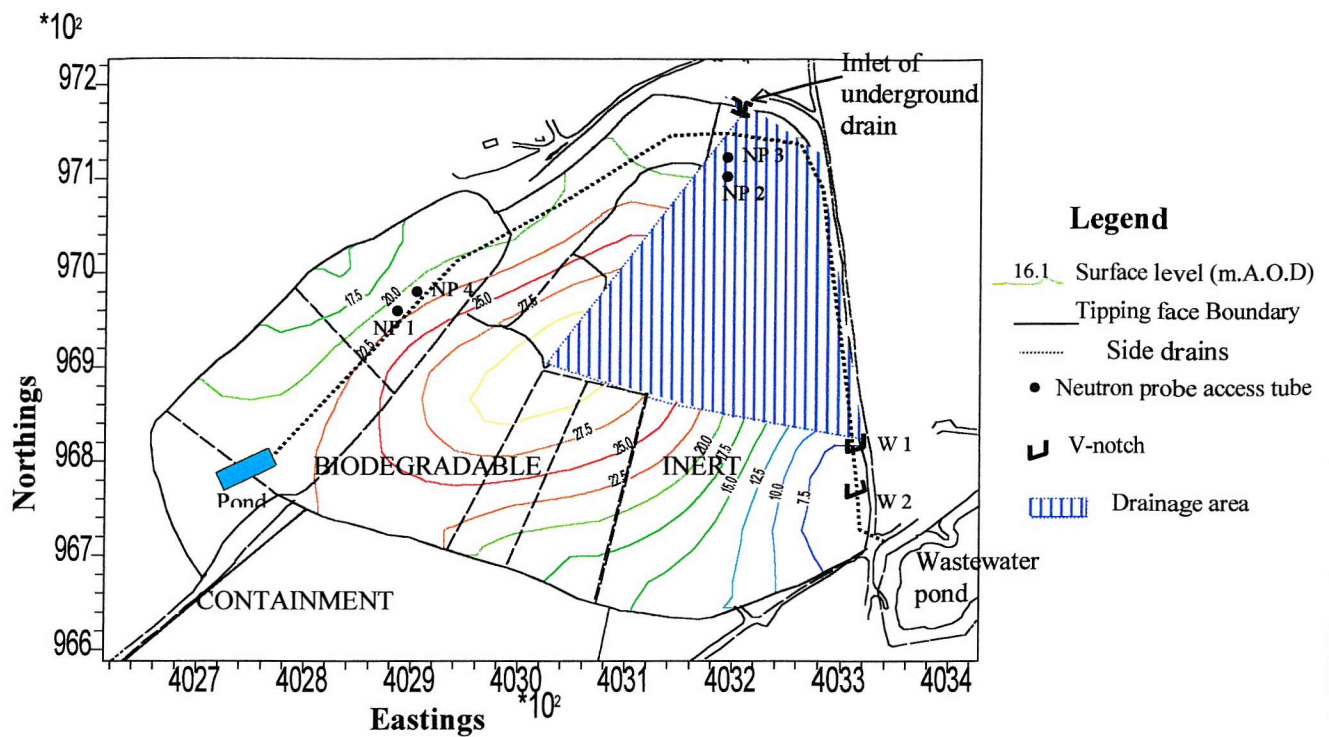


Figure 6.2: Location of neutron probe access tubes and V-notches at the site.

Table 6.1: Calibration of Neutron Probe -Soil moisture and count rate data for NP 1

Depth from top of tube (cm)	Depth from ground level (cm)	Count rate (R)				Count rate ratio (R/R _w)	Moisture content (v/v)
		1	2	3	<u>R</u>		
30	20	247	240	245	244	0.253	0.190
40	30	318	325	322	322	0.334	0.247
50	40	305	310	309	308	0.319	0.250
60	50	310	319	324	317	0.329	0.254
70	60	327	325	322	325	0.337	0.253
80	70	329	328	334	330	0.342	0.260
90	80	364	358	370	364	0.377	0.307
100	90	369	379	371	373	0.387	0.294

R = mean count rate; R_w (Standard count) = 965

Preset time for water standard = 10 x 64 sec; Preset time for water standard = 3 x 64 sec;

6.3.3 Results and Discussion

The volumetric moisture contents for the soil profile at NP 4 were plotted against the corresponding count rate ratios (Figure 6.3). A curve was fitted to the data points to obtain a relationship between the count rate and the volumetric moisture content of the soil profile at NP 4. The curve was assumed to be representative of the site since the topsoil and clay, which comprises of the cover soil system were obtained from the same stockpiles at the site (Huc, 1996). In addition, the vegetation at the restored landfill of the site was fairly uniform. The calibration relationship between count rate and volumetric water content for the site is represented by the equation of the linear fit (Figure 6.3) as:

$$\theta = 0.838 \left(\frac{R}{R_w} \right) - 0.0235 \quad [6.1]$$

where

θ = volumetric water content

R = field count of the neutron probe

R_w = standard count of the neutron probe

The Institute of Hydrology (1979) reported standard equations that can be used for different types of soils. The equations are given as:

$$\text{Sandy, silty or gravelly soils: } \theta = 0.790 \left(\frac{R}{R_w} \right) - 0.024 \quad [6.2]$$

$$\text{Loamy soils: } \theta = 0.867 \left(\frac{R}{R_w} \right) - 0.016 \quad [6.3]$$

$$\text{Clay soils (also peats): } \theta = 0.958 \left(\frac{R}{R_w} \right) - 0.012 \quad [6.4]$$

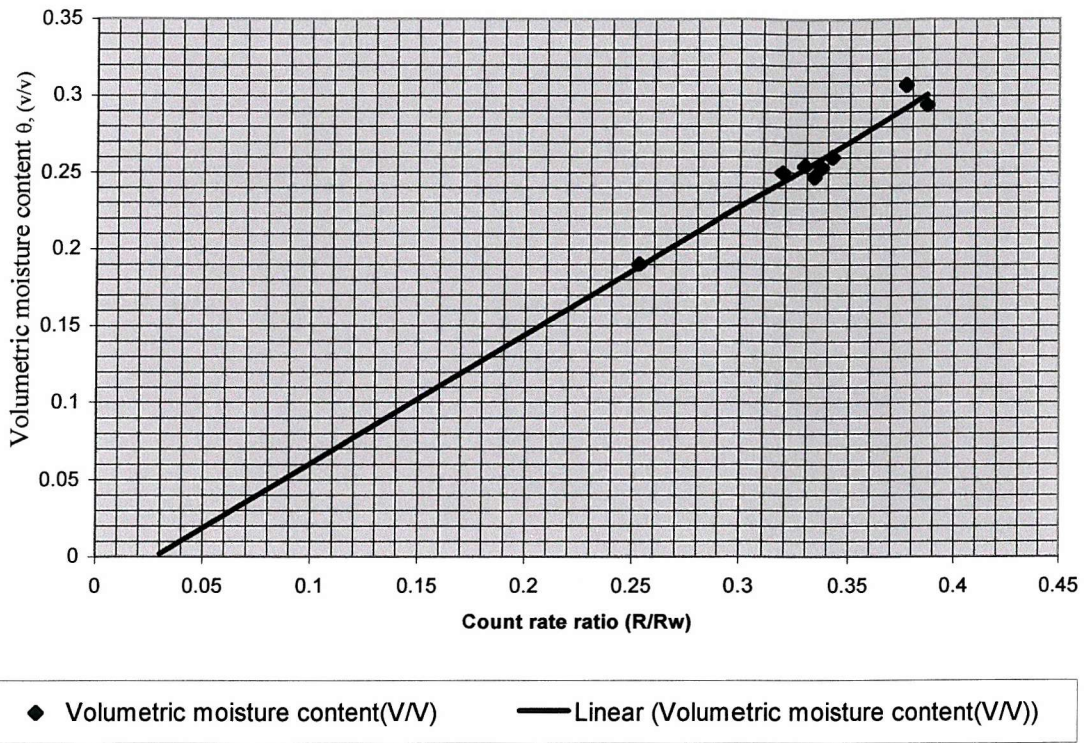


Figure 6.3: Calibration curve for the topsoil at the site.

The Institute of Hydrology (1979) reported that very little error would result from the adoption of the most relevant of the equations in determining subsurface moisture content with a neutron probe. However, errors can be eliminated by calibrating the readings of the neutron probe with site data as was done in this study.

In determining the evaporative zone of the top soil cover at the site, the moisture content profile for the extreme dry and wet periods in a year were plotted in order to discern the effective depth up to which evapotranspiration of moisture occurred in the soil. The moisture data from 1m long access tubes (NP 1, and NP 2) were not plotted since they did not depict the entire variation of moisture content in the topsoil. Moreover, they were similar to the moisture data of the adjacent 2 m tubes.

The volumetric moisture content of the soil profile at NP 3 and NP 4 are shown in Figures 6.4 (a & b) and 6.5 (a & b) respectively. There was a general increase in moisture content from the ground level to a depth of 80 cm, on July, 9, 1997 and

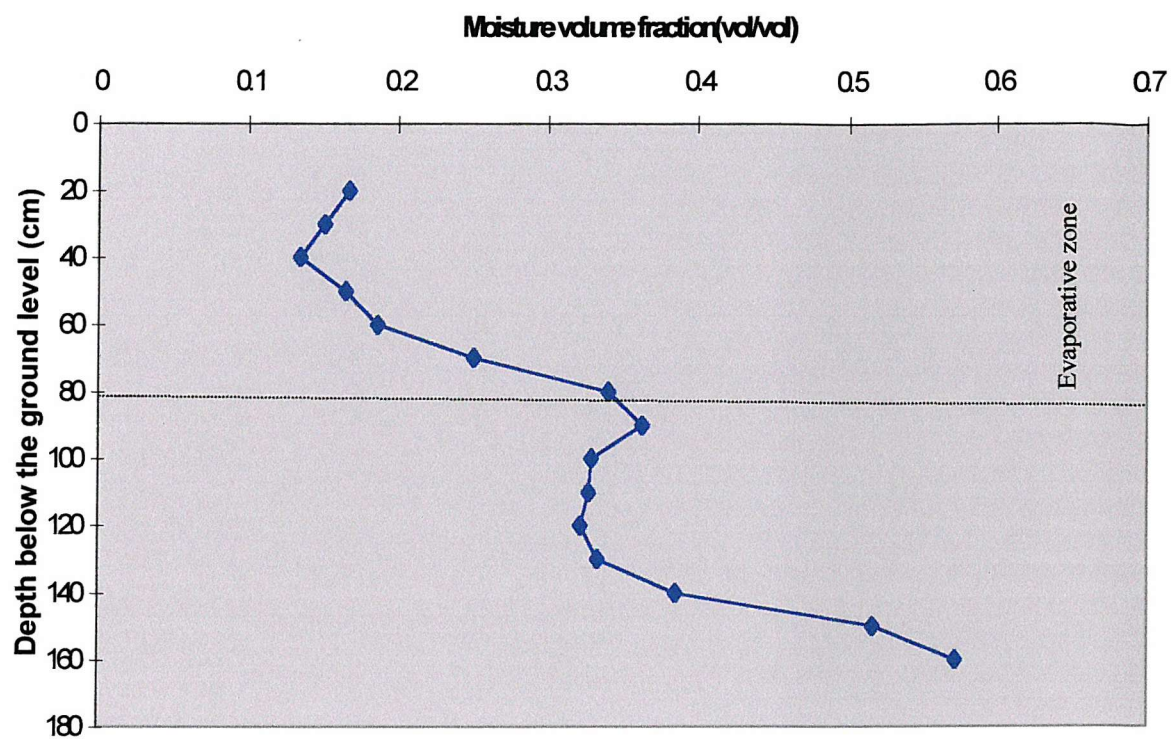


Figure 6.4a: Topsoil moisture profile for point NP 3 at the site on 09/07/1997

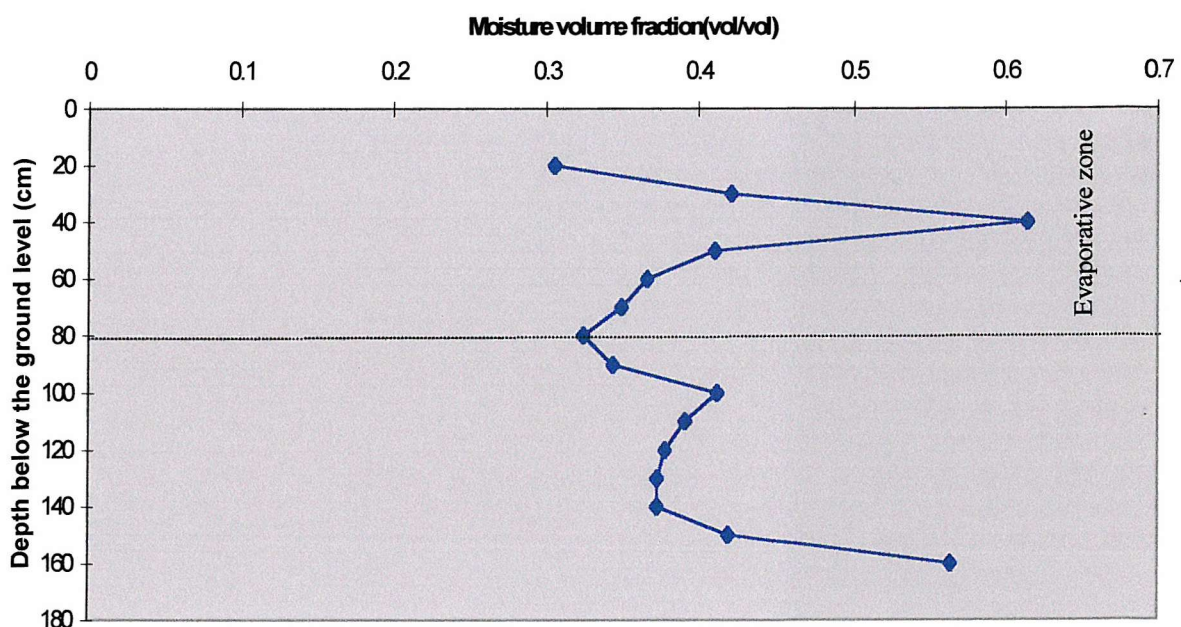


Figure 6.4b: Topsoil moisture profile for point NP 3 at the site on 22/12/1997

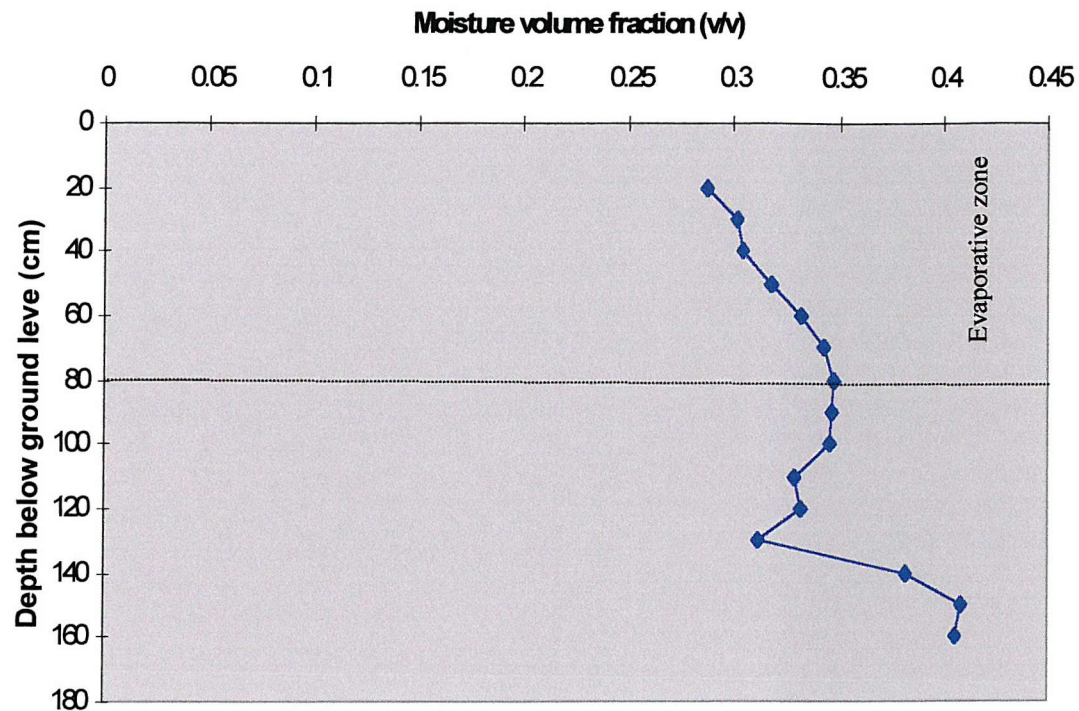


Figure 6.5a: Topsoil moisture profile for point NP 4 at the site on 11/9/1997

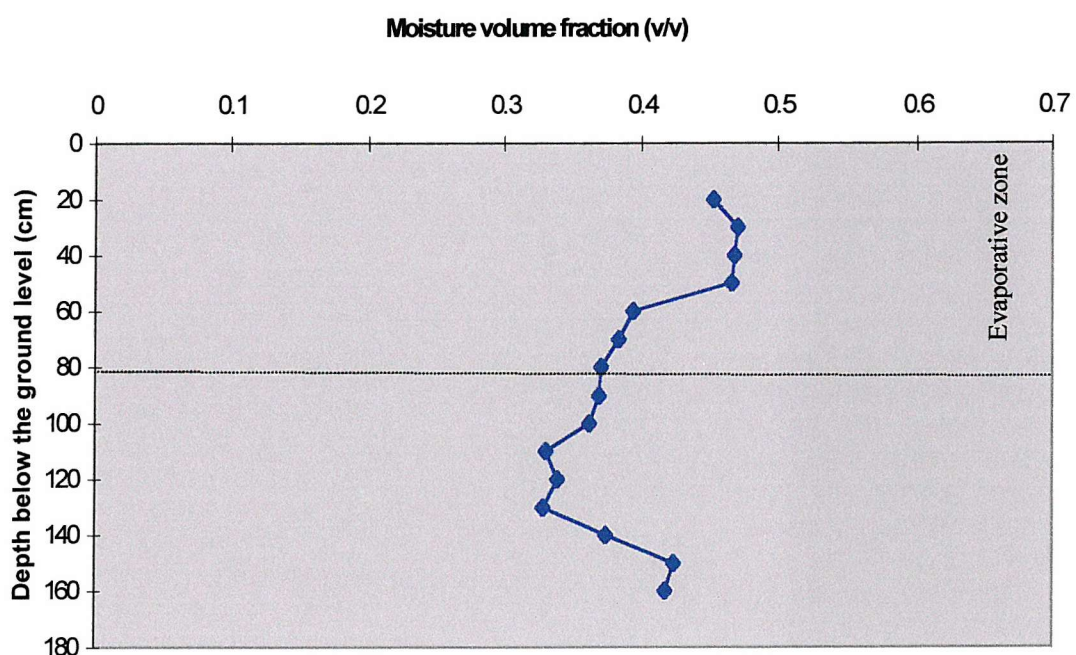


Figure 6.5b: Topsoil moisture profile for point NP 4 at the site on 22/12/1997

September 11, 1997. Weather records (Table 6.2) show that there was very little precipitation in the preceding days and that the ambient temperature during this period was relatively high thus optimising evapotranspiration from the topsoil. However, the moisture content on 22nd of December 1997, shows an abruptness between depths 10 cm and 80 cm below the ground level. The sudden increase was likely to be a result of infiltration of the precipitation (Table 6.2) on September 17, 1997 which would have formed a moisture front, moving downwards into the refuse material.

Generally, the moisture contents at depths greater than 140 cm below ground level at NP 3 and NP 4 seemed to increase sharply with depth. This is apparent in Figure 6.4 b, where the moisture content at a depth of 160 cm was close to the water (saturation) front. This increasing moisture content with depth was in likelihood due to the moisture that might have seeped in or accumulated around the base of the access tube, thereby prompting the instrument to measure near-saturation values towards the base of the hole. As a result, the data beyond 140 cm were discarded in determining the evaporative depth of the soil cover.

The moisture content close to the ground surface during July and September 1997 was about 0.15 compared to a moisture content of about 0.33 (Figure 6.4 b) during the winter period. However, the moisture content between depths of 80 cm and 140 cm below ground level seemed to be less varied and unaffected by evapotranspiration. The average moisture content of the topsoil at this period appeared to be at field capacity and was approximately 0.35 at the test points.

Due to the reduced variation in the temporal moisture content beyond a depth of 80 cm below the ground surface, the evaporative depth of the cover soil systems at the site was taken to be 80 cm. Schroeder et al. (1994) reported that the evaporative depth should be at least equal the depth of root penetration and since the vegetation at the site was mainly grass, (whose average root zone was approximately 40 cm; Vilenski, 1994), the evaporative depth of 80 cm can be considered a reasonable maximum. The evaporative depth showed that moisture would be lost through evapotranspiration from the clay liner beneath the topsoil in the biodegradable area of the site. However,

Table 6.2: 5-day precipitation and temperature before moisture measurement.

Date (1997)	Precipitation (mm)	Mean Temperature (°C)	Applicable diagrams
4/07	0.1	16.3	Figure 6.3a
5/07	0	16.7	
6/07	0	19.6	
7/07	0	20.1	
8/07	0	19.5	
6/09	0	15.1	Figure 6.4a
7/09	0	17.5	
8/09	0	14.7	
9/09	0	14.9	
10/09	0	15.8	
17/12	13.6	5.3	Figures 6.3b & 6.4b
18/12	0	7.1	
19/12	0	6.9	
20/12	0	8.6	
21/12	0	8.5	

refuse areas excessively or repeatedly filled with topsoil due to on going settlement, and the inert fill areas would not be subjected to clay desiccation.

6.4 Surface Runoff Measurements

6.4.1 Introduction

The use of an empirical runoff coefficient, which gives runoff as a fraction of precipitation, is convenient but requires considerable caution (Dass et al., 1977). Landfill sites have potholes and cave-ins (depressions) and the surface runoff does not occur as freely as it does over natural soil slopes, therefore, the use of runoff coefficient is likely to underestimate infiltration (Ettala, 1987; Qasim and Chiang, 1994). Precise measurement of the surface runoff from a landfill is therefore necessary when a water balance method is to be applied for the determination of moisture stored in a landfill.

6.4.2 Field Measurement

Most of the surface runoff from the site drains into peripheral channels, which discharges into a wastewater pond located to southeastern edge of the site (Figure 6.2). Runoff from some areas in the southern part of the site mix with runoff from the containment areas making it difficult to determine the surface flows from the restored landfill areas. Also, part of the runoff from the central part of the site is drained by a subsurface drainage system, the outlet of which is located near the biodegradable/inert area boundary (Figure 6.2). In view of this, a distinct drainage area was carved out of the site for an average runoff measurement of the landfill.

A 3-mm steel plated V-notch weir was used to measure the flow in the drainage ditch at the site (Figure 6.6). Prior to field measurements, the notch was calibrated in the laboratory by measuring different discharges and corresponding heads of water above the V-notch, which was installed in a flume. The head of water was measured by a vernier micrometer, and the discharge was measured with an automatic flow meter.

The equation of the weir, which was obtained by plotting the flow against the head of water (Figure 6.7) runoff measurement at the site, is:

$$Q = 1.4286H^{2.5} \quad (6.5)$$

where

Q = the volumetric flowrate in m^3/s

H = the head of water above weir in m.

Two weirs were installed at points W1, W2 on the side drain of the site, close to waste pond (Figure 6.1). The sitting of the weirs was designed to complement each other in case of unforeseen breakdown or damage to either of them. Prior to installation of the weirs, approximately 10m stretch of the drainage ditch at the point of installation was cleared of silt, debris, vegetation and obstructions that might have affected flow conditions required for standard installation of the weirs (BS 3860, 1981). The weirs were positioned firmly in the ditch with a clay embankment on both the upstream and downstream faces (Plate 6.2).

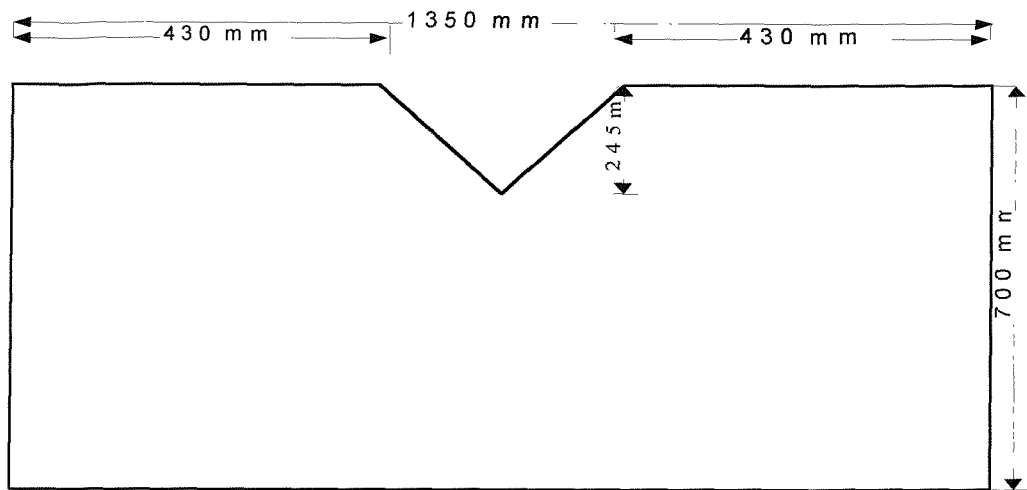


Figure 6.6: The V-notch used at the site

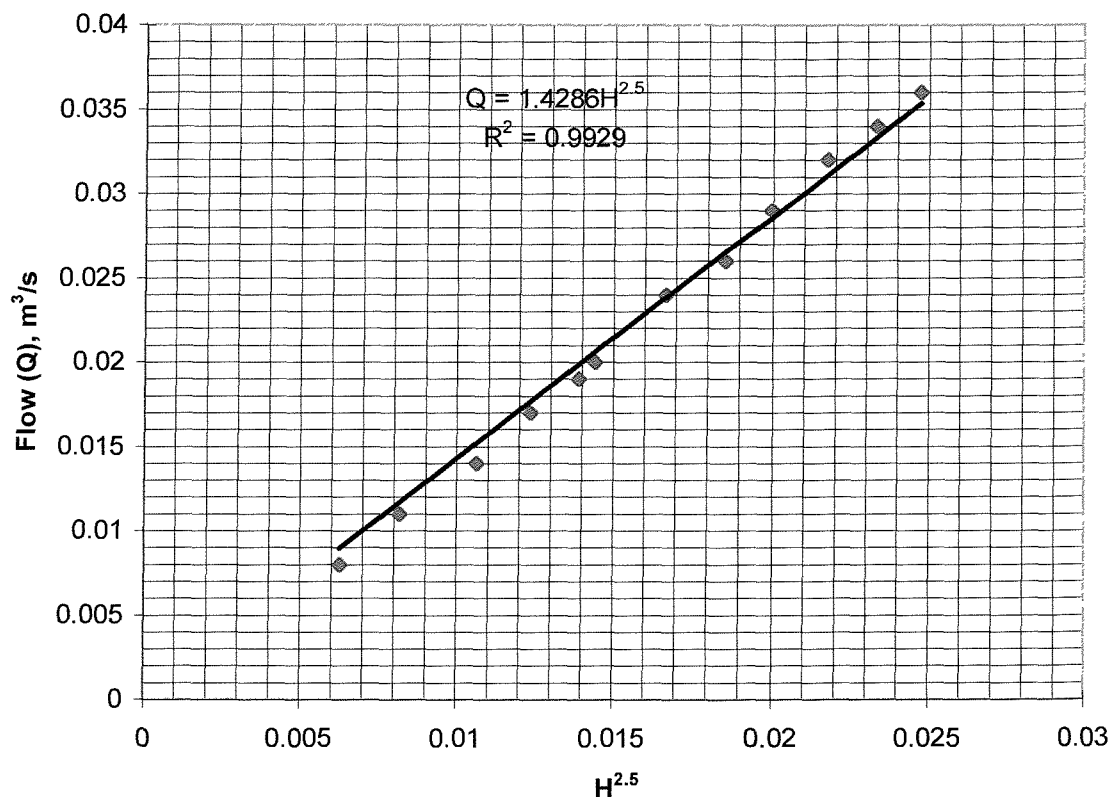


Figure 6.7: Runoff versus $H^{2.5}$



Plate 6.2: Surface runoff measurement at the site.

Continuous measurement of water head above the crest of the weir was undertaken with a water recorder, installed at approximately 1.2 m upstream of the weir. Prior to field measurements, a linear relationship was established between vertical movement of the pen and the vertical movement of the float of the water recorder in the laboratory. The water recorder consists of a float, whose vertical motion moves a pen across a chart. It was attached to a wooden frame with sharp end-studs, which allowed it to be firmly installed by embedding it into the soft soil of the channel. The installation was undertaken such that the base of the stilling well (the tube housing the float) was below the crest of the weir and well clear of the floor of the channel. The elevation of the crest of the weir relative to the base of the stilling well was measured with a level. The immediate floor of the downstream channel was filled with gravel to prevent erosion due to the jump of water flowing over the crest of the weir. The channel and the opening of the stilling well were cleared of silt every week.

The head of water on the weir was regularly measured and compared with calculated values obtained from the horizontal displacement of the pen on the chart to ensure continued validation of the calibration equation. Also, the date and time of each

period of measurement were printed on the chart to detect any error in the clock and rolling mechanism of the instrument between measuring periods.

The pen movement of the gauge recorders was frequently obstructed by the uneven surface of the chart. These situations were, however, promptly remedied, and the data during disrupted periods were excluded from the analysis. The measurement of runoff from the site was undertaken during the period September 10 - December 21, 1998.

6.4.3 Results and Discussion

The measurements of the surface runoff at the site were undertaken during a period when there was a significant variation in temperature to observe the varied surface flows due to effects of evapotranspiration and infiltration in the landfill.

Unfortunately, frequent obstructions of the recorder pen prevented a truly continuous measurement of surface runoff from the site.

The longest continuous period of measurement occurred during September 9 - 26, 1998. The rainfall and runoff during this period is shown in Figure 6.8. The volume of surface runoff was greatly influenced by the quantity of precipitation occurring at the site. The precipitation resulted in immediate short rapid flows, and very small flows occurring almost continuously thereafter. Generally, there was a lag of 8 – 42 hrs between the rainfall and the resulting runoff. The lag was likely to be influenced by the size and the terrain of the catchment area, quantity and intensity of the downpour, type and prior moisture content of topsoil, vegetation, and to a lesser extent, evaporation.

The greatest discharge from the landfill was 21.01 l/s on 26th of September 1998 (377.75 hrs) as a result of a rainfall of 4.7 mm (Tables 6.3) earlier in the day. Often, the recorded runoff was the cumulative effect of two or more separate rainfall incidents thereby making it difficult to separate the individual flows. In determining the runoff coefficient for the period of measurement, a distinct runoff to a specific

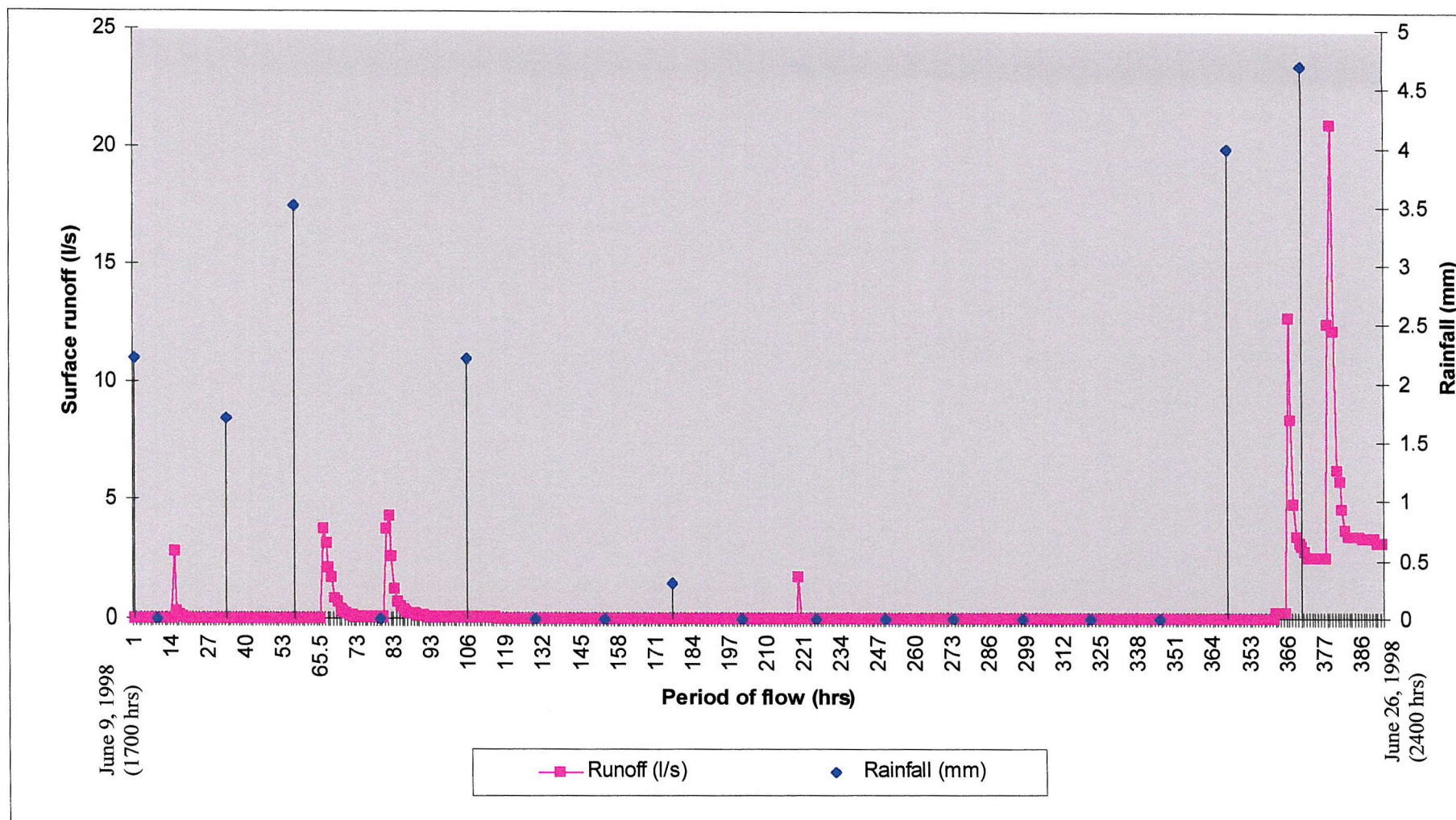


Figure 6.8: The precipitation and runoff at the site

Table: 6.3: The precipitation and temperature during the continuous period of surface runoff measurement

Date (1998)	Precipitation (mm)	Temperature (°C)
9/09	2.2	18.3
10/09	0	18.3
11/09	1.7	14.7
12/09	3.5	11.8
13/09	0	12.6
14/09	2.2	12.4
15/09	0	15.4
16/09	0	14.5
17/09	0.3	14.3
18/09	0	16.7
19/09	0	17.1
20/09	0	16.4
21/09	0	17.5
22/09	0	16.7
23/09	0	16.4
24/09	0	16.6
25/09	4	17
26/09	4.7	16.4

quantity of rainfall was required. This period (PERIOD A in Figure 6.8) occurred between the 15 hrs and 203 hrs of measurement.

The drainage area was mapped out from the surface contours of the site such that areas contributing to an upstream flow, which is drained by a subsurface drain system, was excluded (Figure 6.2). The drainage area was obtained by tracing the outline of the map with a digitiser and computation of the digital data required with a computer program “AREACAL” (Clarke, 1997).

The coefficient of runoff during the period of continuous measurement is calculated as follows:

Period: 15 hrs – 203 hrs

Average flow during the period = 0.0746 l/s (See Table B3)

Time = $189 \times 3600s = 680400s$

Runoff = $(0.0746 \times 10^{-3} \times 680400) m^3/s$
= $50.758 m^3/s$

Total precipitation during period = $(2.2 + 1.7 + 3.5 + 2.2 + 0.3) mm = 9.9mm$

Landfill area contributing to runoff = $56000m^2$

Volume of precipitation received = $(5600 \times 9.9 / 1000) m^3 = 554.4 m^3$

Estimated coefficient of runoff = $50.758 / 554.4 = 0.0916$

From the above calculations, the surface runoff coefficient of the selected portion of the landfill was approximately 0.09 during the period of measurement. It is far less than the empirical runoff coefficients of 0.18 to 0.22 (Table 2.8) being used in drain designs for similar natural surfaces. However, it conforms with the runoff range of 0.07 to 0.02 stated by Qasim and Chiang (1994) for sanitary landfills.

Berger et al. (1996) reported that desiccation of cohesive liners (clay) due to water uptake by plant roots allows cracks to develop, and as such encourages channelling of water through the cover soil systems in refuse fills. The desiccation of the site's clay capping system that was implied in the moisture monitoring of the topsoil cover system will be a contributing factor to the reduction in the surface runoff from the site.

In conclusion, the surface runoff from White's pit is low compared with the runoff from a similar natural surface. Despite the short period of measurement at the site, the measured runoff showed that the infiltration of incident rainfall at the site is greater than as expected on a similar natural surface.

CHAPTER

7

A Laboratory Investigation into Changes in the Properties of Refuse Lifts under Loading

7.1 Summary

In this chapter the determination of compression, dry density, porosity, and the hydraulic conductivity of a refuse fill with, and without a cover soil under incremental applied loads in small-scale cells is presented. The results are compared to those obtained from large-scale cell tests, and the influence of cover materials on the general hydraulic properties of the refuse is discussed.

7.2 Introduction

The hydraulic conductivity (permeability) of refuse is a parameter commonly used in the design and effective management of a municipal refuse disposal facility. The in situ permeability of waste in a landfill is often determined during the intermediate stage of water level recession, after the flow has stabilised and before any debris clogs the voids (Landva and Clark, 1990). Unfortunately, there is a limit to the usefulness of this method because test pits are usually confined to the upper zone of the landfill, therefore, the permeability of underlying refuse layers, which is often the zone of interest, is not determined.

A conventional pumping test, which is often used to determine the hydraulic characteristics of soil aquifers is sometimes used at landfill sites to measure the

hydraulic conductivity of a refuse fill. However, Giardi and Somigli (1997) and Cossu et al., (1997) reported that a conventional pumping test was not particularly reliable in determining the permeability of refuse due to the heterogeneity of waste, well clogging and damage, and the biogas dissolved in leachate and occupying the waste macropores. Parsons (1995) stated that the conditions found in waste do not satisfy the basic underlying assumptions for pumping test theory, and therefore, a pumping test is inappropriate for refuse fills.

Chen and Chynoweth (1995) reported that the hydraulic conductivity of a porous material is affected by particle size, void ratio, composition, pore geometry, fabric, degree of saturation, and the properties of the test fluid. They noted, however, that refuse samples could not be characterised according to these factors because of the heterogeneity of municipal solid waste. Furthermore, water is transmitted through the micropores in refuse; unlike soil grains. Based on this, the hydraulic conductivity of refuse is best determined from permeability tests. The hydraulic conductivity of refuse samples is usually estimated from Darcy's equation as follows:

$$k = Q / (A(\Delta H / L)) \quad [7.1]$$

where

k = hydraulic conductivity of refuse sample

Q = flow rate through the refuse sample

A = cross sectional area of the refuse sample

$\Delta H/L$ = hydraulic gradient in the refuse sample, ΔH is the change in hydraulic head and L is the length of flow.

The determination of the hydraulic properties of refuse under controlled conditions in the laboratory is convenient, but demands caution due to potential experimental scale effects. Due to the extremes in sizes of the typical constituents of landfill refuse, Sowers (1973) suggested that large-scale tests, preferably pilot cells, 1-2 m diameter should be used to conduct such tests on crude refuse. Beaven and Powrie (1995) used a large-scale compression cell, 2 m in diameter by 3 m high, to determine the density, absorptive capacity, porosity and hydraulic conductivity of refuse at various



compressive stresses up to an equivalent of a 60m-deep landfill. In contrast, Chen and Chynoweth (1995) used much smaller test columns, 37.5 cm in diameter by 122 cm high, to determine the hydraulic conductivity of refuse compacted to densities of 160, 320, and 480 kg/m³. They used paper and plastic materials of nominal size of 1.27 x 0.01 cm, and yard waste, shredded to a diameter of approximately 10 cm, due to the smaller cell size. Similarly, Wall and Zeiss (1995) used a smaller cell, 0.57 m diameter by 1.7 m, to study both landfill biodegradation and compression. In these studies, the refuse particles were reduced to 20% of the test cell diameter.

Wall and Zeiss (1995) reported that the main concern regarding the use of shredded refuse is the influence of the larger surface area of the small particles on the biodegradation of refuse. They concluded, however, that in the short-term, results comparable to field values could be obtained from determining refuse properties in small cells if the particle sizes of the refuse sample are scaled to less than 20 % of the diameter of the test cell. The influence of overburden stress on the density, porosity, and field capacity of an emplaced refuse lift was established in the field tests described in Chapter 6. In addition to these physical characteristics, the hydraulic conductivity of a refuse fill (with, and without a cover soil) that is subjected to incremental vertical loading, is presented in the following sections.

7.3 Experimental Set-up

The permeameter (Figure 7.1) used for the experiment was originally designed and used by Naseri (1996 & 1998) to determine the hydraulic conductivity of a clay under compressive loading. The permeameter was adapted for refuse tests, following slight modification to some of its components.

The compression cell comprised a Perspex cylinder, 240 mm internal diameter, 230 mm overall height, and 12 mm thickness (Plate 7.1), and a Perspex plate to seal the base of the cylinder. The entire compression cell was placed and secured in a hollow wooden base plate (Plate 7.2), fastened to the base of a wooden support frame. A gravel layer (10 mm gravel) of approximately 50 mm thickness, placed on the Perspex base plate provided uniform distribution of water through the refuse. Two perforated galvanised steel screens (60% void area) with 8 mm diameter holes served as the

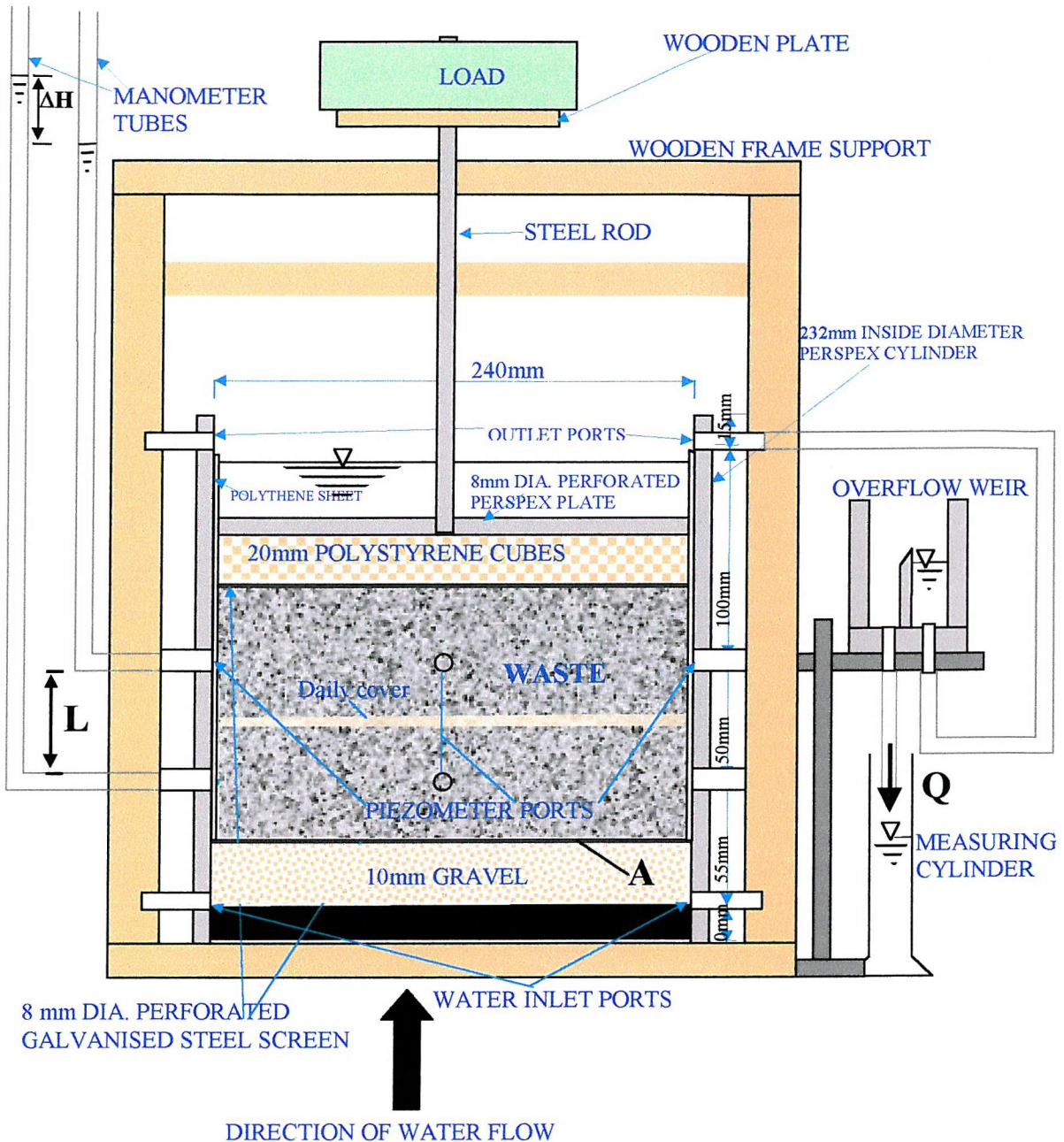


Figure 7.1: The permeameter used for measuring the hydraulic conductivity of waste

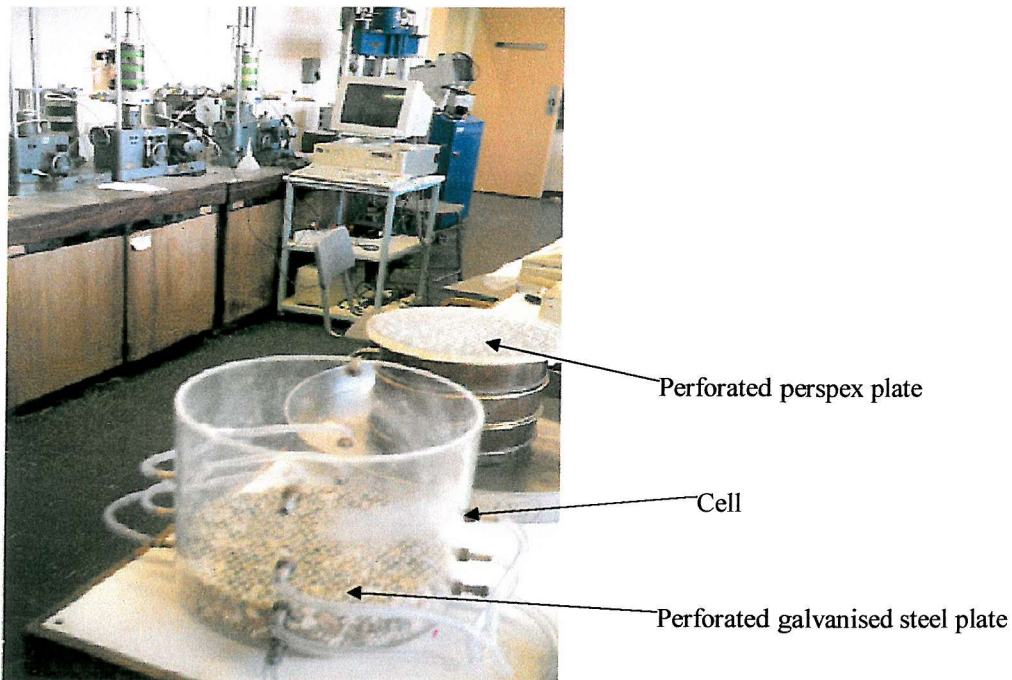


Plate 7.1: Cell and other components

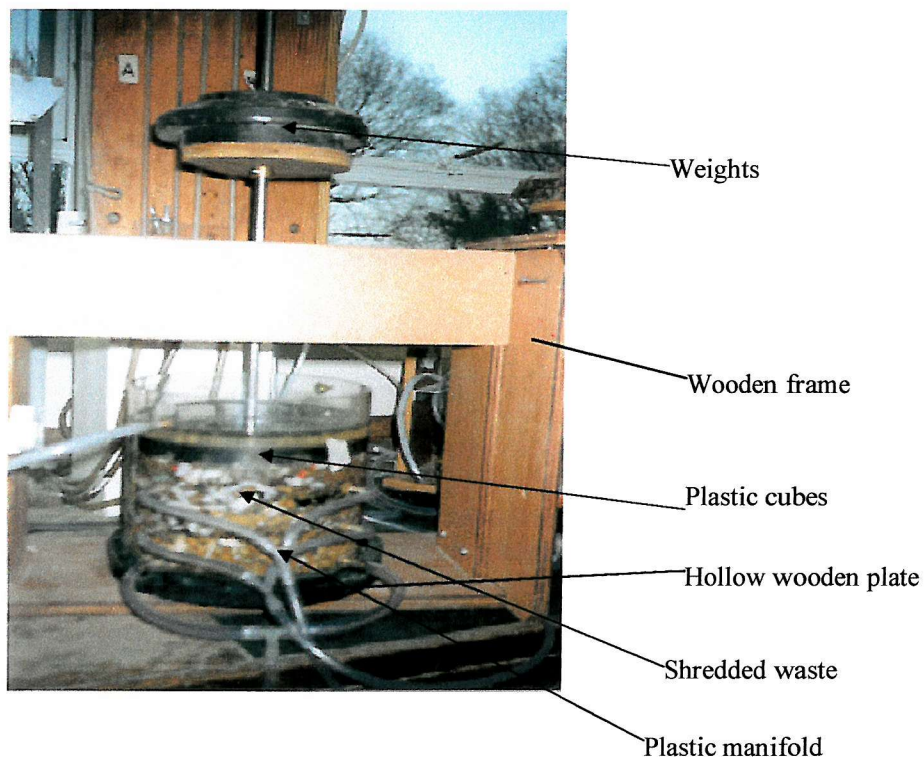


Plate 7.2: Assembled cell in operation

upper and lower boundaries for the refuse sample to prevent the loss of fine particles during the flow of water through them.

The refuse in the cell was compressed by a perforated 240 mm-diameter Perspex platen with an 8 mm-hole diameter, connected by a steel rod to an upper wooden base plate on which metal weights (Plate 7.2) could be placed. In between the Perspex platen and the upper galvanised steel screen was a layer of 20 mm polystyrene cubes, designed to provide a uniformly distributed vertical load to the underlying refuse fill in the cell.

There were four evenly spaced ports on each of three levels on the cell. The basal ports were connected to an elevated constant head tank, which supplied de-aired water to the cell through a manifold, made up of plastic tubes. The ports at the next two levels were connected to Pyrex standpipes, which were fixed to the side of the wooden frame by plastic tubing. The Pyrex standpipes served as manometers for determining pressure at various points in the cell during the experiment.

There were two ports located at the top of the cell. These were the water outlet ports, and were connected to a weir unit, fastened to the side of the wooden frame. The weir units comprised a Perspex cell partitioned evenly into two by a tapered Perspex plate (weir). The water outflow from the weir unit was collected by a measuring cylinder via a plastic tube. The rate of flow of water through the plastic tubing in the permeameter was controlled by means of a pinch clip, fixed close to the side ports.

A problem often encountered during compression tests in laboratory cells is the reduction in the applied stress due to the effects of sidewall friction. Beaven and Powrie (1995) reported that a height:diameter ratio of 1:4 is commonly used in conventional oedometers to minimise these effects. They stated, however, that, with a height:diameter ratio of 3:2 of the Pitsea compression cell, more than 90% of the applied load was transmitted to the base of a 2 m deep refuse fill. Notwithstanding, the following steps were taken in an attempt to reduce the effect of friction in the test cell used in this study:

- A sample height of 110 mm was used, giving a height: diameter ratio of approximately 1:2.2.

- The internal wall of the test cell was lined with a polythene sheet to reduce friction between the waste particles and the cell wall during vertical loading.

In calculating the hydraulic conductivity of a material sample in laboratory test cells, Head (1994) reported that the losses due to fittings, the shape and effect of filter, and ancillary tubes between the inlet and outlet points could be minimised by measuring the hydraulic gradient within the length of the sample. Manometers were used for determining the hydraulic gradient of refuse sample and were spaced at 50mm apart, within the length of the refuse fill in the cell.

7.4 Materials and Methodology

7.4.1 Refuse Material

The refuse material was obtained from the working face of the active (fill) part of White's pit landfill. Due to the nature of the environment within which the experiment was conducted, degraded materials were excluded from the waste mass obtained from the landfill. These putrescible materials were substituted with materials of the same organic content, but which were easier to handle under the prevailing conditions in the laboratory. Food waste was substituted by fresh potato; green/ garden waste was replaced with hay, which has a low degradable rate. Many of the cans in the emplaced waste were extremely distorted and difficult to shred, and so were replaced by food and drink cans collected from waste bins locally. The composition of refuse tested in the laboratory (Table 7.1) was made similar to that of the fresh waste currently deposited at White's pit landfill.

The refuse was reduced to a nominal size of 20 x 5 mm, which was assumed to be compatible with the scale of the experiment (Wall and Zeiss, 1995). A shredder was found to produce a characteristic size which was dissimilar to the scaled size; therefore, a hand (side) cutter was used to cut the textile, grass, paper and cardboard wastes; a mechanical cutter was used to cut the plastic, metals, and wood wastes, and a hammer was used to reduce over sized glass.

Table 7.1: Composition of waste materials used in the permeability test

Waste material	Percent of bulk mass (%)			Gravimetric moisture content of individual components (%)
	Refuse 1 (No cover soil)	Refuse 2 (7.5% cover soil)	Refuse 3 (10% cover soil)	
Paper	30.59	31.94	29.92	57.87
Cardboard	4.32	5.51	5.16	11.46
Plastic	3.70	2.95	2.77	Nd
Thin plastic	5.73	4.58	4.29	Nd
Textile	1.82	1.45	1.36	2.32
Glass	4.29	3.42	3.21	Nd
Food waste	12.48	4.37	4.10	81.48
Ferrous Metals	4.55	2.83	2.65	Nd
Non Ferrous metals	1.49	1.19	1.11	Nd
Combustible	6.43	5.13	4.81	0.63
Green/garden	16.32	9.84	9.22	9.92
Wood	0.61	0.49	0.46	10.65
Fines<10mm	0.78	6.15	5.76	1.49
Sand soil cover	6.89	20.15	25.18	11.07
Total	100.00	100	100	Na
Overall moisture content (%)		35.30	33.59	Na

Nd : Not determined

Na : Not applicable

A daily cover soil, approximately 15 cm thick is placed on 2 m thick of refuse lift at the site, indicating a soil thickness: waste thickness ratio of 0.075: 1. This condition was simulated in the experiment by placing a soil layer equivalent to 3.75 mm of cover soil over 50 mm thickness of refuse layer. In addition, a cover soil layer equivalent to 5 mm of cover soil was placed over 50 mm thickness of refuse layer to examine the impact of various thickness of cover soil on the hydraulic properties of the waste layer. The three possible scenarios of refuse placement simulated in the cells were:

- (a) Test 1: Waste materials only.
- (b) Test 2: Waste materials with a cover material, 7.5% thickness of the underlying refuse layer.
- (c) Test 3: Waste materials with a cover material, 10% thickness of the underlying refuse layer.

The cover material used in the tests was the same daily cover soil used at White's pit landfill, and was obtained from a stockpile at the site. Previous classification of the cover materials indicated the soil to be slightly clayey/silty slightly gravelly sand. Prior to testing, the paper and cardboard was uniformly saturated to field capacity to enhance workability. Samples of the refuse components were dried in an oven at 105°C for 24 hrs (BS 1377: Part 2) to determine their moisture contents (Table 7.1).

7.4.2 Determination of Compression, Porosity, and Hydraulic Conductivity of Refuse (With Cover Soil) under Loading

In Test 1, approximately 1.244 kg¹ (wet mass) of waste material was mixed thoroughly together and uniformly compacted in small loads to a density of approximately 250 kg/m³. In Test 2, approximately 565.5 g² of the shredded waste material was mixed thoroughly and compacted in small layers of 50 mm thickness, to a density of 250 kg/m³. Then, approximately 279 g³ dry mass of sand, equivalent to 7.5% thickness of the underlying refuse layer was placed immediately on the refuse in the cell as cover material. Thereafter, approximately 636 g⁴ of refuse material was placed on the sand and compacted to a density of approximately 250 kg/m³, making up a total sample height of 110 mm in the cell. The same procedure was repeated in Test 3: approximately 372 g dry mass of sand equivalent to 10% thickness of the underlying 50 mm layer of refuse, and 622 g⁵ of shredded refuse were placed sequentially in the cell. Due to the size of the cell, clay lumps greater than nominal size of the waste particles were removed from the cover soil placed on the waste fill in the cell.

¹ Wet mass of 110mm refuse in Test 1 = 250 kg/m³ * 3.142 * 0.24m²/4 * 0.110 m = 1244.07g

² Wet mass of underlying 50 mm refuse layer in Test 2 = 250 kg/m³ * 0.002262 m³ = 565. 5g

³ Thickness of cover soil in Test 2 = 7.5*50mm/100 = 3.75mm. Equivalent in situ mass =

1851.3 kg/m³* 0.0001696 m³ = 314.0g. Dry mass = 314g/(1+0.1245) = 279.3g

For Test 3, thickness of cover soil = 5mm; Wet mass = 418.75g, Dry mass = 418.75g/1.1245 = 372.4g

⁴ Mass of refuse layer overlying cover soil in Test 2 = 250 kg/m³ * 3.142 * 0.24m²/4 * 0.05625 m =636.2g

⁵ Mass of refuse layer overlying cover soil in Test 2 = 250 kg/m³ * 3.142 * 0.24m²/4 * 0.055 m =622.0g

After placement, the sample was loaded in approximately eight sequential 44.5 N increments by placing weights on the wooden plate connected to the Perspex loading platen. At each loading (compression) increment, the sample was allowed to consolidate until there was less than 1% change in its thickness. The full loading condition was achieved over a period of 1 to 3 days. The thickness of the sample was determined by measuring the elevation of the perforated Perspex plate from the top of the cell by a vernier calliper. Due to uneven compression of the refuse in the cell, the thickness of the sample was determined from the mean of eight evenly spaced measurements taken around the surface perimeter of the sample.

Immediately after measuring the thickness, the sample was saturated sequentially by passing de-aired water, supplied from a constant head overhead tank through the basal ports of the cell. Applying a low inflow of water from the bottom of the cell allowed entrapped air to be purged from the cell. Uniform saturation of the refuse materials was achieved by allowing the water in the manometer tubes to settle before each addition of small volume of water. Once the sample was fully saturated, the water outlets to the manometer tubes were closed. The water in the sample was then drained under gravity into a measuring cylinder to measure the effective porosity of the refuse fill.

For the determination of the saturated hydraulic conductivity, a continuous upward flow of de-aired water through the sample from the bottom of the cell was established. The water outflow from the cell passed through a weir unit, which discharged to a measuring cylinder. Prior to measurements, the air bubbles in the manometer tubes were dislodged by removing the initial water build-up in these tubes. Regular measurements of the pressure head in the waste (as shown by the manometer) and the flow rate through the sample were taken to obtain the hydraulic conductivity of the refuse in the cell. The hydraulic conductivity during was calculated using the Darcy's equation (Equation 7.1). The hydraulic conductivity for the refuse loading was taken when there was less than 5 % changes in the hydraulic conductivity measurements within a 6-hr period. Finally, the sample was drained prior to another cycle of operation.

In addition to the refuse-testing programme, the cell was used to measure the permeability of the daily cover soil used at the site. The apparatus set-up and procedures for the permeability measurement were similar to that employed with the refuse sample. However, the drainage medium was 3.35 mm gravel, and a vertical stress of 7.92 kPa was applied to keep the soil sample in-place during the upward flow of water. The density of the sand in the cell was 1850 kg/m³. The hydraulic conductivity of 6.35×10^{-7} m/s obtained from the cell compared well with measurements undertaken with a standard permeameter cell of 75 mm diameter (according to BS 1377: Part 5: 1990).

7.5 Results

The height, effective porosity, dry density, and hydraulic conductivity of the refuse samples at different applied loads are shown in Table 7.2. The relationships and terms used in calculating the geotechnical properties of refuse are stated in Appendix A. In calculating the total applied load on the refuse in the cell, the submerged masses of the perforated steel plate, Perspex plate, plastic cubes, and the mass of the steel rod and wooden plate were determined and added to the load applied through the loading platen by the metal weights. The applied vertical stress on the refuse samples, which ranged from 1.04 kPa to 7.92 kPa, is equivalent to 104 mm and 792 mm of emplaced refuse fill, having a bulk density of 1 Mg/m³.

The height of the refuse sample before the application of load was 110 mm. The maximum compression occurred in Test 1, where the sample compressed to a height of 61.37 mm under an applied vertical stress of 7.92 kPa. At this load, the compressions of the refuse samples in Tests 2 and 3 were 63.81 mm and 63.86 mm respectively. The compression of the refuse samples is plotted in Figure 7.2. As expected, the compression of the refuse increased with increasing applied vertical stress. However, the rate of increase of compression decreased as the applied vertical stress increased.

Table 7.2: Effective porosity, dry density, and hydraulic conductivity of refuse at different applied stresses.

Test 1- Waste only						
Applied vertical stress (kPa)	Equivalent depth of emplaced refuse fill (mm)	Total height of refuse in cell (mm)	Dry density kg/m ³	Drainage volume (ml)	Effective porosity (%)	Hydraulic conductivity (m/s)
Initial	-	110	175.26	2510	50.43	Nd
1.04	104	96.56	199.65	1940	44.41	3.60E-02
2.02	202	87.18	221.14	1470	37.27	6.09E-03
3.00	300	82.26	234.36	1265	33.99	5.62E-03
3.99	399	75.57	255.12	960	28.08	2.50E-03
4.97	497	71.78	268.56	790	24.32	1.79E-03
5.96	596	66.33	290.63	635	21.16	1.37E-03
6.94	694	63.73	302.52	505	17.52	8.16E-04
7.92	792	61.37	314.15	425	16.21	6.53E-04
Test 2 (Waste + 7.5% (by vol.) cover material)						
Applied vertical stress (kPa)	Equivalent depth of emplaced refuse fill (mm)	Total height of refuse in cell (mm)	Dry density kg/m ³	Drainage volume (ml)	Effective porosity (%)	Hydraulic conductivity (m/s)
Initial	-	110	225.39	2495	50.13	Nd
1.04	104	100.33	247.10	2070	45.60	1.17E-03
2.02	202	87.98	281.28	1500	37.68	4.01E-03
3.00	300	83.97	295.27	1295	34.09	3.28E-03
3.99	399	78.44	316.07	1070	30.15	2.22E-03
4.97	497	74.66	332.08	900	26.64	1.18E-03
5.96	596	70.25	352.92	730	22.97	9.38E-04
6.94	694	66.43	373.20	605	20.13	6.98E-04
7.92	792	63.81	388.55	495	17.15	4.41E-04
Test 3 (Waste + 10% (by vol.) cover material)						
Applied vertical stress (kPa)	Equivalent depth of emplaced refuse fill (mm)	Total height of refuse in cell (mm)	Dry density kg/m ³	Drainage volume (ml)	Effective porosity (%)	Hydraulic conductivity (m/s)
Initial	-	110	242.14	2470	49.63	Nd
1.04	104	101.20	263.16	2090	45.65	4.72E-03
2.02	202	89.13	298.79	1535	38.06	2.11E-03
3.00	300	84.68	314.52	1305	34.06	1.96E-03
3.99	399	79.60	334.62	1115	30.96	1.44E-03
4.97	497	75.10	354.62	935	27.52	1.03E-03
5.96	596	70.32	378.74	735	23.10	7.75E-04
6.94	694	66.93	397.89	625	20.64	5.20E-04
7.92	792	63.86	417.10	505	17.48	4.04E-04

Nd – Not determined

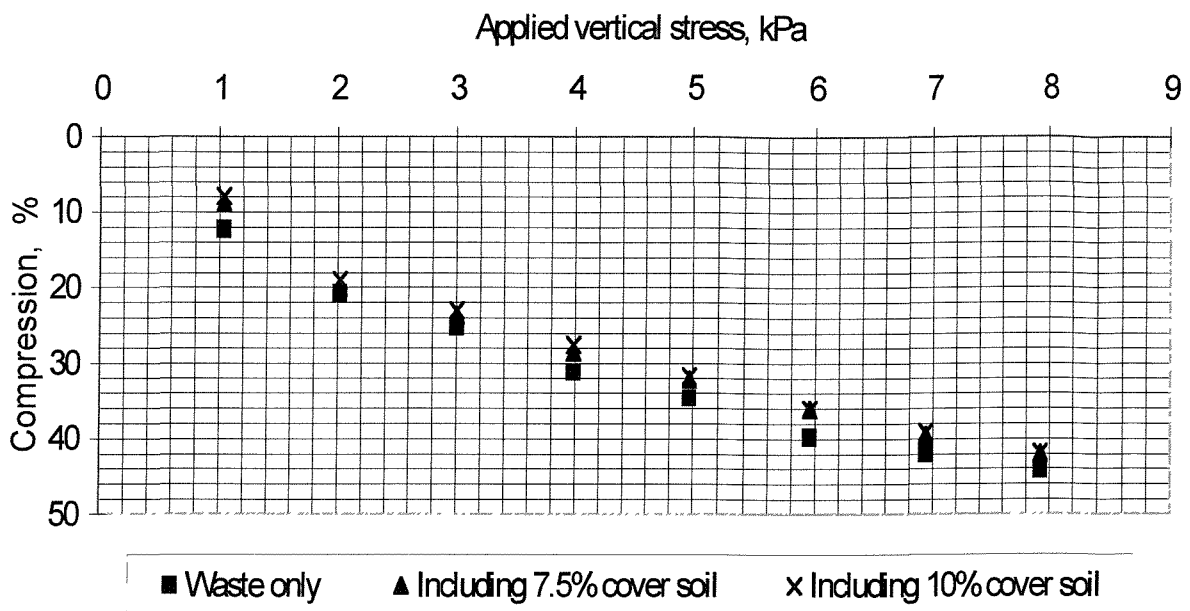


Figure 7.2: Compression of refuse at different applied vertical stress

The dry density of the refuse in Test 1 (refuse-only) was lower than the refuse in Tests 2 and 3 (refuse with cover soil) under the same vertical loading (Figure 7.3). The dry density of refuse in Test 1 increased from 225.39 kg/m^3 without any load application to 314.15 kg/m^3 at an applied vertical stress of 7.92 kPa. Similarly, the dry density of refuse in Test 2 and Test 3 increased from 225.39 kg/m^3 and 242.14 kg/m^3 to 388.55 kg/m^3 and 417.10 kg/m^3 respectively.

The volume of water drained from the saturated refuse samples at field capacity decreased with increasing load application. This is as expected since the volume of pores in the refuse sample decreased with increased compression. The maximum and minimum drainage volumes of water from the samples occurred in Test 1, and were 2510 ml and 425 ml under no loading and a vertical stress application of 7.92 kPa respectively.

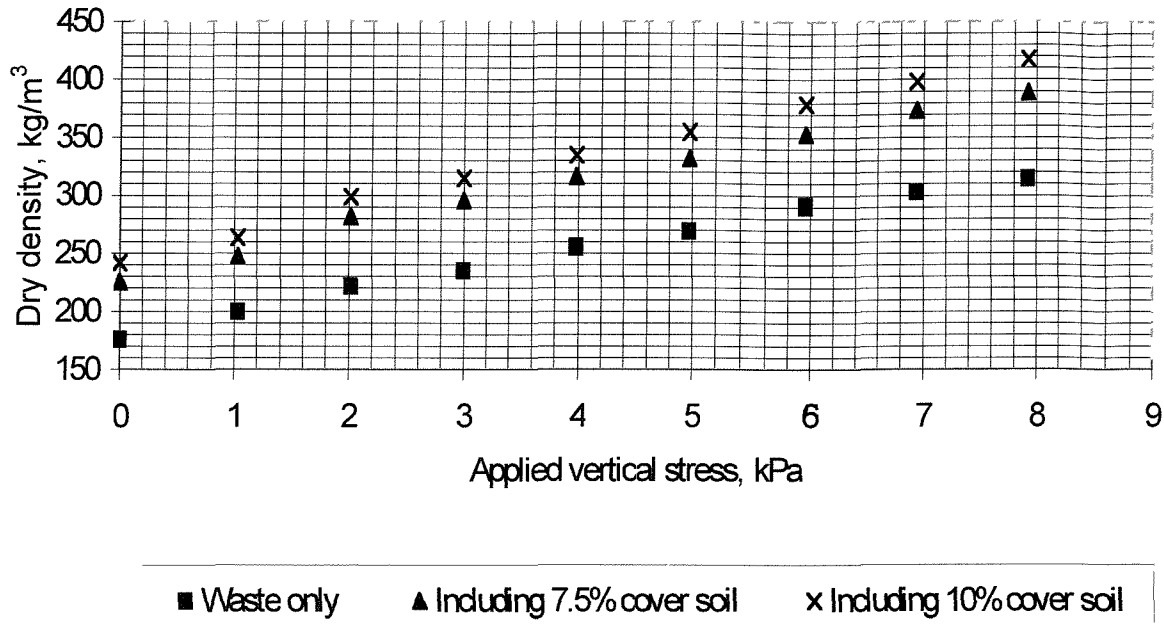


Figure 7.3: The dry density of refuse at different applied vertical stresses

The effective porosity is plotted against the dry density of the refuse samples in Figure 7.4. As expected, the porosity of the refuse samples decreased with increasing dry density. The dry density of waste with cover soil was however higher than the waste-only fill at the same porosities. A relationship between effective porosity and dry density was obtained by fitting a trend curve to the data plotted in Figure 7.4. The characteristic equations are:

$$n = 2 \times 10^6 \rho_{dry}^{-2} \quad (\text{Test 1}) \quad [7.2]$$

$$n = 2 \times 10^6 \rho_{dry}^{-1.95} \quad (\text{Test 2}) \quad [7.3]$$

$$n = 2 \times 10^6 \rho_{dry}^{-1.9} \quad (\text{Test 3}) \quad [7.4]$$

where:

n = effective porosity of refuse in %

ρ_{dry} = dry density of refuse in kg/m^3

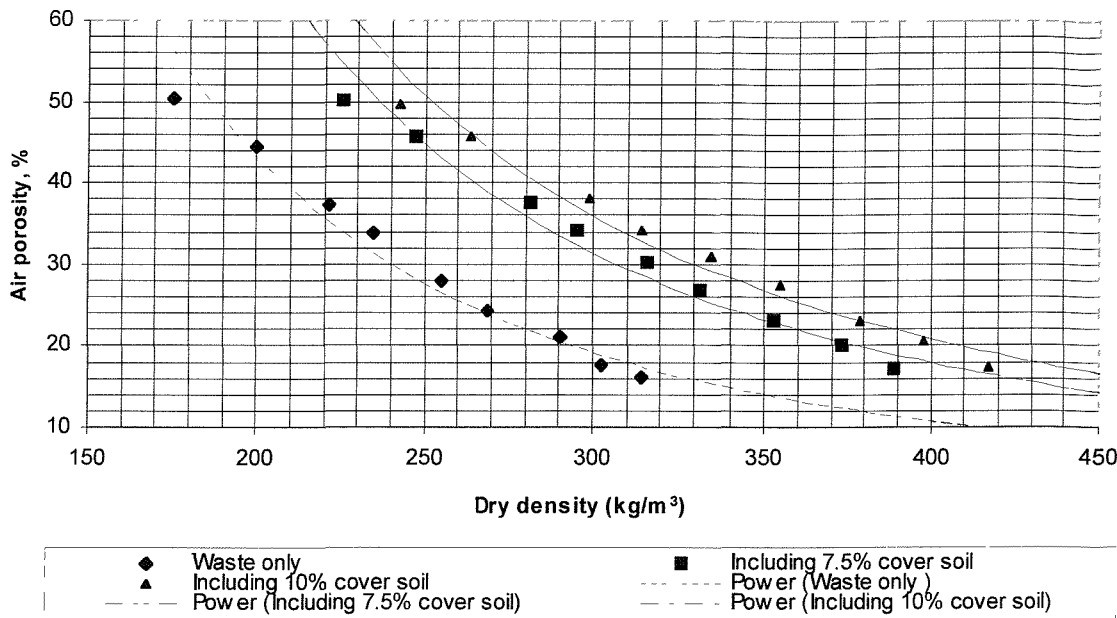


Figure 7.4: The effective porosity of refuse at different dry densities

The correlation of the fits to the data for Tests 1, 2, and 3 were 0.974, 0.973, and 0.971 respectively.

The hydraulic conductivity of the refuse at different applied stresses is shown in Figures 7.5 (a & b). Generally, the hydraulic conductivity of refuse decreased with an increase in applied vertical stress. The hydraulic conductivity of the refuse samples in Test 1 was higher than the refuse with cover soil in Tests 2 and 3, under the same vertical loading. The hydraulic conductivity of refuse samples in Test 1 decreased from 3.60×10^{-2} m/s under a loading of 1.04 kPa to 6.53×10^{-4} m/s under a vertical loading of 7.92 kPa. Also, the refuse in used in Test 3, which had a relatively lower hydraulic conductivity, decreased from 4.72×10^{-3} m/s to 4.04×10^{-4} m/s.

The hydraulic conductivity of a composite soil layer is determined from the following equation (Freeze and Cherry, 1979; Schroeder et al, 1994):

$$K_e = \frac{T_e}{\sum_{i=1}^n \frac{T_i}{K_i}} \quad [7.5]$$

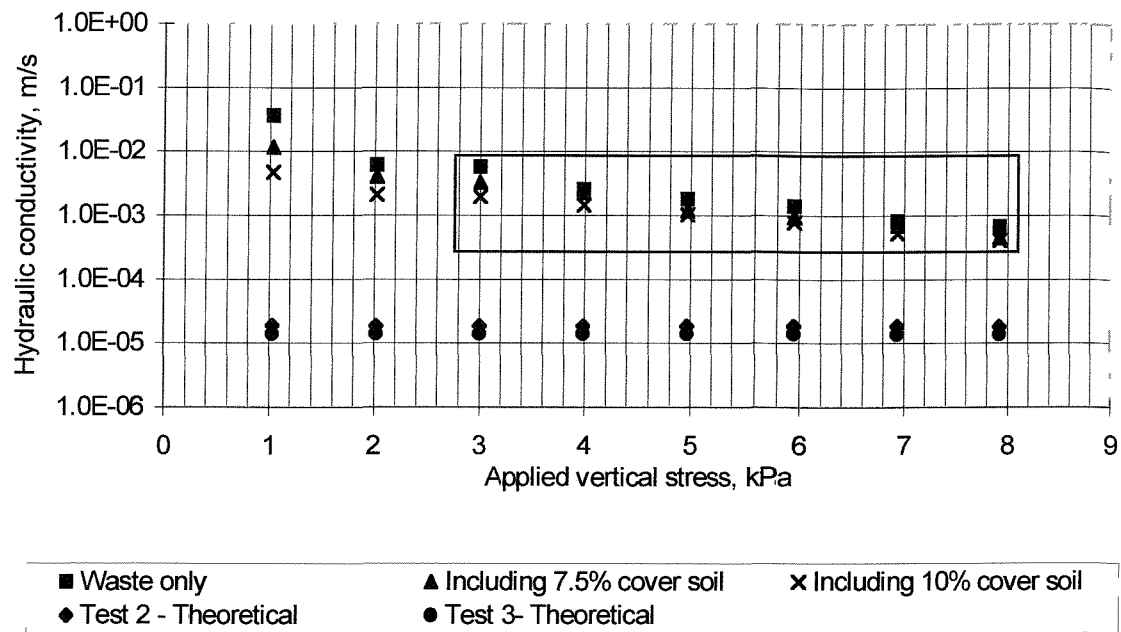


Figure 7.5a: Hydraulic conductivity of refuse vs. applied vertical stress

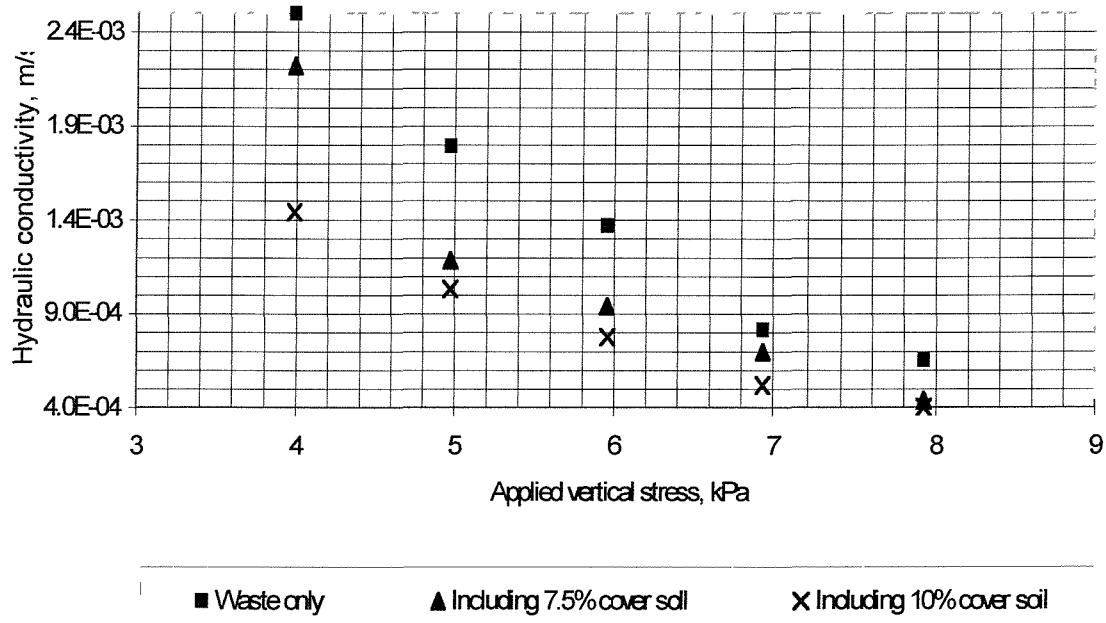


Figure 7.5b: Expanded hydraulic conductivity vs. applied vertical stress

where

K_e = effective saturated hydraulic conductivity of the combined layer

T_e = effective thickness of combined layer

T_i = thickness of layer i

K_i = saturated hydraulic conductivity of layer i

n = number of layers in the combined layer

The hydraulic conductivity of refuse samples in Tests 2 and 3 was determined using Equation [7.5] and plotted in Figure 7.5 a. There was no apparent change in the hydraulic conductivity of the refuse in Tests 2 and 3 with increased vertical loading. The hydraulic conductivity according to equation 7.5 was lower than the experimental hydraulic conductivity by a factor of 10^3 . However, the difference in these values decreases with increasing overburden (Figures 7.5a and B1).

In calculating the hydraulic conductivity of the composite layer of refuse and soil in Tests 2 and 3, the hydraulic conductivity of refuse-only used at different applied vertical stresses was that obtained from the experiment. Similarly, the hydraulic conductivity of emplaced cover soil, determined earlier in the laboratory, was used for the soil layer.

The hydraulic conductivity of the refuse fills in the cells at different dry densities is shown in Figure 7.6. The data were fitted using a trend line to provide a relationship between the hydraulic conductivity and dry density of the refuse samples within the range of applied loads in the experiment. The correlation of the data points was 0.95, 0.99, and 0.99 respectively.

The characteristic equations are given as follows:

$$HC = 5 \times 10^{16} \rho_{dry}^{-7.98} \quad (\text{Test 1}) \quad [7.6]$$

$$HC = 6 \times 10^{14} \rho_{dry}^{-7} \quad (\text{Test 2}) \quad [7.7]$$

$$HC = 2 \times 10^{10} \rho_{dry}^{-5.18} \quad (\text{Test 3}) \quad [7.8]$$

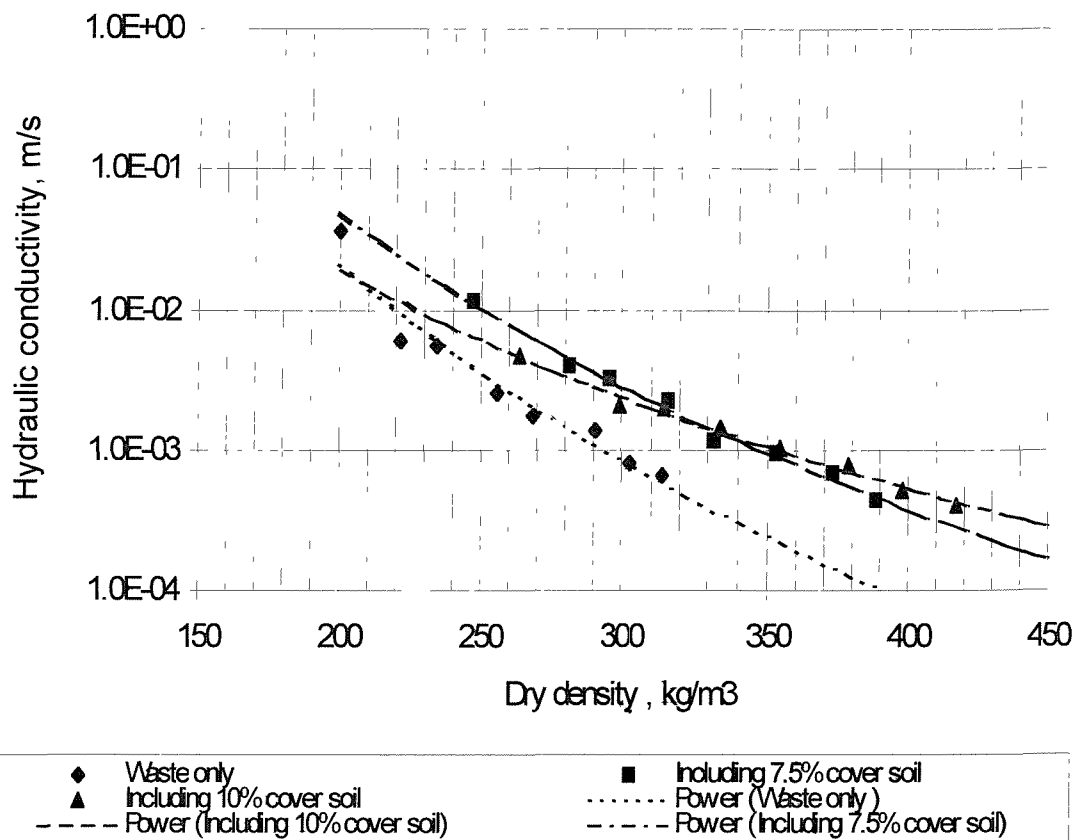


Figure 7.6: Hydraulic conductivity vs. dry density

where:

HC = hydraulic conductivity of refuse fill in m/s

ρ_{dry} = dry density of refuse fill in kg m^{-3}

The hydraulic conductivity of the refuse decreased with an increase in dry density.

Within the range of data, the hydraulic conductivity of the refuse-only samples was less than the composite refuse fills (Tests 2 and 3).

The hydraulic conductivity of the refuse fills in the cells at different porosities is plotted in Figure 7.7. In general, the hydraulic conductivity of the refuse increases with increasing porosity, however, the hydraulic conductivity of the refuse-only fill was higher than the refuse with cover soil.

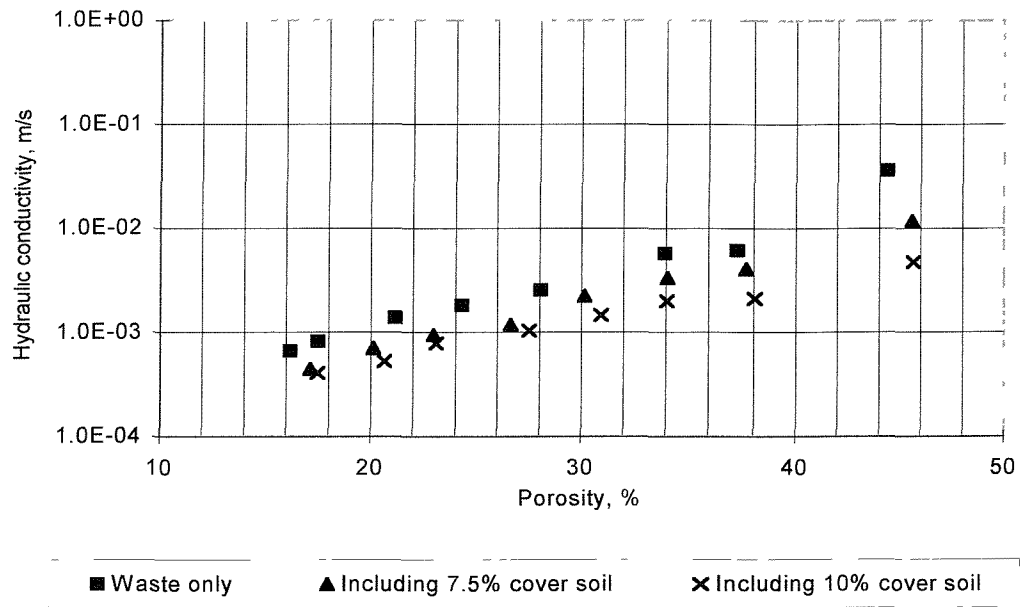


Figure 7.7: Hydraulic conductivity vs. Effective porosity

7.6 Discussion

The impact of applied vertical stress on both the geotechnical and hydraulic properties of three different types of emplaced refuse lifts in landfill was investigated using small-scale cells in the laboratory. Unlike previous laboratory investigations (Wall and Zeiss, 1995; Chen and Chynoweth, 1995; Beaven and Powrie, 1995), a soil layer, consisting of soil materials used as daily cover at White's pit landfill, Wimborne, Dorset, was interbedded between refuse fills in two of the tests undertaken (Test 2 – 7.5% cover soil; Test 3 – 10% cover soil) in the present study.

One of the problems commonly encountered in the testing of refuse in experimental cells is the impact of biodegradation on the properties of the refuse. Chen and Chynoweth (1995) reported that the hydraulic conductivity of refuse should be monitored over a considerable period to expend the gas produced by easily biodegradable substrate in the refuse. They obtained steady state conditions up to two weeks after refuse placement in 0.38 m diameter, 1.22 m long test columns during hydraulic conductivity tests on shredded compacted municipal refuse.

In contrast, steady state conditions were obtained within a week during refuse testing in present tests probably due to less easily biodegradable components in the refuse. In addition to excluding putrescible materials in the samples (Section 7.4.1), the tests were conducted in an unconfined cell to minimise errors in measurement of the hydraulic conductivity of the refuse fill by gas production from anaerobic biodegradation. Preferential flow (channelling) of water within the waste and along the cell wall, especially at low applied stress was also minimised by the uniform placement of waste samples in the test cell. The pressure exerted on the cell wall by waste particles, as the applied vertical load increased would further reduced the channelling of water along the cell wall.

The results of the properties of refuse fills at various applied vertical stresses in the experimental cells are discussed in the following sections. Due to the small thickness of the waste samples, the variation in the applied stress with the depth within the refuse was assumed to be very small. Consequently, the variation in porosity, density, and hydraulic conductivity of the refuse with depth was not considered to be significant.

7.6.1 Compression and Density of the refuse fill

As expected, the compression of the refuse samples increased with increasing applied vertical load. As the vertical load was increased, the intercontact area of the refuse increased, leading to a greater portion of the refuse fabric supporting the load. The increased resistance to compression through increased structural support by the waste fabric resulted in low compression, which is also common to soil.

The compression of the refuse samples with daily cover (Tests 2 and 3) was similar over the range of applied stresses, as there was little difference in the quantities of the cover soil in them. The compression of the refuse-only fill, however, was greater than the refuse with cover soil at the same applied vertical stresses (Figure 7.2). At an applied vertical stress of 7.92 kPa, the refuse-only fill had a compression of 44.21% while the compression of the refuse with a 10% cover soil was 41.95%. The difference in the compression of the waste types was therefore due to the soil layer in the refuse fill. If the final thickness of the samples (Table 7.2) is considered, a volume

of approximately 50%⁶ of the cover soil would have ravelled into the waste mass since placement in the cell. The soil material would have ravelled into the pores in the underlying waste layer during its placement in the cells and subsequently during the application of vertical stresses (Figure 5.3). As the ravelled soil materials would provide additional resistance to the compression of the refuse fills due to its relatively higher structural strength, the estimated ravelling of 50% into the refuse with 10% cover soil (see footnote) from the samples' settlement was taken as a maximum value.

The dry density of the samples increased with an increase in applied vertical load. The dry density of the waste-only sample was significantly lower than the refuse samples with cover soil over the range of applied vertical stresses. As no significant loss of mass was evident during the experiment, the relative increase in the dry density of the composite refuse samples was due to the heavier soil particles within the waste fill.

7.6.2 Porosity and Hydraulic Conductivity

The porosity of the refuse fills in the cells, as expected decreased with increasing dry density (Figure 7.4). The hydraulic conductivity of the refuse fills increased with porosity (Figure 7.7), and thus increased with increasing applied vertical stress and dry density (Figures 7.5 and 7.6). When the applied stress was increased from 1.04 kPa to 7.92 kPa, the hydraulic conductivity of the refuse-only decreased from 3.6×10^{-2} m/s to 6.5×10^{-4} m/s while that of the refuse with 10 % cover soil decreased from 4.7×10^{-3} m/s to 4.04×10^{-4} m/s. The flow of water through the refuse-only fill was greater than in refuse with cover soil at the same applied stresses and porosities (Figures 7.5 (a,b) and 7.7) due to many factors including the relatively low permeability of the cover soil and the high microporosities of the refuse components compared to the soil particles.

⁶ Initial sample thickness = 110 mm; At 7.92 kPa, thickness of refuse-only sample = 61.37 mm, thickness of refuse+10% soil = 63.86 mm; Difference in thickness = 2.49 mm; Initial thickness of cover soil = 5 mm.

There was a disparity in the calculated and experimental permeability of the refuse fills. If a trend line is fitted to the plot in Figure 7.5a, the experimental values will equal the calculated values (according to equation 7.5) at applied stresses in excess of 50 kPa (Figure B1). This indicates that the permeability of the cover soil layer in the cell was less than its typical field value (Mott MacDonald, 1990b; Section 7.4.2), which was used in the calculation using equation 7.5. This is not surprising since the relative loose placement of the cover soil would result in a greater flow of water through the refuse fill than the calculated values. However, increased densification of the soil layer would result from increasing overburden, and the permeability of the cover soil will reduce to the in-situ (Figure B1) at high stresses. At this stage, the permeability of the cover soil layer would be as low as the emplaced refuse lifts and therefore inconsequential to the water flow in the entire refuse fill.

In essence, the flow of water through the refuse fill at White's pit cannot be determined from theoretical estimation based on soil mechanics principles due to the loose placement of the cover soil and the continuing decrease in its thickness due to ravelling into the waste mass.

A trend line was fitted to the plots in Figures 7.4 and 7.6 to obtain a relationship between effective porosity, hydraulic conductivity and dry density of the refuse fills over the range of applied vertical stresses in the experiment. The high correlation of the characteristic curves in Figures 7.4 and 7.6 demonstrates that derived characteristic equations (equations 7.2 -7.4; 7.6 – 7.8) from the experimental data can be used to predict the effective porosity and hydraulic conductivity of the refuse fill at White's pit from its dry density, within the limits of scale effects of the experiment.

7.6.3 Comparison of Experimental Results with Data Obtained from Beaven and Powrie (1995) Large-scale Cells

The results of the data obtained from tests (small) cells in present study are compared with that obtained from large-scale cells by Beaven and Powrie (1995). In their work, a 2 m diameter and 3 m high steel cylinder was used and is one of the largest test cell

Percentage of ravelling (approximate) = $(2.49 \text{ mm} / 5 \text{ mm}) \times 100 = 49.8\%$

used to determine the properties of municipal waste. Wall and Zeiss (1995) reported that reducing the characteristic refuse particle size to less than 20% of the test cell's diameter will give reasonable results from refuse testing in a cell whose diameter is less than 1m. Consequently, the refuse samples of were reduced to a nominal particle size of 20 x 5mm.

The effective porosity, hydraulic conductivity, porosity, and field capacity of the crude refuse in the large-scale tests at different dry densities are shown in Figure 7.8 – 7.11. As in the experimental tests (tests 1, 2, and 3), a trend line was fitted to the data points in Figures 7.8 and 7.9 and 7.11 to establish the relationships between the effective porosity, hydraulic conductivity, field capacity and dry density of the refuse tested in the large-scale cells. The resulting characteristic equations are:

$$n = 10^{11} \rho_{dry}^{-3.8} \quad [7.9]$$

$$HC = 10^{20} \rho_{dry}^{-9.5} \quad [7.10]$$

$$FC = 14.82 \rho_{dry}^{0.18} \quad [7.11]$$

where

n = effective porosity of refuse in %

HC = hydraulic conductivity of refuse fill in m/s

FC = field capacity of refuse in %

ρ_{dry} = dry density of refuse in kg/m³

The equations of the characteristic curves in Figures 7.8 and 7.9 ought to be valid within the limit of the test data. But, by extending the trend curves to the ranges encountered in Tests 1, 2, and 3 and the large scale testing, a good comparison can be made between the different scale of experiments.

There is a slight difference in the magnitude of refuse properties in the both scales of experiments (Figure 7.8 & 7.9). However, if the differences in the density, routing of moisture, settlement, and other scale factors of both sets of tests are taken into consideration, the experimental data compared well with the data of the large-scale tests.

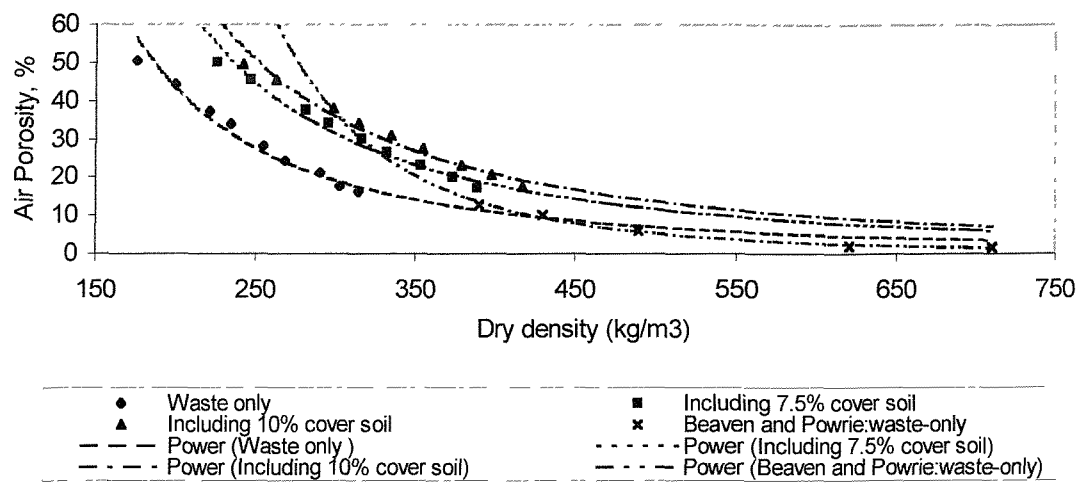


Figure 7.8: Effective porosity versus dry density of refuse tested in small cells and large-cell

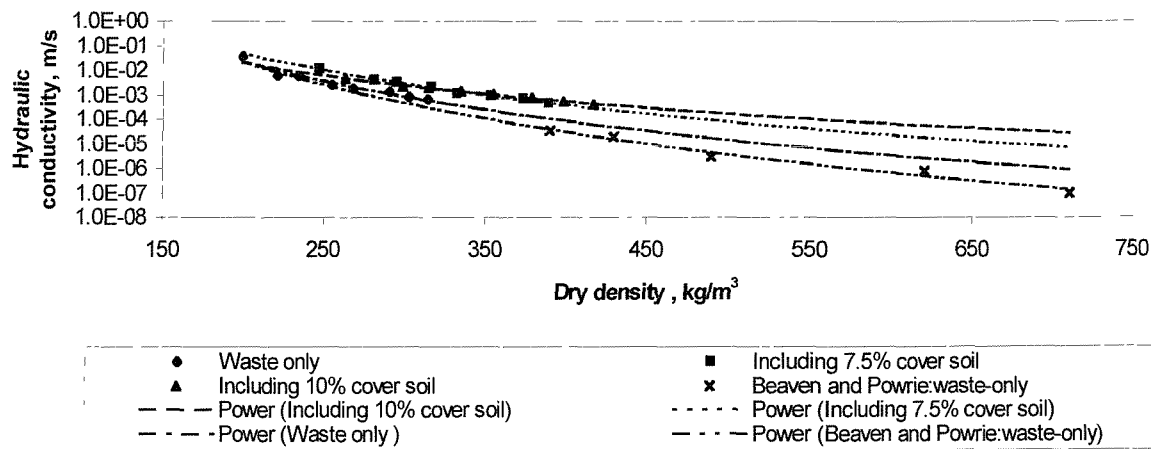


Figure 7.9: Hydraulic conductivity versus dry density of refuse tested in small cells and large cell

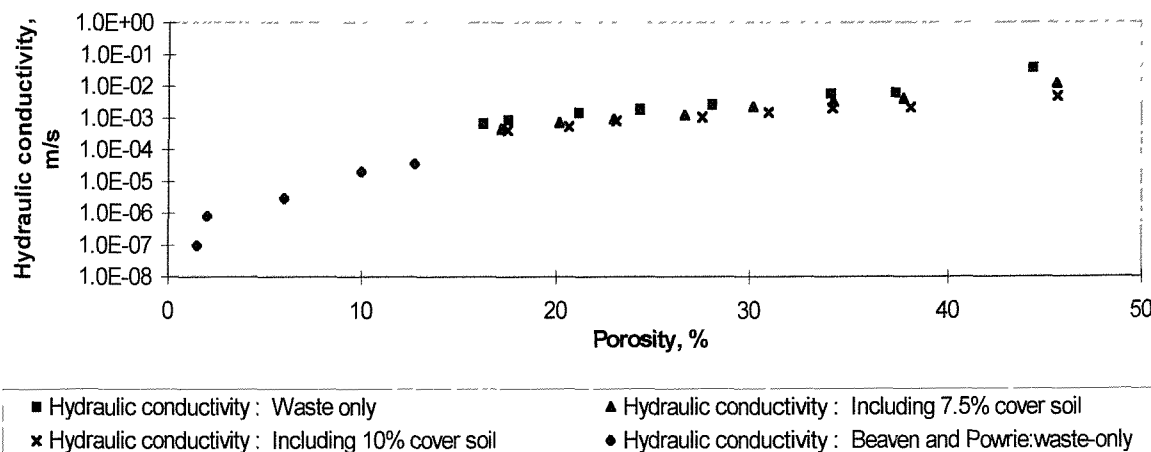


Figure 7.10: Hydraulic conductivity versus effective porosity of refuse tested in small cells and large-scale cell

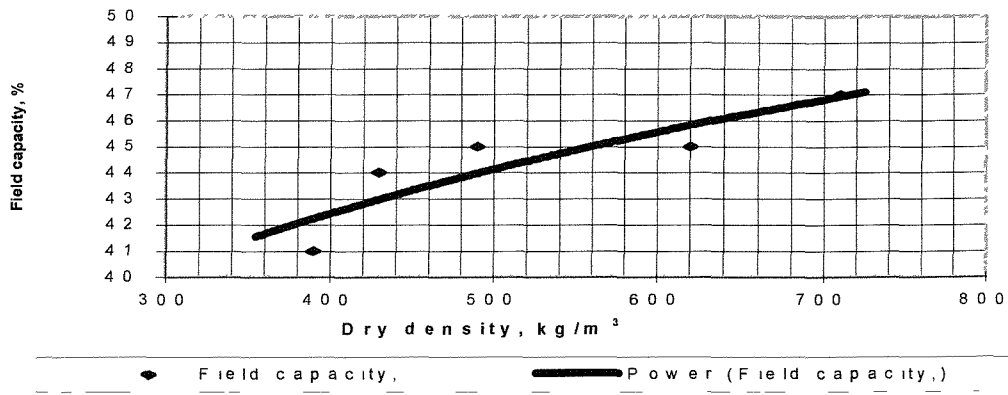


Figure 7.11: Field capacity vs dry density (Beaven, 2000)

There is a substantial similarity in the magnitude of the dry density, used as a determinant parameter for determining the effective porosity of refuse in equations 7.2 and 7.9, and for hydraulic conductivity in equations 7.6 and 7.10, for the large-scale and the refuse-only data. This is not surprising since the refuse samples used in both cases did not contain a layer of cover material as in Tests 2 and 3.

Besides the similarity with the large-scale cell data, the relationship between effective porosity and dry density in the small-scale experiment is also akin to that obtained from tests undertaken in recompacted crude waste in 210 litre-drums (Table 5.6). The similarity between the data at both scales of experiments is best depicted in the plot of hydraulic conductivity against effective porosity in Figure 7.10. Despite the difference in sizes of the cell and waste components, and the range of applied stresses in both tests, the data points, which shows an increase in the permeability of refuse with increasing effective porosity, appears similar for each experiment.

In general, the results obtained from tests on refuse in a small cell (Tests 1, 2, and 3) showed substantially similar trends of waste behaviour to that observed in the large-scale compression cell (Beaven and Powrie, 1995). In particular, the reduction in waste particle sizes in relation to the size of the test cell was found to be appropriate when using small cells for testing municipal refuse materials. The test methodology, together with the low cost of the apparatus, showed the experiment to be cost-effective. Such tests will be valuable in preliminary investigations on the behaviour of

waste, and also in researches carried out in developing countries; where there is currently an increased awareness of the damage and effects poor waste management have on environment, but with few testing facilities.

7.6.4 The Impact of Cover Soil on the Properties of Refuse Layer and Implications for Landfilling

The placement of a cover soil on a refuse layer was found to affect the overall geotechnical and hydraulic properties of the refuse fill. The refuse samples with cover soil materials assimilated into the waste was found to be slightly less compressible than the waste-only sample. Under a vertical loading of 7.92 kPa, the compression of the refuse-only fill (44.21 %) was 2.26% more than that of refuse with 10 % cover soil. In contrast, the dry density of the refuse with 10% cover soil (417 kg/m³) was more than 30% greater than the refuse-only fill.

Whereas the landfill operator may benefit from the space occupied by the daily soil cover and extra space created in the settlement of refuse-only fills, the use of a cover soil, which may also hinder biodegradation, may appear uneconomical. However, the daily soil cover may densify the refuse fill and its function, which includes limiting infiltration and preventing fly infestation, is vital to effective landfill practice.

One of the main concerns in using cover soils in landfills is the impact they may have on the hydraulic conductivity of the refuse fills. The permeability of a refuse fill with the cover soil used at White's pit (slightly clayey/silty slightly gravelly sand) was found to be slightly less than that of refuse-only fills. In particular, the observed hydraulic conductivity of the composite fill was found to be less than its calculated values (equation 7.5) due to the loose placement of the soil cover. This behaviour is likely to be observed in large-scale landfills as daily soil cover is also placed loosely on emplaced waste layers in MSW landfills.

CHAPTER

8

The Help Model - An Overview

8.1 Summary

The basic concepts of the Hydrologic Evaluation of Landfill Performance (HELP) computer program, which is commonly used for estimating leachate volume in MSW landfills, is described in this chapter.

8.2 The HELP Model

The HELP computer program is a quasi-two-dimensional hydrological model of water movement across, into, through and out of landfills. HELP (Version 3.01) model was developed by the U.S Army Engineer Waterways Experiment Station (WES), Vicksburg, for the U.S. Environmental Protection Agency (EPA), Risk Reduction Engineering Laboratory, Cincinnati, OH. The model accepts weather, soil and design data, and uses solution techniques that account for the effects of surface storage, snowmelt, runoff, infiltration, evapotranspiration, vegetative growth, soil moisture storage, lateral subsurface drainage, leachate recirculation, unsaturated vertical drainage, and leakage through soil, geomembrane or composite liner systems.

The program can model whole landfill systems including various combinations of vegetation, cover soils, waste cells, lateral drain layers, low permeability barrier soils, and composite liners incorporating synthetic geomembrane liners. HELP (v.3.01) was developed to assist with water balance analyses of solid waste disposal facilities, including the landfill cover systems. The model conducts rapid estimation of key parameters such as runoff, evapotranspiration, drainage, leachate collection and liner

leakage that may be expected to occur during the operation and post closure period of a wide variety of landfill designs. HELP is especially useful for the comparison of alternative landfill designs and their impacts on water balances.

8.2.1 Modelling Procedure

The hydrologic conditions modelled in a MSW landfill can be categorised as surface and subsurface processes. The surface processes include interception of rainfall by vegetation, snowmelt, surface runoff, and evaporation of water. The subsurface processes include plant transpiration, vertical unsaturated drainage, evaporation of water from the soil, geomembrane liner leakage, barrier soil liner percolation and lateral saturated drainage.

To illustrate the modelling concept using the HELP program, a schematic profile of a typical hazardous waste landfill is shown in Figure 8.1. In reality, modern MSW landfills will often have a reduced provision for base drainage than that shown in Figure 8.1. The majority of old dilute and disperse landfills are likely to have no liner provision.

The daily infiltration into the landfill is obtained indirectly from the water balance of the surface water quantities. In the absence of a snow cover, the infiltration is:

$$INF_i = PRE_i + GM_i - INT_i - Q_i \quad [8.1]$$

In the presence of a snow cover, the infiltration is:

$$INF_i = O_i + GM_i - EMELT_i - Q_i \quad [8.2]$$

where:

INF_i = infiltration on day i , mm

PRE_i = precipitation on day i , mm

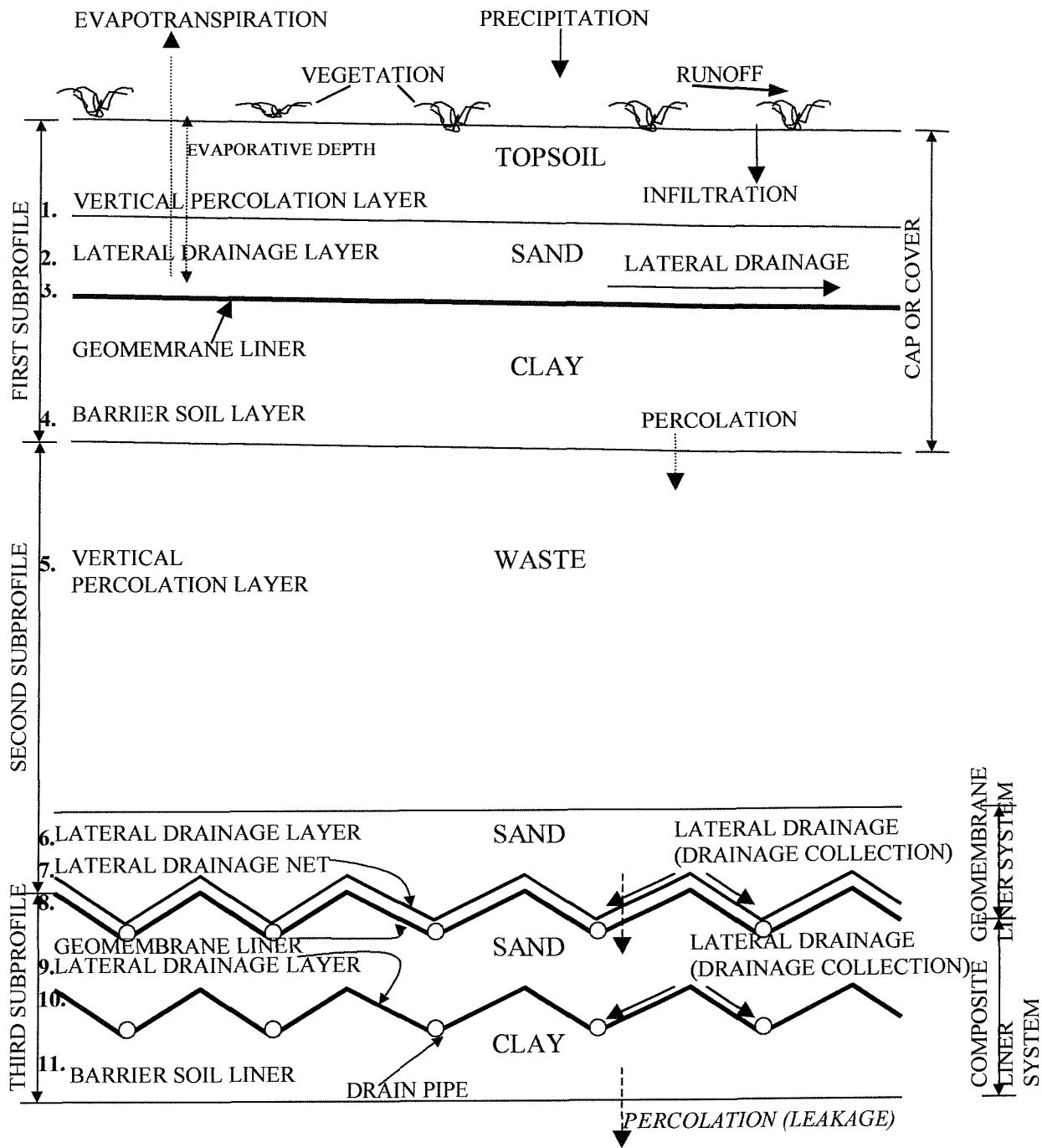


Figure 8.1: Schematic profile view of a typical hazardous waste landfill (Schroeder et al, 1994).

GM_i = groundmelt on day i , mm

INT_i = interception of rainfall by vegetation on day i , mm

$EMELT_i$ = surface melt that is evaporated on day i , mm

Q_i = is the actual runoff on day i , mm

O_i = outflow from snow cover on day i available for evaporation, runoff, and infiltration, mm

Precipitation data can be obtained from the Meteorological Office. Groundmelt are empirical values. The rainfall-runoff is modelled using the Soil Conservation Service (SCS) curve number as presented in Section 4 of the National Engineering Handbook of US Department of Agriculture (Schroeder et al, 1994). The equations for the hydrological sub-models (INT_i , $EMELT_i$, O_i) are stated in the HELP documentation. The liquid water is not held in surface storage from one day to the next except in the snow cover or when the topsoil is saturated and runoff is not permitted.

The daily surface water routing can be described as follows. The precipitation (snowfall and rainfall) is added to the surface snow storage (if present), and snowmelt and excess storage of water is computed. The entire outflow from the snow cover is considered simply as rainfall when computing the runoff. The surface evaporation is then calculated but it is not allowed to exceed the sum of surface snow storage and intercepted rainfall. In addition, interception is computed only for rainfall, not for outflow from the snow cover. The quantity of rainfall and snowmelt that does not run off or evaporate is assumed to infiltrate into the landfill. In situations where the computed infiltration is greater than the drainage and storage capacity of the soil, the excess water is routed back to the surface and added to the runoff. If runoff is restricted, the excess water is ponded on the surface and subjected to evaporation and infiltration during the next day.

The first subsurface process involves evapotranspiration from the evaporative zone of the upper subprofile (Figure 8.1). As evapotranspiration decreases with depth, the evaporative zone of the upper subprofile (cover soil) is divided into seven modelling segments. The top segment and the second segment of the evaporative zone are set at one thirty-sixths and five thirty-sixths of the thickness of the evaporative depth respectively. Each of the bottom five segments is set at one-sixths of the thickness of

the evaporative depth. The evapotranspiration demand is calculated daily and distributed among the segments; the demand decreases with the depth of the segment. A vegetative growth model is used for the daily growth and decay of the surface vegetation.

The remaining subsurface processes are simulated within each subprofile in turn, from top to bottom using a design dependent time step. The time step is sized to ensure that the lateral drainage layer if initially wetted to field capacity, cannot be saturated in a single time step, even in the absence of drainage from the layer. The number of time steps, which is based on empirical estimation from field conditions, varies from 4 to 48 per day.

A storage–routing procedure is used to redistribute the soil water among the modelling segments of the subprofile. A mid-point routing of storage at each time step thereby provides simulation of simultaneous incoming and outgoing drainage processes. Mid-point routing tends to produce relatively smooth, gradual changes in flow conditions, avoiding the abrupt changes that result from applying the full amount of moisture to the segment at the beginning of the time step. Using time steps shorter than the period of interest (0.5hr – 6hrs) further smoothes the simulation process. The mid-point routing is based on the following equation of continuity for a segment:

$$\Delta \text{Storage} = \text{Drainage In} - \text{Drainage Out} - \text{Evapotranspiration} + \text{Leachate Recirculation} + \text{Subsurface Inflow} \quad [8.3]$$

The unsaturated hydraulic conductivity is related to the saturated hydraulic conductivity as follows (Schroeder et al, 1994):

$$K_u = K_s \left[\frac{\theta - \theta_r}{\phi - \theta_r} \right]^{3+\left(\frac{2}{\lambda}\right)} \quad [8.4]$$

where:

K_u = unsaturated hydraulic conductivity, cm/sec

K_s = saturated hydraulic conductivity, cm/sec

θ = actual volumetric water content, vol/vol

θ_r = residual volumetric water content, vol/vol

ϕ = total porosity, vol/vol

λ = pore-size distribution index, dimensionless

The unsaturated vertical drainage and soil water storage for each segment are calculated from a solution of equations 8.3 and 8.4, and the Darcy's equation (equation 7.1].

In situations where the subprofile has a liner, water-routing or drainage from the segment directly above the liner is computed as leakage or percolation through the liner, and lateral drainage to the collection system, if present. An estimate of the lateral drainage and leakage/percolation is first used to compute the moisture storage and head on the liner. The calculated head is used to compute the leakage and lateral drainage, which is compared to the initial estimate. The procedure is repeated until an acceptable convergence is achieved. The liner is assumed to be saturated, so any drainage into the liner results in an equal drainage out of the liner. There is no lateral drainage if the subprofile does not contain any liner; vertical drainage from the bottom subprofile in such a case is calculated as the upper modelling segments.

8.2.2 Limitations in the Application

The program performs water balance analysis for a minimum of one year. All simulations start on the January 1 and end on December 31. The physical characteristics of the landfill specified by the user remain constant throughout the simulation period. No adjustments are made for the changes that occur in these characteristics as the landfill ages. Furthermore, the program cannot model the filling process within a single simulation. Ageing of materials and staging of the landfill operation must therefore be modelled by successive simulations.

The values for the maximum leaf index may range from 0 for bare ground to 5 for excellent vegetation of grass. Greater leaf indices do not have an impact on the

results. For numerical stability, the minimum evaporative zone should be at least 8 cm. The program computes evaporation coefficient based on their soil properties. The default values for the evaporation coefficient are based on experimental results. The basis for the calculation of these default values is described by Schroeder et al. (1994). The model imposes upper and lower limits of 5.1 and 3.3 for the evaporation coefficient so as not to exceed the range of experimental data.

The model can simulate water routing in twenty layers of soil, waste, geosynthetics, or other materials for a period of 1 to 100 years. As many as five liner systems, either barrier soil, geomembrane or composite liners can be used. However, each of the layers must be described as being one of four operational types: vertical percolation, lateral, barrier soil liner or geomembrane. The model does not permit a vertical percolation layer to be placed directly below a lateral drainage layer. A barrier soil liner may not be placed directly below another barrier soil liner. A geomembrane liner may not be placed directly below another geomembrane liner. Three or more liners, barrier soil or geomembrane cannot be placed adjacent to each other. The top barrier shall not be a barrier soil or geomembrane liner.

The porosity, field capacity and wilting point can theoretically range from 0 to 1 (units of volume per volume), however, the porosity must be greater than the field capacity, which must be greater than the wilting point. The initial moisture storage must be greater than or equal to the wilting point and less than or equal to the porosity. In addition, the initial moisture content of liners must be equal to the porosity and the liners remain saturated throughout the life of the landfill.

The limits of the application ensures that the results are valid, based on the theory and the range of data of the empirical sub-models used for simulating the physical processes occurring in the landfill. It also ensures the stability of the numerical manipulation in the program. The assumptions made in the solution methods of the program are documented in the User's Guide (Schroeder et al, 1994).

Despite the fact that the HELP model was initially developed for the US, experiences in various countries (Chapter 3) have shown that HELP will yield reasonable results when applied to any landfill, if the input data are accurate. Considering the limit on

the change in physical characteristics of the landfill within the minimum simulation period, the HELP model was used to model the moisture storage in refuse lifts at White's pit and is described in Chapter 9.

CHAPTER

9

Simulation of Moisture Stored in Refuse Lifts in a Municipal Landfill

9.1 Summary

A back analysis of the long-term effects on moisture stored within the lifts of a refuse fill is presented. The moisture routing analysis is undertaken with the Hydrologic Evaluation of Landfill Performance (HELP) computer model and has been modified to consider changes in compression, dry density, porosity, field capacity, and hydraulic conductivity of the emplaced refuse lifts. The results are compared with field data, and an assessment of the modified HELP analysis is discussed.

9.2 Introduction

The ability to simulate accurately moisture storage in a MSW landfill is a requirement of any landfill planning application as it significantly enhances the operation of a waste disposal facility. The majority of studies involving moisture routing in refuse fills have been undertaken on restored landfills (Dass et al, 1977; Holmes, 1980; Campbell, 1983). However, Bleiker et al (1995) simulated the moisture stored in incompressible refuse layers with the HELP model, when demonstrating the formation of leachate mounds in refuse landfills. A rheological model (Edil et al, 1990) was used to determine the thickness of the refuse layers at a post-closure period when physical compression was considered to be insignificant.

Possible reasons for the inability of researchers to simulate accurately moisture routing during the filling period of the landfill include:

- The water balance equation method commonly applied to waste sites does not consider changes in key parameters such as porosity, density, and hydraulic conductivity of the waste fill over time.
- There is no widely available model, which has been formulated to estimate geotechnical and hydraulic properties of refuse under different loading conditions, or long term changes.

In the present study, the moisture stored in refuse lifts during both the active and post-closure periods of the restored landfill at White's Pit, Poole, was simulated. The conventional use of the HELP model was modified to account for the temporal changes in porosity, field capacity, density, and hydraulic conductivity of emplaced refuse lifts at landfill site. In addition, the impact of the cover materials (both daily and final capping) on refuse properties and moisture storage is considered with reference to the field and experimental works described in Chapters 5-7.

9.3 The Empirical Models for Refuse Properties

It is extremely difficult to make a precise prediction of refuse properties because of the heterogeneity of waste. Unlike soils, some refuse components degrade, and the rate and amount of biodegradation of a refuse mass is very difficult to estimate because of the factors that may influence them. The hydraulic and geotechnical tests of refuse in test cells (Beaven, 2000; Chapter 7) have generally been undertaken in short periods of time to minimise the impact of long term biodegradation of refuse.

The projection of characteristic curves for the small scale cell results of this study (Figure 7.10) to the range of applied stresses in large compression cells of Beaven and Powrie (1995), showed that the derived characteristic equations (equations 7.2-7.4, 7.6-7.8) can be used to estimate waste properties at stresses at landfills. In determining the temporal changes in the properties of refuse lifts placed at White's Pit landfill, characteristic equations derived from refuse samples with 7.5% cover soil, which is representative of the landfill process at White's Pit, was used.

The characteristic equations for determining the air porosity and hydraulic conductivity of the refuse with 7.5% cover soil are shown in equations 7.3 and 7.7. Dry density is the dependent parameter for determining other refuse properties in these equations due to the following reasons:

- Among the refuse parameters, the dry density is easily estimated from the vertical compression of refuse layers, which can also be estimated from a compression model.
- Dry density is the density refuse has at same void ratio. The effect of the moisture contents of different emplaced refuse lifts is eliminated, thereby minimising the unknown parameters of the modelling; thus enhancing the accuracy of prediction.
- The ability to estimate other refuse parameters from the dry density of municipal refuse reduces the need to undertake several refuse tests at the site. It significantly minimises the cost and time used in simulating the moisture routing of the refuse fill.

The vertical compression of refuse lifts due to overburden during the fill period of the landfill is estimated from equation 2.2 while the post-closure settlement is determined from equation 2.3. These equations, which are based on empirical observations, are preferred to the models proposed by Watts and Charles (1999) because of their convenience and compatibility with the procedure of moisture simulation with the HELP model. By using the secondary compression index of 0.09 obtained in Chapter 6 and an average primary compression index of 0.2 (Table 5.9), the empirical compression models are stated as follows:

$$S_p = 0.3H_t \log \frac{\sigma^1}{\sigma} \quad [9.1]$$

$$S_s = 0.09H_t \log \frac{t}{t_p} \quad [9.2]$$

where

S_p = primary settlement occurring in the refuse lift being considered

S_s = secondary settlement occurring in the refuse lift being considered

H_t = initial thickness of the refuse lift being considered

σ^1 = existing applied vertical stress acting at the mid-level of the refuse lift

σ = previous applied vertical stress acting at the mid-level of the refuse lift

t = present time or period at which settlement is desired

t_p = starting time or period at which secondary settlement is desired. t_p is usually taken as one month (Sowers, 1973).

9.4 Moisture Simulation at White's Pit Landfill

9.4.1 Introduction

A back simulation of moisture stored in the restored biodegradable landfill at White's Pit from 1986 to 1998 was conducted mainly to determine the impact of sequential emplacement of refuse on the moisture content of emplaced lifts. To simplify the simulation due to the multiple filling sequence in the landfill, a tipping area G (Figure 4.5) was selected for analysis. This tipping area (G) was also chosen to observe the moisture storage during the inactive fill period (1991) within the tipping regime of the fill area. As a result of the complex conditions existing in the landfill, the following assumptions were made for the simulation:

- The simulation area represented a refuse column, consisting of individual lifts (cells) of waste.
- The only source of infiltrating water was precipitation.
- There was spatial uniformity in the climatic and landfill conditions on site.
- There was spatial uniformity in compaction, composition, and compression of the emplaced refuse layers.
- The hydraulic and geotechnical properties of individual refuse lifts were considered to be uniform. These were taken to be the mean values of the properties in each lift.
- The net horizontal inflow of water into the refuse column was zero.
- Each additional refuse lift was placed, only when the previous emplaced lifts had been completely laid on the fill area.
- Each further placement of refuse on a refuse lift was taken as additional imposed load.

- The pore pressure in the emplaced refuse layers was considered to be negligible (see Figure 5.7) during the active filling period of the landfill.
- There will be leakage through the top cover soil system as its integrity depreciates.
- The leachate mound drains from the sand drainage layer overlying the basal liner (Broadstone clay)

9.4.2 HELP INPUT

The input requirements for the HELP analyses are shown in the flow diagram in Figure 9.1. The daily precipitation, daily temperature, and daily solar radiation for the area were obtained from the Meteorological Office at Bracknell (UK Meteorological Office, 1999).

The evaporative depth was determined from monitoring moisture content in the topsoil of the site (Figures 6.4 and 6.5). The maximum leaf area index (LAI) is defined as the dimensionless ratio of the leaf area of actively transpiring vegetation to the nominal surface area of the land on which vegetation is growing. Based on the guidelines in the HELP user's guide and field observations in chapter 6, LAI value of 0, which corresponds to bare ground was assumed for the period of refuse infilling. LAI value of 2 that corresponds to a poor stand of grass was assumed for the first year following clay capping. Thereafter, LAI value of 3.5, which corresponds to a good stand of grass was assumed for the landfill for all subsequent periods.

Due to limitations in the simulation period in the HELP model, a refuse lift (cell) comprised refuse layers and cover materials placed in a single year. One of the most difficult aspects of the simulation was in predicting the original thickness of the refuse lifts because a detailed temporal breakdown of elevation data for the fill in zone G was not available. However, this was estimated from the 1990 mean thickness of refuse fill G, 19.35 m, and the sequence of waste filling at the site, shown in Table 3.3. The refuse column was divided into nine periods of tipping, each equivalent to 2.15 m thickness of refuse lift. The extra capacity generated by the settlement of the refuse lifts before 1990 was filled with waste, prior to the final clay capping system being constructed.

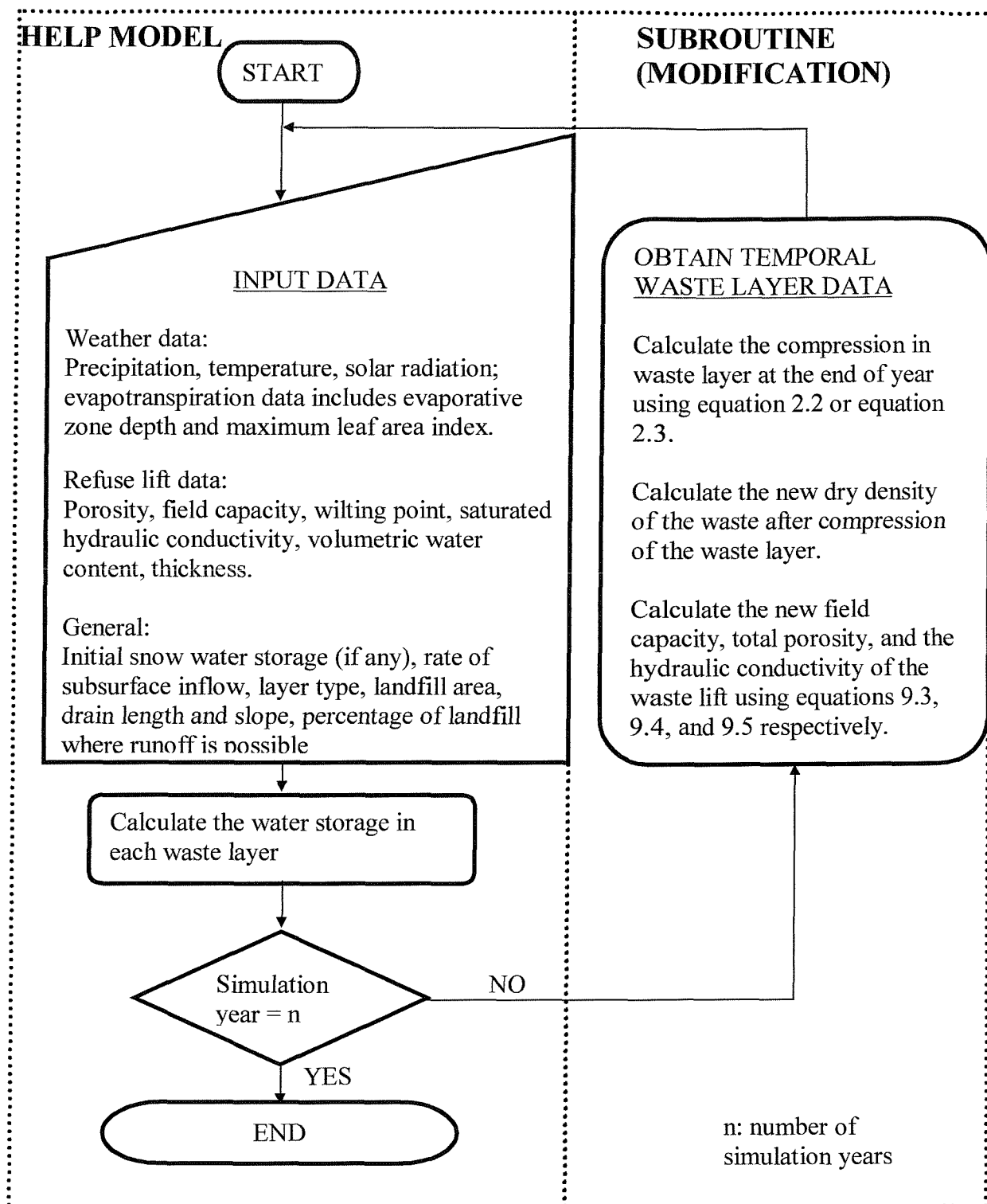


Figure 9.1: Flow chart for the simulation of moisture routing in refuse lifts at White's Pit.

The previous assumption by Bleiker (1995) that the cover soil is incompressible was disregarded due to the findings in Chapter 7. The refuse layer and the overlying cover soil were considered as a composite refuse layer. The combined density and moisture content of a composite layer comprising waste and cover soil were estimated as follows:

Thickness of a refuse layer = 2m; Thickness of daily soil cover = 0.15m

Emplacement density of waste = 600 kg/m³; moisture content (m) = 0.39

Emplacement dry density of waste = $600 / 1.39 \text{ kg/m}^3 = 431.65 \text{ kg/m}^3$

Emplacement density of daily cover = 1850 kg/m³ moisture content = 0.1245

Emplacement dry density of daily cover = $1850 / 1.1245 \text{ kg/m}^3 = 1645.18 \text{ kg/m}^3$

Combined emplacement density = $(600 \times 2/2.15) + (1850 \times 0.15/2.15) \text{ kg/m}^3$

$$= 687.2 \text{ kg/m}^3$$

Combined emplacement dry density = $(435.65 \times 2/2.15) + (1645.18 \times 0.15/2.15) \text{ kg/m}^3$

$$= 516.31 \text{ kg/m}^3$$

Combined emplacement gravimetric moisture content = $(687 / 516.31) - 1$
= 0.331

Combined emplacement volumetric moisture content = $0.331 \times 516 / 1000 = 0.1709$

The porosity and hydraulic conductivity of the lifts were obtained by substituting the composite dry density in the characteristic equations given in equations 7.3, 7.7 and 7.11. The refuse field capacity was not determined in the present experiment, therefore, the characteristic equation derived from the large-scale data (Figure 7.11) was used for temporal estimation of field capacity in the simulation.

The total porosity of the refuse was obtained from the sum of the air porosity and field capacity. The initial geotechnical properties of emplaced fresh refuse (Table 9.1 – 9.3) calculated using the composite density (687.2 kg/m³) were similar to that determined in the 210 litre drums (Table 5.6). This indicates that the model is appropriate for predicting the properties of refuse lifts under different loading.

The characteristics of sandy loam (Section 6.3.3) given in the HELP manual (Schroeder et al, 1994) was used for the topsoil of White's Pit. To account for the leakage of surface water through the top cover soil system (Section 6.4.3), the

properties of sandy clay (HELP no 10) was used instead of the less permeable stiff Broadstone clay of White's Pit in the simulation. This is reasonable as there is no suitable model for the temporal integrity of the liner since the formation of macropores in clay capping system, and the flow through is extremely difficult to model (Berger et al., 1996). The wilting point was obtained from the user's guide for the HELP model. No initial snow water storage was assumed in the simulation. A run-off (surface) slope of 2.5% was estimated from the survey maps (Dorset County Council, 1997) of the site. A run-off (surface) slope of 1.7 % was also obtained for the basal Broadstone clay from the map of the top of the clay in Figure 4.3.

9.4.3 Solution method

The flow diagram for the simulation of moisture stored in refuse lifts at the restored landfill of the site is shown in Figure 9.1. The simulation involves the input of initial data into the HELP program, which calculates the moisture stored in the refuse lift at the end of first year (year 1). No waste compression is assumed to have occurred due to the initial self-weight of the refuse lift, therefore, the initial porosity, field capacity, and hydraulic conductivity of the emplaced refuse lift is not altered during year 1.

During the second year, a new refuse lift (lift 2) is placed directly onto lift 1. First, the moisture content in lifts 1 and 2 are calculated with the HELP program, using initial waste properties of both lifts at the start of year 2. The initial properties of waste lift 1 at the beginning of year 2 is the waste properties of the lift at the end of year 1 while the initial waste properties for lift 2 is similar to lift 1 in year 1. Due to the assimilation of moisture in lift 1 in year 1, the bulk wet density of lift 1 has increased and is calculated for the start of year 2 (or end of year 1) as follows (Schroeder, 1994):

$$\rho_{wet} = \rho_{dry} \left(1 + \left(\frac{\theta \rho_w}{\rho_{dry}} \right) \right) \quad [9.6]$$

where:

ρ_{wet} = wet bulk density of the waste lift

ρ_{dry} = dry bulk density of the waste lift

ρ_w = density of water

θ = volumetric moisture content of the waste lift

Adjustments are then made to lift 1's waste properties to account for the applied vertical stresses caused by the placement of lift 2. The compression of the refuse lift 1 is then calculated through the subroutine using equation 2.2. The total vertical stresses on lift 1 in year 2 include the stresses due to the overlying lift 2 and the self-weight of lift 1. The compression in lift 1 is then reflected in the density of the lift. Thus, the dry density of lift 1 at the end of year 2 is obtained as follows:

$$\rho_{1,2} = \rho_{1,1} \left(\frac{H_{1,1}}{H_{1,2}} \right) \quad [9.7]$$

where:

$\rho_{1,1}$ = dry density of lift 1 in year 1

$\rho_{1,2}$ = dry density of lift 1 in year 2

$H_{1,1}$ = Height or thickness of lift 1 in year 1

$H_{1,2}$ = Height or thickness of lift 1 in year 2

The calculated dry density of lift 1(post-compression) is then used to calculate the field capacity, porosity, and hydraulic conductivity of lift 1 at the end of year 2. Furthermore, the moisture content of lift 2, earlier obtained with the initial (non-settlement) properties of the lift using the HELP model is then adjusted for the compression of lift 1 during year 2. This is calculated as follows:

$$\theta_{\text{adj}} = \theta_{\text{HELP}} \left(\frac{H_i}{H_f} \right) \quad [9.8]$$

where:

θ_{adj} = adjusted volumetric moisture content of the lift in year 2.

θ_{HELP} = initial volumetric moisture content of lift obtained from HELP model in year 2

H_i = initial lift thickness used during HELP simulation in year 2.

H_f = final lift thickness due to compression in year 2.

The moisture stored in lift 2 during year 2 is calculated as in lift 1; year 1. This process is repeated for all emplaced refuse lifts during the active fill period of the landfill. During the post-closure period, however, the compression of the refuse lifts is calculated from equation 2.3, but all other procedures remain identical.

9.5 Actual Leachate Level in the Landfill

Comparison of the actual and simulated moisture conditions in the landfill is vital for the validity of this investigation. The direct method of determining the volume of leachate stored up in a landfill is by measuring the head of the standing water in wells (Figure 4.1) located within the landfill (Holmes, 1984, Watts and Charles, 1999).

The head of the standing leachate in some wells located at the site (Figure 9.2) was measured by lowering a steel tape, attached to a electrical sounder, slowly in and out of the leachate in the well at least twice, to determine the actual surface level.

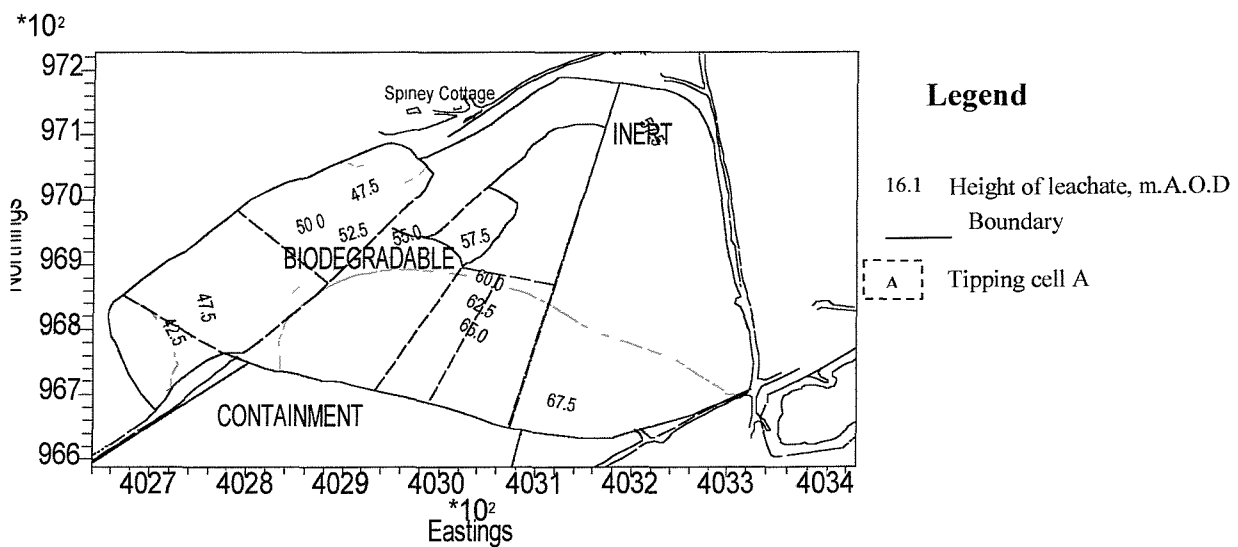


Figure 9.2: Standing leachate levels at White's Pit in December 1998

The standpipes in the wells were slotted, and extended down to the basal Broadstone clay liner (C L Associates. 1991). Regular monitoring of the selected wells indicated that they are functioning (Huc, 1997), therefore, the phreatic surface of the standing leachate in the refuse at the site was assumed to be measured.

9.6 Results

The simulated moisture storage of lifts 1, 2 and 3 are shown in Tables 9.1, 9.2, and 9.3 respectively. The moisture content in lift 1 increased from 0.1709 to 0.5236 from placement in 1986 to the end of 1998. The highest absorption of moisture in the lift during this period occurred during placement. The temporal physical properties of the lifts are well defined by the characteristic equations. The wet density of the lift increased from 687 kg/m^3 to 1258 kg/m^3 while the field capacity increased from 44.37% to 47.2%. The thickness of the lift, however, decreased from 6.45 m to 4.55 m, the porosity decreased from 54.63% to 52.36%, and the hydraulic conductivity decreased from $6.13 \times 10^{-5} \text{ m/s}$ to $5.23 \times 10^{-6} \text{ m/s}$.

Similarly, the moisture content in lift 2 increased from 0.1709 to 0.4753 between 1987 and 1998. The wet density increased from 687 kg/m^3 to 1160 kg/m^3 , and the field capacity increased from 44.37% to 46.63%. During this period, the thickness of the lift decreased from 8.6 m to 6.48 m, the porosity decreased from 54.63 % to 52.54 %, and the hydraulic conductivity decreased from $6.13 \times 10^{-5} \text{ m/s}$ to $8.48 \times 10^{-6} \text{ m/s}$. In the same vein, the moisture content in lift 3 during 1989 to 1998 increased from 0.1709 to 0.4671, the wet density increased from 687 kg/m^3 to 1141 kg/m^3 , while the field capacity increased from 44.37% to 46.5%. The thickness of the lift decreased from 5.73m to 4.38m, the porosity decreased from 54.63% to 52.59%, and the hydraulic conductivity decreased from $6.13 \times 10^{-5} \text{ m/s}$ to $9.49 \times 10^{-6} \text{ m/s}$.

The temporal height of waste lifts above basal Broadstone clay liner is shown in Figure 9.3. The height of the waste lifts decreased since placement at the site. The compression of the lifts was more pronounced in the early stages, and by 1998, the settlement was very small. The cumulative settlement of the refuse lifts is reflected at the top of the landfill (lift 3). In all, the refuse fill has settled by approximately 20 %,

Table 9.1: Simulated temporal moisture content and properties of refuse lift 1

Calendar year	Simulation year	Refuse lift 1								
		Moisture Cont	Wdensity, kg/m3	A stress, kPa	Thickness, m	Ddensity, kg/m3	Air porosity, %	Total porosity, %	Vol FC, %	HC, m/s
1986	1 (Initial)	0 1709	687 00			516 31	10 25	54 63	44 37	6 13E-05
	1(final)	0 2633	779 61	24 65	6 45	516 31	10 25	54 63	44 37	6 13E-05
1987	2	0 2633	779 61	87 49	6 45	516 31	10 25	54 63	44 37	6 13E-05
	(adjusted)	0 2958	G E 875 98	87 49	5 74	580 13	8 17	53 46	45 29	2 71E-05
1988	3	0 2954	I 875 53	92 51	5 74	580 13	8 17	53 46	45 29	2 71E-05
	(adjusted)	0 2968	879 80	92 51	5 71	582 96	8 09	53 42	45 33	2 62E-05
1989	4 A	0 3015	884 46	115 89	5 71	582 96	8 09	53 42	45 33	2 62E-05
	(adjusted)	0 3075	902 11	127 73	5 60	594 59	7 79	53 27	45 49	2 28E-05
1990	C 5	0 3353	F 929 89	143 55	5 60	594 59	7 79	53 27	45 49	2 28E-05
	(adjusted)	0 3387	H 939 42	143 51	5 54	600 69	7 63	53 20	45 57	2 13E-05
Post closure										
1991	1	0 3643	964 99		5 54	600 69	7 63	53 20	45 57	2 13E-05
	(adjusted)	0 4035	1068 79		5 01	665 31	6 25	52 65	46 39	1 04E-05
1992	2	0 4242	1089 51		5 01	665 31	6 25	52 65	46 39	1 04E-05
	(adjusted)	0 4373	1123 21		4 86	685 89	5 89	52 53	46 64	8 40E-06
1993	3	0 4826	1168 49		4 86	685 89	5 89	52 53	46 64	8 40E-06
	(adjusted)	0 4915	1190 02		4 77	698 53	5 69	52 48	46 79	7 39E-06
1994	4	0 5248	1223 33		4 77	698 53	5 69	52 48	46 79	7 39E-06
	(adjusted)	0 5244	1232 21		4 71	707 78	5 54	52 44	46 90	6 74E-06
1995	5	0 5244	1232 21		4 71	707 78	5 54	52 44	46 90	6 74E-06
	(adjusted)	0 5242	1239 31		4 66	715 13	5 43	52 42	46 99	6 27E-06
1996	6	0 5242	1239 31		4 66	715 13	5 43	52 42	46 99	6 27E-06
	(adjusted)	0 5240	1245 23		4 62	721 25	5 34	52 40	47 06	5 91E-06
1997	7	0 5240	1245 23		4 62	721 25	5 34	52 40	47 06	5 91E-06
	(adjusted)	0 5238	1250 34		4 58	726 51	5 27	52 38	47 12	5 62E-06
1998	8	0 5238	1250 34		4 60	726 51	5 27	52 38	47 12	5 62E-06
	(adjusted)	0 5236	1257 66		4 55	734 02	5 16	52 36	47 20	5 23E-06

Wdensity: Wet density;

Ddensity: Dry density;

FC: Field capacity;

Vol. HC: Volumetric hydraulic conductivity;

A. Stress: Applied stress

Table 9.2: Simulated temporal moisture content and properties of refuse lift 2

		Moisture Cont	Wdensity, kg/m ³	A stress, kPa	Thickness, m	Ddensity, kg/m ³	Air porosity, %	Total porosity, %	Vol FC, %	HC, m/s
1987	1 (Initial)	0 1709	687 00			516 31	10 25	54 63	44 37	6 13E-05
	1(final)	0 2288	745 11	31 42	8 60	516 31	10 25	54 63	44 37	6 13E-05
1988	2	0 2890	805 31	33 96	8 60	516 31	10 25	54 63	44 37	6 13E-05
	(adjusted)	0 2910	810 78	33 96	8 54	519 82	10 12	54 54	44 43	5 85E-05
1989	3	0 3086	828 42	68 31	8 54	519 82	10 12	54 54	44 43	5 85E-05
	(adjusted)	0 3285	881 96	68 31	8 02	553 41	8 96	53 87	44 92	3 77E-05
1990	4	0 3380	891 41	82 95	8 02	553 41	8 96	53 87	44 92	3 77E-05
	(adjusted)	0 3438	906 71	82 95	7 89	562 91	8 66	53 71	45 05	3 35E-05
Post closure										
1991	1	0 3660	928 91		7 89	562 91	8 66	53 71	45 05	3 35E-05
	(adjusted)	0 4053	1028 58		7 12	623 31	7 10	52 97	45 86	1 64E-05
1992	2	0 4258	1049 11		7 12	623 31	7 10	52 97	45 86	1 64E-05
	(adjusted)	0 4390	1081 57		6 91	642 59	6 69	52 80	46 11	1 33E-05
1993	3	0 4611	1103 69		6 91	642 59	6 69	52 80	46 11	1 33E-05
	(adjusted)	0 4696	1124 03		6 78	654 44	6 46	52 72	46 26	1 17E-05
1994	4	0 4634	1117 84		6 78	654 44	6 46	52 72	46 26	1 17E-05
	(adjusted)	0 4695	1132 65		6 70	663 11	6 29	52 66	46 37	1 06E-05
1995	5	0 4693	1132 41		6 70	663 11	6 29	52 66	46 37	1 06E-05
	(adjusted)	0 4742	1144 17		6 63	669 99	6 17	52 62	46 45	9 90E-06
1996	6	0 4645	1134 49		6 63	669 99	6 17	52 62	46 45	9 90E-06
	(adjusted)	0 4685	1144 20		6 57	675 73	6 07	52 59	46 52	9 33E-06
1997	7	0 4732	1148 93		6 57	675 73	6 07	52 59	46 52	9 33E-06
	(adjusted)	0 4766	1157 30		6 52	680 65	5 98	52 56	46 58	8 87E-06
1998	8	0 4723	1152 95		6 52	680 65	5 98	52 56	46 58	8 87E-06
	(adjusted)	0 4753	1160 27		6 48	684 97	5 91	52 54	46 63	8 48E-06

Wdensity: Wet density; Ddensity: Dry density; FC: Field capacity;

Vol. HC: Volumetric hydraulic conductivity;

A. Stress: Applied stress

Table 9.3: Simulated temporal moisture content and properties of refuse lift 3

Calendar year	Simulation year	Refuse lift 3								
		Moisture Cont	Wdensity, kg/m3	A stress, kPa	Thickness, m	Ddensity, kg/m3	Air porosity, %	Total porosity, %	Vol FC, %	HC, m/s
1989	1 (Initial)	0 1709	687 00			516 31	10 25	54 63	44 37	6 13E-05
	1(final)	0 2808	797 11	16 81	4 30	516 31	10 25	54 63	44 37	6 13E-05
1990	capping	0 3365	852 81	23 94	5 73	516 31	10 25	54 63	44 37	6 13E-05
	final	0 3611	915 03	52 38	5 34	553 98	8 94	53 86	44 93	3 75E-05
Post closure										
1991	1	0 3671	921 08		5 34	553 98	8 94	53 86	44 93	3 75E-05
	(adjusted)	0 4066	1020 17		4 82	613 58	7 32	53 06	45 74	1 83E-05
1992	2	0 4266	1040 44		4 81	613 84	7 32	53 06	45 74	1 83E-05
	(adjusted)	0 4394	1071 76		4 67	632 32	6 91	52 89	45 98	1 48E-05
1993	3	0 4598	1092 63		4 67	632 83	6 89	52 88	45 99	1 48E-05
	(adjusted)	0 4679	1111 86		4 59	643 97	6 66	52 79	46 13	1 31E-05
1994	4	0 4613	1105 79		4 59	644 49	6 65	52 79	46 13	1 30E-05
	(adjusted)	0 4670	1119 53		4 53	652 50	6 50	52 73	46 24	1 19E-05
1995	5	0 4624	1115 43		4 53	653 03	6 48	52 73	46 24	1 18E-05
	(adjusted)	0 4668	1126 10		4 48	659 28	6 37	52 68	46 32	1 11E-05
1996	6	0 4632	1123 01		4 48	659 81	6 36	52 68	46 33	1 10E-05
	(adjusted)	0 4668	1131 70		4 44	664 92	6 26	52 65	46 39	1 04E-05
1997	7	0 4639	1129 36		4 44	665 46	6 25	52 65	46 39	1 04E-05
	(adjusted)	0 4669	1136 66		4 41	669 76	6 17	52 62	46 45	9 92E-06
1998	8	0 4645	1134 81		4 41	670 31	6 16	52 62	46 45	9 87E-06
	(adjusted)	0 4651	1141 09		4 38	674 02	6 10	52 60	46 50	9 49E-06

Wdensity: Wet density;

Ddensity: Dry density;

FC: Field capacity;

Vol. HC: Volumetric hydraulic conductivity;

A. Stress: Applied stress

from the start of clay capping in 1990, to the period the field tests were carried out at the landfill in 1998.

The temporal dry density and field capacity of the refuse lifts are shown in Figures 9.4 and 9.5 while the temporal porosity and hydraulic conductivity of the lifts are plotted in Figures 9.6 and 9.7. As expected, the dry density of the refuse lifts increased significantly with time since placement. Also, the porosity and hydraulic conductivity of the refuse lifts decreased since placement. The rate of increase in the dry density was higher in lift 1 and was more pronounced during the period when the compression was due to physical mechanisms caused by the overburden (until 1991). The same behaviour was also characteristic of the field capacity, porosity and hydraulic conductivity of the refuse lifts during the filling period. This is not surprising since compression is the primary factor affecting the physical changes in the emplaced refuse lifts.

The temporal moisture content of the refuse lifts at the tipping area G of White's Pit is plotted in Figure 9.8. The initial moisture conditions were plotted as moisture storage at the end of year prior to placement of subsequent lifts to depict the rapid increase in moisture contents of the lifts during placement. In general, there was an appreciable increase in the moisture content of the lifts before the landfill was completely capped in 1991. The moisture content of the lifts increased at a considerably lower rate thereafter. In 1998, the moisture storage in lift 1 was greater than in lift 2, which in turn was greater than lift 3, as moisture percolated downwards through the waste following moisture absorption to field capacity.

The simulated and measured moisture content from the ground surface of tipping area G in 1998 and the corresponding simulated and actual standing leachate levels are depicted in Figure 9.9. While there is a similarity in simulated and measured moisture storage of the refuse lifts, the measured volumetric moisture content in lift 2 (0.509) is greater than the simulated values (0.475). The measured and simulated standing leachate levels are 7.71 m and 11.37 m from the ground surface. The measured leachate level plotted in Figure 9.9 was converted to volumetric moisture content as follows:

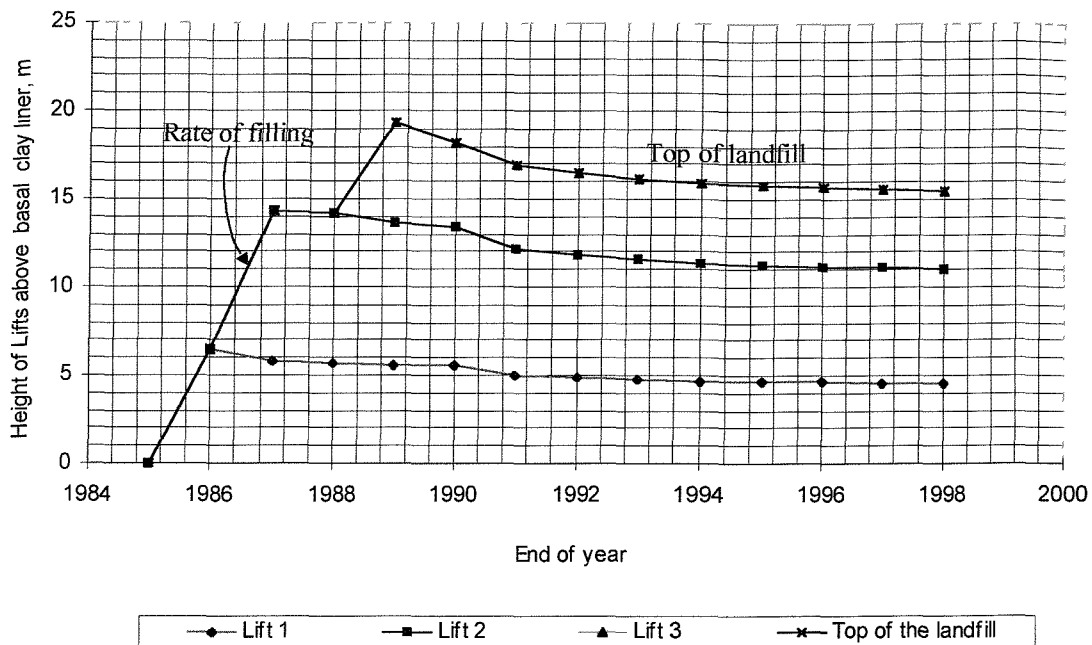


Figure 9.3: Simulated height of waste lifts above basal clay liner

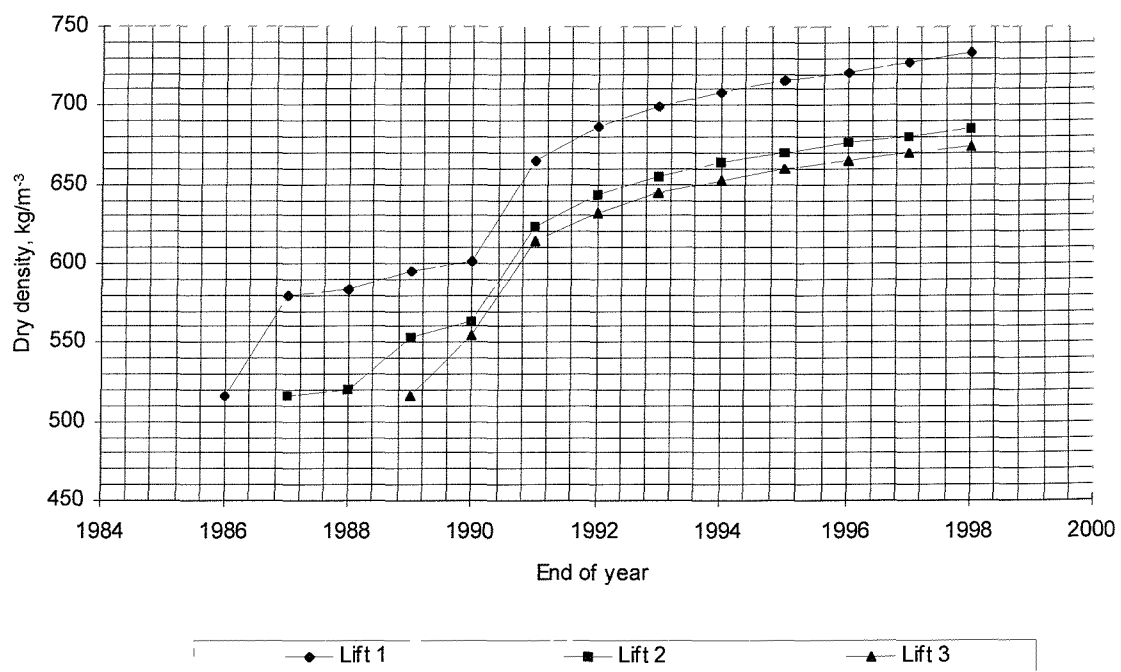


Figure 9.4: Simulated dry density of waste lifts.

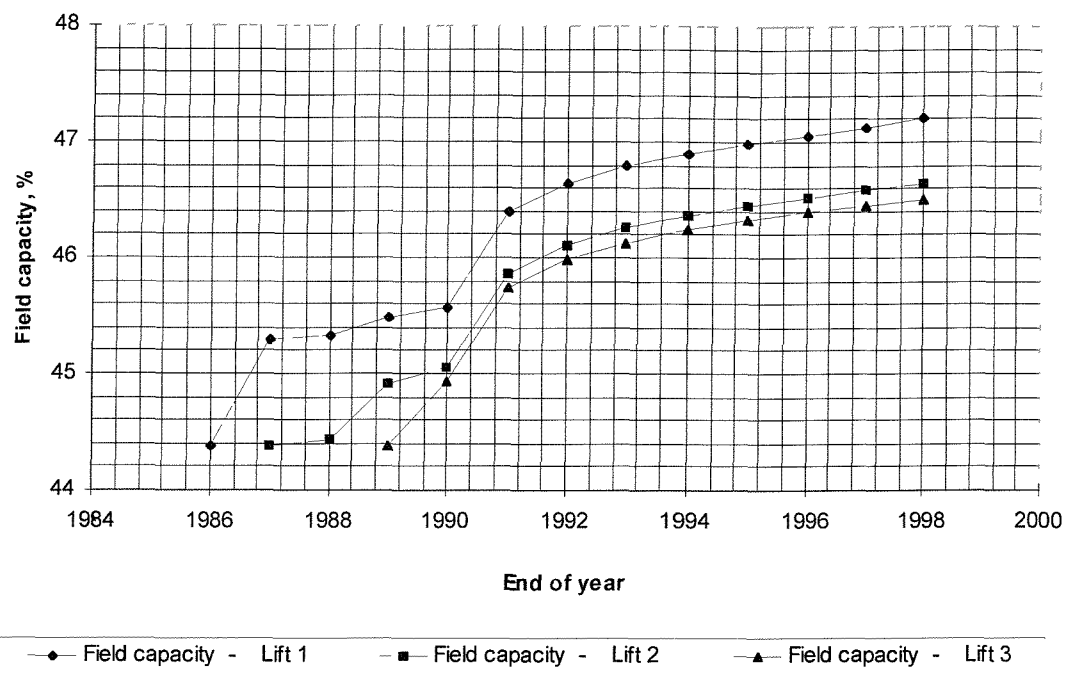


Figure 9.5: Simulated field capacity of the waste lifts

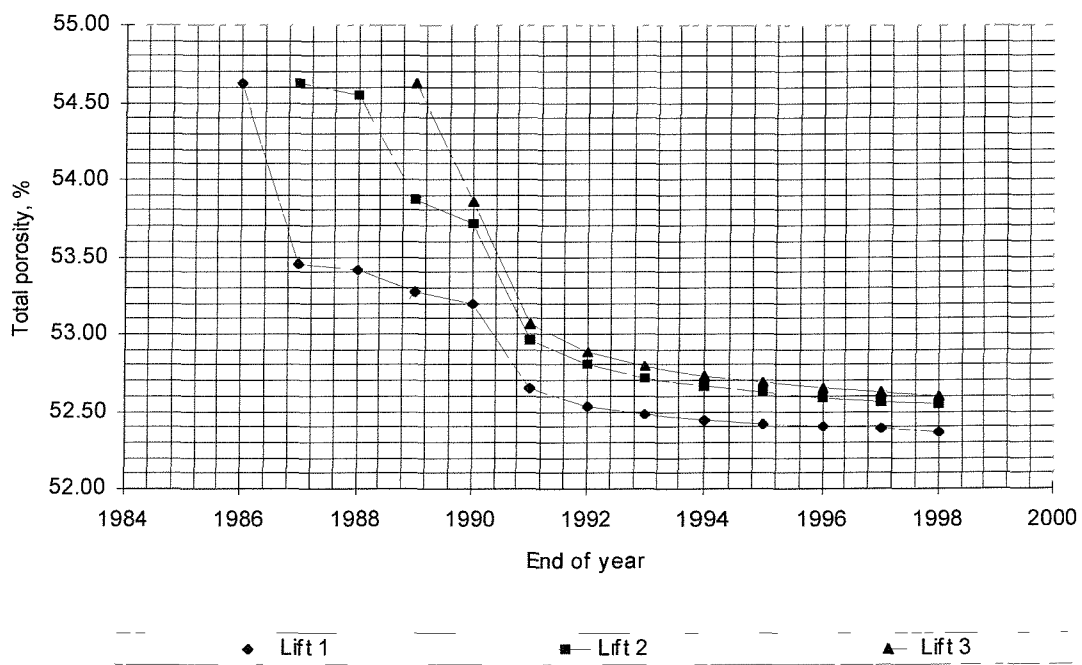


Figure 9.6: Simulated porosity of the waste lifts

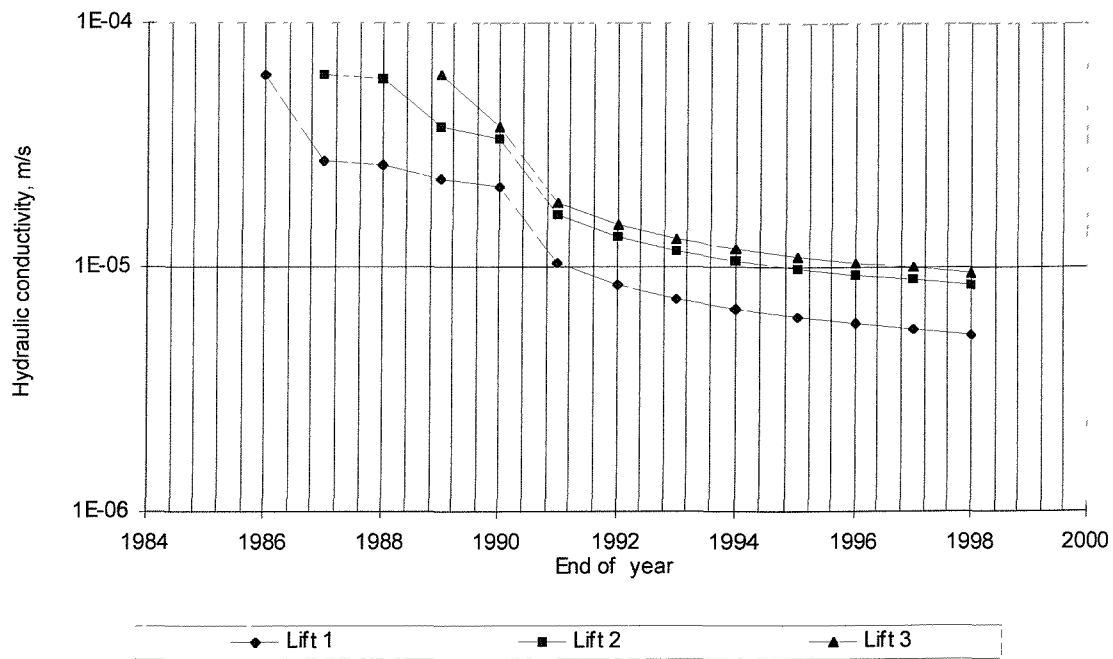


Figure 9.7: Simulated hydraulic conductivity of waste layers

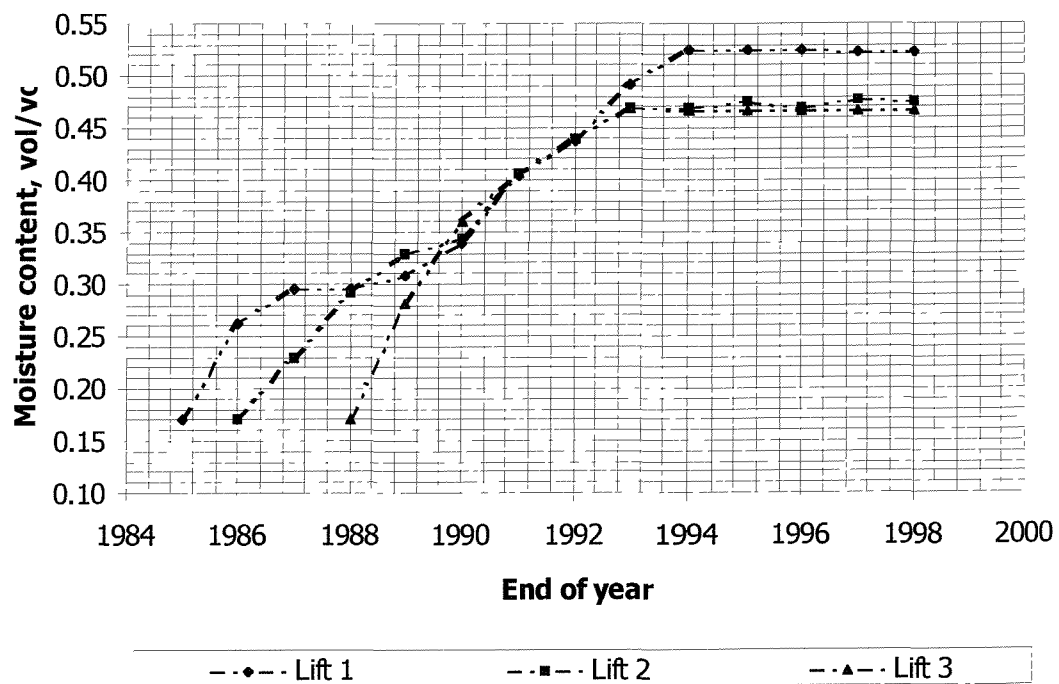
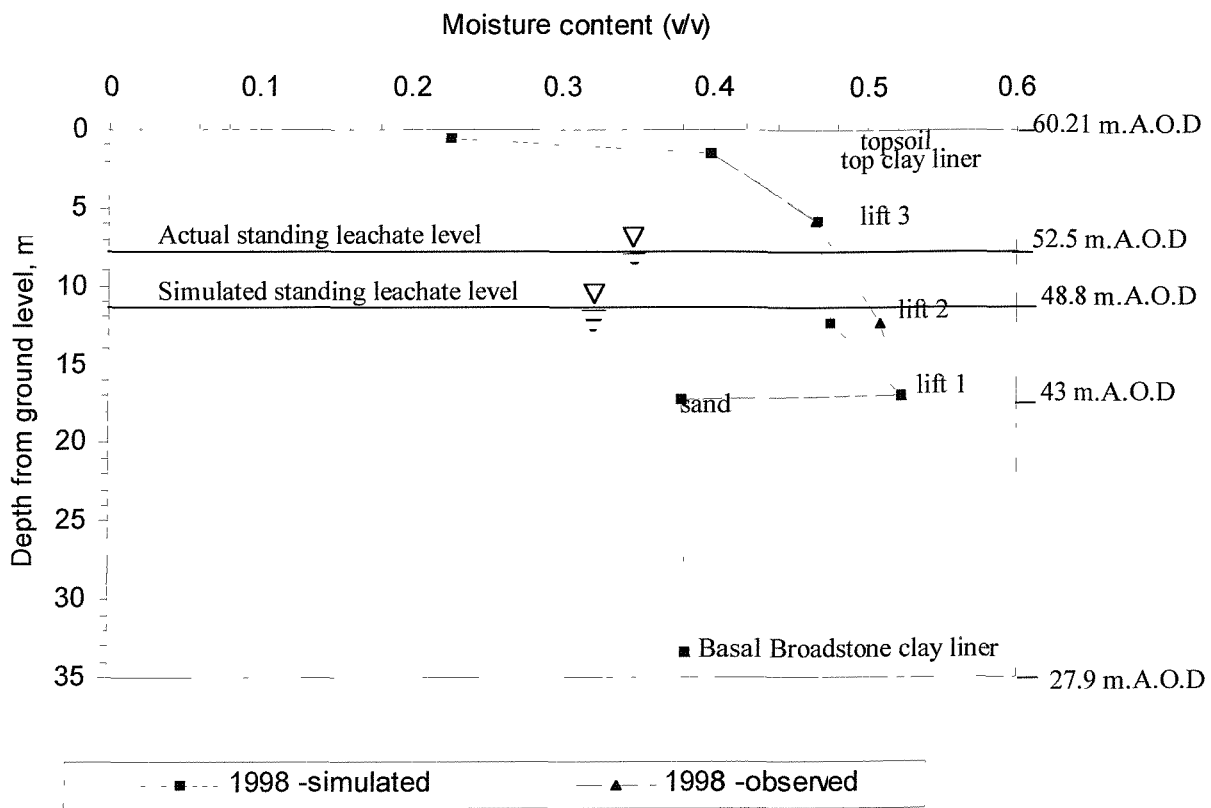


Figure 9.8: Simulated moisture content of waste lifts



NB – The moisture content is indicated at the base of each refuse lift and soil layer

Figure 9.9: Comparison of simulated and measured moisture content

The measured mean leachate level of 52.5 m A.O.D at tipping area G (Figure 9.2), indicates a mean standing leachate depth of 9.5 m above the basal Broadstone clay (~ 43 m A.O.D; Figure 4.4).

At the end of 1998 (Tables 9.1-9.3),

Thicknesses of lifts 1, 2, 3 and sand layer are 4.55 m, 6.48 m and 4.38 m and 0.3m. Thus, the sand layer and lift 1 are saturated while lift 2 is partly saturated.

$$\begin{aligned}
 \text{The moisture content in lift 2 (v/v)} &= 0.4663 + ((9.5 - (0.3 + 4.55)) / 6.48) \times (0.5254 - 0.4663) \\
 &= 0.509 - (\text{porosity \& FC of lift 2 are } 0.5254 \text{ \& } 0.4663).
 \end{aligned}$$

Similarly, the simulated moisture content was also converted to a leachate level by assuming that the moisture values above field capacity drains freely to form a standing leachate layer at the bottom of the lift. Thus:

The simulated moisture in lift 1 is saturated (Table 9.1)

$$\begin{aligned} \text{The height of simulated leachate in lift 2} &= ((0.4753-0.4663)/(.5254-0.4663)) \times 6.48 \\ &= 0.987 \text{ m} \end{aligned}$$

$$\begin{aligned} \text{Total simulated leachate height above clay} &= (0.3 + 4.55 + 0.987) \\ &= 5.837 \text{ m} (\sim 49 \text{ m. A.O.D}) \end{aligned}$$

The unsaturated measured moisture content plotted in Figure 9.9 is at field capacity (Section 5.3.4).

In order to determine the impact of compression on moisture content of the emplaced lifts, the moisture content in the refuse lifts was simulated with and without adjustments for temporal changes in refuse properties. In this case, the in situ properties of the Basal Broadstone clay were input in the simulation of the post-closure period. The moisture content of the uncompressed refuse lifts (Figure 9.10) is less than that of the compressed lifts (with temporal adjustment) under the same simulated climatic conditions. Unlike the compressed lifts, the moisture content in uncompressed lifts was constant after the clay capping.

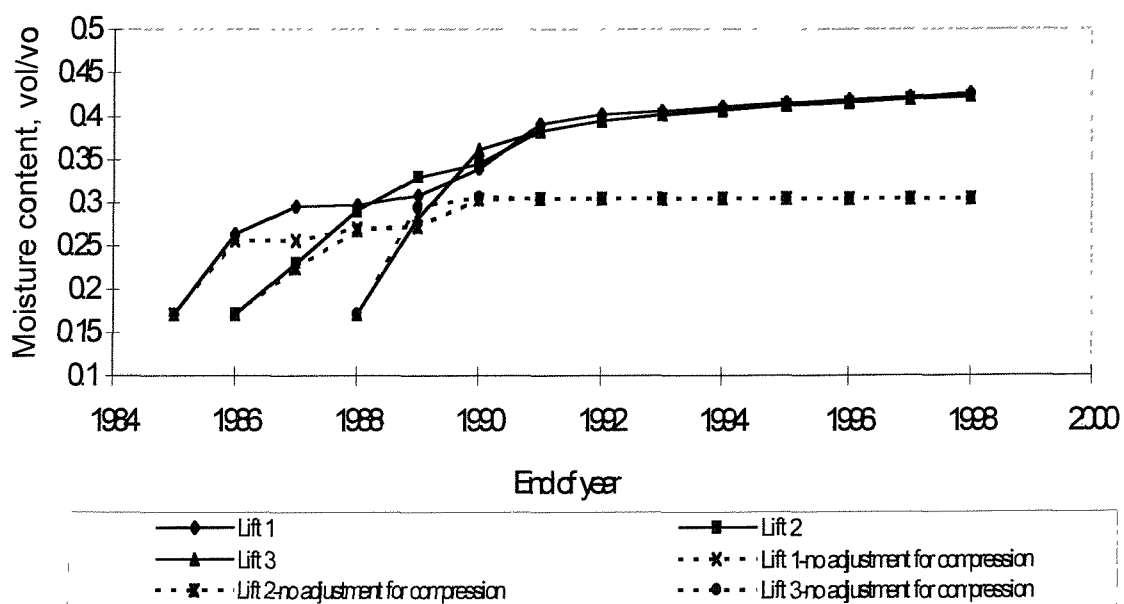


Figure 9.10: Simulated moisture content of waste lifts with and without compression

9.7 Discussion

A back analysis of the moisture stored in refuse lifts in the restored landfill part of the site was undertaken from start of refuse infilling at the site in 1986 to the period of field measurements in 1998.

In addition to the assumptions documented in the HELP manual (Schroeder et al, 1994), due to limitations of the HELP model, certain assumptions (Section 9.4.1) had to be made to simplify the processes involved in the moisture simulation due to the complex nature of the fill operations and factors influencing leachate production in refuse landfills. The findings from previous investigations (Chapters 5 – 7) were used to enhance the accuracy of the simulation technique. For instance, the assumption of the cover soil being incompressible by Bleiker et al, (1995) was disregarded due to the ravelling of the cover soil materials into the waste mass (Chapter 7). The refuse layer and daily cover were considered as a composite material with combined density of 687 kg/m^3 .

The characteristic equations (equations 7.3, 7.7 and 7.11) do not apply to pre-compactated waste. The equivalent effective stress of the waste (dry density = 516.3 kg/m^3) is approximately 34 kPa (equation C3), and as such, less effective (overburden) stress was considered not to have any effect on the properties of the emplaced waste.

9.7.1 Modelling Results

As expected, the behaviour of the simulated refuse lifts was similar to the characteristics exhibited by refuse layers under loading (Section 7.5). There was a general decrease in thickness of the refuse lifts, with a majority of the compression in the lifts occurring during the fill, and up to one year after closure. Watts and Charles (1999) reported that the compression during this period results from the increase in vertical effective stress caused by the overburden load. The highest compression rate during the fill period occurred in lift 1 as a result of the cumulative overburden of lifts 2 and 3 (Tables 8.1 –

8.3). The simulated cumulative settlement is approximately 20% of the original thickness of the refuse fill.

As expected, there was a temporal increase in the density and the field capacity of the lifts, which was very significant during the period of refuse tipping. Similarly, there was a decrease in the temporal porosity of refuse lifts layers during this period. In view of this, the hydraulic conductivity of the refuse lifts decreased considerably during the period of refuse infilling. Chen and Chynoweth (1995) stated that the hydraulic conductivity of a porous material is affected by particle size, void ratio, composition, pore geometry, fabric, degree of saturation, and the properties of the test fluid. The structural factors (void ratio, pore geometry) are greatly influenced by the overburden load, and therefore it is not surprising that the hydraulic conductivity of lift 1 was less than that of lifts 2 and 3.

The moisture content of the lifts increased over the period of refuse emplacement. During the first year of refuse landfill, in 1986, moisture accumulated in lift 1. As soon as the second lift was fully in place in the second year, the moisture infiltration due to precipitation was absorbed in lift 2. But, while lift 2 was absorbing the infiltrated moisture, the volumetric moisture content of lift 1 increased because of the reduction in the porosity (volume) of the lift, due to applied load exerted by overlying lift 2. This trend continued in lift 1 in 1988, but at a reduced rate since there was no refuse placement during this year and the extra compression of the lift was due only to the weight of precipitation absorbed by the overlying lift 2 during this period.

In 1989, the infiltrated moisture was absorbed mainly in emplaced lift 3. As before, the slight increase in the moisture content of lifts 1 and 2 during this period was a result of the compression of refuse by the overburden weight of the lift 3. In general, the volume of water absorbed during placement was more pronounced in lift 3 than lift 1, and lift 1 than lift 2. The rainfall for 1986, 1987, and 1989 when the lifts 1, lift 2, and lift 3 were placed were 908.6mm, 720.4mm, and 830.4mm respectively. If the infiltration due to the incidental rainfalls in these years is similar, then the variation in the increased moisture

content in the lifts was due to the amount of waste in the lifts, which is higher in lift 2 than lifts 1 and 3.

Construction of the final cover soil system and eventual establishment of vegetation over the site was modelled from 1991 to 1998. The barrier to infiltration of precipitation by the clay capping system was reflected in the large reduction in moisture content in all the refuse lifts post-1990. The small increase in the volumetric moisture content of the refuse lifts during the post-closure was caused by the continued small settlement in the lifts.

The magnitude of the impact of compression (caused immediately by refuse infilling and later biodegradation) on the moisture content of emplaced refuse lifts was determined by simulating the moisture content in emplaced lifts without any adjustments for compression and physical properties of the refuse. Comparison of the two cases of simulations (Figure 9.10) indicates an underestimation of the volumetric moisture content of refuse lifts when the causes and effects of compression is not considered in moisture simulation of the refuse lifts.

Whereas, the degree of saturation of refuse lifts is increased during the active filling period of the landfill, the hydraulic conductivity of the refuse is reduced, leading to poor drainage due to a low percolation rate. Consequently, the retention period of the infiltrated water within the waste mass is increased while the rate of water accumulation at the bottom of a containment landfill is reduced; a vital consideration in the design of leachate recirculation system. In reality, these effects will be reduced by the transmission of moisture through the micropores of some waste components like paper and cardboard.

Some of the assumptions in the simulation technique include uniformity in compaction and spatial distribution of the properties of the emplaced waste. However, the placement of non-uniform layers of refuse will result in waste characteristics, which are dissimilar to the simulation results presented in this chapter. Localised moisture saturation (water logging) will occur if the hydraulic conductivity of a refuse layer is very small compared with the overlying and underlying lifts.

9.7.2 Validity of the Simulation Technique

The moisture simulation technique was validated by comparing the predicted volumetric moisture content with the measured standing leachate at the site in 1998. Although there is a slight difference in the simulated and measured volumetric moisture content in lift 2, which is depicted as a difference of 3.66 m in leachate levels, a reasonable similarity exists between simulated and measured leachate volumes considering the complex nature of waste.

One of the problems in the application of this technique is the choice of top liner (clay capping) that will simulate infiltration similar to infiltration rates caused by a loss of integrity of the liner. An underestimation of the runoff from the landfill (Chapter 6) indicates an increase in infiltration due the macropores in the cover soil system of a landfill. In this study, the properties of sandy clay (HELP no 10), which was used instead of that of the in situ Broadstone clay appears to have successfully simulated the leakage through the top liner. A similar soil was also used by Bleiker et al. (1995) to model the leakage of the top liner in a study of landfill settlement, site capacity and refuse hydraulic conductivity. However, this type of soil may not be universally applicable due to complex factors that may influence the leakage through the top cover system. e.g. differential settlement and, type of liner material.

Also of significance is the similarity between the simulated density of lift 3 (1135 kg/m^3) with the field density (1198 kg/m^3) determined for the topmost refuse layer at the site through a pit test (Section 5.6.3). This tends to support the validity of certain assumptions used in the modified simulation.

Sensitivity analysis could not be conducted on the HELP program, as the hydraulic conductivity of the basal liner used in the simulation was more than that of the in situ Broadstone clay at White's to allow infiltration similar to the vertical leakage expected at the site.

In summary, the modified simulation of moisture stored in the refuse landfill (tipping area G) has captured key characteristics of sequential filling on leachate volume in refuse lifts. The moisture content of the lifts increased rapidly during refuse infilling due to direct infiltration of precipitation. In addition, the volumetric moisture content of the underlying refuse lifts also increased during this period due to the reduction in porosity of the refuse. In effect, the tendency for the refuse lifts to be saturated was increased, but the drainage potential was also decreased. Sequential infilling of non-uniform waste layers will encourage localised saturation (perched water) of some parts of the landfill. (As observed in Section 5.5).

The modified simulation technique used in this study substantially replicated the moisture routing for both the active and post-closure periods of a landfill. The simulation results provide confidence for the examination of alternative designs and planning strategies for risk assessment of waste disposal facilities. To overcome the shortfall in the simulated and field moisture storage of the refuse fill during post closure, the field value of the effective permeability of the top soil system (clay + topsoil) should be increased in the simulation to enable small quantities of infiltrated water, similar to the channelled water, into the emplaced refuse fill.

CHAPTER 10

General Discussion and Recommendations

10.1 Summary

A general discussion of the results of the investigations undertaken on the impact of overburden stress on the refuse properties and moisture volumes in refuse lifts is presented. It includes a summary of the discussions in previous chapters and the findings to the practice of refuse landfilling.

10.2 General Discussion

As discussed in Chapters 2 and 4, the properties of the emplaced lifts (or cells) in a MSW landfill change as a result of further tipping of refuse and daily soil cover. Prior to this investigation, these changes have been studied by applying vertical loads on non-degraded refuse placed in test cells (Beaven and Powrie, 1995, Wall and Zeiss, 1995). However, none of the waste samples used in these studies included a cover material layer, commonly placed on a waste lift (cell) as daily cover to limit infiltration and prevent insect infestation in MSW landfills. Consequently, the data from these tests will not be exact with the in situ waste properties. Other factors that may contribute to the variation in the result of the cell tests with field observations include heterogeneity and biodegradation, and in particular, the varying degree of air, water and gas in waste.

In this study, the classification of the physical components of refuse excavated from experimental pits at White's pit landfill, Poole showed an interaction between the

daily cover material and the underlying refuse mass. The fines (< 10 mm) in the fresh, 5–year old, and 14-year waste fills in the pits were found to be 6.89%, 11.87%, and 49.78% respectively. The particle size distribution of the fines (Figure 5.4) suggests that the majority of the extra fines in the aged refuse appeared to have come from the daily cover overlying the refuse. Visual observation during the manual sorting of the refuse components also supports this observation.

The density of the excavated refuse increased with increasing overburden stress and age. The high unit weight of the 14 year old refuse (11.75 kN/m^3) compared to the fresh refuse (5.89 kN/m^3) suggests the ravelling of the daily cover, which has a relative higher specific gravity of ~2.65 (Terzaghi et al, 1996) into the emplaced aged refuse. However, the individual contribution of overburden and biodegradation, which are the causative factors of ravelling could not be determined from pit (physical) tests alone, as refuse biodegradation depends on many factors including pH of interstitial water, and presence of oxygen (Lu et al., 1985). The impact of the test cell excavation process on the quantity of the daily cover assimilated into the waste sample was considered to be small due to the precautions taken in the sample removal (Section 5.4.2).

Having observed the sifting of daily cover into the refuse during the field tests, laboratory tests were conducted on refuse samples with, and without a cover soil layer interbedded in the waste mass under increasing vertical loads in test cells, 240 mm diameter and 230 mm height. Despite the relatively small scale of these experiments, their results compared well with 6 m^3 larger scale test cells (Beaven and Powrie 1995). Both the refuse with, and without cover soil showed similar behaviour under increasing applied vertical stress. However, there were significant differences in the properties of these two waste samples.

The density of refuse with 10 % (by volume) of cover soil (417 kg/m^3) was greater than the refuse-only (314 kg/m^3) under an applied vertical stress of 8 kPa due to the heavier particles of the soil. At this vertical stress, the compression of the waste with cover soil was 41.9% while that for refuse-only was 44.2 %. This will lead to the landfill accepting less waste during its active phase and may reduce the economic viability of the site. However, the benefits of an increased waste stability due to the

increased density and less biodegradation in waste fills with cover soil appears to exceed the economic benefits of waste only fills. Modelling of compression of refuse based on data from refuse-only samples will tend to overestimate the extra void caused by settlement.

Apart from the classification tests, no other tests were undertaken to support the concept of ravelling of the daily cover into the waste mass. However, if the height of the refuse-only sample (61.37 mm) and the refuse with 10% cover soil (63.86 mm) at the final applied stress of approximately 8 kPa are considered, up to 50 %* (see section 7.4.2) of the cover soil must have migrated into the underlying refuse layer, as the estimation is based on the assumption that the compression of the refuse mass in both samples is uniform. This supports the assumption by Morris and Woods (1990) that the thickness of daily soil cover ultimately reduces to 25% of its original thickness.

Perhaps the most significant concern in the use of cover soil is its impact on the hydraulic conductivity of the refuse fill. The hydraulic conductivity of refuse samples with daily soil cover used at the study site, which was classified as slightly silty/ slightly clayey gravelly sand was found to be less than that of refuse-only. The influence of daily soil cover on the hydraulic conductivity of refuse, however, decreased with increasing overburden stress. The difference in the hydraulic conductivity of the waste with and without soil cover at the maximum applied stress (8 kPa) in the experiment is very small (10^{-4} m/s). Some of the reasons for this behaviour include the relative low hydraulic conductivity of the soil layer and the reduction in the effective (macro) porosity of the waste mass due to ravelling. The impact of these factors will tend to reduce as the macropores in the waste mass reduce at high overburden stresses. Beaven (2000) reported that the water flow through refuse when the macropores collapse at dry densities usually higher than 500 kg/m^3 will be through the micropores and along the interface of individual particles

* Calculated thickness of 10% cover soil = $0.1 \times 50 = 5 \text{ mm}$

Final thickness of 10% cover soil = 2.49 mm

Unit volume of ravelled soil = $(2.51 / 5) * 100 = 50.2 \%$

The impact of cover soil on the general properties of a refuse fill is likely to be greater in reality because of the relative small scale of the tests. i.e. reduced waste particles, low applied stress, small soil thickness, and cell size etc. As a result of the small thickness and the loose placement of the cover soil, the hydraulic conductivity of the soil layer in the test cell will be considerably greater than that of a thicker layer or formation of compacted cover soil. Channelling through the interstices between the cell wall and the soil layer will also increase the overall hydraulic conductivity values of the soil layer.

In practice, the main problem of increasing overburden stress in landfills is the resulting decrease in hydraulic conductivity of the refuse. Current landfill practice limits water infiltration during refuse tipping (Tchobanoglous, 1993) leading to an unsaturated fill, whose hydraulic conductivity will decrease with increasing effective stress (depth) at closure. The implications of low permeability of refuse on the leachate control and design of leachate recirculation systems have been adequately analysed and reported by Powrie and Beaven (1999) and Beaven (2000). These analyses have not been repeated in this study, but instead, used to infer the impact of waste with a daily cover on sustainable landfilling, based on the current findings of the influence of daily cover on the properties of refuse.

Beaven (2000) reported that the control of leachate within 2 metres of the base of a 40 m deep refuse fill, assuming an infiltration of 100 mm/annum, with abstractions from vertical wells is impracticable because of the low permeability of the basal refuse layers. With the infiltration rate (m/year) required to flush contaminants from a landfill in a 30-year period taken as the height of landfill divided by 10, he also demonstrated that the maximum depth of an unsaturated waste fill at which the required flushing rate can be achieved with downward vertical flow is 40 metres. While acknowledging the decrease in infiltration rate with low permeability, Powrie and Beaven (1999) showed that pre-compaction of refuse further reduce the infiltration in both saturated and unsaturated conditions of a refuse fill. Pre-compaction is similar to the inclusion of cover soil in the sense that both increase waste density and hydraulic conductivity (Figures 7.3 & 7.5). Consequently, the

impact of low refuse hydraulic conductivity on leachate control and flushing reported by Beaven (2000) should therefore be considered as the threshold values for field conditions. Accurate analysis of the impact of low permeability of refuse fills on sustainable refuse landfilling should be based on data derived from refuse with a cover material.

Beaven (2000) reported that the impact of the effective stress, especially on the hydraulic conductivity of the refuse in deep landfills can be reduced by controlled saturation of the refuse fill as its depth increases since refuse rebound is very small. In contrast, the adverse impacts of a low permeability daily cover on the properties of refuse can only be rectified by re-excavation and re-filling of the refuse fill. Beaven (2000) stated that 0.5 m layer of material (e.g. stiff clay), which a hydraulic conductivity of $1 \times 10^{-9} \text{ ms}^{-1}$ restricted the flushing rates drastically below the required design rate in landfills. It implies that the daily soil cover used in a landfill should be well selected (devoid of clays) to prevent adverse effects on the overall permeability of the refuse fill.

The moisture stored in the dilute and disperse landfill at White's pit was simulated with the HELP model and characteristic models derived from the data of refuse with cover soil. White's pit is underlain completely by approximately 16 m stiff Broadstone clay, which serves as a natural basal liner for the landfill. The majority of the input data used in the modelling were obtained from the site in order to enhance simulation results. The data measured at the site include the evaporative root zone and runoff from the site. The measured evaporative depth (80 cm) indicated that evapotranspiration was occurring in the top clay liner during the field measurements. The seasonal pattern of moisture transport also suggests possible desiccation of the liner. Cracks caused by desiccation of the liner was assumed to contribute to channelling of water, which resulted in standing leachate observed at the site (Figure 9.8). The runoff coefficient (9 %) measured at the site was smaller than typical runoff coefficients of 18% to 22% commonly used in sewer designs for similar natural surfaces. This further indicates leakage of water through the macropores in the clay capping system, possibly caused by differential settlement of the underlying waste, in addition to desiccation.

The moisture simulation of the site showed that the volumetric moisture content in the waste lifts increased significantly during placement. The volumetric moisture content of the lifts also increased due to a decrease in porosity (volume) caused by increasing effective vertical stress as further waste was applied above. This led to an increase in the degree of saturation of the entire waste fill. A good estimate of the moisture stored in emplaced refuse during the active period is therefore needed for effective design, planning, and operation of a landfill.

The simulation moisture volume for the site (tipping area G) compared well with the leachate volume that was calculated from observed leachate levels considering the complex conditions that may influence the emplaced waste. Simulation results were improved by increasing the hydraulic conductivity of the top Broadstone clay liner to allow water infiltration similar to the leakage caused as the integrity of the clay capping system depreciated. The simulation technique is thus suitable for predicting the leachate volumes in both active and post closure periods of a MSW landfill.

In general, the impact of overburden stress on refuse properties have been considered in the present study without considering in details various factors including: - (a) pre – consolidation or different degrees of compact effort on the waste lifts placed; (b) channelling of water into the refuse mass, (c) long term effects- biodegradation and (d) increasing particle size of waste particles. Factors influencing waste behaviour are very complex. Nevertheless, the present findings are very useful for integrated waste management, and should be investigated further.

10.3 Recommendations for future investigations

The present work has improved the understanding of the temporal properties of emplaced refuse lifts in municipal landfill. However, some of the tests undertaken were influenced by both financial and time constraints. Further work on some aspects of the investigations is therefore necessary to validate and improve present findings, thereby enhancing the design, planning and operation of future municipal landfills.

Some of the recommendations for future work are as follows:

- The temporal changes in the properties of emplaced lifts should be measured in situ. Methods and equipment should be developed to measure the average porosity, density, and hydraulic conductivity of a refuse lift, since placement to the closure of the landfill site.
- The impact of cover soil materials on the properties of emplaced refuse lifts subjected to vertical applied stresses should be further determined in the Beaven and Powrie (1995) large scale cell. The tests could be undertaken on crude refuse samples underlying various thickness and types of soils commonly used as daily cover materials in municipal landfills. The quantity of cover soil that have sifted into the underlying refuse layer should be determined, possibly through material classification studies.
- The impact of biodegradation on the properties of the refuse fills under constant loading should be tested in the large-scale cell used by Beaven and Powrie (1995). This can be accomplished by measuring the hydraulic and geotechnical properties of refuse samples (including a cover soil) under a constant overburden load, at different time intervals considered to be effective for biodegradation with the refuse mass.
- The lateral flow characteristics of the refuse fill (including cover soil) under increasing overburden load in the large-scale cell should be measured. This will provide further understanding of the flow regimes in a waste fill. The flow of water through refuse is calculated with Darcy's one-dimensional flow equation in the HELP model. Zeiss (1997) reported that the prediction of leachate in landfills could be improved if a two dimensional flow approach is applied.
- The sequential simulation used for determining moisture in refuse lifts in this study is quasi-manual because adjustments to temporal changes in the geotechnical and hydraulic properties of the refuse lifts were done on a spreadsheet. It is suggested that all the processes in this subroutine should be written in code and be compatible for inclusion in the computer program of the HELP model for robustness of the simulation.
- Investigations on the formation of macropores and their flow characteristics should be intensified, so models can be formulated to estimate the channelling of water into the waste fill after clay capping (restoration). The integrity of different

cover soil systems should also be studied, so that a system can be designed, which can withstand differential settlement, to assist landfill operators and designers.

- The veracity of the similarity between waste properties determined from small cells in the present study, and Beaven and Powrie's large-scale tests should be further investigated by conducting several tests on refuse obtained from the same landfill site in both cells. The particle size of the refuse used in the small cells should be same as in the present study, while crude refuse should be used in the larger cell. These further tests are urgently recommended, as they may have positive implications for refuse testing in countries that cannot afford sophisticated and costly large-scale testing facilities such as those at Pitsea (Beaven, 2000).

CHAPTER

11

Conclusions

11.1 Conclusions

This study reaffirms the change in the thickness, porosity, density, and hydraulic conductivity of a refuse layer with increasing vertical applied loads, which was reported in previous investigations (Bleiker et, 1995; Beaven and Powrie 1995). For instance, the hydraulic conductivity of a refuse layer in test cells decreased from 3.62×10^{-2} m/s to 6.53×10^{-4} m/s when the overburden was increased from 1kPa to 8kPa. The porosity of the refuse decreased from 44% to 16% during this period. As such, a refuse landfill consists of emplaced refuse lifts with different hydraulic and geotechnical properties. The simulation of individual refuse lift rather than the entire refuse fill will be representative of the actual landfill process and thus enhance simulation results.

The daily soil cover (slightly clay/silt sand) affected the properties of the refuse placed in the test cells. The hydraulic conductivity of the refuse fill was reduced while its density was increased. The measured permeability of a composite lift comprising of refuse with a cover soil was found to be less than its theoretical values calculated from soil mechanics principles.

There was a particular similarity between the trend of refuse properties obtained using a Perspex cylinder, 240 mm diameter, and 230mm overall height in this study, and the steel cylinder, 2 metre in diameter and 3 metre high used by Beaven and Powrie

(1995). With this, small cell tests appear suitable for preliminary study of waste characteristics if the waste components are reduced in proportion to the size of the test cell.

The similarity between the two scales of experiments also enabled empirical models to be derived from experimental data. These models, which are characteristic equations fitted to the plot of the test data, can be used to estimate hydraulic conductivity, field capacity, and porosity of refuse from its dry density.

The volumetric moisture content of the emplaced refuse lifts at White's pit increased during the active period of refuse filling due to infiltration from precipitation, and also from compression of the particulate waste. The degree of saturation of the lifts was increased while their absorption capacity decreased. The observed and measured moisture storage at White's pit compare very well considering the complexity of the nature of an emplaced refuse fill. Consequently, the simulation technique used in this study was deemed appropriate for moisture estimation in comparative planning and design of a MSW landfill.

REFERENCES

Advisory Group on Computer Graphics. 1994. Uniras training materials. Unimap Solutions, Loughborough, UK.

ASCE, 1959. Refuse volume reduction in a sanitary landfill. Journal of the Sanitary Engineering Division, ASCE, 85 (SA6): pp. 37 – 50.

Balaz, M. A., Ham, R. K., and Schaefer, D. M. 1989. Mass balance analysis of anaerobically decomposed refuse. Journal of Environmental Engineering, 6 (115): pp. 1088-1102.

Ball, J. M., and Blight, G. E. 1986. Groundwater pollution downstream of a long established sanitary landfill. Proceedings, International Symposium on Environmental Geotechnology, Allentown, pp. 149-157.

Beaven, R. P. 2000. The hydrogeological and geotechnical properties of household waste in relation to sustainable landfilling. PhD Thesis, Queen Mary and Westfield College, University of London, London.

Beaven, R. P., and Powrie, W. 1995. Hydrogeological and geotechnical properties of refuse using a large-scale compression cell. Proceedings Sardinia 95, Fifth International Landfill Symposium, Cagliari, Italy, pp. 745–760.

Beaven, R. P., and Powrie, W. 1996. Determination of the hydrogeological and geotechnical properties of refuse in relation to sustainable landfilling. 19th International Madison Waste Conference, Department of Engineering Professional Development, University of Wisconsin, Madison, pp. 435-454.

Bengtsson, L., Bendz, D., Hogland, W., Rosqvist, H., and Akesson, M. 1994. Water balance for landfills of different age. Journal of Hydrology, 158: pp. 203-217.

Berger, K., Melchior, S., and Miehlich, G. 1996. Suitability of hydrologic evaluation of landfill performance (HELP) model of the US Environmental Protection Agency for the simulation of the water balance of landfill cover systems. Environmental Geology, 28 (4): pp. 181–189.

Beven, K., and Germann, P. 1982. Macropores and water flow in soils. Water Resources Research, 18(5): pp. 1311-1325.

Biffaward, 2000, Landfill tax credit scheme.

<<http://www.biffaward.org/biffawardlandfilltax.html>> (Accessed August, 17, 2000).

Bingemer, H.G., and Crutzen, P. J. 1987. The production of methane frm solid wastes. Journal of Geophysical Research, 92 (D2): pp. 2181-2187.

Blakey, N. C. 1982. Infiltration and absorption of water by domestic wastes in landfills-Research carried out by the WRC. Landfill Leachate Symposium, Harwell, UK.

Bleiker, D. E., Farquhar, G., and McBean, E. 1995. Landfill settlement and the impact on site capacity and refuse hydraulic conductivity. Waste Management and Research, 13: pp. 533-534.

Blight, G. E., Ball, J. M., and Blight, J. J. 1992. Moisture and suction in sanitary landfills in semiarid areas. ASCE Journal of Environmental Engineering, 118 (6): pp. 865-877.

Blight, G. E., Hojem, D.J., and Ball, J. M. 1989. Generation of leachate from landfills in water-deficient areas. Proceedings Sardinia 89, Second International Landfill Symposium, Cagliari, Italy, XXVI-1 – XXVI-15.

Bookter, T. J., and Ham, R. K. 1982. Stabilisation of solid waste in landfills. Journal of the Environmental Engineering Division, ASCE, and 108 (EE6): pp. 1089-1100.

British Geological Survey. 1962. Dorset - Hampshire (Sheet 329). Ordnance Survey Office, Southampton.

BSI, 1990. BS 1377: Part 2. Soils for civil engineering purposes-Classification tests. British Standards Institute.

BSI. 1981. BS 3680: Part 4A: Liquid flow in open channels - Thin-plate weirs. British Standards Institute.

BSI. 1990. BS 1377: Part 5: Soils for civil engineering purposes - Compressibility, permeability and durability tests, British Standards Institute.

Buisman, A. S. K. 1936. Results of long duration settlement tests. Proceedings, 1st International Conference on Soil Mechanics, pp. 103-106.

C L Associates. 1991. Well logs for White's Pit landfill extension. Magna Road, Wimborne, Dorset.

C.H. Steavenson. 1992. Well logs for White's Pit landfill extension. Magna Road, Wimborne, Dorset.

Campbell, D. J. V. 1983. Understanding water balance in landfill sites. Waste Management, November, pp. 594-605.

Cartographical Services. 1987. Aerial photograph of Canford Heath (No 1389), Southampton.

Charles, J. A., and Burland, J. B. 1982. Geotechnical considerations in the design of foundations for buildings on deep deposits of waste materials. The Structural Engineer, 60A (1): pp. 8-14.

Chen, T., and Chynoweth, D. P. 1995. Hydraulic conductivity of compacted municipal solid waste. *Bioresource Technology*, 51: 205-212.

Cheremisinoff, P. N., K. A. Gigliello and O'Neill, T. K. 1984. *Groundwater-Leachate*. Technomic Publishing Inc. Pennsylvania.

Chian, E. S. K., DeWalle, F. B. 1976. Sanitary landfill leachate and their treatment. *ASCE Journal of the Environmental Engineering Division*, 102 (EE2): pp. 411-431.

Christensen, T. H., Nielsen, P. H., and Bjerg, P. L. 1995. Degradation of organic chemicals in a leachate pollution plume: An in- situ experiment, *Proceedings Sardinia '95, Fifth International Landfill Symposium*, pp. 621-628.

Clarke, D. 1997. Computer program "AREACAL" for calculating areas using digital data. *Irrigation Studies*, Department of Civil and Environmental Engineering, University of Southampton, Southampton.

Clayton, C. R. I., Matthews, M. C., and Simons, N. E. 1995. *Site Investigation*. Blackwell Science Ltd.

Conduto, P. D., and Huitric, R. 1990. Monitoring landfill movements using precise instruments. *Geotechnics of wastefills—Theory and practice: ASTM STP 1070*, Philadelphia, pp. 358-370.

Demetracopoulos, A. C. 1986. Modelling leachate production from municipal landfills. *Journal of Environmental Engineering-ASCE*, 112 (5): pp. 849-866.

DOE, 1992. A review of options. UK Department of Environment, Waste Management Paper No 1, HMSO, London.

DOE, 1995A. Landfill completion. Waste Management Paper No 26A, Department of the Environment, HMSO, London.

DOE, 1995B. Landfill design, construction and operational practice. Waste Management Paper 26B, HMSO, London.

Dorset County Council. 1997. Survey Maps for White's pit (1985-1990).

Dorset Drilling Services. 1994. Borehole logs for White's Pit landfill. Magna Road, Wimborne, Dorset.

Dorset Drilling Services. 1996. Borehole logs for White's Pit landfill. Magna Road, Wimborne, Dorset.

Edil, B. T., Ranguette, V. J., and Wuellner, W. W. 1990. Settlement of municipal refuse. Geotechnics of wastefills-Theory and practice: ASTM STP 1070, Philadelphia, pp. 225-239.

El-Fadel, M., Findikakis, A. N., and Leckie, J. O. 1997. Environmental impacts of solid waste landfilling. Journal of Environmental Management, 50: pp. 1-25.

Environment Agency. 1996. Well logs for Spiney Cottage, Magna Road, Wimborne, Dorset.

Ettala, M. 1987. Infiltration and hydraulic conductivity at a Sanitary Landfill. *Aqua Fennica*, 17 (2): pp. 231-237.

Ettala, M. 1987. Infiltration and hydraulic conductivity at a sanitary landfill. *Aqua Fennica*, 17 (2): pp. 231-237.

Farquhar, G. J. 1989. Leachate: production and characterisation. *Canadian Journal of Civil Engineering*, 16 (3): pp. 317-325.

Farquhar, G. J., Rovers, F. A. 1973. Gas production during refuse decomposition. Water, Air, and Soil Pollution, 2: pp. 483-495.

Fetter, 1981. Determination of the direction of groundwater flow. GWMR, pp. 28-31.

Freeze, R. A., and Cherry, J.A. 1979. Groundwater. Prentice-Hall, New Jersey.

Freshney, E. C., Bristow, C. R., and Williams, B. J. 1985. Geology of Bournemouth-Poole-Wimborne, Dorset (Sheet SZ 09). Geological report for DOE: Land Use Panning. British Geological Survey, Exeter.

Garmin Corporation, 1996. GPS 45XL Personal Navigator, Owners Manual and References. Romsey, UK.

Gee, J. R. 1981. Prediction of leachate accumulation in sanitary landfills. Proceedings of the Fourth Annual Madison Conference of Applied Research Practice on Municipal and Industrial Waste. Dept. of Engineering and Applied Science, University of Madison Extension, Madison, WI, pp. 170-190.

Georgious, B. 1998. Standard cone penetration tests, Whites pit landfill, Magna Road, Wimborne, Dorset. GEOCONE, Environmental Services Ltd., Leamington spa.

Gifford, P., Landva, A.O., and Hoffman, V.C. 1990. Geotechnical consideration when planning construction on a landfill. Geotechnics of wastefills—Theory and practice: ASTM STP 1070, Philadelphia, pp. 41-56.

Hampshire County Council. 1993. Analysis of wheeled bin waste-Summary of results.

Head, K. H. 1994. Manual of Soil Laboratory Testing: Volume 2: Permeability, Shear Strength and Compressibility Tests. John Wiley & Sons, New York.

Holmes, R. 1980. The water balance method of estimating leachate production from landfill sites. *Solid Wastes*. January, 1980. pp. 20 –33.

Holmes, R. 1984. Comparison of different methods of infiltration at a landfill site in the south Essex with implications for leachate management and control. *J. Eng. Geol.*, 17: pp. 9-18.

Huc, E. 1997. Personal communication.

Hutchinson, D. A. 1990. Phases of Tipping at White's Pit, Arrowsmith Road, Poole. Dorset County Council.

Hutchinson, D. A. 1995. Waste disposal issues statement: Towards a Dorset waste disposal strategy for the next millennium. *The Waste Challenge*, Dorset County Council, Dorchester.

Institute of Hydrology, 1979. Neutron Probe System 1H II. Instruction Manual. The Natural Environment Research Council, Wallingford, Oxon.

Ishii, M., Ashimura, K., and Nakayama, T. 1992. Environmental. *Geology, Water Science*, 19 (3): pp. 169-178.

Johnson, T. M., Cartwright, K., and Schuller, R. M. 1981. Monitoring of leachate migration in the unsaturated zone in the vicinity of Sanitary landfills. *GWMR*, pp. 55-63.

Fryett, J. 1997. Personal Communication.

Kao, J., Lin, H, and Chen, W. 1997. Network geographical information system for landfill siting. *Waste Mangement Research*, 15: pp. 239-253.

Kelly, W. E. 1976. Groundwater pollution near a landfill. Journal of the Environmental Engineering Division, ASCE, 102 (EE6): pp. 1189-1199.

Kjeldsen, P. 1993. Groundwater pollution source characterisation of an old landfill, Journal of Hydrology, 412: pp. 349-371.

Knox, K. 1998. Practical benefits for the waste industry from the UK's landfill test cell programme. Wastes Management, pp. 18-19.

Landva, A O., and Clark, J. I. 1990. Geotechnics of waste fill. Geotechnics of wastefills—Theory and practice: ASTM STP 1070, Philadelphia, pp. 87-103.

Leach, A. 1994. White's Pit - Landfill Gas Resource Assessment, Second Report.

Leckie, J. O., and Pacey, J. G. 1973. Journal of Environmental Engineering Division, ASCE, and 105 (EE2): pp. 337 – 355.

Leskiw, E. J., Sego, D. C. and Smith, D. W. 1992. Potential leachate production due to cold weather effects. Canadian Journal of Civil Engineering, 19 (4): pp. 660-667.

Ling, H. I., Leshchinsky, D., Mohri, Y., and Kawabata, T. 1998. Estimation of municipal solid waste landfill settlement. Journal of Geotechnical and Geoenvironmental Engineering, ASCE, 124 (1): pp. 21 – 28.

Linsley, R. K., Kohler, M. A., and Paulhus, J. L. H. 1982. Hydrology for Engineers. McGraw-Hill, Japan.

Lu, J. C. S., Eichenberger, B., and Stearns, R. J. 1985. Leachate from Municipal Landfills. Noyes Publication, New Jersey.

Lyngkilde, J., and Christensen, T. H. 1992. Redox zones of a landfill leachate pollution plume. Journal of Contaminant Hydrology, 10: pp. 273-289.

M J Carter Associates. 1989. Borehole logs for White's Pit landfill, Magna Road, Wimborne, Dorset.

Martin, J. H., Colins, A. R., and Diener, R. G. 1995. A sampling protocol for composting, recycling, and re-use of municipal solid waste. *Journal of Air & Waste Management Association*, 45: pp. 864-870.

McCarthy, D. F. 1982. *Essentials of Soil Mechanics and Foundations*. Prentice-Hall, Virginia.

Morris, D. V., and Woods, C. E. 1990. Settlement and engineering considerations in landfill and final cover design. *Geotechnics of wastefills – Theory and practice: ASTM STP 1070*, Philadelphia, pp. 41 – 56.

Mott MacDonald. 1990a. *Factual Report on Site Investigation*. White's Pit, Canford Heath, Magna Road, Wimborne, Dorset.

Mott MacDonald. 1990b. *Ground Investigation*. Report No. S1526, White's Pit, Canford Heath, Magna Road, Wimborne, Dorset.

Musa, E., and Ho, G. E. 1981. Optimum sample size in refuse analysis. *Journal of Environmental Engineering*, ASCE 107 (EE6): pp. 1247-1259.

Naseri, A. A. 1996. Impact of leaching on the hydraulic conductivity of aggregated clay soils. *MPhil/PhD Transfer Report*, University of Southampton, Southampton.

Naseri, A. A. 1998. The hydraulic conductivity of aggregated clay soils under loading, leaching and reclamation. *PhD Thesis*, University of Southampton, Southampton, UK.

Nixon, W. B., Murphy, R. J., and Stessel, R. I. 1997. An Empirical approach to the the performance assessment of solid waste landfills. *Waste Management and Research*, 15: pp. 607-626.

NRA, 1995. Landfill and the water environment. NRA Position Statement, National Rivers Authority, UK.

Ordnance Survey. 1988. Pathfinder 1301: Wimborne Minster and Bournemouth (West), HMSO, Southampton.

Oweis, I. S., and Khera, R. 1986. Criteria for geotechnical construction on sanitary landfills. Proceedings International Symposium on Environmental Geotechnology, Allentown, 1: pp. 205-223.

Parker, K. H., Mehta, R. V., and Caro, C. G. 1987. Steady flow in porous, elastically deformable materials. *Journal of Applied Mechanics.* pp. 794-800.

Parsons, R. 1995. Water balance method to predict leachate generation: Geohydrological experiences. Proceedings Sardinia 95, Fifth International Landfill Symposium, Cagliari, Italy, pp. 275-284.

Perrier, E. R., and Gibson, A. C. 1981. Hydrologic simulation on solid waste disposal sites. EPA-530/SW-868, US EPA, Cincinnati.

Pohland, F.G. 1980. Leachate recycle as a landfill management option. *Journal of Environmental Engineering Division, ASCE, and 106 (EE6):* pp. 1057-1069.

Powrie, W., and Beaven, R. P. 1999. Hydraulic properties of household waste and implications for landfills. *Proceedings of the Institution of the Civil Engineers, Geotechnical Engineering.* 137: pp. 235-247.

Price, M. 1985. Introducing groundwater. Chapman and Hall, London.

Qasim, S. R., and Chiang, W. 1994. Sanitary Landfill Leachate. Technomic Publishing Company, Pennsylvania.

Qdais, H. A. A., Hamoda, M. F., and Newham, J. 1997. Analysis of residential solid waste at generation sites. *Waste Management & Research*, 15: pp. 395-406.

Rao, S. K., Moulton, L. K., and Seals, R.K. 1977. Settlement of refuse landfills. *Geotechnical practice for disposal of solid waste materials*, ASCE, New York, pp. 574-598.

Reinhart, D. R., and Al-Yousfi, A. B. 1996. The impact of leachate recirculation on municipal solid waste landfill operating characteristics. *Waste Management Research*, 14: pp. 337-346.

Richards, D., Powrie, W., and Beaven, R. 1997. Factors relevant to the determination of final fill levels in landfills. *Proceedings of the 6th Sardinia International Landfill Symposium*, Cagliari, Italy, 3: pp. 413-420.

Rovers, F. A., and Farquhar, G. J. 1973. Infiltration and landfill behaviour. *Journal of the Environmental Division*, ASCE, 99 (EE5): pp. 671-690.

Rowe, R. K. 1998. Recent advances in understanding and modelling of clogging in landfill leachate collection systems. Seminar, University of Southampton, Southampton, UK.

Rowe, R. K., and Booker, J. R. 1991. Modelling two-dimensional contaminant migration in a layered and fractured zone beneath landfills. *Canadian Geotechnical Journal*, 28: pp. 338-352.

Schroeder, P. R., Dozier, T. S., Zappi, P. A., McEnroe, B. M., Sjostrom, J. W., and Peyton, R. L. 1994. *The Hydrologic Evaluation of Landfill Performance (HELP) Model: Engineering Documentation for Version 3*, EPA/600/9-94/xxx, U.S. Environmental Protection Agency Risk Reduction Engineering Laboratory, Cincinnati, OH.

Skempton, A. W. 1960. Effective Stress in Soils, Concrete and Rock. Pore pressure and suction in soils, pp. 4 –6.

Solomat, 1994. Multiparameter Water Quality Probe, Sonde 803PS-User Manual, Solomat Limited, Herts, U.K.

Sowers, G. F. 1968. Foundation problems in sanitary landfills. Journal of Sanitary Engineering Division. ASCE. 94 (SA1): pp. 103-116.

Sowers, G. F. 1973. Settlement of waste disposal fills. Proceedings, 8th International Conference on Soil Mechanics and Foundation Engineering, Moscow, pp. 207-210.

Tchobanoglous, G., Theisen, H., and Vigil, S. A. 1993. Integrated Solid Waste Management, Engineering Principles and Management. McGraw-Hill, Singapore.

Terzaghi, K., Peck, R. B., and Mesri, G. 1996. Soil mechanics in engineering practice. John Wiley and Sons Inc., Canada.

The Engineering Council. 1994. Guidelines on Environmental Issues. Department of Environment, UK.

The UK Meteorological Office. 1981. Soil Moisture - Monitoring on a National Scale: Scientific Background. Meteorological Office, Bracknell, UK.

The UK Meteorological Office. 1999. Daily rainfall, temperature and radiation, normal average annual wind speed, and quarterly relative humidity for Poole (1985-1998). Meteorological Office, Bracknell, UK.

Thompson, B., and Zandi, I. 1975. Future of sanitary landfill. Journal of Environmental Engineering Division, ASCE, 101 (EE1): pp. 41-53.

UNIRAS. 1989. UNIMAP 2000, Users Manual. UNIRAS A/S, Søborg, Denmark.

Vilenskii, D. G. 1957. Soil Science. Israel Program for Scientific translations, 3rd Edition.

W. S. Atkins Environment. 1994. White's Pit: Landfill gas potential estimate of landfill gas production, Draft document.

Wall, D. K., and Zeiss, C. 1995. Municipal landfill biodegradation and settlement. Journal of Environmental Engineering, ASCE, 121 (3): pp. 214-223.

Waste Management, 1998. Special feature: Landfill Technology. Waste management, November, 1998, pp. 24–25.

Watt, K. S. 1999. Settlement characteristics of landfill wastes. Proceedings of the Institution of the Civil Engineers, Geotechnical Engineering, 137: pp. 225-233.

Weymouth and Sherborne Recycling. 1997. Waste analysis results. Bournemouth Borough Council, Bournemouth.

WH White Plc. 1996. Wise-up to Waste! White's Pit landfill introductory pamphlet, Site Control Centre, Magna Road, Wimborne, Dorset.

Yen, B. C., and Sealon, B. 1975. Sanitary landfill settlement rates. Journal of the Geotechnical Engineering Division, ASCE, 101(5): pp. 475-487.

BIBLIOGRAPHY

Atkinson, J. 1993. An introduction to the mechanics of soil and foundations. McGraw-Hill, Berkshire.

Briscoe, M. H. 1990. A researcher's guide to scientific and medical illustrations. Springer-Verlag, New York.

Craig, R. F. 1983. Soil mechanics. Van Nostrand Reinhold, Wokingham, UK.

Daniel, D. E. 1993. Geotechnical practice for waste disposal. Chapman & Hall, London.

Day, J. C., and Athey, T. H. 1990. Microcomputers and applications. Scott, Foresman and Company.

Gere, J. M., and Timoshenko, S. P. 1991. Mechanics of materials. Chapman & Hall, London.

Mott MacDonald. 1991. Modelled surface contours of Broadstone clay at White's Pit Landfill, Canford Heath, Magna Road, Wimborne, Dorset.

Oakley, R. E. 1990. Case history: Use of the cone penetrometer to calculate the settlement of a chemically stabilised landfill. Geotechnics of wastefills – Theory and practice: ASTM STP 1070, Philadelphia, pp. 345-357.

Powrie, W. 1997. Soil Mechanics, Concepts and Applications. Chapman and Hall, London.

Ritzema, H. 1994. Drainage, Principles and Applications, ILRI Publication 16, International Institute for Land Reclamation and Improvement, Netherlands.

Saines, M. 1981. Errors in interpretation of groundwater level data. GWMR, pp. 56-61.

Star, J., and Estes, J. 1990. Geographical Information Systems - An Introduction. Prentice-Hall Inc., London.

Stoud, K. A. 1990. Further Engineering Mathematics. Macmillan, London.

Stoud, K. A. 1995. Engineering Mathematics. Macmillan, London.

Streeter, V. L., and Wyle, E. B. 1975. Fluid mechanics. McGraw-Hill, Kogakusha. pp. 473-483.

Whitlow, R. 1983. Basic soil mechanics. Longman Inc., New York.

Williams, G. M., and Higgo, J. J. W. 1994. In situ and laboratory investigations into contaminant migration, *Journal of Hydrology*, 159: pp. 1-25.

Williams, G. M., Ross, A. M., Stuart, A., Hitchman, S. P., and Alexander, L. S. 1984. Controls on contamination migration at Villa Lagoons, *Journal of Engineering Geology*, 17: pp. 39-55.

Zeiss, C. 1997. A comparison of approaches to the prediction of landfill leachate generation. *Proceedings Sardinia 97*, Proceedings of the 6th Sardinia International Landfill Symposium, Cagliari, Italy, 1: pp. 13-22.

Zeiss, C. A., and Atwater, J. 1989. Waste facility impacts on residential property values. *Journal of Urban Planning and Development*, ASCE, 115(2), pp. 64-80.

APPENDICES

APPENDIX A
ERRORS IN MEASUREMENT AND
SOME USEFUL GEOTECHNICAL TERMS

Errors in Field Measurement

Pit/Experimental test:

Measurement using the Distomat	±10 mm
Surface length:	2000 – 5000 mm
Error in measuring the surface length	<±0.2 – 0.5%
Width	1000 mm
Error in measuring the width	<±1%
Gradations on the measuring stick	10mm
Depth	300 - 3000mm
Error in measuring the depth	<±0.33 – 3.33%
Measurement with weighbridge	<± 10 kg
Mass of excavated spoil (including mass of skip)	22000 – 32000 kg
Error in measuring the depth	<±0.03 – 0.045%

Drum tests:

Load:

Minimum load measurement using the weighing equipment	±0.01 kg
Minimum load measured	126 kg
Error	<±0.01%

Volume:

Measurement with measuring cylinder	±0.01 lt.
Volume of leachate drained	30 – 70 lt.
Error	<±0.01 - 0.03%

Classification tests:

Load readings	±1g
Error	<±1%

Refuse testing in cells:

Accuracy of the Vernier (calliper) scale	± 0.01 mm
Error in diameter of refuse sample	$<\pm 0.01\%$
Error in length of refuse sample	$<\pm 0.01\%$
Error in measurement of head in piezometer tubes	$<\pm 1\%$
Accuracy of measuring cylinder	± 1 ml
Min. volume of water drained	<500 ml
Error in volume of water drained from sample	$<\pm 1\%$
Accuracy in load measurement	± 1 g
Min measurement of sample	~ 280 g
Error	$<\pm 1\%$

Some Useful Geotechnical Terms

Unlike soil, waste contains compressible particles and the particle density increase with overburden stress (Beaven, 2000). In the absence of research into the impact of varying particle density on properties, some of the basic terms in soil mechanics are still applied to waste technology. A typical phase diagram for soil material is shown in Figure A1 below

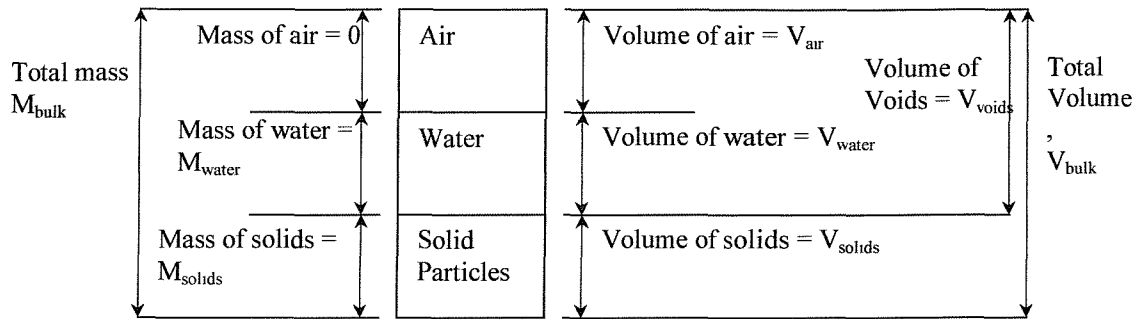


Figure A1: Phase diagram for a waste/soil material

The most common characteristic of refuse that is often quoted in various forms is the moisture content. The moisture content of waste is often reported in terms of the wet mass of refuse (Tchobanoglou et al, 1993), but sometimes quoted in terms of the dry mass of refuse. The relationships between these terms for a waste/soil material are:

$$m_{dry} = \frac{m_{wet}}{(1 - m_{wet})} \quad (A1)$$

$$m_{wet} = \frac{m_{dry}}{(1 + m_{dry})} \quad (A2)$$

$$\rho_{dry} = \frac{\rho_{wet}}{(1 + m_{dry})} \quad (A3)$$

$$\rho_{dry} = \rho_{wet} (1 - m_{wet}) \quad (A4)$$

where

m_{dry} = the gravimetric dry moisture content of the refuse/soil material

m_{wet} = the gravimetric wet (or bulk) moisture content of the refuse/soil material

ρ_{dry} = the dry density of the refuse/soil material

ρ_{wet} = wet (bulk) density of the refuse/soil material

In soil science, moisture content of soil is expressed in volumetric ratio but engineers often report this in gravimetric ratio in waste and soil investigations. In the HELP model, water content of waste and soil materials are expressed in volumetric terms. Schroeder et al. (1994) and Blight et al. (1992) reported the relationship between volumetric (θ) and gravimetric expression of water storage (m). This can be derived as shown below:

The volume of water in a waste/soil material is given as:

$$V_{water} = \frac{M_{water}}{\rho_{water}} \quad (A5)$$

The volume of a dry bulk of the material is:

$$V_{dbulk} = \frac{M_{dbulk}}{\rho_{dbulk}} \quad (A6)$$

Dividing equation (A5) by (A6) gives

$$\frac{V_{water}}{V_{dbulk}} = \left(\frac{M_{water}}{M_{dbulk}} \right) \left(\frac{\rho_{dbulk}}{\rho_{water}} \right) \quad (A7)$$

The expression on the left side of equation (A7) is the volumetric water content θ and can be written as

$$\theta = m_{dry} \frac{\rho_{dbulk}}{\rho_w} = m_{dry} \Gamma_{dbulk} \quad [A8]$$

$$\theta = \left(\frac{m_{wet}}{1 + m_{wet}} \right) \left(\frac{\rho_{bulk}}{\rho_{water}} \right) = \left(\frac{m_{wet}}{1 + m_{wet}} \right) \Gamma_{wbulk} \quad [A9]$$

$$\theta = \left(\frac{m_{dry}}{1 + m_{dry}} \right) \left(\frac{\rho_{bulk}}{\rho_{water}} \right) = \left(\frac{m_{dry}}{1 + m_{dry}} \right) \Gamma_{wbulk} \quad [A10]$$

where

V_{water} = volume of water

M_{water} = Mass of water

ρ_{water} = density of water

V_{dbulk} = volume of dry bulk of refuse/soil material

M_{dbulk} = Mass of refuse/soil material

ρ_{dbulk} = density of refuse/soil material

Γ_{dbulk} = dry bulk specific gravity of the refuse/soil material.

Γ_{wbulk} = wet bulk specific gravity of the refuse/soil material

Some other basic terms used in the thesis include:

Porosity = volume of voids / bulk volume of the refuse

Air porosity = drainage porosity = effective porosity = porosity at field capacity.

Total porosity = field capacity of waste + drainage porosity of waste.

Absorption capacity = field capacity of waste – prevailing moisture content in waste.

Degree of saturation = volume of water in waste / volume of voids in refuse.

APPENDIX B

TABLES AND CURVES

Table B1: Neutron probe readings for NP 3

Depth from GL (cm)	06/05/98	31/3/98	02/2/98	28/01/98	22/12/97	8/12/97	11/11/97	11/9/97	9/07/97	13/6/97
	NP 3	NP 3	NP 3	NP 3	NP 3	NP 3	NP 3	NP 3	NP 3	NP 3
20	0 292	0 318	0 282	0 295	0 306	0 592	0 259	0 185	0 167	0 154
30	0 289	0 333	0 288	0 322	0 422	0 574	0 306	0 189	0 151	0 151
40	0 282	0 326	0 266	0 314	0 615	0 630	0 347	0 163	0 135	0 152
50	0 365	0 390	0 324	0 382	0 412	0 434	0 390	0 149	0 165	0 149
60	0 387	0 385	0 358	0 393	0 367	0 395	0 351	0 158	0 187	0 149
70	0 382	0 385	0 354	0 385	0 350	0 373	0 361	0 177	0 251	0 158
80	0 370	0 385	0 350	0 387	0 325	0 353	0 365	0 215	0 341	0 176
90	0 396	0 404	0 377	0 407	0 344	0 390	0 358	0 311	0 364	0 214
100	0 442	0 417	0 409	0 442	0 413	0 427	0 415	0 327	0 329	0 228
110	0 396	0 386	0 383	0 410	0 392	0 407	0 390	0 382	0 328	0 239
120	0 381	0 381	0 383	0 397	0 379	0 396	0 381	0 373	0 322	0 241
130	0 378	0 381	0 378	0 388	0 374	0 387	0 373	0 369	0 334	0 241
140	0 379	0 383	0 370	0 397	0 374	0 390	0 393	0 375	0 386	0 257
150	0 414	0 443	0 409	0 421	0 421	0 409	0 442	0 435	0 516	0 327
160	0 547	0 558	-	0 572	0 564	0 566	0 551	0 576	0 472	0 411
170	0 506	0 543	-	-	-	-	0 535	-	-	-

Table B2: Neutron probe readings for NP 4

Depth from GL (cm)	06/05/98	31/3/98	02/2/98	28/01/98	22/12/97	8/12/97	11/11/97	11/9/97	9/07/97
	NP 4	NP 4	NP 4	NP 4	NP 4	NP 4	NP 4	NP 4	NP 4
20	0 337	0 494	0 332	0 355	0 453	0 490	0 464	0 287	0 347
30	0 361	0 486	0 365	0 415	0 471	0 496	0 468	0 302	0 367
40	0 373	0 471	0 395	0 463	0 469	0 477	0 460	0 305	0 373
50	0 374	0 401	0 448	0 461	0 467	0 475	0 463	0 319	0 374
60	0 381	0 378	0 397	0 403	0 394	0 414	0 402	0 332	0 369
70	0 350	0 377	0 382	0 375	0 384	0 388	0 379	0 342	0 364
80	0 348	0 365	0 369	0 352	0 371	0 368	0 374	0 347	0 376
90	0 349	0 360	0 368	0 355	0 370	0 370	0 367	0 346	0 367
100	0 352	0 323	0 357	0 352	0 363	0 366	0 370	0 345	0 349
110	0 337	0 336	0 348	0 319	0 331	0 329	0 347	0 329	0 351
120	0 340	0 321	0 344	0 327	0 340	0 344	0 346	0 332	0 329
130	0 323	0 378	0 349	0 327	0 329	0 335	0 334	0 312	0 395
140	0 383	0 418	0 387	0 354	0 375	0 371	0 354	0 382	0 406
150	0 416	0 412	0 434	0 405	0 425	0 430	0 383	0 409	0 408
160	0 417	-	0 429	0 412	0 418	0 425	0 384	0 406	-

GL – ground level

Table B3: Runoff data

Runoff Data								Computer Statistics- 15 – 203 hrs (9 - 26 Sept 1998)	
Time (hr)	Reading on graph paper (mm)	Depth of water in stilling well (mm)	Height of water above V-notch (mm)	Runoff (l/s)	Rainfall (mm)	Date (1998)		Mean	0 075
1	40	99 80	8 80	1 04E-02				Standard Error	0 022
2	40	99 80	8 80	1 04E-02				Median	0 007
3	40	99 80	8 80	1 04E-02				Mode	0 007
4	40	99 80	8 80	1 04E-02				Standard Deviation	0 306
5	40	99 80	8 80	1 04E-02				Sample Variance	0 094
6	39 75	99 48	8 48	9 45E-03				Kurtosis	58 332
7	39 5	99 16	8 16	8 59E-03				Skewness	7 313
8	39 4	99 03	8 03	8 26E-03			end of 9/9		
9	39	98 52	7 52	7 00E-03			0	Range	2 829
10	38 5	97 88	6 88	5 61E-03				Minimum	0 000
11	38	97 24	6 24	4 40E-03				Maximum	2 829
12	38	97 24	6 24	4 40E-03				Sum	14 101
13	38	97 24	6 24	4 40E-03				Count	189 000
14	38	97 24	6 24	4 40E-03				Largest(1)	2 829
15	98	173 92	82 92	2 83E+00				Smallest(1)	0 000
16	58	122 80	31 80	2 58E-01				Confidence Level(95 0%)	0 044
17	51	113 86	22 86	1 13E-01					
18	45	106 19	15 19	4 06E-02					
19	41	101 08	10 08	1 46E-02					
20	40	99 80	8 80	1 04E-02					
21	40	99 80	8 80	1 04E-02					
22	40	99 80	8 80	1 04E-02					
23	40	99 80	8 80	1 04E-02					
24	40	99 80	8 80	1 04E-02					
25	40	99 80	8 80	1 04E-02					
26	40	99 80	8 80	1 04E-02					
27	40	99 80	8 80	1 04E-02					
28	40	99 80	8 80	1 04E-02					
29	40	99 80	8 80	1 04E-02					
30	40	99 80	8 80	1 04E-02					
31	40	99 80	8 80	1 04E-02			end of 10/9		
32	40	99 80	8 80	1 04E-02					
33	40	99 80	8 80	1 04E-02			1 7		
34	40	99 80	8 80	1 04E-02					
35	40	99 80	8 80	1 04E-02					
36	40	99 80	8 80	1 04E-02					
37	40	99 80	8 80	1 04E-02					
38	40	99 80	8 80	1 04E-02					
39	40	99 80	8 80	1 04E-02					
40	39 75	99 48	8 48	9 45E-03					
41	39 5	99 16	8 16	8 59E-03					
42	39 5	99 16	8 16	8 59E-03					
43	39	98 52	7 52	7 00E-03					
44	39	98 52	7 52	7 00E-03					
45	39	98 52	7 52	7 00E-03					
46	39	98 52	7 52	7 00E-03					
47	39	98 52	7 52	7 00E-03					
48	39	98 52	7 52	7 00E-03					
49	39	98 52	7 52	7 00E-03					
50	39	98 52	7 52	7 00E-03					
51	39	98 52	7 52	7 00E-03					
52	39	98 52	7 52	7 00E-03					
53	39	98 52	7 52	7 00E-03					
54	39	98 52	7 52	7 00E-03					
55	39	98 52	7 52	7 00E-03					
56	39	98 52	7 52	7 00E-03					
57	39	98 52	7 52	7 00E-03					
58	39	98 52	7 52	7 00E-03			3 5		

Time (hr)	Reading on graph paper (mm)	Depth of water in stilling well (mm)	Height of water above V-notch (mm)	Runoff (l/s)	Rainfall (mm)	Date (1998)
59	39	98 52	7 52	7 00E-03		
60	39	98 52	7 52	7 00E-03		
61	39	98 52	7 52	7 00E-03		
62	39	98 52	7 52	7 00E-03		
63	39	98 52	7 52	7 00E-03		
64	39	98 52	7 52	7 00E-03		
65	39	98 52	7 52	7 00E-03		
65 5	39	98 52	7 52	7 00E-03		
65 75	106	184 15	93 15	3 78E+00		
66	101	177 76	86 76	3 17E+00		
66 25	91	164 98	73 98	2 13E+00		
66 5	86	158 59	67 59	1 70E+00		
66 75	73	141 97	50 97	8 38E-01		
67	70	138 14	47 14	6 89E-01		
67 5	62	127 91	36 91	3 74E-01		
68	59	124 08	33 08	2 84E-01		
69	55	118 97	27 97	1 87E-01		
70	53	116 41	25 41	1 47E-01		
71	52	115 13	24 13	1 29E-01		
72	50	112 58	21 58	9 77E-02		
73	48	110 02	19 02	7 13E-02		
74	47	108 74	17 74	5 99E-02		
75	47	108 74	17 74	5 99E-02		
76	47	108 74	17 74	5 99E-02		
77	47	108 74	17 74	5 99E-02		
78	47	108 74	17 74	5 99E-02		
79	47	108 74	17 74	5 99E-02		
80	47	108 74	17 74	5 99E-02		end of 12/9
81	47	108 74	17 74	5 99E-02	0	
81 25	47	108 74	17 74	5 99E-02		
82	106	184 15	93 15	3 78E+00		
82 25	110	189 26	98 26	4 32E+00		
82 5	96	171 37	80 37	2 62E+00		
83	80	150 92	59 92	1 26E+00		
83 5	70	138 14	47 14	6 89E-01		
84	65	131 75	40 75	4 79E-01		
84 5	61	126 64	35 64	3 42E-01		
85	59 5	124 72	33 72	2 98E-01		
85 5	57	121 52	30 52	2 33E-01		
86	56 5	120 88	29 88	2 21E-01		
87	56	120 25	29 25	2 09E-01		
88	54	117 69	26 69	1 66E-01		
89	53	116 41	25 41	1 47E-01		
90	51	113 86	22 86	1 13E-01		
91	49	111 30	20 30	8 39E-02		
92	47	108 74	17 74	5 99E-02		
93	46 5	108 10	17 10	5 47E-02		
94	46	107 47	16 47	4 97E-02		
95	46	107 47	16 47	4 97E-02		
96	45 5	106 83	15 83	4 50E-02		
97	45	106 19	15 19	4 06E-02		
98	45	106 19	15 19	4 06E-02		
99	45	106 19	15 19	4 06E-02		
100	45	106 19	15 19	4 06E-02		
101	45	106 19	15 19	4 06E-02		
102	45	106 19	15 19	4 06E-02		
103	45	106 19	15 19	4 06E-02		
104	45	106 19	15 19	4 06E-02		end of 13/9

Time (hr)	Reading on graph paper (mm)	Depth of water in stilling well (mm)	Height of water above V-notch (mm)	Runoff (l/s)	Rainfall (mm)	Date (1998)
105	45	106 19	15 19	4 06E-02		
106	45	106 19	15 19	4 06E-02		
107	45	106 19	15 19	4 06E-02		
108	45	106 19	15 19	4 06E-02		
109	45	106 19	15 19	4 06E-02		
110	45	106 19	15 19	4 06E-02		
111	45	106 19	15 19	4 06E-02		
112	45	106 19	15 19	4 06E-02		
113	45	106 19	15 19	4 06E-02		
114	45	106 19	15 19	4 06E-02		
115	44 5	105 55	14 55	3 65E-02		
116	43 5	104 27	13 27	2 90E-02		
117	41 5	101 71	10 71	1 70E-02		
118	40 5	100 44	9 44	1 24E-02		
119	40	99 80	8 80	1 04E-02		
120	39 5	99 16	8 16	8 59E-03		
121	39	98 52	7 52	7 00E-03		
122	39	98 52	7 52	7 00E-03		
123	39	98 52	7 52	7 00E-03		
124	39	98 52	7 52	7 00E-03		
125	39	98 52	7 52	7 00E-03		
126	39	98 52	7 52	7 00E-03		
127	39	98 52	7 52	7 00E-03		
128	39	98 52	7 52	7 00E-03	end of 14/9	
129	39	98 52	7 52	7 00E-03	0	
130	39	98 52	7 52	7 00E-03		
131	39	98 52	7 52	7 00E-03		
132	39	98 52	7 52	7 00E-03		
133	39	98 52	7 52	7 00E-03		
134	39	98 52	7 52	7 00E-03		
135	39	98 52	7 52	7 00E-03		
136	39	98 52	7 52	7 00E-03		
137	40	99 80	8 80	1 04E-02		
138	39 5	99 16	8 16	8 59E-03		
139	39	98 52	7 52	7 00E-03		
140	39	98 52	7 52	7 00E-03		
141	39	98 52	7 52	7 00E-03		
142	39	98 52	7 52	7 00E-03		
143	39	98 52	7 52	7 00E-03		
144	39	98 52	7 52	7 00E-03		
145	39	98 52	7 52	7 00E-03		
146	39	98 52	7 52	7 00E-03		
147	39	98 52	7 52	7 00E-03		
148	39	98 52	7 52	7 00E-03		
149	39	98 52	7 52	7 00E-03		
150	39	98 52	7 52	7 00E-03		
151	39	98 52	7 52	7 00E-03		
152	39	98 52	7 52	7 00E-03	end of 15/9	
153	39	98 52	7 52	7 00E-03	0	
154	39	98 52	7 52	7 00E-03		
155	39	98 52	7 52	7 00E-03		
156	39	98 52	7 52	7 00E-03		
157	39	98 52	7 52	7 00E-03		
158	39	98 52	7 52	7 00E-03		
159	39	98 52	7 52	7 00E-03		
160	39	98 52	7 52	7 00E-03		
161	39	98 52	7 52	7 00E-03		
162	39	98 52	7 52	7 00E-03		
163	39	98 52	7 52	7 00E-03		
164	39	98 52	7 52	7 00E-03		
165	39	98 52	7 52	7 00E-03		
166	39	98 52	7 52	7 00E-03		
167	39	98 52	7 52	7 00E-03		
168	39	98 52	7 52	7 00E-03		
169	39	98 52	7 52	7 00E-03		
170	39	98 52	7 52	7 00E-03		
171	39	98 52	7 52	7 00E-03		
172	39	98 52	7 52	7 00E-03		
173	38 5	97 88	6 88	5 61E-03		
174	38 5	97 88	6 88	5 61E-03		
175	38 5	97 88	6 88	5 61E-03		
176	38 5	97 88	6 88	5 61E-03	end of 16/9	
177	38 5	97 88	6 88	5 61E-03	0 3	
178	38	97 24	6 24	4 40E-03		
179	38	97 24	6 24	4 40E-03		
180	38	97 24	6 24	4 40E-03		
181	38	97 24	6 24	4 40E-03		
182	38	97 24	6 24	4 40E-03		
183	38	97 24	6 24	4 40E-03		
184	38	97 24	6 24	4 40E-03		
185	38	97 24	6 24	4 40E-03		

Time (hr)	Reading on graph paper (mm)	Depth of water in stilling well (mm)	Height of water above V-notch (mm)	Runoff (l/s)	Rainfall (mm)	Date (1998)
186	38	97 24	6 24	4 40E-03		
187	38	97 24	6 24	4 40E-03		
188	38	97 24	6 24	4 40E-03		
189	38	97 24	6 24	4 40E-03		
190	38	97 24	6 24	4 40E-03		
191	38	97 24	6 24	4 40E-03		
192	38	97 24	6 24	4 40E-03		
193	38	97 24	6 24	4 40E-03		
194	38	97 24	6 24	4 40E-03		
195	38	97 24	6 24	4 40E-03		
196	37	95 96	4 96	2 48E-03		
197	36	94 69	3 69	1 18E-03		
198	35	93 41	2 41	4 06E-04		
199	34	92 13	1 13	6 12E-05		
200	34	92 13	1 13	6 12E-05		end of 17/9
201	33 5	91 49	0 49	7 59E-06	0	
202	33 5	91 49	0 49	7 59E-06		
203	33 25	91 17	0 17	5 42E-07		
204	33	90 85	-0 15	0 00E+00		
205	33	90 85	-0 15	0 00E+00		
206	33	90 85	-0 15	0 00E+00		
207	33	90 85	-0 15	0 00E+00		
208	33	90 85	-0 15	0 00E+00		
209	33	90 85	-0 15	0 00E+00		
210	33	90 85	-0 15	0 00E+00		
211	33	90 85	-0 15	0 00E+00		
212	33	90 85	-0 15	0 00E+00		
213	33	90 85	-0 15	0 00E+00		
214	33	90 85	-0 15	0 00E+00		
215	33	90 85	-0 15	0 00E+00		
216	33	90 85	-0 15	0 00E+00		
217	33	90 85	-0 15	0 00E+00		
218	32 75	90 53	-0 47	0 00E+00		
219	32	89 57	-1 43	0 00E+00		
219 85	29	85 74	-5 26	0 00E+00		
219 93	87	159 86	68 86	1 78E+00		
220	35	93 41	2 41	4 06E-04		
221	41	101 08	10 08	1 46E-02		
222	40	99 80	8 80	1 04E-02		
223	39	98 52	7 52	7 00E-03		
224	39	98 52	7 52	7 00E-03		end of 18/9
225	39	98 52	7 52	7 00E-03	0	
226	39	98 52	7 52	7 00E-03		
227	39	98 52	7 52	7 00E-03		
228	39	98 52	7 52	7 00E-03		
229	39	98 52	7 52	7 00E-03		
230	39	98 52	7 52	7 00E-03		
231	38 75	98 20	7 20	6 28E-03		
232	38 75	98 20	7 20	6 28E-03		
233	38 75	98 20	7 20	6 28E-03		
234	38 75	98 20	7 20	6 28E-03		
235	38 75	98 20	7 20	6 28E-03		
236	38 75	98 20	7 20	6 28E-03		
237	38 75	98 20	7 20	6 28E-03		
238	38 75	98 20	7 20	6 28E-03		
239	38	97 24	6 24	4 40E-03		
240	37 5	96 60	5 60	3 36E-03		
241	36 75	95 64	4 64	2 10E-03		
242	36	94 69	3 69	1 18E-03		
243	36	94 69	3 69	1 18E-03		
244	36	94 69	3 69	1 18E-03		
245	33 75	91 81	0 81	2 66E-05		
246	35	93 41	2 41	4 06E-04		
247	35	93 41	2 41	4 06E-04		
248	35	93 41	2 41	4 06E-04		end of 19/9

Time (hr)	Reading on graph paper (mm)	Depth of water in stilling well (mm)	Height of water above V-notch (mm)	Runoff (l/s)	Rainfall (mm)	Date (1998)
249	35	93 41	2 41	4 06E-04	0	
250	35	93 41	2 41	4 06E-04		
251	35	93 41	2 41	4 06E-04		
252	35	93 41	2 41	4 06E-04		
253	35	93 41	2 41	4 06E-04		
254	35	93 41	2 41	4 06E-04		
255	35	93 41	2 41	4 06E-04		
256	35	93 41	2 41	4 06E-04		
257	34 75	93 09	2 09	2 84E-04		
258	34 75	93 09	2 09	2 84E-04		
259	34 75	93 09	2 09	2 84E-04		
260	34 75	93 09	2 09	2 84E-04		
261	34 75	93 09	2 09	2 84E-04		
262	34 25	92 45	1 45	1 14E-04		
263	33	90 85	-0 15	0 00E+00		
264	31	88 30	-2 71	0 00E+00		
265	30	87 02	-3 98	0 00E+00		
266	29 75	86 70	-4 30	0 00E+00		
267	29 5	86 38	-4 62	0 00E+00		
268	29 25	86 06	-4 94	0 00E+00		
269	29	85 74	-5 26	0 00E+00		
270	29	85 74	-5 26	0 00E+00		
271	29	85 74	-5 26	0 00E+00		
272	29	85 74	-5 26	0 00E+00		end of 20/9
273	29	85 74	-5 26	0 00E+00	0	
274	29	85 74	-5 26	0 00E+00		
275	29	85 74	-5 26	0 00E+00		
276	29	85 74	-5 26	0 00E+00		
277	29	85 74	-5 26	0 00E+00		
278	29	85 74	-5 26	0 00E+00		
279	29	85 74	-5 26	0 00E+00		
280	29	85 74	-5 26	0 00E+00		
281	29	85 74	-5 26	0 00E+00		
282	29	85 74	-5 26	0 00E+00		
283	29	85 74	-5 26	0 00E+00		
284	29	85 74	-5 26	0 00E+00		
285	29	85 74	-5 26	0 00E+00		
286	29	85 74	-5 26	0 00E+00		
287	29	85 74	-5 26	0 00E+00		
288	29	85 74	-5 26	0 00E+00		
289	29	85 74	-5 26	0 00E+00		
290	29	85 74	-5 26	0 00E+00		
291	29	85 74	-5 26	0 00E+00		
292	29	85 74	-5 26	0 00E+00		
293	29	85 74	-5 26	0 00E+00		
294	29	85 74	-5 26	0 00E+00		
295	29	85 74	-5 26	0 00E+00		
296	29	85 74	-5 26	0 00E+00		end of 21/9
297	29	85 74	-5 26	0 00E+00	0	
298	29	85 74	-5 26	0 00E+00		
299	29	85 74	-5 26	0 00E+00		
300	29	85 74	-5 26	0 00E+00		
301	29	85 74	-5 26	0 00E+00		
302	29	85 74	-5 26	0 00E+00		
303	29	85 74	-5 26	0 00E+00		
304	29	85 74	-5 26	0 00E+00		
305	29	85 74	-5 26	0 00E+00		
306	29	85 74	-5 26	0 00E+00		
307	29	85 74	-5 26	0 00E+00		
308	29	85 74	-5 26	0 00E+00		
309	29	85 74	-5 26	0 00E+00		
310	29	85 74	-5 26	0 00E+00		
311	29	85 74	-5 26	0 00E+00		

Time (hr)	Reading on graph paper (mm)	Depth of water in stilling well (mm)	Height of water above V-notch (mm)	Runoff (l/s)	Rainfall (mm)	Date (1998)
312	29	85 74	-5 26	0 00E+00		
313	28	84 46	-6 54	0 00E+00		
314	28	84 46	-6 54	0 00E+00		
315	28	84 46	-6 54	0 00E+00		
316	28	84 46	-6 54	0 00E+00		
317	28	84 46	-6 54	0 00E+00		
318	28	84 46	-6 54	0 00E+00		
319	28	84 46	-6 54	0 00E+00		
320	28	84 46	-6 54	0 00E+00		end of 22/9
321	28	84 46	-6 54	0 00E+00	0	
322	28	84 46	-6 54	0 00E+00		
323	28	84 46	-6 54	0 00E+00		
324	28	84 46	-6 54	0 00E+00		
325	28	84 46	-6 54	0 00E+00		
326	28	84 46	-6 54	0 00E+00		
327	28	84 46	-6 54	0 00E+00		
328	28	84 46	-6 54	0 00E+00		
329	28	84 46	-6 54	0 00E+00		
330	28	84 46	-6 54	0 00E+00		
331	28	84 46	-6 54	0 00E+00		
332	28	84 46	-6 54	0 00E+00		
333	28	84 46	-6 54	0 00E+00		
334	28	84 46	-6 54	0 00E+00		
335	28	84 46	-6 54	0 00E+00		
336	28	84 46	-6 54	0 00E+00		
337	28	84 46	-6 54	0 00E+00		
338	28	84 46	-6 54	0 00E+00		
339	28	84 46	-6 54	0 00E+00		
340	28	84 46	-6 54	0 00E+00		
341	28	84 46	-6 54	0 00E+00		
342	28	84 46	-6 54	0 00E+00		
343	28	84 46	-6 54	0 00E+00		
344	28	84 46	-6 54	0 00E+00		end of 23/9
345	28	84 46	-6 54	0 00E+00	0	
346	28	84 46	-6 54	0 00E+00		
347	28	84 46	-6 54	0 00E+00		
348	28	84 46	-6 54	0 00E+00		
349	28	84 46	-6 54	0 00E+00		
350	28	84 46	-6 54	0 00E+00		
351	28	84 46	-6 54	0 00E+00		
352	28	84 46	-6 54	0 00E+00		
353	28	84 46	-6 54	0 00E+00		
354	28	84 46	-6 54	0 00E+00		
355	28	84 46	-6 54	0 00E+00		
356	28	84 46	-6 54	0 00E+00		
357	28	84 46	-6 54	0 00E+00		
358	28	84 46	-6 54	0 00E+00		
359	28	84 46	-6 54	0 00E+00		
360	28	84 46	-6 54	0 00E+00		
361	28	84 46	-6 54	0 00E+00		
362	28	84 46	-6 54	0 00E+00		
363	28	84 46	-6 54	0 00E+00		
364	28	84 46	-6 54	0 00E+00		
365	28	84 46	-6 54	0 00E+00		
366	28	84 46	-6 54	0 00E+00		
367	28	84 46	-6 54	0 00E+00		
368	28	84 46	-6 54	0 00E+00		end of 24/9
345	28	84 46	-6 54	0 00E+00	4	
346	28	84 46	-6 54	0 00E+00		
347	28	84 46	-6 54	0 00E+00		
348	28	84 46	-6 54	0 00E+00		
349	28	84 46	-6 54	0 00E+00		
350	28	84 46	-6 54	0 00E+00		
351	28	84 46	-6 54	0 00E+00		
352	28	84 46	-6 54	0 00E+00		

Time (hr)	Reading on graph paper (mm)	Depth of water in stilling well (mm)	Height of water above V-notch (mm)	Runoff (l/s)	Rainfall (mm)	Date (1998)
353	28	84 46	-6 54	0 00E+00		
354	28	84 46	-6 54	0 00E+00		
355	28	84 46	-6 54	0 00E+00		
356	28	84 46	-6 54	0 00E+00		
357	28	84 46	-6 54	0 00E+00		
358	28	84 46	-6 54	0 00E+00		
359	28	84 46	-6 54	0 00E+00		
360	28	84 46	-6 54	0 00E+00		
361	28	84 46	-6 54	0 00E+00		
362	28	122 58	31 58	2 53E-01		
363	28	122 58	31 58	2 53E-01		
364	28	122 58	31 58	2 53E-01		
365	28	122 58	31 58	2 53E-01		
366	122	242 71	151 71	1 28E+01		
366 25	104	219 71	128 71	8 49E+00		
366 5	84	194 15	103 15	4 88E+00		
367	74	181 37	90 37	3 51E+00		
368	72	178 81	87 81	3 26E+00		
					end of 25/9	
369	70 5	176 90	85 90	3 09E+00	4 7	
370	68 5	174 34	83 34	2 86E+00		
371	66 5	171 78	80 78	2 65E+00		
372	66	171 15	80 15	2 60E+00		
373	66	171 15	80 15	2 60E+00		
374	66	171 15	80 15	2 60E+00		
375	66	171 15	80 15	2 60E+00		
376	66	171 15	80 15	2 60E+00		
377	66	171 15	80 15	2 60E+00		
377 5	121	241 44	150 44	1 25E+01		
377 75	148	275 94	184 94	2 10E+01		
378	120	240 16	149 16	1 23E+01		
378 5	93	205 65	114 65	6 36E+00		
379	90	201 82	110 82	5 84E+00		
380	82 5	192 23	101 23	4 66E+00		
380 5	76	183 93	92 93	3 76E+00		
381	74	181 37	90 37	3 51E+00		
382	74	181 37	90 37	3 51E+00		
383	74	181 37	90 37	3 51E+00		
384	74	181 37	90 37	3 51E+00		
385	74	181 37	90 37	3 51E+00		
386	73 5	180 73	89 73	3 45E+00		
387	73 5	180 73	89 73	3 45E+00		
388	73 5	180 73	89 73	3 45E+00		
389	73 5	180 73	89 73	3 45E+00		
389 5	73 5	180 73	89 73	3 45E+00		
390	72	178 81	87 81	3 26E+00		
391	72	178 81	87 81	3 26E+00		
392	72	178 81	87 81	3 26E+00		
					end of 26/9	

Table B4: Temporal moisture content and properties of refuse lift 1 (without clay capping)

Calendar year	Simulation year	Refuse lift 1								
		Moisture Cont	Wdensity, kg/m ³	A stress, kPa	Thickness, m	Ddensity, kg/m ³	Air porosity, %	Total porosity, %	Vol FC, %	HC, m/s
1986	1 (Initial)	0 1709	687 00			516 31	10 25	54 63	44 37	6 13E-05
	1(final)	0 2633	779 61	24 65	6 45	516 31	10 25	54 63	44 37	6 13E-05
1987	2	0 2633	779 61	87 49	6 45	516 31	10 25	54 63	44 37	6 13E-05
	(adjusted)	0 2958	875 98	87 49	5 74	580 13	8 17	53 46	45 29	2 71E-05
1988	3	0 2954	875 53	92 51	5 74	580 13	8 17	53 46	45 29	2 71E-05
	(adjusted)	0 2968	879 80	92 51	5 71	582 96	8 09	53 42	45 33	2 62E-05
1989	4	0 3015	884 46	115 89	5 71	582 96	8 09	53 42	45 33	2 62E-05
	(adjusted)	0 3075	902 11	127 73	5 60	594 59	7 79	53 27	45 49	2 28E-05
1990	5	0 3353	929 89	143 55	5 60	594 59	7 79	53 27	45 49	2 28E-05
	(adjusted)	0 3387	939 42	143 51	5 54	600 69	7 63	53 20	45 57	2 13E-05
Post closure										
1991	1	0 3763	976 99		5 54	600 69	7 63	53 20	45 57	2 13E-05
	(adjusted)	0 4168	1082 09		5 01	665 31	6 25	52 65	46 39	1 04E-05
1992	2	0 4491	1114 41		5 01	665 31	6 25	52 65	46 39	1 04E-05
	(adjusted)	0 4630	1148 88		4 86	685 89	5 89	52 53	46 64	8 40E-06
1993	3	0 5253	1211 24		4 86	685 89	5 89	52 53	46 64	8 40E-06
	(adjusted)	0 5248	1223 31		4 77	698 53	5 69	52 48	46 79	7 39E-06
1994	4	0 5248	1223 31		4 77	698 53	5 69	52 48	46 79	7 39E-06
	(adjusted)	0 5244	1232 21		4 71	707 78	5 54	52 44	46 90	6 74E-06
1995	5	0 5244	1232 21		4 71	707 78	5 54	52 44	46 90	6 74E-06
	(adjusted)	0 5242	1239 31		4 66	715 13	5 43	52 42	46 99	6 27E-06
1996	6	0 5242	1239 31		4 66	715 13	5 43	52 42	46 99	6 27E-06
	(adjusted)	0 5240	1245 23		4 62	721 25	5 34	52 40	47 06	5 91E-06
1997	7	0 5240	1245 23		4 62	721 25	5 34	52 40	47 06	5 91E-06
	(adjusted)	0 5238	1250 34		4 58	726 51	5 27	52 38	47 12	5 62E-06
1998	8	0 5238	1250 34		4 60	726 51	5 27	52 38	47 12	5 62E-06
	(adjusted)	0 5236	1257 66		4 55	734 02	5 16	52 36	47 20	5 23E-06

Wdensity: Wet density;

Ddensity: Dry density

FC: Field capacity;

HC: Hydraulic conductivity;

A. Stress: Applied stress

Table B5: Temporal moisture content and properties of refuse lift 2 (without clay capping)

Calendar year	Simulation year	Refuse lift 2									
		Moisture Cont	Wdensity, kg/m ³	A stress, kPa	Thickness, m	Ddensity, kg/m ³	Air porosity, %	Total porosity, %	Vol FC, %	HC, m/s	
1987	1 (Initial)	0 1709	687 00			516 31	10 25	54 63	44 37	6 13E-05	
	1(final)	0 2288	745 11	31 42	8 60	516 31	10 25	54 63	44 37	6 13E-05	
1988	2	0 2890	805 31	33 96	8 60	516 31	10 25	54 63	44 37	6 13E-05	
	(adjusted)	0 2910	810 78	33 96	8 54	519 82	10 12	54 54	44 43	5 85E-05	
1989	3	0 3086	828 42	68 31	8 54	519 82	10 12	54 54	44 43	5 85E-05	
	(adjusted)	0 3285	881 96	68 31	8 02	553 41	8 96	53 87	44 92	3 77E-05	
1990	4	0 3380	891 41	82 95	8 02	553 41	8 96	53 87	44 92	3 77E-05	
	(adjusted)	0 3438	906 71	82 95	7 89	562 91	8 66	53 71	45 05	3 35E-05	
Post closure											
1991	1	0 3770	939 91		7 89	562 91	8 66	53 71	45 05	3 35E-05	
	(adjusted)	0 4175	1040 76		7 12	623 31	7 10	52 97	45 86	1 64E-05	
1992	2	0 4489	1072 21		7 12	623 31	7 10	52 97	45 86	1 64E-05	
	(adjusted)	0 4628	1105 38		6 91	642 59	6 69	52 80	46 11	1 33E-05	
1993	3	0 4779	1120 49		6 91	642 59	6 69	52 80	46 11	1 33E-05	
	(adjusted)	0 4867	1141 14		6 78	654 44	6 46	52 72	46 26	1 17E-05	
1994	4	0 4765	1130 94		6 78	654 44	6 46	52 72	46 26	1 17E-05	
	(adjusted)	0 4828	1145 92		6 70	663 11	6 29	52 66	46 37	1 06E-05	
1995	5	0 4770	1140 11		6 70	663 11	6 29	52 66	46 37	1 06E-05	
	(adjusted)	0 4820	1151 95		6 63	669 99	6 17	52 62	46 45	9 90E-06	
1996	6	0 4748	1144 79		6 63	669 99	6 17	52 62	46 45	9 90E-06	
	(adjusted)	0 4789	1154 59		6 57	675 73	6 07	52 59	46 52	9 33E-06	
1997	7	0 4890	1164 73		6 57	675 73	6 07	52 59	46 52	9 33E-06	
	(adjusted)	0 4926	1173 21		6 52	680 65	5 98	52 56	46 58	8 87E-06	
1998	8	0 4835	1164 15		6 52	680 65	5 98	52 56	46 58	8 87E-06	
	(adjusted)	0 4866	1171 55		6 48	684 97	5 91	52 54	46 63	8 48E-06	

Wdensity: Wet density;

Ddensity: Dry density

FC: Field capacity;

HC: Hydraulic conductivity;

A. Stress: Applied stress

Table B6: Temporal moisture content and properties of refuse lift 3 (without clay capping)

Calendar year	Simulation year	Refuse lift 3									
		Moisture Cont	Wdensity, kg/m ³	A stress, kPa	Thickness, m	Ddensity, kg/m ³	Air porosity, %	Total porosity, %	Vol	FC, %	HC, m/s
1989	1 (Initial)	0 1709	687 00			516 31	10 25	54 63	44 37	6 13E-05	
	1 (final)	0 2808	797 11	16 81	4 30	516 31	10 25	54 63	44 37	6 13E-05	
1990	capping	0 3365	852 81	23 94	5 73	516 31	10 25	54 63	44 37	6 13E-05	
	final	0 3611	915 03	52 38	5 34	553 98	8 94	53 86	44 93	3 75E-05	
Post closure											
1991	1	0 3725	926 48		5 34	553 98	8 94	53 86	44 93	3 75E-05	
	(adjusted)	0 4126	1026 15		4 82	613 58	7 32	53 06	45 74	1 83E-05	
1992	2	0 4418	1055 38		4 82	613 58	7 32	53 06	45 74	1 83E-05	
	(adjusted)	0 4555	1088 02		4 67	632 56	6 90	52 88	45 98	1 48E-05	
1993	3	0 4536	1086 16		4 67	632 56	6 90	52 88	45 98	1 48E-05	
	(adjusted)	0 4620	1106 17		4 59	644 21	6 66	52 79	46 13	1 30E-05	
1994	4	0 4552	1099 41		4 59	644 21	6 66	52 79	46 13	1 30E-05	
	(adjusted)	0 4612	1113 98		4 53	652 75	6 49	52 73	46 24	1 19E-05	
1995	5	0 4561	1108 85		4 53	652 75	6 49	52 73	46 24	1 19E-05	
	(adjusted)	0 4608	1120 36		4 48	659 53	6 36	52 68	46 32	1 11E-05	
1996	6	0 4553	1114 83		4 48	659 53	6 36	52 68	46 32	1 11E-05	
	(adjusted)	0 4592	1124 37		4 44	665 17	6 26	52 65	46 39	1 04E-05	
1997	7	0 4576	1122 77		4 44	665 17	6 26	52 65	46 39	1 04E-05	
	(adjusted)	0 4609	1130 95		4 41	670 02	6 17	52 62	46 45	9 90E-06	
1998	8	0 4579	1127 92		4 41	670 02	6 17	52 62	46 45	9 90E-06	
	(adjusted)	0 4608	1135 08		4 38	674 28	6 09	52 59	46 50	9 47E-06	

Wdensity: Wet density;

Ddensity: Dry density

FC: Field capacity;

HC: Hydraulic conductivity;

A. Stress: Applied stress

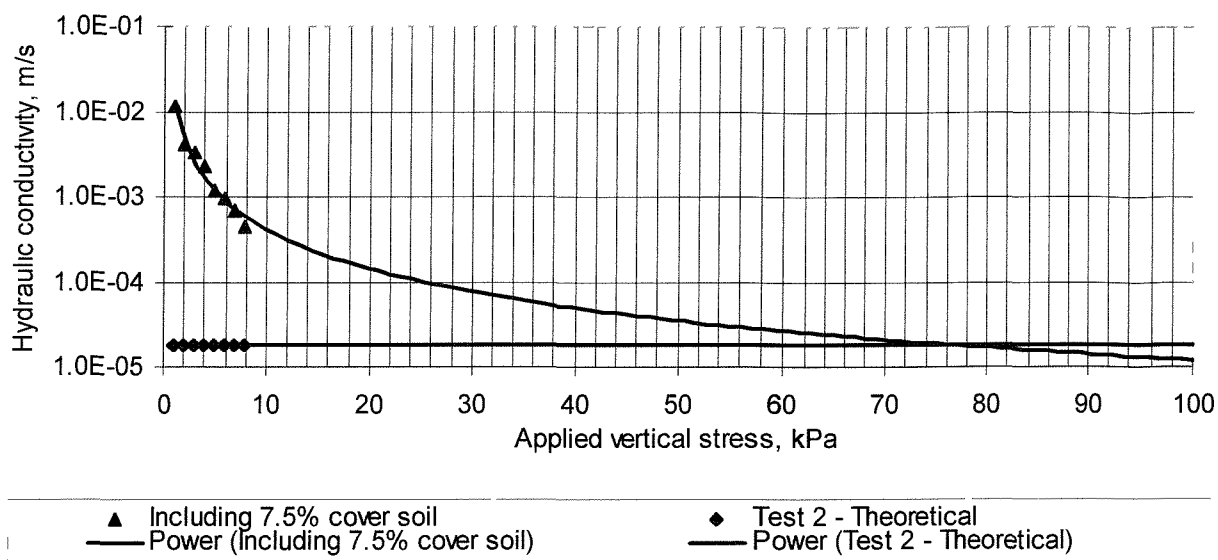
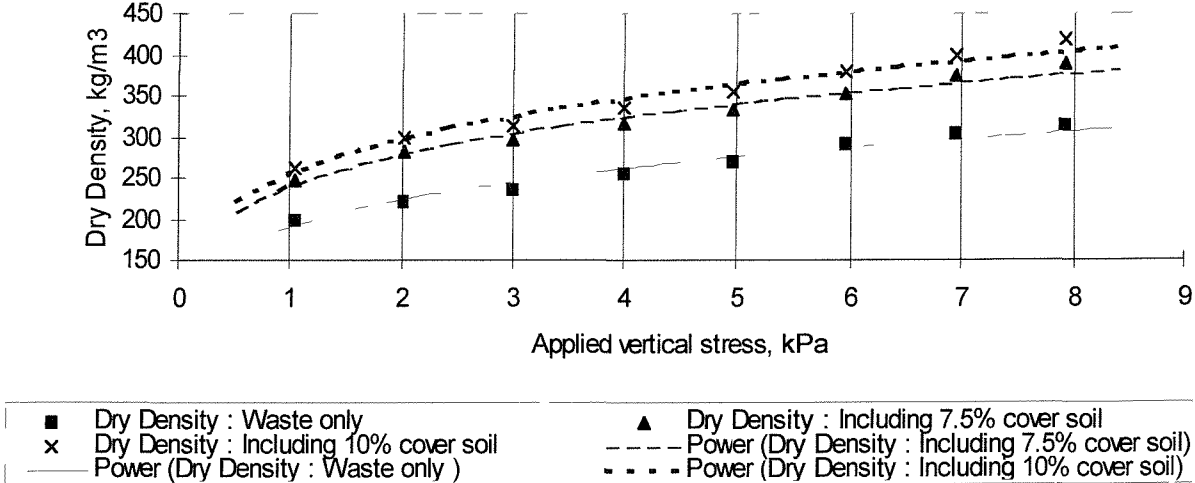


Figure B1: The extended characteristic curves of the experimental and theoretical hydraulic conductivity of refuse with 7.5 % cover soil



The characteristic equations of the above curves are:

$$\rho_{dry} = 190\sigma_e^{0.228} \quad (\text{refuse only}) \quad [\text{B1}]$$

$$\rho_{dry} = 239\sigma_e^{0.2182} \quad (\text{with 7.5% cover soil}) \quad [\text{B2}]$$

$$\rho_{dry} = 254\sigma_e^{0.2219} \quad (\text{with 10% cover soil}) \quad [\text{B3}]$$

where

ρ_{dry} = dry density of refuse in kg/m³

σ_e = effective stress